

The antimicrobial activity of carrier-coupled  
antisense peptide nucleic acids (PNAs) on  
streptococci

Dissertation

zur

Erlangung des akademischen Grades

doctor rerum naturalium (Dr. rer. nat.)

der Mathematisch-Naturwissenschaftlichen Fakultät

der Universität Rostock

vorgelegt von

Corina Abt-Becker (geb. Abt), geb. am 29.03.1996 in Geislingen an der Steige  
aus Rostock

Rostock, 21.06.2023

Reviewer of the doctoral defense, held on November 17, 2023

**Dr. Nadja Patenge**

Institute of Medical Microbiology, Virology and Hygiene, University of Rostock

**Dr. Mirko Basen**

Institute of Biosciences, University of Rostock

**Dr. Ulrike Gimsa**

Research Institute for Farm Animal Biology (FBN)  
and Professor of Immunology at the University of Rostock

# Corina Abt-Becker

Day and place of birth: 29.03.1996 at Geislingen a. d. Steige

## Education

- 2020 – 2023 **Institute for Medical Microbiology, Virology and Hygiene**  
Degree: Dr rer. nat.  
Funding: : Scholarship from the Mecklenburg-West Pomeranian Graduate Fund
- 2017 – 2019 **M.Sc. Medical Biotechnology, University of Rostock**  
Degree: Master of Science
- 2014 – 2017 **B.Sc. Applied Biology, Hochschule Bonn-Rhein-Sieg**  
Degree: Bachelor of Science
- 2006 – 2014 **Michelberggymnasium Geislingen a. d. Steige**  
Degree: Abitur

---

## Publication

- Publication: **Barkowsky G\*, Abt C\***, Pöhner I, Bieda A, Hammerschmidt S, Jacob A, Kreikemeyer B, Patenge N. Antimicrobial Activity of Peptide-Coupled Antisense Peptide Nucleic Acids in *Streptococcus pneumoniae*. *Microbiol Spectr.* 2022 Dec 21;10(6):e0049722. doi: 10.1128/spectrum.00497-22. Epub 2022 Nov 2. PMID: 36321914; PMCID: PMC9784828. (\*shared first authorship)
- Abt C**, Gerlach LM, Bull J, Jacob A, Kreikemeyer B, Patenge N. Pyrenebutyrate Enhances the Antibacterial Effect of Peptide-Coupled Antisense Peptide Nucleic Acids in *Streptococcus pyogenes*. *Microorganisms.* 2023 Aug 22;11(9):2131. doi: 10.3390/microorganisms11092131. PMID: 37763975; PMCID: PMC10537354.
- Presentation: Talk at the Lancefield Symposium 2022 in Stockholm

---

*C. Abt-Becker*

Corina Abt-Becker, 14.12.2023

**Doktorandinnen/Doktoranden-Erklärung gemäß § 4 Absatz 1 Buchstaben g und h  
der Promotionsordnung  
der Mathematisch-Naturwissenschaftlichen Fakultät  
der Universität Rostock**

**Name:** Abt-Becker, Corina Rebekka

Ich habe eine Dissertation zum Thema

The antimicrobial activity of carrier-coupled antisense peptide nucleic acids (PNAs) in streptococci.

Die antimikrobielle Wirkung von Carrier-gekoppelten Antisense-Peptidnukleinsäuren (PNAs) in Streptokokken

an der Mathematisch-Naturwissenschaftlichen Fakultät der Universität Rostock angefertigt. Dabei wurde ich von

Dr Bernd Kreikemeyer und Dr Nadja Patenge

betreut.

Ich gebe folgende Erklärung ab:

1. Die Gelegenheit zum vorliegenden Promotionsvorhaben ist mir nicht kommerziell vermittelt worden. Insbesondere habe ich keine Organisation eingeschaltet, die gegen Entgelt Betreuerinnen/Betreuer für die Anfertigung von Dissertationen sucht oder die mir obliegenden Pflichten hinsichtlich der Prüfungsleistungen für mich ganz oder teilweise erledigt.

2. Ich versichere hiermit an Eides statt, dass ich die vorliegende Arbeit selbstständig angefertigt und ohne fremde Hilfe verfasst habe. Dazu habe ich keine außer den von mir angegebenen Hilfsmitteln und Quellen verwendet und die den benutzten Werken inhaltlich und wörtlich entnommenen Stellen habe ich als solche kenntlich gemacht.

....., den .....

## **Acknowledgment**

I would like to express my deepest gratitude to my supervisors Dr. Bernd Kreikemeyer and Dr. Nadja Patenge for the advice and support. Additionally, this endeavor would not have been possible without the generous funding from the Landesgraduiertenförderung Mecklenburg-Vorpommern. I am also thankful for the great atmosphere and fun in the lab, which is largely thanks to Dr. Gina Barkowsky. Special thanks to Jana Bull and Yvonne Humboldt for the wonderful breakfast breaks, the open ears, and for the help. And last but not least, I would like to thank my incredibly great friends, especially Irina Pöhner and Annika Eichhorst, and my love Kanti.



**Universität  
Rostock**



Traditio et Innovatio



**Mecklenburg-Vorpommern**  
Ministerium für Wissenschaft,  
Kultur, Bundes- und  
Europaangelegenheiten



EUROPÄISCHE UNION  
Europäischer Sozialfonds



Europäische Fonds EFRE, ESF und ELER  
in Mecklenburg-Vorpommern 2014-2020



# Table of content

Abbreviations.....	V
List of Tables.....	VIII
List of Figures.....	IX
Summary.....	- 1 -
Zusammenfassung.....	- 2 -
<b>1. Introduction</b> .....	- 4 -
<b>1.1 Streptococcus</b> .....	- 4 -
1.1.1 General properties and clinical relevance of <i>Streptococcus pneumoniae</i> .....	- 4 -
1.1.2 General properties and clinical relevance of <i>Streptococcus pyogenes</i> .....	- 7 -
<b>1.2 Carrier-coupled antisense peptide nucleic acids</b> .....	- 9 -
1.2.1 Peptide nucleic acids (PNAs).....	- 9 -
1.2.2 Carrier-coupled peptide nucleic acids.....	- 11 -
1.2.3 Pyrenebutyrate as enhancer of antimicrobial activity of CPP-PNA.....	- 13 -
1.2.4 Off target effects of carrier-coupled PNAs.....	- 14 -
<b>1.3 The infection model organism <i>Galleria mellonella</i></b> .....	- 16 -
1.3.1 <i>Galleria mellonella</i> as infection model organism.....	- 16 -
1.3.2 The immune system of <i>Galleria mellonella</i> .....	- 17 -
<b>1.4 Aim of this work</b> .....	- 19 -
<b>2. Materials and Methods</b> .....	- 20 -
<b>2.1 Materials</b> .....	- 20 -
<b>2.2 Methods</b> .....	- 24 -
2.2.1 Media and buffer preparation.....	- 24 -
2.2.2 CPP-PNA handling.....	- 25 -
2.2.3 Bacterial maintenance.....	- 25 -
2.2.3.1 Bacterial cultures.....	- 25 -
2.2.3.2 Storage of bacteria.....	- 25 -
2.2.3.3 Determination of the number of colony forming units (CFU).....	- 25 -
2.2.4 Determination of the antimicrobial activity.....	- 25 -
2.2.5 Determination of uptake of fluorescently labeled carrier into <i>S. pyogenes</i> .....	- 26 -
2.2.6 Determination of relative gene expression.....	- 26 -
2.2.6.1 Treatment of <i>S. pneumoniae</i> with CPP-PNA.....	- 26 -
2.2.6.2 Isolation of RNA from CPP-PNA treated <i>S. pneumoniae</i> .....	- 26 -
2.2.6.3 Cleaning of RNA and determination of quantity and quality.....	- 27 -
2.2.6.4 cDNA Synthesis.....	- 27 -

2.2.6.5	Quantitative PCR (qPCR).....	- 27 -
2.2.7	Transcriptomic analysis .....	- 28 -
2.2.7.1	Treatment of streptococci with CPP-PNA.....	- 28 -
2.2.7.2	RNA isolation .....	- 28 -
2.2.7.3	Cleaning RNA, determination of quality and quantity of RNA, and target gene expression .....	- 28 -
2.2.7.4	Transcriptomic analysis .....	- 29 -
2.2.8	Cell-based infection system .....	- 29 -
2.2.8.1	Detroit 562 cultivation and maintenance.....	- 29 -
2.2.8.2	Antimicrobial effects of CPP-PNA conjugates in cell based infection model.....	- 29 -
2.2.8.3	Viability of Detroit 562 cells: LDH leakage assay and crystal violet staining.....	- 29 -
2.2.9	Infection model organism <i>Galleria mellonella</i> larvae .....	- 30 -
2.2.9.1	Maintenance of <i>G. mellonella</i> larvae.....	- 30 -
2.2.9.2	Infection and treatment of <i>G. mellonella</i> larvae .....	- 30 -
2.2.9.3	Determination of bacteria load in <i>G. mellonella</i> larvae.....	- 31 -
2.2.9.4	Proteomics analysis of the immune response of infected <i>G. mellonella</i> larvae ...	- 33 -
<b>3.</b>	<b>Results</b> .....	- 34 -
<b>3.1</b>	<b>Antimicrobial effect of antisense CPP-PNAs on <i>Streptococcus pneumoniae</i>.</b>	- 34 -
3.1.1	Identification of effective CPP-PNA conjugates .....	- 34 -
3.1.2	Kill kinetics of (RXR) <sub>4</sub> XB- and TAT-PNA.....	- 38 -
3.1.3	Target specificity.....	- 39 -
3.1.4	CPP-PNA in a cell-based infection system.....	- 40 -
3.1.5	CPP-PNA as therapeutic in the infection model organism <i>Galleria melonella</i>	- 42 -
<b>3.2</b>	<b>Improving the antimicrobial effect of CPP-PNA with pyrenebutyrate.....</b>	- 45 -
<b>3.3</b>	<b>Transcriptomic analyses of CPP-PNA treated streptococci</b> .....	- 50 -
3.3.1	Transcriptomic response of <i>Streptococcus pneumoniae</i> .....	- 51 -
3.3.2	Transcriptomic response of <i>Streptococcus pyogenes</i> .....	- 54 -
<b>3.4</b>	<b>Investigation of the immune response of <i>Galleria mellonella</i> to <i>Streptococcus pyogenes</i> infection using a proteomics approach</b> .....	- 59 -
3.4.1	Proteins of the humoral immune response .....	- 62 -
3.4.2	Proteins of cellular immune response .....	- 66 -
3.4.3	Proteins not associated with the immune response.....	- 67 -
<b>4.</b>	<b>Discussion</b> .....	- 71 -
<b>4.1</b>	<b>Antimicrobial effect of antisense CPP-PNAs on <i>Streptococcus pneumoniae</i>.</b>	- 71 -



## Appreviations

4.1.1	CPP-PNA conjugates with antimicrobial activity in <i>S. pneumoniae</i> .....	- 71 -
4.1.2	Target specificity of PNAs.....	- 73 -
4.1.3	Evaluation of CPP-PNAs <i>in vivo</i> using an infection model organism.....	- 75 -
4.1.4	Perspective of CPP-PNA treatment in pneumococci.....	- 76 -
<b>4.2</b>	<b>Improving the antimicrobial effect of CPP-PNA with pyrenebutyrate.....</b>	<b>- 78 -</b>
<b>4.3</b>	<b>Transcriptomic analyses of CPP-PNA treated streptococci .....</b>	<b>- 80 -</b>
4.3.1	Transcriptomic changes in pneumococci after (RXR) <sub>4</sub> XB-PNA treatment .....	- 80 -
4.3.2	Transcriptomic changes in <i>S. pyogenes</i> treated with (RXR) <sub>4</sub> XB- and TAT-PNA ....	- 82 -
4.3.3	Limitations of the experimental setting and prospect of improvement .....	- 84 -
<b>4.4</b>	<b>Proteome profiling of model organism <i>G. mellonella</i> during GAS infection</b>	<b>- 85 -</b>
4.4.1	Specificity of <i>G. mellonella</i> immune response .....	- 86 -
4.4.2	Similarity of the <i>G. mellonella</i> immune response and the mammalian innate immune system .....	- 89 -
4.4.3	Complexity of <i>G. mellonella</i> immune response .....	- 92 -
4.4.4	<i>G. mellonella</i> as a model organism for the investigation of immune responses-	- 94 -
<b>References</b>	.....	<b>- 97 -</b>
<b>Appendix</b>	.....	<b>- 118 -</b>

## Abbreviations

AMPs	Antimicrobial peptides
ATP	Adenosine triphosphate
$\beta$ -1,3-glucan BPs	$\beta$ -1,3-glucan binding proteins
BHI	Brain heart infusion
bp	Base pairs
<i>C. albicans</i>	<i>Candida albicans</i>
CDC	Centers for disease control and prevention
cDNA	Copy DNA
CFU	Colony forming units
CPP	Cell-penetrating peptides
Ct	Cycle threshold
CTL	C-type-lectin
<i>D. melanogaster</i>	<i>Drosophila melanogaster</i>
DAMP	Damage-associated molecular pattern
DEPC	Diethylpyrocarbonate
DNA	Deoxyribonucleic acid
<i>E. coli</i>	<i>Escherichia coli</i>
e. g.	Exempli gratia
F-actin	Filamentous actin
g	Gramm, or gravity force
<i>G. mellonella</i>	<i>Galleria mellonella</i>
GAS	Group A streptococcus
GmCP8	Cationic peptide 8
GNB	Gram-negative bacteria binding proteins
GRC	Gustatory receptor candidate
h	Hours
HSP	Heat shock protein
IMPI	Inducible metalloproteinase inhibitor
IPD	Invasive pneumococcal disease
IR	Immune response
JH	Juvenile hormone
l	Liter

## Abbreviations

LDH	Lactate dehydrogenase
<i>L. monocytogenes</i>	<i>Listeria monocytogenes</i>
LPS	Lipopolysaccharides
LTA	Lipoteichoic acid
M	Molar
min	Minutes
ml	Milliliter
mRNA	Messenger RNA
NA	Nucleic acid
n.d.	Not determined
NET	Neutrophil extracellular trap
OD	Optical density
p.i.	Post infection
PAMP	Pathogen-associated molecular pattern
PB	Pyrenebutyrate
PBS	Phosphate buffered saline
PCV	Pneumococcal conjugate vaccine
PG	Peptidoglycan
PGRP	Peptidoglycan recognition protein
PNA	Peptide nucleic acid
PO system	Phenol oxidase system
PPSV	Pneumococcal polysaccharide vaccine
PRR	Pattern recognition receptor
qPCR	Quantitative real-time polymerase chain reaction
RHD	Rheumatic heart disease
RNA	Ribonucleic acid
ROS	Reactive oxygen species
rpm	Revolutions per minute
RT	Room temperature
<i>S. aureus</i>	<i>Staphylococcus aureus</i>
<i>S. enterica</i>	<i>Salmonella enterica</i>
<i>S. pneumoniae</i>	<i>Streptococcus pneumoniae</i>
<i>S. pyogenes</i>	<i>Streptococcus pyogenes</i>
scr	Scrambled

## Abbreviations

sec	Seconds
SP	Serine protease
THY	Todd hewitt bouillon
™	Unregistered trademark
WHO	World health organization
xg	Gravity
®	Registered trademark
μl	Microliter

## List of Tables

Table 1: Chemicals and enzymes .....	- 20 -
Table 2: Consumable supplies.....	- 21 -
Table 3: Devices.....	- 21 -
Table 4: Bacterial strains.....	- 22 -
Table 5: Cell line .....	- 22 -
Table 6: Antibiotic .....	- 22 -
Table 7: Oligonucleotides .....	- 22 -
Table 8: Kits .....	- 23 -
Table 9: Software .....	- 23 -
Table 10: Sequences of PNAs.....	- 23 -
Table 11: Sequences of the peptide carriers used in this work .....	- 23 -
Table 12: Composition of DEPC-H <sub>2</sub> O, media, and 10x PBS buffer.....	- 24 -
Table 13: Mastermix for qPCR, per sample.....	- 28 -
Table 14: Amplification program for qPCR.....	- 28 -
Table 15: Feed of <i>G. mellonella</i> larvae .....	- 30 -
Table 16: Reaction mixture for colony PCR.....	- 32 -
Table 17: Amplification program for colony PCR.....	- 32 -
Table 18: Antimicrobial effect of CPP-PNAs on <i>S. pneumoniae</i> strain TIGR4 and strain 19F. - 37 -	
Table 19: Relative LDH release of Detroit 562 cells upon CPP-PNA treatment.....	- 41 -
Table 20: Positive amino acid residues per CPP.....	- 46 -
Table 21: Number of differentially expressed genes in <i>S. pneumoniae</i> TIGR4 after treatment with CPP-PNA, CPP-scrPNA and CPP.....	- 52 -
Table 22: Number of differentially expressed genes in <i>S. pyogenes</i> 591 after treatment with CPP-PNA, CPP-scrPNA and CPP.....	- 55 -
Table 23: Proteins with altered amount in cell-free hemolymph 4, 24, and 72h p.i. ....	- 60 -
Table 24: Accession number and description of putative antimicrobial peptides (AMPs) with fold changes at three different time points in infected larvae compared to control. ....	- 64 -
Table 25: Effect of pyrenebutyrate on antimicrobial cell count reduction of CPP-PNA on <i>S. pneumoniae</i> .....	- 119 -
Table 26: Effect of pyrenebutyrate on antimicrobial cell count reduction of CPP-PNA on <i>S.</i> <i>pyogenes</i> . .....	- 120 -
Table 27: Proteins with altered abundance in infected larvae compared to control larvae at 4, 24, and 72 h post infection.....	- 122 -

## List of Figures

Figure 1: Chemical structure of PNA.....	10 -
Figure 2: Models of direct translocation of CPPs (Szabó et al., 2022).....	13 -
Figure 3: Main effectors and their function in <i>G. mellonella</i> larval immune system. ....	17 -
Figure 4: Anatomy of <i>G. mellonella</i> larvae (modified) (Durieux et al., 2021; Singkum et al., 2019), which adapted from (Engel and Moran, 2013; Singkum et al., 2019).. ....	31 -
Figure 5: Concentration-dependent reduction of bacterial cell count following treatment of <i>S. pneumoniae</i> TIGR4 with cell-penetrating peptide (CPP)-antisense PNAs for 6 h..	35 -
Figure 6: Toxicity of CPPs (RXR) <sub>4</sub> XB and TAT in <i>S. pneumoniae</i> strain TIGR4.....	36 -
Figure 7: Killing kinetics of CPP-anti- <i>gyrA</i> PNA treatment in <i>S. pneumoniae</i> strain TIGR4.....	38 -
Figure 8: Relative expression of target genes in <i>S. pneumoniae</i> strain TIGR4 following treatment with CPP-antisense PNAs. ....	39 -
Figure 9: Relative expression of virulence genes in <i>S. pneumoniae</i> strain TIGR4 following treatment with CPP-anti- <i>rpoB</i> PNAs.....	40 -
Figure 10: Antimicrobial effect of (RXR) <sub>4</sub> XB-anti- <i>gyrA</i> in a cell-based infection system. ....	41 -
Figure 11: Cell viability of Detroit 562 cells upon treatment with CPP-PNAs. ....	42 -
Figure 12: Survival of <i>Galleria mellonella</i> larvae treated with 10 nmol CPP-PNAs following infection with <i>S. pneumoniae</i> strain TIGR4. ....	43 -
Figure 13: Bacterial load of <i>G. mellonella</i> larvae infected with <i>S. pneumoniae</i> strain TIGR4 and treated with (RXR) <sub>4</sub> XB- <i>gyrA</i> .....	44 -
Figure 14: Effect of different concentrations of pyrenebutyrate on bacterial cell count of (a) <i>S. pneumoniae</i> TIGR4 and (b) <i>S. pyogenes</i> 591.....	45 -
Figure 15: Effect of pyrenebutyrate on cell count reduction of CPP-PNA on <i>streptococci</i> . ....	46 -
Figure 16: Kinetics of effect of pyrenebutyrate on antimicrobial cell count reduction of CPP-PNA on <i>S. pyogenes</i> 591.. ....	48 -
Figure 17: Uptake of K8-FITC into in <i>S. pyogenes</i> in presence and absence of PB.....	49 -
Figure 18: Workflow for the investigation of transcriptomic effects of CPP-PNA or CPP treatment on streptococcal species.. ....	50 -
Figure 19: Principal component analysis (PCA) of the different treatment conditions with <i>S. pneumoniae</i> .....	52 -
Figure 20: Transcriptomic responses of <i>S. pneumoniae</i> strain TIGR4 upon CPP-PNA and CPP treatment. ....	53 -
Figure 21: Pathways with differentially expressed genes of <i>S. pneumoniae</i> strain TIGR4 upon CPP-PNA and CPP treatment.....	54 -
Figure 22: Principal component analysis (PCA) of the different treatment conditions of <i>S. pyogenes</i> . ....	55 -
Figure 23: Transcriptomic responses of <i>S. pyogenes</i> upon CPP-PNA and CPP treatment. ....	56 -
Figure 24: Pathways with differentially expressed genes of <i>S. pyogenes</i> upon CPP-PNA and CPP treatment. ....	58 -
Figure 25: Workflow of proteomics analysis of cell-free hemolymph of infected <i>G. mellonella</i> larvae.. ....	59 -
Figure 26: Proteomic response of <i>Galleria mellonella</i> larvae infected with 2 – 4 x 10 <sup>6</sup> CFU of <i>S. pyogenes</i> 591 after (A) 4 h, (B) 24 h, and (C) 72 h p.i. ....	61 -
Figure 27: Proteins associated with non-self recognition. ....	63 -

List of Figures

Figure 28: Antimicrobial peptides (AMPs).....	- 65 -
Figure 29: Putative immune-relevant proteins. ....	- 66 -
Figure 30: Sequence alignment of endonucleases.....	- 67 -
Figure 31: Tissue proteins. ....	- 68 -
Figure 32: Silk proteins. ....	- 69 -
Figure 33: Proteins involved in metabolism.. ....	- 69 -
Figure 34: Overview of main findings of this work of the <i>G. mellonella</i> immune response to GAS infection concerning the relative specificity, similarity to the mammalian innate immune response, and complexity. ....	- 96 -
Figure 35: Concentration-dependent reduction of bacterial cell count following treatment of <i>S. pneumoniae</i> D39 with cell-penetrating peptide (CPP)-antisense PNAs for 6 h.....	- 118 -
Figure 36: Concentration-dependent reduction of bacterial cell count following treatment of <i>S. pneumoniae</i> 19F with cell-penetrating peptide (CPP)-antisense PNAs for 6 h. ....	- 119 -
Figure 37: RNA isolated of streptococci after treatment with lethal concentration of CPP-PNA. ....	- 120 -
Figure 38: Bacterial load and survival rate of <i>G. mellonella</i> infected with <i>S. pyogenes</i> 591. ....	- 121 -

## Summary

The pathogens *Streptococcus pneumoniae* and *Streptococcus pyogenes* can cause serious diseases and are of high clinical relevance. In this work effective carrier-coupled antisense peptide nucleic acids (PNAs) against *S. pneumoniae* were identified. PNAs were designed complementary to the start region of the mRNA of target genes to suppress translational initiation. The relative transcript abundance of the target genes *gyrA* and *rpoB* were significantly reduced following antisense PNA treatment. Uptake of PNA into pneumococci was mediated by the cell penetrating peptides (CPPs) (RXR)<sub>4</sub>XB and TAT. Treatment with the (RXR)<sub>4</sub>XB-anti-*gyrA* PNA conjugate resulted in complete eradication of *S. pneumoniae in vitro*. The effectivity of the CPP- antisense PNA was further shown in a cell-based system with the human pharyngeal epithelial cell line Detroit 562. In the invertebrate model organism *Galleria mellonella*, treatment of infected larvae with the CPP-PNA conjugates reduced the pneumococcal load and resulted in increased survival rates.

The counteranion pyrenebutyrate (PB) was investigated for its ability to improve uptake of CPP-PNAs in streptococci *in vitro*. Preincubation with PB increased the uptake of fluorescently labeled K8 by 4.5-fold in *Streptococcus pyogenes*, and improved the antibacterial effect of CPP-antisense PNA in *S. pneumoniae* and *S. pyogenes*. The effect of PB on the uptake of CPP-cargo conjugates had been studied only in eukaryotes, and so far, only an effect on the uptake of arginine-rich CPPs had been reported. In this work, it was discovered that PB can also be applied to bacteria. Additionally, PB was effectively supporting uptake of lysine-rich CPPs.

Transcriptomic effects of CPP-PNA on streptococci were investigated using a sublethal concentration over an extended incubation time. This resulted in low transcriptomic alterations. Among those were several genes involved in uptake and metabolism of carbohydrates, and genes putatively associated with the bacterial stress response. In future experiments, higher CPP-PNA concentrations should be applied for reduced treatment times to achieve pronounced transcriptomic changes. This will lead to information about knock-down effects, off-target effects, and possible resistance mechanisms and stress responses against CPP-PNA.

As *G. mellonella* is an increasingly popular infection model organism, the *S. pyogenes* specific immune response of the larvae was investigated using a proteomics approach. The immune response of larvae showed relative specificity to *S. pyogenes* infection, high similarity to the mammalian innate immune response, and a greater complexity than appreciated today. The data qualify the insect organism as simplified model of the mammalian innate immune response, and make a valuable contribution to reduce the use of murine infection models.



## Zusammenfassung

Der Krankheitserreger *Streptococcus pneumoniae* und *Streptococcus pyogenes* können schwerwiegende Erkrankungen verursachen und sind von hoher klinischer Relevanz. In dieser Arbeit wurden wirksame Carrier-gekoppelte Peptidnukleinsäuren (peptide nucleic acids, PNAs) gegen *S. pneumoniae* identifiziert. PNAs, welche komplementär zur Startregion der mRNA eines Zielgens sind, führen zur Inhibierung der Translation dieses Gens. Die relative Transkripthäufigkeit der essentiellen Zielgene *gyrA* und *rpoB* wurde mit Antisense-PNAs signifikant reduziert. Die Aufnahme von PNA in Pneumokokken wurde durch die zellpenetrierenden Peptide (cell penetrating peptides, CPPs) (RXR)<sub>4</sub>XB und TAT vermittelt. Mit (RXR)<sub>4</sub>XB-anti-*gyrA* PNA wurde *in vitro* eine vollständige Eradikation von *S. pneumoniae* erreicht. Die Wirksamkeit wurde zudem in einem zellbasierten System mit der menschlichen Pharynxepithelzelllinie Detroit 562 gezeigt. Die Behandlung von infizierten Larven des wirbellosen Modellorganismus *Galleria mellonella* mit CPP-PNAs reduzierte die Pneumokokken-Belastung und steigerte die Überlebensrate.

Es wurde untersucht, ob das Gegenanion Pyrenebutyrinsäure (PB) die Aufnahme von CPP-PNA in Streptokokken *in vitro* verbessern kann. Vorinkubation mit PB erhöhte die Aufnahme von fluoreszenzmarkiertem K8 um das 4.5-fache in *Streptococcus pyogenes* und verbesserte die antibakterielle Wirkung von CPP-PNA in *S. pneumoniae* und *S. pyogenes*. Der Effekt von PB auf die Aufnahme von CPP-Cargo-Konjugaten war bisher nur in Eukaryoten untersucht worden, wobei nur eine Wirkung von PB auf argininreiche CPPs bekannt war. In dieser Arbeit wurde gezeigt, dass PB auch bei Bakterien eingesetzt werden kann, und dort auch die Aufnahme lysinreicher CPP verbessert.

Auswirkungen von CPP-PNA auf das Transkriptom von Streptokokken wurden mit subletalen Konzentrationen über eine längere Inkubationszeit untersucht. Dies führte zu einer geringen transkriptomischen Veränderung. Darunter befanden sich mehrere Gene, die an der Aufnahme und dem Metabolismus von Kohlenhydraten beteiligt sind, sowie Gene, die mit bakteriellen Stressreaktionen in Verbindung gebracht werden. Zukünftige Experimente sollten mit erhöhter CPP-PNA-Konzentration bei reduzierter Behandlungszeit durchgeführt werden, um eine stärkere Änderung des Transkriptoms zu erreichen. Die Daten aus der RNAseq-Analyse können Informationen über Knock-down-Effekte, Off-Target-Effekte, mögliche Resistenzmechanismen und Stressreaktionen gegen CPP-PNA liefern.

Da *G. mellonella* zunehmend als Infektionsmodellorganismus genutzt wird, wurde die *S. pyogenes*-spezifische Immunantwort der Larven mit einem Proteomik-Ansatz untersucht.

Die Immunantwort der Larven zeigte eine relative Spezifität gegen *S. pyogenes*-Infektionen, eine sehr große Ähnlichkeit zu der angeborenen Immunantwort von Säugetieren, sowie eine höhere Komplexität als bislang angenommen. Die Daten qualifizieren den Insektenorganismus als vereinfachtes Modell der angeborenen Immunantwort von Säugetieren und leisten einen wertvollen Beitrag, um den Einsatz von murinen Infektionsmodellen reduzieren zu können.

# 1. Introduction

## 1.1 Streptococcus

The genus *Streptococcus* belongs to the family of *Streptococcaeae* and includes many pathogenic species (Krzyściak et al., 2013). Streptococci are gram-positive cocci forming pairs or chains. They are nonmotile, nonsporeforming, and catalase-, oxidase-, and nitrate-negative (Hossain, 2014). Most streptococcal species, as *S. pneumoniae* and *S. pyogenes*, are aerotolerant (Todar, 2015). Streptococci are chemoorganotrophic, and via their fermentative metabolism of carbohydrates, mainly lactic acid, ethanol, and acetate are produced (Hossain, 2014).

Most commonly, streptococci are classified serologically, and according to their hemolytic phenotype. The Lancefield grouping is based on the presence of polysaccharide and teichoic acid antigens on the cell wall. This classification includes 20 groups (A – V, without I and J), yet some species as *S. pneumoniae*, *S. mutans* and streptococci of the *viridans* group lack such antigens and are categorized independently of the Lancefield grouping (Slater, 2007). According to the hemolytic phenotype on blood agar, streptococci can be divided into  $\alpha$ -,  $\beta$ - and  $\gamma$ -hemolytic.  $\alpha$ -hemolysis describes partial breakdown of red blood cells, as secreted hydrogen peroxide causes oxidization of iron in hemoglobin and the resulting methemoglobin forms a visible green zone on blood agar plates.  $\beta$ -hemolytic streptococci perform complete lysis of the red blood cell, leading to clear zones on blood agar, while  $\gamma$ -hemolytic species do not cause typical lysis, but slight discolouration may occur (Hossain, 2014).

### 1.1.1 General properties and clinical relevance of *Streptococcus pneumoniae*

*Streptococcus pneumoniae*, also known as pneumococcus, is a lancet-shaped diplococcus,  $\alpha$ -hemolytic in the presence of oxygen, optochin-sensitive and lysed by bile. In 2020, 100 serotypes were known, distinguished by their chemically and immunogenically distinct polysaccharide capsule (Centers for Disease Control and Prevention (U.S.), 2021).

The pneumococcus is an obligate human and opportunistic pathogen (Zafar, Wang et al., 2017) responsible for diseases that range from mild mucosal infections as otitis media and sinusitis to more severe diseases such as pneumonia, bacteremia, meningitis, osteomyelitis, and septic arthritis (Centers for Disease Control and Prevention (U.S.), 2021; Thadchanamoorthy and Dayasiri, 2021).

Infections with *S. pneumoniae* can lead to severe clinical outcomes and especially invasive pneumococcal diseases (IPD) are associated with high morbidity and mortality worldwide (Chan et al., 2020). In fact, pneumococci are the most common cause of bacterial pneumonia and the leading contributor to pneumonia-related mortality worldwide (Sattar and Sharma, 2022; World Health Organization, 2021). They are also the most common causative agent of bacterial meningitis in children above one month and in adults (Mańdziuk and Kuchar, 2022). It was estimated in 2009, that pneumococcal disease causes death of up to one million children below the age of five years annually, accountings to 5 – 11 % of deaths in this population (Maimaiti et al., 2013; O'Brien et al., 2009; World Health Organization, 2003, 2007).

Transmission is mediated through respiratory droplets of both, asymptomatic carriers and patients with pneumococcal disease (Donkor, 2013). The opportunistic pathogen resides asymptotically in the upper respiratory tract with typical carriage duration of 2 – 16 weeks. Carriage rates vary among geographical areas, ethnical groups, season (higher in winter and early spring), and age groups, with carriage rates of approximately 20 – 60 % in school kids and 5 – 10 % of healthy adults (Centers for Disease Control and Prevention (U.S.), 2021). Interaction of pneumococci with epithelial cells of the nasopharynx is a prerequisite for the development of an infection. But whether the interaction leads to clearance and specific immunity or to disease is likely to depend on the immune status of the host at the time of colonization and on the virulence of the particular strain (AlonsoDeVelasco et al., 1995; Loughran et al., 2019).

To successfully distribute throughout the body, adapt to niches, and evade the immune response, pneumococcus has distinct mechanisms and virulence factors. Starting from the nasopharynx, pneumococci can ascend the Eustachian tube to reach the middle ears, leading to otitis media, which is especially common in children (Henriques-Normark and Tuomanen, 2013; Loughran et al., 2019). Accession to the lower respiratory tract, by overcoming specific (IgA) and nonspecific defenses (e.g. mucus, cough reflex, ciliary escalator), leads eventually to inflammation of bronchi and alveoli (AlonsoDeVelasco et al., 1995). Especially secretion of hydrogen peroxide and release of the intracellular toxin pneumolysin causes damage of host monolayer and thereby dissemination of pneumococci into the blood stream (Loughran et al., 2019). Pneumococcal bacteremia can develop from pneumococcal pneumonia, but also via other routes. Bacteremia without a known primary focus of the infection is the most common invasive pneumococcal infection in children below the age of two years (Centers for Disease Control and Prevention (U.S.), 2021). From the bloodstream, pneumococci disseminate to

many organs. A common complication of IPD is cardiac dysfunction, with microscopically visible lesions in the myocardium (Brown et al., 2014). After overcoming the blood-brain-barrier, *S. pneumoniae* can infect the meninges. Pneumococcal meningitis is associated with high mortality rates of up to 30 %, and neurological sequelae in up to 50 % of surviving patients (Mook-Kanamori et al., 2011).

The distinctive property of pneumococci to undergo autolysis, which describes the autoinduced disruption of the bacterial cell wall under stationary growth conditions by activation of the enzyme LytA, is among the reasons for success of pneumococci in infection of host and dissemination (Martner et al., 2008). Pneumococcal lysis results in the release of pneumococcal surface components, intracellular toxin pneumolysin, hydrogen peroxide, but also several secreted proteins, triggering multiple inflammation cascades (Loughran et al., 2019). The combination of host damaging effects of pneumococci and the inflammatory host immune response seems to be the cause of high mortality and morbidity of invasive pneumococcal infections (AlonsoDeVelasco et al., 1995).

A successful strategy for preventing pneumococcal infections is vaccination against the serotypes most prevalent in IPD. Two basic types of pneumococcal vaccine are used, the pneumococcal polysaccharide vaccine (PPSV), licensed in 1977, and pneumococcal conjugate vaccine (PCV), used since 2000 (Grabenstein and Klugman, 2012). PPSV-23 contains purified capsular polysaccharides of the 23 most common serotypes causing IPD. It is suitable for adults but poorly immunogenic to children below the age of two years. Furthermore, it does not reduce carriage, and induces a T-cell-independent response. Thus, no booster effect is achieved with repeated administration. In contrast, PCV-7, -10, and -13 protect against 7, 10 and 13 prevalent IPD-causing serotypes, are suitable for infants, reduce asymptomatic carriage and induce immunogenic memory via the T-cell response. Therefore PCV-7 is part of the routine childhood immunization program of most European countries (Roux et al., 2008). Introduction of PCV-7 has dramatically reduced the burden of pneumococcal disease by decreasing the incidence in immunized individuals and also indirectly of the non-immunized population (especially the elderly) via the herd effect (Weinberger et al., 2011). As most of the serotypes covered by PCV-10 and -13 are associated with 90% of the antibiotic-resistant strains responsible for IPD in children, introduction of PCVs led to reduction of non-sensitive serotypes (Klugman and Black, 2018). Nevertheless, following the introduction of PVC-7, non-vaccine serotypes are emerging in asymptomatic carriers and, to a lesser extent, in IPD, in a process called serotype replacement (Weinberger et al., 2011).

IPD are treated with  $\beta$ -lactams, macrolides, and fluoroquinolones, but increasing numbers of antibiotic resistant pneumococci strains are a major global concern (Cillóniz et al., 2018). Drug-resistant *S. pneumoniae* was included on the priority list to guide discovery, research and development of new antibiotics for drug-resistant bacterial infections by the WHO in 2017 (World Health Organization, 2017). Also, the CDC's 2019 Antibiotic Resistance Threats Report scored drug-resistant *S. pneumoniae* as serious threat and estimated, that in more than 30 % of infections in the United States, pneumococci are resistant to one or more antibiotics (Centers for Disease Control and Prevention (U.S.), 2019). This concerning evaluation is consistent with data from other studies, whereby it has to be taken into account that the prevalence of antibiotic resistant pneumococci varies greatly worldwide (Cherazard et al., 2017; Lynch and Zhanel, 2009).

### **1.1.2 General properties and clinical relevance of *Streptococcus pyogenes***

*Streptococcus pyogenes* is an aerotolerant (Todar, 2015),  $\beta$ -hemolytic, and strictly human pathogen. It is the only member of the Lancefield group A and therefore referred to as group A streptococcus (GAS) (Kanwal and Vaitla, 2022).

*S. pyogenes* colonizes asymptotically mostly the nasopharynx, which is also the main site of infection and transmission (LaRock et al., 2020), as well as anus, vagina, skin (DeMuri and Wald, 2014). Transmission is mediated by respiratory droplets and contact with contaminated objects and surfaces (Kanwal and Vaitla, 2022). GAS is a high global burden, as it is a major cause of death and disability, especially in low- and middle-income countries (Sims Sanyahumbi et al., 2016). It causes multiple clinical manifestations ranging from mild and localized infection, such as impetigo, pharyngitis, infection of vaginal and uterine mucosa, muscles and fascia, to severe invasive diseases (Kanwal and Vaitla, 2022). GAS is the leading cause of pharyngitis with more than 600 million incident cases annually (World Health Organization, 2005). A strep throat or streptococcal skin infection can further develop into scarlet fever, when the patient is infected with specific GAS strains producing streptococcal pyrogenic exotoxins (Center for Disease Control and Prevention, 2022; Nelson, 2016).

Invasive diseases, such as bacteremia, the streptococcal toxic shock syndrome (STSS), and type II necrotizing fasciitis, as well as post-infectious sequelae are responsible for the high morbidity and mortality of GAS infections. Untreated GAS infection can develop into acute rheumatic fever, which is especially devastating when it occurs in the heart (rheumatic heart disease, RHD), and post-streptococcal glomerulonephritis (Kanwal and Vaitla, 2022). RHD has a

prevalence of more than 15 million cases and causes annually death of more than 230 000 patients worldwide (Carapetis et al., 2005).

The ability to infect multiple body sites and to cause a wide array of diverse clinical manifestations is achieved by several important virulence factors of GAS. Among them are the capsule and the M protein protecting against phagocytosis (Ashbaugh et al., 2000; Fischetti, 1989), proteins necessary for attachment to host cells, exotoxins (Hallas, 1985), as well as proteins like streptokinase and streptolysin involved in for tissue invasion (Coleman and Benach, 1999; Kanwal and Vaitla, 2022; Khil et al., 2003). Sequencing of the *emm*-gene, encoding the M-Protein, is used for molecular typing. Today more than 200 *emm*-types are known (Smeesters et al., 2009). The M protein is a fimbrial protein with coiled-coil dimer structure, composed of a conserved cell wall-bound C-terminal region, multiple segments with functional attributes, and the characteristically hypervariable N-terminal type-specific segment (Fischetti, 2016; Phillips et al., 1981).

Despite decades of major research efforts, there is still no vaccine available. Among the main reasons are biological, technical and economic impediments (Brouwer et al., 2023; Carapetis et al., 2005). One important problem is the possibility of triggering acute rheumatic fever by unknown autoimmune epitopes of the vaccine (Dale et al., 2016). A further difficulty is the complex epidemiology, partly caused by the geographic strain diversity (Steer et al., 2009). Limitations in the use of animal models arise from the fact that GAS is an exclusively human pathogen (Dale and Walker, 2020). In addition, the development of a vaccine was considered in the past to be not very economically profitable, since severe GAS diseases are more likely to be preventable and less common in high-income countries (Carapetis et al., 2005). The importance of developing a GAS vaccine has now been clearly recognized by key stakeholders (Brouwer et al., 2023). On the global resolution on rheumatic fever and rheumatic heart disease of the WHO in 2018, the development of a GAS vaccine was announced as a priority (World Health Organization, 2018). Further, the efforts are supported by new estimates showing the high financial damage caused by GAS infections, and that the use of an appropriate vaccine could prevent GAS-associated costs of \$1 billion annually in the US alone (Andrejko et al., 2022).

The gold standard of antibiotic treatment for many GAS infections is the  $\beta$ -lactam penicillin. Alternative antibiotics are macrolides and cephalosporins. Clindamycin and vancomycin are used to treat severe infections. Development of resistance is observed in most antibiotics despite penicillin, but to a lesser extent than for most other pathogens (Bisno et al., 2002; Johnson and

LaRock, 2021). However, there are concerning reports of GAS isolates with reduced susceptibility to beta-lactams caused by mutations in penicillin binding proteins (Chochua et al., 2017; Hayes et al., 2020; Musser et al., 2020). The major challenge is not antibiotics resistance development but treatment failure in GAS infection (Johnson and LaRock, 2021). Treatment failure can have several causes, including biofilm formation in which bacteria are protected by the extracellular matrix (Baldassarri et al., 2006), invasion of host cells (Sela et al., 2000), or reduced perfusion of antibiotics through infected tissue (Johnson and LaRock, 2021).  $\beta$ -lactamase producing microbiota protect sensitive bacteria in a mechanisms termed community-mediated resistance (Gjonbalaj et al., 2020). Another problem is penicillin allergy, affecting around 1 % of people (Bhattacharya, 2010). Taken together, there is an urgent need for alternative treatment options.

## **1.2 Carrier-coupled antisense peptide nucleic acids**

One promising approach for alternative treatment options to antibiotics is the application of antisense molecules. Antisense molecules are able to bind complementary nucleic acids and have therefore proven useful for many applications, most notably as a therapeutic approach (Potaczek et al., 2016). Common antisense molecules are antisense oligonucleotides (Askari and McDonnell, 1996), small interfering RNA (siRNA) (Hammond et al., 2000), ribozymes (Rossi, 1995; Tarle and Radoś, 1991), and DNAzymes (Breaker and Joyce, 1994; Chandra et al., 2009). Among them, oligonucleotides are especially simple and easy to design (Temsamani J, 1997). Several chemically modified oligonucleotides as locked nucleic acids (LNAs) (Singh et al., 1998), morpholino compounds (Brakel, 1989), and peptide nucleic acids (PNAs) (Nielsen et al., 1991) have been designed to improve oligonucleotide properties according to their application (Karkare and Bhatnagar, 2006).

### **1.2.1 Peptide nucleic acids (PNAs)**

Peptide nucleic acid (PNA) is a synthetic nucleic acid (NA) derivative that can bind sequence-specific and in a reversible manner to complementary NA (Nielsen and Egholm, 1999). It was invented by P.E. Nielsen (University Copenhagen), M. Egholm (U.C.), R.H. Berg (Risø National Laboratory), and O. Buchardt (U.C.) in 1991 (Nielsen et al., 1991). In the DNA analogue, the deoxyribose phosphodiester backbone is replaced by a pseudo-peptide backbone consisting of N(2-aminoethyl)-glycine units that are linked by amide bonds (Figure 1). The



purine and pyrimidine bases are attached to that polyamide backbone via methylene carbonyl linkages.

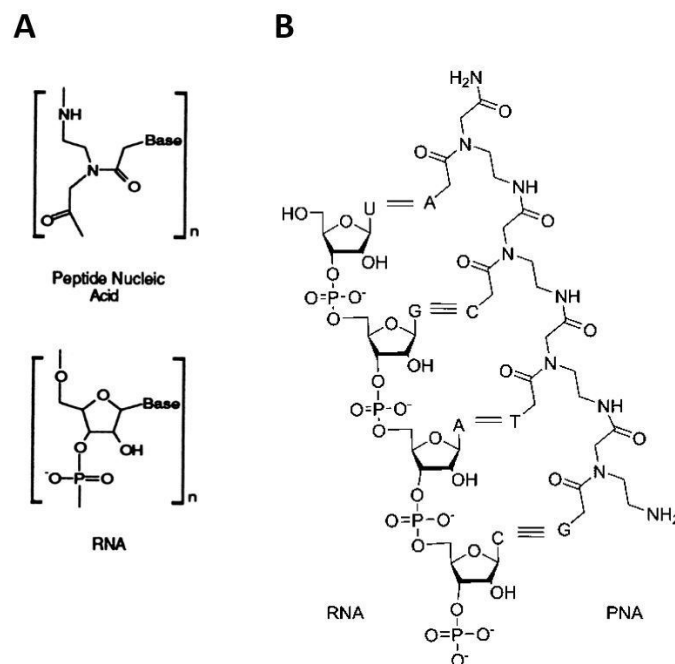


**Figure 1: Chemical structure of PNA.** (A) Comparison of PNA and RNA monomers (Nelson et al., 2000) (modified). (B) Schematic model of base pairing between complementary PNA and RNA molecules (Równicki et al., 2019).

This hybrid molecule has a higher chemical and biological stability compared to DNA. Additionally, PNA bind with higher affinity and specificity to complementary NA. As PNA has no sugar moiety and no phosphate group but a neutral backbone, there is no electrostatic repulsion between the hybrid molecule and complementary NA strands. Therefore, the binding between PNA and NA is stronger, which is reflected in a higher melting temperature of PNA-NA duplexes than of the corresponding NA-NA duplexes. Strong binding also increases specificity, as mismatches result in a greater reduction of melting temperature, which allows enhanced discrimination between fully complementary and mismatched duplexes. Furthermore, PNA binding is independent of the salt concentration (Nielsen and Egholm, 1999), and the molecule is more stable in the acidic pH range (4.5 – 6.5) (Montazersaheb et al., 2018). Due to the unique structure of the hybrid molecule, it is no substrate for neither nucleases nor peptidases, resulting in its high serum stability (Demidov et al., 1994).

The synthetic oligonucleotides can form duplexes with single-stranded NA via Watson-Crick base pairing, and also triplexes that additionally employ Hoogsteen base pairing. Triplexes can be formed by two PNA molecules with a single strand DNA molecule, or by strand invasion of double strand DNA with a PNA molecule. Less relevant are triplex invasion, duplex invasion and double duplex invasion complexes (Nielsen and Egholm, 1999). Due to the ability of PNA to form these complexes, it can be applied to alter gene expression. Sequence-specific PNA-

DNA triplex formation in the coding region of a target gene leads to inhibition of its transcription, making PNA an antigene agent. By forming PNA-mRNA duplexes at the translation initiation region of mRNA, PNA acts as antisense agent preventing the translation of the sequence (Dryselius et al., 2003). Translation inhibition is in contrast to other antisense approaches not achieved by activation of RNase H, but most likely by sterical hindrance as the hybrid-mRNA complex blocks the ribosome (Knudsen and Nielsen, 1996). Furthermore, PNAs are employed in diagnostics and as molecular tool for numerous applications. Due to their exceptional physicochemical properties, they are applied e.g. in PCR reactions for modulation or detection of single base pair mutations, as probes for *fluorescence in situ hybridization* (FISH) and in microarrays, or as biosensors (Singh et al., 2019.).

When antisense PNA is used as antimicrobial agent, the synthetic oligonucleotide is designed complementary to the start region (Bennett and Swayze, 2010; Dryselius et al., 2003) of transcripts of an essential gene. The resulting translational repression leads consequently to the death of the targeted microbe. Using PNA as antibacterial therapeutic offers several advantages. In contrast to antibiotics, the antisense approach enables the selection of any gene for inhibition and therefore allows a free choice of target. Furthermore, this potential therapeutic agent provides species-specificity, due to the choice of the target gene and the sequence variability of a particular gene between different species. Therefore, among other things, the beneficial host microbiome remains unaffected, there is less selective pressure on microbiota for the development of antibiotic resistance, and the consecutive spread of resistance is reduced. Development of resistance to the synthetic oligonucleotide could be responded to by adapting the antisense sequence or choosing a different target gene (Hegarty and Stewart, 2018). Common targets for antisense agents are the genes *acpP* (Good et al., 2001; Rawlings M, Cronan JE Jr., 1992) and *fabI* (Dryselius et al., 2005), essential for fatty acid biosynthesis, genes involved in surface synthesis (Mondhe et al., 2014), genes coding for RNA polymerase subunits necessary for translation (Alajlouni and Seleem, 2013; Bai et al., 2012), and *gyrA*, as the type 2 topoisomerase subunit A is required for DNA replication (Hatamoto et al., 2010; Patenge et al., 2013). The ubiquitous and essential enzyme gyrase is a validated and effective target for antibacterial activity and is inhibited by quinolones and aminocoumarins antibiotics (Collin et al., 2011).

### **1.2.2 Carrier-coupled peptide nucleic acids**

PNAs are hydrophilic macromolecules with a neutral backbone. Thus, cellular uptake is restricted. In bacteria, surface barriers, including the cell wall, cell membrane, and the capsule,

if present, can hamper the translocation of PNA (Good et al., 2000; Good et al., 2001; Good and Nielsen, 1998a, 1998b; Wojciechowska et al., 2020). Various transport systems exist for intracellular delivery of small molecules. Cargos can be taken up via liposomes (Fenske and Cullis, 2005) and nanoparticles with or without different coatings (Chithrani et al., 2010). Further, cargos can be coupled to molecules which are essential for the target cell and are therefore actively taken up (Równicki et al., 2017). A well-studied carrier of various molecules such as proteins and oligonucleotides into cells are cell penetrating peptides (CPPs). In this work, PNAs are coupled to CPPs for intracellular delivery into bacterial cells.

CPPs are short oligopeptides with the ability to penetrate cellular membranes. They typically consist of 5 – 30 amino acids and exhibit high chemical and structural variability (Böhmová et al., 2018). CPPs can be classified on the basis of their origin as synthetic, protein-derived or chimeric. They can also be grouped according to their function e.g. as transcriptomic factor-derived or antimicrobial peptide-derived. Furthermore, these molecules can be distinguished by their uptake mechanism. Most commonly, they are categorized as cationic, amphipathic or hydrophobic based on their physico-chemical properties (Böhmová et al., 2018; Pooga and Langel, 2015).

CPPs can enter lipid bilayers via energy-dependent endocytosis and via energy-independent direct translocation. The main mechanisms of direct translocation rely on pore formation or destabilization of the membrane, whereby the first is described by the barrel-stave model and the toroidal pore model, and the second by the carpet-like model and the inverted micelle formation mechanism (Figure 2) (Böhmová et al., 2018). Depending on the type of CPP, its concentration, the incubation time and temperature, the cargo, and the membrane structure of the respective target cell type, CPPs can switch between different membrane uptake mechanisms (Buccini et al., 2020; El-Andaloussi et al., 2007). As the cellular surface of eukaryotes and prokaryotes, of bacterial species and even of serotypes of a given species differs greatly, the uptake efficacy of different CPPs depends to a great extent on the particular target cell (Abushahba, Mohammad, Thangamani et al., 2016; Barkowsky et al., 2019; Jha et al., 2011).

While PNAs have no toxic effects on cells (Pellestor and Paulasova, 2004), CPPs can be cytotoxic, depending on the target cells. However, coupling of CPPs to a cargo has been shown to reduce toxicity of some CPPs (El-Andaloussi et al., 2007).

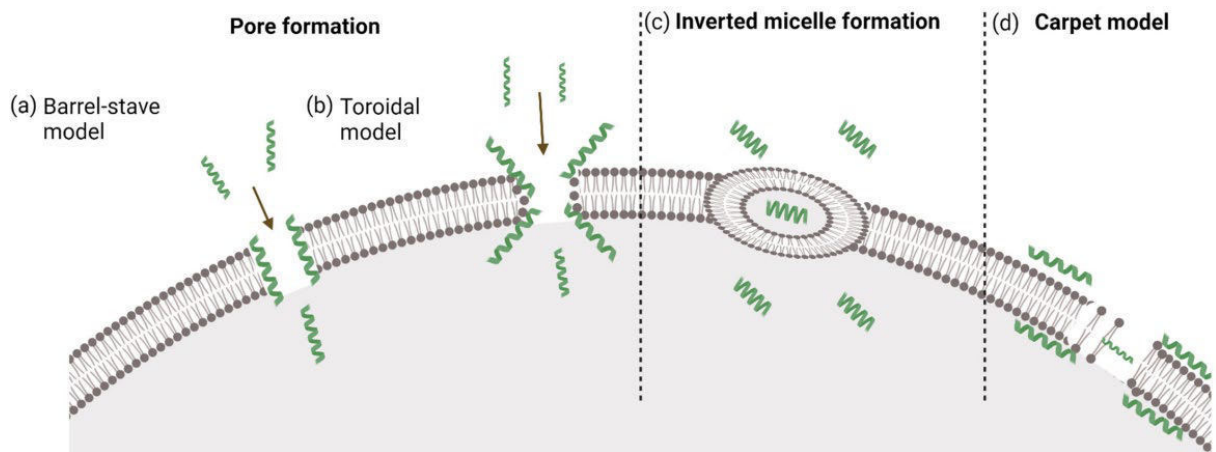


**Figure 2: Models of direct translocation of CPPs (Szabó et al., 2022).** CPPs translocate by formation of pores, inverted micelles, or as described with the carpet model. In pore formation, two models are distinguished: in the barrel-stave model, CPPs interact with the membrane and form a bundle with a channel inside (Shai, 1999; Yang et al., 2001). In the toroidal pore model, CPPs cause bending of the bilayer resulting in pore formation (Hercé et al., 2009). Electrostatic interaction disturbing the membrane structure can cause membrane curvature resulting in formation of inverted micelles with hydrophilic inlayer (Alves et al., 2010). Internalization of CPPs binding electrostatically to membrane in high local concentration is described with the carpet model (Shai, 1999).

### 1.2.3 Pyrenebutyrate as enhancer of antimicrobial activity of CPP-PNA

The costs of *in vitro* experiments using CPP-PNAs to alter gene expression could be reduced by increasing the uptake efficacy of CPP-PNAs, as the amount of conjugate required could be minimized.

Addition of counteranions has been shown to improve uptake of positively charged CPPs, especially oligoarginines, in eukaryotes (Guterstam et al., 2009; Katayama et al., 2013; Takeuchi et al., 2006). A substance that has already been studied for this approach is 4-(1-pyrenyl)-butyric acid, also known as pyrenebutyrate (PB) (Katayama et al., 2013). The pyrene derivate PB is hydrophobic due to its aromatic ring system and negatively charged by its carboxylic group.

Cell fluometry and confocal microscopy demonstrated, that the uptake of oligoarginine-cargo conjugates into various cell lines was increased in the presence of PB (Guterstam et al., 2009; Katayama et al., 2013; Takeuchi et al., 2006). This observation could be confirmed by bioactive cargo delivery experiments (Guterstam et al., 2009; Takeuchi et al., 2006).

The effect of PB was shown to depend on the arginine content of a CPP and to decrease with increasing hydrophobicity of the CPPs (Guterstam et al., 2009). Electrostatic interaction of the negatively charged counteranion with the positively charged oligoarginine is the proposed mechanism by which PB enhances uptake of oligoarginine-cargo conjugates (Katayama et al., 2013; Takeuchi et al., 2006). This interaction results in increased net hydrophobicity of the

CPP, which enhances the potential of the CPP to interact with the lipid bilayer (Futaki et al., 2004), thereby facilitating its translocation (Perret et al., 2005; Takeuchi et al., 2006). Of importance are the guanidinium cations of the arginine residues that are crucial for the translocation of arginine-rich CPPs (Futaki et al., 2001; Umezawa et al., 2002; Wright et al., 2003), and are able to bind tightly to counteranions (Sakai et al., 2003; Sakai et al., 2005; Sakai and Matile, 2003). Guanidinium cations can form bidentate hydrogen bonds and are thought to enable the formation of ion pair complexes with the carboxyl group of PB and with phospholipids of membrane bilayers (Rothbard et al., 2004; Sakai et al., 2005; Sakai and Matile, 2003).

The concentration of PB necessary to increase CPP-cargo uptake into cells did not harm the cellular membrane integrity and was not cytotoxic (Mishra et al., 2009; Sakai et al., 2005). However, the benefit of PB is limited, because it is not effective in the presence of medium or serum. Ionic species in complex solutions compete with the CPP for interaction with PB, thereby reducing the improvement of CPP translocation (Sakai et al., 2005). Therefore, the application of the counterion is limited to *in vitro* experiments in the absence of complex solutions.

Whether PB has an effect on CPP translocation into bacteria is not known. In contrast to mammalian cells, bacteria form structures that provide a barrier to both CPPs and PB. They have a cell wall, which is composed mainly of peptidoglycan. Additionally, many bacteria, such as streptococci, produce a polysaccharide capsule. Moreover, the plasma membrane of bacteria differs from the mammalian cell membrane in its transmembrane potential and lipid composition (Sani et al., 2015). Bacteria have a high proportion of negatively charged phospholipids as cardiolipin and phosphatidylglycerol (Strahl and Errington, 2017), while the mammalian membrane contains mostly neutral lipids as cholesterol, phosphatidylcholine and sphingomyelin (Luchini and Vitiello, 2020).

This work will examine the effect of PB on the antimicrobial effect of CPP-PNA in gram-positive bacterial species.

#### **1.2.4 Off target effects of carrier-coupled PNAs**

Antisense therapeutics act specifically on a target gene. In addition, there are knock-down consequences, i.e. genes that are regulated in response to the reduction of target gene expression. Furthermore, ‘off target’ effects can occur as a result of sequence similarity, binding of CPP-PNA molecules to cellular structures or through defense reactions of the organism to

the CPPs (AMP resistance) (Holgerson et al., 2021; Popella et al., 2021; Popella et al., 2022; Shen, W. et al., 2018; Yoshida et al., 2019).

To gain information about direct and indirect sequence-specific effects and off-target effects of carrier-coupled antisense PNAs, transcriptomic analyses of bacteria after treatment with CPP-PNA can be performed. Cellular responses to the CPP carrier molecule can be elucidated by comparing treatment with CPPs to treatment with CPP-PNA conjugates.

Transcriptome data will provide fundamental information about underlying mechanisms of antisense PNA activity and will support the design of efficient CPP-PNA constructs (Jung et al., 2023). Furthermore, the exact mechanism of PNA on translational inhibition is not clearly understood. PNAs are thought to act in an RNase H-independent manner (Knudsen and Nielsen, 1996) by sterical hindrance of translation initiation due to binding to the start region of the target mRNA (Dryselius et al., 2003). They were shown to affect the steady-state-level of the target mRNA and cause its rapid decay in *Salmonella enterica*, *Escherichia coli*, *Klebsiella pneumoniae*, and *Shigella flexneri* (Bai et al., 2012; Massé et al., 2005; Popella et al., 2021). Nevertheless, the mechanism of target mRNA decay is not yet understood.

CPP and CPP-PNA conjugates are responsible for phenotypic off-target effects arising from their activity on the bacterial surface and general interactions with the cell. Cellular recognition and CPP-PNA-mediated activation of stress pathways and surface homeostasis are dependent on carrier- and cell-type (Popella et al., 2021; Popella et al., 2022). Identification of uptake and response pathways is essential to predict potential resistance mechanisms that might develop, for example, by altering transporter systems (Popella et al., 2021).

In summary, transcriptomic analysis might give information on PNA-mediated mRNA decay, knock-down effects, and ‘off target’ effects. It could allow the identification of intrinsic resistance mechanisms and stress responses, and the detection of differential gene regulation in response to distinct CPPs. So far, the transcriptomic responses of CPP-PNA treatment have only been studied in gram-negative species. In this work could compare the transcriptomic response of two different gram-positive species to CPP-PNA treatment will be compared with each other and with the results from studies in *E. coli* and *S. enterica* (Popella et al., 2021; Popella et al., 2022).

## **1.3 The infection model organism *Galleria mellonella***

### **1.3.1 *Galleria mellonella* as infection model organism**

*Galleria mellonella*, also known as greater wax moth or honeycomb moth, is an insect of the family Pyralidae of the Lepidopteran order. The moth inhabits beehives and is a pest of honeybees feeding on wax and pollen. The holometabolous insect undergoes a complete metamorphosis that includes the egg, larvae, pupa and adult stages. The length of the life cycle depends on biotic factors as nutrition and abiotic factors as temperature. Larval stages last of 6 – 7 weeks, pupation 1 – 8 weeks (Ellis et al., 2013) and the adult life span is 8 - 15 days for females and 21 - 30 days for males (El-Sawaf, 1950). Larvae usually reach a size of 23 mm with a weight of 0.2 g. Female adults have a body size of 15 – 20 mm with 1.6 g, while male adults are smaller and can be further distinguished from females by their lighter colouration (Paddock, 1918).

The larvae of *G. mellonella* are increasingly popular as infection model organisms to study virulence mechanisms and pathogenicity of bacteria and fungi, and to investigate the efficacy of antimicrobial agents (Jorjão et al., 2018; Wojda et al., 2020). Employing the larvae as model organism has several advantages over vertebrate models. For one thing, there fewer ethical concerns associated with their use. For another, in purchase, husbandry, and handling are less expensive. Further, the short life cycle, high availability and easy handling allow large-scale and high throughput experiments that quickly provide statistically relevant data (Wojda et al., 2020).

One main advantage over other commonly used invertebrate models as fruit flies or the nematode *Caenorhabditis elegans* is the option to keep the larvae at 37°C, allowing investigation of pathogens at mammalian body temperature (Jorjão et al., 2018). Drawbacks are the lack of guidelines for handling and treatment conditions, and the absence of stock centers. This results in differing genotypes of larvae, and variation of breeding conditions and maintenance (Tsai et al., 2016). Although the immune system of insects has many similarities to the innate immune system of mammals, they lack adaptive immune responses. Therefore, this infection model cannot be considered as a full alternative to mammalian models, but can serve as pre-screening tool to reduce the number of mammalian experiments required (Tsai et al., 2016).

### 1.3.2 The immune system of *Galleria mellonella*

The immune response of the insect *G. mellonella* has many structural and functional similarities to the innate immune response of vertebrates, and comprises both a cellular and a humoral branch that are tightly interconnected (Pereira et al., 2018). The *G. mellonella* cellular immune response is mediated by hemocytes circulating in the hemolymph and performing the main functions of phagocytosis, encapsulation and clotting of pathogens. The humoral response involves various soluble effector molecules as complement-like proteins, antimicrobial peptides (AMPs), and effectors of the phenol oxidase pathway (Tsai et al., 2016; Wu et al., 2016). The main components of the larval immune system are illustrated in Figure 3.

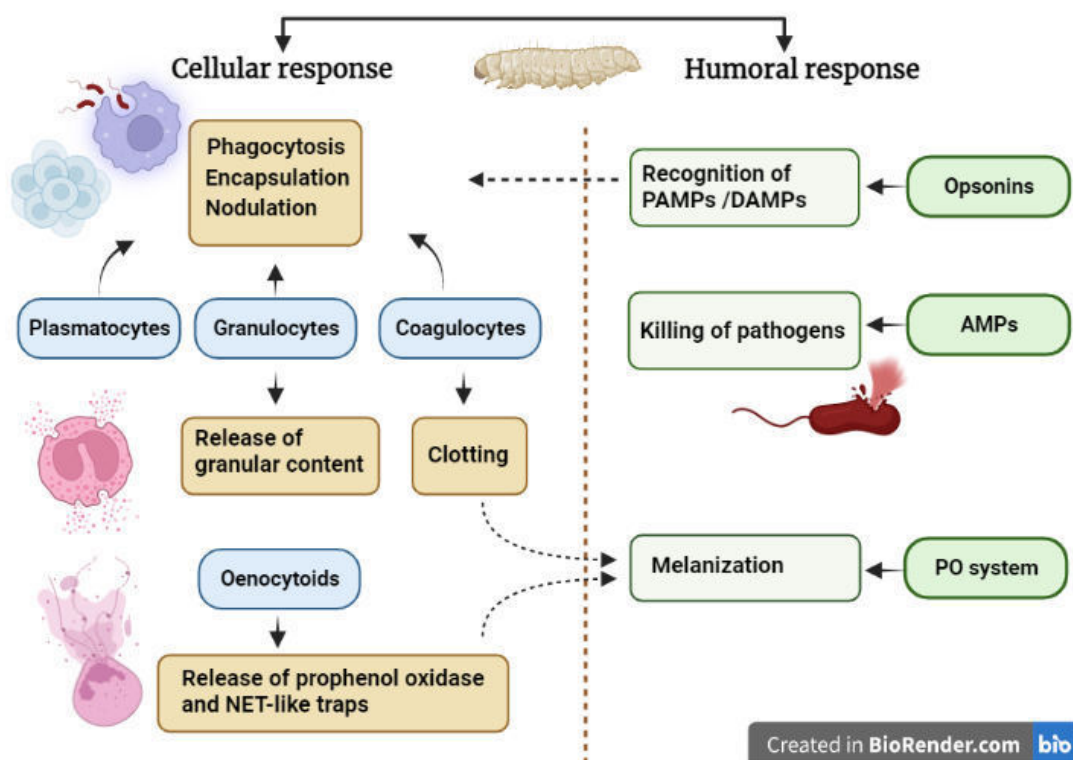


**Figure 3: Main effectors and their function in *G. mellonella* larval immune system.** Hemocytes (blue) and the performed immune responses (yellow), as well as humoral effectors (darker green) and the corresponding processes (lighter green) are illustrated in a schematic diagram. Cellular response: plasmatocytes, granulocytes and coagulocytes perform phagocytosis, encapsulation, and nodulation (Wu et al. 2016; Tojo et al. 2000). Granulocytes release additionally granular content (Pech und Strand 1996). Coagulocytes are involved in the clotting process. Oenocytoids release prophenol oxidase and neutrophil extracellular traps (NETs)-like structures (Eleftherianos und Revenis 2011; Chen und Keddie 2021). Clotting and release of prophenol oxidase contribute to the melanization process (Eleftherianos and Revenis, 2011). Humoral immune response: Opsonins and recognition proteins detect PAMPs and DAMPs (pathogen/damage associated patterns). Antimicrobial peptides (AMPs) kill pathogens and activation of phenol oxidase system results in melanization (Tsai et al. 2016). The schematic diagram was generated with BioRender.com and is based on Ménard et al. 2021.

*G. mellonella* has four types of hemocytes: plasmatocytes, granulocytes, oenocytoids, and spherulocytes (Wu et al., 2016). Additionally, stem cell-like prohemocytes are present (Wu et al., 2016). Plasmatocytes and granulocytes are the most numerous and, like oenocytoids, act as phagocytes (Tojo et al., 2000; Wu et al., 2016). Phagocytosis of insects is similar to that of



mammals in terms of recognition, internalization mechanism, and killing. The latter is mediated by reactive oxygen species of the oxygen burst generated by the NADPH oxidase mechanism, as performed by neutrophils (Tsai et al., 2016; Wu et al., 2016).

Granulocytes attach to large microbes such as protozoa and nematodes in a process called encapsulation. The release of material from their granules promotes attachment of plasmatocytes leading to the formation of a smooth capsule consisting of multiple cellular layers (Pech and Strand, 1996). During nodule formation, several hemocytes form an overlapping shield to entrap and remove high numbers of bacteria from the hemolymph. Eventually, upon activation of the phenol oxidase pathway the cellular aggregates become melanised (Lavine and Strand, 2002; Tsai et al., 2016).

The phenol oxidase system is responsible for synthesis and deposition of melanin during wound healing and around invading microbes during infection. Oenocytes and granulocytes release the proenzyme prophenol oxidase, which after cleavage to active phenol oxidase, catalyses the synthesis of melanin (Eleftherianos and Revenis, 2011; Wojda et al., 2020). Coagulation and opsonization is analogous to abscess formation in mammals (Tang, 2009).

Important humoral effectors are opsonins, which are complement-like proteins. These multifunctional plasma proteins are involved in recognition and binding to conserved microbial components (Tsai et al., 2016). Common opsonins of *G. mellonella* are peptidoglycan recognition proteins (PGRPs), cationic protein 8 (GmCP8), and Apolipoprotein III (apoLp-III). ApoLp-III has a strong affinity to the bacterial cell wall components lipopolysaccharide (LPS) and lipoteichoic acid (LTA) and is highly homologous to human apolipoprotein E (Halwani et al., 2000; Pratt and Weers, 2004). Recognition of foreign material activates the signalling cascades Toll and immune deficiency (IMD), which both result mostly in expression of antimicrobial peptides (Sheehan, Garvey et al., 2018; Tanji et al., 2007).

The larvae synthesize a broad spectrum of antimicrobial peptides like moricins and cecropins, that act by forming cytoplasmic pores resulting in ion leakage from targeted bacteria, and enzymes like lysozyme, which degrades the peptidoglycan of the bacterial cell wall (Dai et al., 2008; Efimova et al., 2014; Tsai et al., 2016).

Within the framework of the principles of replacement, reduction and refinement (3R) (European Medicines Agency, 2016), *G. mellonella* larvae are increasingly used as infection and therapy model organism for the investigation of pathogenic bacteria and fungi. In order to more reliably transfer experimental data from the invertebrate animal model to other model

organisms or the human host in the future, further characterization of the model is necessary. One possible approach is the detailed investigation of the specific immune response of the larvae to infection with *S. pyogenes* using proteomic analyses.

## **1.4 Aim of this work**

In this work, effective CPP-PNAs will be identified for *Streptococcus pneumoniae*. To achieve this aim, screening for effective carrier-systems and testing suitability of potential PNA targets, proving target specificity, and evaluating CPP-PNA conjugates as therapeutic agents using an invertebrate model organism will be performed.

The effect of application of the counteranion pyrenebutyrate on CPP-PNA translocation will be examined in the gram-positive bacterial species *Streptococcus pyogenes* and *S. pneumoniae in vitro*.

To determine potential off-target effects, to distinguish between PNA-sequence specific and CPP-mediated effects, and to identify species-specific responses, transcriptomic analyses of CPP-PNA treated *S. pyogenes* and *S. pneumoniae* will be performed in cooperation with Prof. Dr. Jörg Vogel (Helmholtz Institute for RNA-based Infection Research, Würzburg).

The larvae of the invertebrate infection model organism *Galleria mellonella* become increasingly popular as invertebrate infection model organism for the investigation of antimicrobial agents. The immune response is being investigated for transferability to mammals and especially humans. For this purpose, a proteomic analysis of *S. pyogenes*-infected and non-infected larvae is carried out at different time points.

## 2. Materials and Methods

### 2.1 Materials

**Table 1: Chemicals and enzymes**

<b>Chemicals and enzymes</b>	<b>Manufacturer</b>
Accutase™ Solution	Merck KGaA, Darmstadt, GE
Acetic acid	AppliChem GmbH, Darmstadt, GE
Agar	Oxoid Ltd., Basingstoke, UK
Agarose Standard	Carl Roth GmbH & Co. KG, Karlsruhe, GE
Ampuwa®	Fresenius Kabi, Bad Homburg, GE
Brain heart infusion broth	Oxoid Ltd., Basingstoke, UK
Brewers yeast	Makana Produktion u. Vertrieb GmbH, Offenbach, GE
Chloroform	Merck KGaA, Darmstadt, GE
Columbia Agar with 5 % Sheep blood	BD, Maryland, USA
Columbia CNA Agar with 5 % Sheep Blood	BD, Maryland, USA
Crystal violet	Merck KGaA, Darmstadt, GE
Cuvettes 10 x 4 x 45 mm	Sarstedt, Nümbrecht, DE
Diethyl pyrocarbonate	Sigma-Aldrich, St. Louis, USA
Dimethyl sulfoxide (DMSO)	Thermo Fisher Scientific, Waltham, USA
Dinatriumhydrogenphosphat	Carl Roth GmbH & Co. KG, Karlsruhe, GE
DMEM (Dulbecco's Modified Eagle Medium) F-12 Nutrient Mix with 10 % FKS	GIBCO, Life Technologies, Paisley, UK
DNA Loading Dye (6 x)	Thermo Fisher Scientific, Waltham, USA
dNTP Mix	Thermo Fisher Scientific, Waltham, USA
Ethanol	Walter CMP, Kiel, DE
Ethidium bromide (1 % [w/v] in H <sub>2</sub> O)	Carl Roth GmbH & Co. KG, Karlsruhe, GE
Ethylenediaminetetraacetic acid (EDTA)	Merck KGaA, Darmstadt, GE
GeneRuler 1 kb DNA-Ladder	Thermo Fisher Scientific, Waltham, USA
Glucose	Oxoid Ltd., Basingstoke, UK
Glycerol (99 %)	Carl Roth GmbH & Co. KG, Karlsruhe, GE
Glycogen (20 mg/ml)	Thermo Scientific™
Honey	Alnatura GmbH, Darmstadt, GE
Maxima SYBR Green/ROX qPCR Master Mix	Thermo Fisher Scientific, Waltham, USA
Milk powder	Sucofin, Zeven, GE
Monopotassium phosphate	J. T. Baker, Deventer, NL
N-Phenylthiourea	Merck KGaA, Darmstadt, GE
Oatmeal	Bauck GmbH, Rosche, GE
Oligonucleotides (primer)	Eurogentec Germany GmbH, Cologne, GE
PCR Reaction buffer (10 x)	QIAGEN GmbH, Hilden, GE
Phenol:Chloroform:Isoamylalcohol (25:24:1, v/v) (UltraPure™)	Invitrogen, Waltham, USA
Pierce™ Coomassie (Bradford) Protein-Assay-K	Thermo Fisher Scientific, Waltham, USA
Polyiosinic acid potassium salt	Sigma-Aldrich, St. Louis, USA
Potassium chloride	J. T. Baker, Deventer, NL
Sodium acetate (2 M)	Merck KGaA, Darmstadt, GE
Sodium chloride	Roth, Karlsruhe, GE
TAE Puffer (50 x)	Carl Roth GmbH & Co. KG, Karlsruhe, GE
Taq DNA Polymerase	QIAGEN GmbH, Hilden, GE
Todd Hewitt Broth	Oxoid Ltd., Basingstoke, UK

**Table 1: Chemicals and enzymes (continued)**

<b>Chemicals and enzymes</b>	<b>Manufacturer</b>
Tris(hydroxymethyl)aminomethane (TRIS)	Merck KGaA, Darmstadt, GE
Trisodium citrate	Merck KGaA, Darmstadt, GE
TRIzol™	Invitrogen, Waltham, USA
Wheat Bran	Futterhandel Frank Butter, Döbern, GE
Yeast extrakt	Oxoid Ltd., Basingstoke, UK

**Table 2: Consumable supplies**

<b>Consumable supplies</b>	<b>Manufacturer</b>
Cell culture 96 well plate (flat bottom)	Greiner Bio-One, Kremsmünster, AUT
Cell culture flask (75 cm <sup>2</sup> )	Greiner Bio-One, Kremsmünster, AUT
Cuvettes (10 x 4 x 45 mm)	Sartstedt, Nümbrecht, GE
Disinfectants BacilloI® AF	Bode Chemie, Hamburg, GE
Disposable Inoculation Loops (10 µl, 1 µl)	Greiner Bio-One, Kremsmünster, AUT
Falcon (15 ml, 50 ml)	Sarstedt, Nümbrecht, GE
Glass beads (0.10 - 0.11 mm)	Sartorius, Gottingen, GE
Grinding balls/ plastic beads (0.5 cm)	QIAGEN GmbH, Hilden, GE
MicroAmp® Fast 96-Well Reaction Plate	Thermo Fisher Scientific, Waltham, USA
Micro-Screwcaps 2 ml	Sartstedt, Nümbrecht, GE
Omnican®-F Fine dosing syringes with integrated cannula, 0.01 - 1 ml, 0.30 x 12 mm	B.Braun, Melsunge, GE
PCR Soft tubes (0.2 ml)	Biozym, Hessisch Oldendorf, GE
Petri discs	Sartstedt, Nümbrecht, GE
Pipette tips (10, 20, 100, 200, 1000 µl)	Sartstedt, Nümbrecht, GE
RNA Nano Chips	Agilent Technologies, Inc. Santa Clara, USA
Screw tubes (2 ml)	Sartstedt, Nümbrecht, GE
Serological Pipettetips (5 - 25 ml)	Sartstedt, Nümbrecht, GE

**Table 3: Devices**

<b>Devices</b>	<b>Manufacturer</b>
Agilent Bioanalyzer	Agilent Technologies, Inc. Santa Clara, USA
Analytical balance Type BP4100S	Sartorius, Göttingen, GE
Biological safety cabinet class II	Thermo Fisher Scientific, Waltham, USA
CO <sub>2</sub> -Incubator CB160	Binder, Tuttlingen, GE
Freezer Comfort – 20 °C	Liebherr, Switzerland, CH
LightCycler 480 b	Roche, Switzerland, CH
Microapplicator	World Precision Instruments, Sarasota, USA
Microscope CKX41	Olympus Deutschland GmbH, Hamburg, GE
Pipette (10 µl- 1000 µl)	Eppendorf, Hamburg, GE
Refrigerated centrifuge Type 5417R	Eppendorf, Hamburg, GE
Precellys 24 Tissue Homogenizer	Bertin Instruments, Montigny-le-Bretonneux, FR
Spectrophotometer SmartSpec™ 3000	Bio-Rad-Laboratories GmbH, Munich, GE
Stuart Tube Rotator SB3	Antylia Scientific, Vernon Hills, USA
ThermoMixer compact	Eppendorf, Hamburg, GE
VersaMax ELISA Microplate Reader	Molecular Devices, LCC, USA
Vortex-Genie Touch Mixer	Scientific Industries, Bohemia, NY, USA
Biometra Tpersonal Thermocycler	Analytik Jena, Jena, GE
UVP GelStudio	Analytik Jena, Jena, GE

**Table 3: Devices (continued)**

Devices	Manufacturer
IKA® VORTEX 3 (Vortex)	Sigma-Aldrich, St. Louis, USA
BP 41005 balance	Sartorius, Göttingen, GE

**Table 4: Bacterial strains**

Bacterial strain	Serotype	Strain number <sup>1</sup>	Origin
<i>Streptococcus pyogenes</i> 591	M49	4649	Skin isolate, provided by R. Lütticken (Aachen, Germany)
<i>Streptococcus pneumoniae</i> TIGR4 BAA-334	4	5095	Blood isolate (Tettelin et al., 2001)
<i>Streptococcus pneumoniae</i> 19F	19F	3724	Robert Koch Institute 704
<i>Streptococcus pneumoniae</i> D39 NCTC 7466	2	4995	not recorded; provided by Dr Siemens (Greifswald, Germany)

<sup>1</sup>Strain collection IMIKRO, Rostock**Table 5: Cell line**

Cell line	Morphology and tissue	Origin
Detroit 562 (ATCC CCL138)	Human epithelial cells from the pharynx	Pharynx of a pharyngeal cancer patient (female)

**Table 6: Antibiotic**

Antibiotic	Solvent	Manufacturer
Levofloxacin	DMSO	Sigma-Aldrich, St Louis, USA
Liofilchem® MTS™ gradient test, Levofloxacin	-	Liofilchem, Roseto degli Abruzzi, Italy

**Table 7: Oligonucleotides**

Oligonucleotides	Sequence
<i>S. pneumoniae_gyraseA_fwd</i>	CTGAGTATGACCTCTTGGC
<i>S. pneumoniae_gyraseA_rev</i>	CCAATCAACTCTGTACGGC
<i>S. pneumoniae_rpoB_fwd</i>	GGACCATACTCAACTGTTACCC
<i>S. pneumoniae_rpoB_rev</i>	TCCATTCCTTCATCCAAGTCGC
<i>S. pneumoniae_5S_fwd</i>	CGATAGCCTAGGAGATACACC
<i>S. pneumoniae_5S_rev</i>	GGGCTTAACTTCTGTGTT-GG
<i>S. pneumoniae_ply_fwd</i>	TTCCGCACTAGTGGCAAATCGG
<i>S. pneumoniae_ply_rev</i>	CTTTACAG AGATCATCCAGGC
<i>S. pneumoniae_pspA_fwd</i>	TTCCTGAACCAAATGCGTTGGC
<i>S. pneumoniae_pspA_rev</i>	GTCTTACCTTCAGGATCAAGGC
<i>S. pyogenes_allM_fwd</i>	ATAAGGAGCATAAAAATGGCT
<i>S. pyogenes_allM_rev</i>	AGCTTAGTTTTCTTCTTTGCG

**Table 8: Kits**

<b>Kit</b>	<b>Manufacturer</b>
Agilent RNA 6000 Nano Kit	Agilent Technologies, Santa Clara, USA
Coomassie (Bradford) Protein-Assay-Kit	Thermo Fisher Scientific, Waltham, USA
CyQUANT™ LDH Zytotoxizitäts-Assay	Invitrogen, Waltham, USA
DNeasy® Blood & Tissue Kit	QIAGEN GmbH, Hilden, DE
FastRNA™ Pro Blue Kit	MP Biomedicals, Eschwege, GE
Qubit™ RNA Broad range (BR) Assay Kit	Invitrogen, Waltham, USA
RNA Clean & Concentrator™-5 kit	Zymo Research, Irvine, USA
SuperScript™ First-Strand Synthesis System for RT-PCR	Life Technologies, Carlsbad, USA
TURBO DNA-free™ Kit	Life Technologies, Carlsbad, USA

**Table 9: Software**

<b>Software</b>	<b>Manufacturer</b>
GraphPad Prism 8	GraphPad Software Inc., USA
Microsoft Office	Microsoft, USA
Progenesis QI for Proteomics	Nonlinear Dynamics, Newcastle upon Tyne, UK
SoftMax Pro 6.2	Moecular Devices, LCC, USA
VisionWorks (for UVP GelStudio)	Analytic Jena, Jena, GE

**Table 10: Sequences of PNAs**

<b>PNAs specific for <i>S. pneumoniae</i></b>	
Anti- <i>gyrA</i> PNA	tgcattaata
Scr (anti- <i>gyrA</i> ) PNA	aatgattact
Anti- <i>rpoB</i> PNA	ctgccaagatga
Scr (anti- <i>rpoB</i> ) PNA	cgtagtccaaag
<b>PNAs specific for <i>S. pyogenes</i></b>	
Anti- <i>gyrA</i> PNA	tgcatttaag
Scr (anti- <i>gyrA</i> ) PNA	attagactgt

Antisense PNAs were designed complementary target gene position - 5 to 5 bp and hybridize to the translation initiation region of the target mRNA.

**Table 11: Sequences of the peptide carriers used in this work**

<b>Carrier</b>	<b>Sequence</b>	<b>Reference</b>
(KFF)3K	KFFKFFKFFK	(Iubatti et al., 2022; Popella et al., 2022; Yavari et al., 2021)
(RFR)4XB	RFRRFRFRFRXRB	(Abushahba, Mohammad, Thangamani et al., 2016)
(RXR)4XB	R-Ahx-RR-Ahx-RR-Ahx-RR-Ahx-R-Ahx-bA	(Abes et al., 2008)
AB2	YARVRRRGPRGYARVRRRGPRR	(Wesolowski et al., 2011)
AmiA-ligand	AKTIKITQTR	(Nasher et al., 2018)
Bac7(15-24)	PRPLPFPRPG	(Sadler et al., 2002)
BUF 5 - 19	RAGLQFPVGRVHRL	(Park et al., 2000)
CADY	GLWRALWRLLRSLWRLWRA	(Konate et al., 2010)

**Table 11: Sequences of the peptide carriers used in this work (continued)**

Carrier	Sequence	Reference
gH625-MK	HGLASTLTRWAHYNALIRAFGCGKKKK	(Falanga et al., 2017)
gH625-MR	HGLASTLTRWAHYNALIRAFGCGRRRR	(Falanga et al., 2017)
HIV-1Rev	TRQARRNRRRRWRERQR	(Oikawa et al., 2018)
K8	KKKKKKKK	(Mitchell et al., 2000)
pANTpHD	RQIKIWFNRRMKWKK	(Derossi et al., 1994; Numata et al., 2018; Oikawa et al., 2018)
PDESTK	PDESTK	(Roth et al., 1998)
PenArg	RQIRIWFQNRRMRWRR	(Derossi et al., 1994; Hansen et al., 2008)
pVec (truncated)	RRRIRKQAHASK	(Alaybeyoglu et al., 2018)
R9	RRRRRRRRR	(Allolio et al., 2018)
R9-TAT	GRRRRRRRRPPQ	(Futaki et al., 2001; Oikawa et al., 2018)
RSV-A9	RRIPNRRPRR	(Kersemans et al., 2008; Wolfe et al., 2018)
SARS-CoV-2 (predicted seq.)	KKSAEASKKPRQKRTATKAY	(Kardani and Bolhassani, 2021)
Sc18	GLRKRLRKFRNKIKEK	(Hoyer et al., 2012)
SynB3	RRLSYSRRRF	(Drin et al., 2003)
TAT	GRKKRRQRRRYK	(Green and Loewenstein, 1988; Vivès et al., 1997)
TLM	PLSSIFSRIGDP	(Manceur et al., 2007)
TP10	AGYLLGKINLKALAALAKKIL	(Arrighi et al., 2008; Ruczyński et al., 2019)

## 2.2 Methods

### 2.2.1 Media and buffer preparation

DEPC-H<sub>2</sub>O, culture media, and 10 x PBS buffer were sterilized in an autoclave for 20 min at 121°C and 1 bar over pressure. For preparation of solid media, 1.5 % agar was added to broth media and poured in petri dishes after sterilization.

**Table 12: Composition of DEPC-H<sub>2</sub>O, media, and 10x PBS buffer**

Diethylpyrocarbonate-H <sub>2</sub> O (DEPC-H <sub>2</sub> O)	500 ml ultrapure water 500 µl Diethylpyrocarbonate (DEPC) Incubated o/n, 37°C
BHI medium	37 g Brain-Heart-Infusion Ad 1 l ultrapure water
THY medium	36.4 g Todd Hewitt Broth 4.5 g Yest extract Ad 1 l ultrapure water
10 x Phosphate Buffered Saline (PBS)	2.00 g Potassium Chloride (KCl) 0.27 g Potassium hydrogen phosphate (KH <sub>2</sub> PO <sub>4</sub> ) 80.01 g Sodium Chloride (NaCl) 14.20 g Disodiumhydrogenphosphate (Na <sub>2</sub> HPO <sub>4</sub> ) Ad 1000 ml ultrapure water Adjustment of the pH to 7.4

## **2.2.2 CPP-PNA handling**

The peptide nucleic acids (PNAs) were synthesized, linked covalently to cell-penetrating peptides (CPPs) via ethylene glycol linkers (8-amino-3,6-Dioxaoctan acid), and purified by HPLC at Peps4LS GmbH, Heidelberg. The PNA sequences used in this work are shown in Table 10, the CPP sequences are listed in Table 11.

To prepare 1 mM CPP-PNA stocks, lyophilized CPP-PNAs were reconstituted in the appropriate volume of sterile molecular biology grade water and allowed to swell for 10 min. The samples were vortexed, centrifuged and then heated to 60°C for at least 10 min. Afterwards, they were vortexed, centrifuged and incubated at 4°C for at least two days to achieve complete dissolution. CPP-PNAs were stored at 4°C and heated before use to 60°C for 10 min.

## **2.2.3 Bacterial maintenance**

### **2.2.3.1 Bacterial cultures**

*Streptococcus pyogenes* and *Streptococcus pneumoniae* were cultured by transferring a single colony from Columbia agar with 5 % sheep blood to 10 ml THY medium and incubated at 37°C under a 5 % CO<sub>2</sub> atmosphere. *S. pyogenes* cultures were incubated for a maximum of 16 hours, *S. pneumoniae* cultures for a maximum of 5 h.

### **2.2.3.2 Storage of bacteria**

700 µl of bacterial culture was mixed with 300 µl sterile glycerol, shock frozen using liquid nitrogen, and stored at -80°C for long term, or -20°C for short term storage (up to three months).

### **2.2.3.3 Determination of the number of colony forming units (CFU)**

For determination of colony count, samples were serially diluted in PBS and plated on THY agar plates. After incubation at 37°C overnight, the colonies were counted and the number of CFU/ml was determined.

## **2.2.4 Determination of the antimicrobial activity**

*S. pneumoniae* or *S. pyogenes* cultures were diluted 1:1000 in PBS with 5 % THY or with 20 % BHI medium, respectively, to approximately 10<sup>5</sup> CFU/ml. 450 µl of bacterial suspension were mixed with 50 µl antimicrobial substance (CPP, CPP-PNA, or antibiotics). Ampuwa® served as mock control. Samples were incubated in 2 ml reaction tubes for 6 h at 37°C and 7 rpm (Rotor SB3). Afterwards, the CFU was determined.

When determining the effect of pyrenebutyrate (PB) on the antimicrobial activity of CPP-PNA, cultures of *S. pneumoniae* or *S. pyogenes* were diluted as described above. 400 µl of the bacterial suspension was preincubated with 50 µl PB or PBS (mock control) for 10 min at 37°C



in 2 ml reaction tubes. Then 50 µl of CPP-PNA or Ampuwa® (mock control) were added and the samples were incubated for 6 h at 37°C and 7 rpm (Rotor SB3). Afterwards, the number of CFU/ml was determined.

## **2.2.5 Determination of uptake of fluorescently labeled carrier into**

### ***S. pyogenes***

An overnight culture of *S. pyogenes* was diluted 1:20 in THY and grown to an optical density of OD<sub>600</sub> = 0.5. After 1:100 dilution in PBS, 400 µl of bacterial culture were pre-incubated with 50 µl PB for 10 min at 37°C. Then 50 µl K8-FITC was added and incubated for 30 min at 37° C. Final concentration of PB: 100 µM; of K8-FITC: 10 µM. The bacterial suspension was centrifuged (4500 g, 5 min), washed with PBS, and centrifuged again. The bacterial pellet was lysed with the lysisbuffer of the DNeasy Blood & Tissue Kit (Qiagen) for 120 min at 37°C. After centrifugation, the supernatant was transferred to a microplate and the fluorescence intensity at 490 nm was measured with a microplate reader.

## **2.2.6 Determination of relative gene expression**

### **2.2.6.1 Treatment of *S. pneumoniae* with CPP-PNA**

A 4 h culture of *S. pneumoniae* was diluted 1:200 in BHI medium. Aliquots of 450 µl bacterial suspension were mixed with either 50 µl of CPP-PNA or Ampuwa® (mock control) and incubated in 2 ml reaction tubes for 5 h at 37°C, 7 rpm. *S. pneumoniae* was treated with 7.5 µM (RXR)<sub>4</sub>XB- and TAT-anti-*gyrA* PNA or 10 µM (RXR)<sub>4</sub>XB- and TAT-*rpoB* PNA. Per treatment condition, five aliquots were centrifuged (13 000 g, 10 min, 4°C), washed with ice cold PBS, pooled, and centrifuged again. The pellets were frozen via liquid nitrogen and stored at - 80°C.

### **2.2.6.2 Isolation of RNA from CPP-PNA treated *S. pneumoniae***

3 µl polyinosinic acid (10 mg/ml) were added to the bacterial pellet on ice and after 10 min, the pellets were suspended in 1 ml TRIzol™ and incubated for 3 min on ice. The suspension was transferred to a 2 ml screw cap tube and ribolyzed at 6500 rpm for 30 sec with a homogenizer. 200 µl chloroform were added, the samples were vortexed for 1 min, incubated for 3 min at RT, and centrifuged at 13 000 g for 15 min at 4°C. The upper aqueous phase was transferred to a fresh 2 ml reaction tube and again 200 µl chloroform were added, vortexed and centrifuged. The upper aqueous phase was transferred to a fresh 2 ml reaction tube and 5 µl glycogen (20 mg/ml) was added. After inversion, 500 µl isopropanol was added and the mixture was inverted 20 times. The sample was incubated for 30 min at RT and then centrifuged (13 000 g, 15 min, 4°C). After removal of the supernatant, 1 ml 75 % ethanol was added, centrifuged (13 000 g, 10 min, 4°C), and the supernatant was carefully removed without disturbance of the

pellet. After repetition of the ethanol wash, the pellet was dried on ice for 15 min, then 200  $\mu$ l of DEPC-H<sub>2</sub>O were added and the solution was heated for 10 min at 60°C. 800  $\mu$ l of phenol:chloroform:isoamylalcohol (25:24:1, v/v) and 20  $\mu$ l of 2 M sodium acetate were added, mixed, and transferred to a 2 ml screw cap tube. The mixture was ribolysed two times at 4000 rpm for 10 sec, incubated for 5 min at RT and then centrifuged (7600 g, 5 min, 4°C). The upper aqueous phase was transferred to a fresh 2 ml screw cap tube and the washing step with phenol:chloroform:isoamylalcohol (25:24:1, v/v) and sodium acetate was repeated two times. The upper aqueous phase was then transferred into a 2 ml reaction tube, 1 ml of 100 % ethanol was added, inverted 10 x and frozen at -10°C for two days to allow precipitation of the RNA. The sample was centrifuged (13 000 g, 1 h, 4°C) and the supernatant was removed. The pellet was washed with 1 ml 75 % ethanol and then dried for 30 min on ice. After addition of 25  $\mu$ l DEPC-H<sub>2</sub>O to the RNA pellet, the sample was heated for 10 min at 60°C.

#### **2.2.6.3 Cleaning of RNA and determination of quantity and quality**

After isolation of RNA, remaining DNA was removed using TURBO DNA-free™ Kit (Life Technologies) according to the manufacturer's manual. The incubation time was increased to 3 h. Afterwards, RNA samples were cleaned using RNA Clean & Concentrator™-5 kit (Zymogen Research).

For determination of the RNA quantity, the Qubit™ RNA Broad Range (BR) Assay kit (Invitrogen™) was used according to the manufacturer's protocol. The RNA quality was controlled with the Agilent RNA 6000 Nano Kit (Agilent Technologies).

#### **2.2.6.4 cDNA Synthesis**

cDNA was synthesized of template RNA using the SuperScript™ First-Strand Synthesis System for RT-PCR (Life Technologies) according to manufacturer's protocol (per reaction mixture 250 ng template RNA was used). The cDNA synthesis was carried out in a thermocycler with the following steps: Annealing phase at 25°C for 25 min, synthesis phase at 37°C for 30 min, heat inactivation of enzyme at 85°C for 1 min. Afterwards, samples were cooled for 10 min on ice and then RNA was digested with RNase H (provided in the kit) for 20 min at 37°C.

#### **2.2.6.5 Quantitative PCR (qPCR)**

Quantitative PCR (qPCR) was performed in MicroAmp® Fast 96-Well reaction plates. cDNA was diluted in DEPC-H<sub>2</sub>O and 4  $\mu$ l diluted cDNA and 16  $\mu$ l mastermix (Table 13) were added per well. The reaction was performed with the LightCycler 480 b (Roche) with the steps listed in Table 14.

**Table 13: Mastermix for qPCR, per sample**

Component	Amount
2 x Maxima SYBR™ Green	10 µl
Primer forward (1 mM)	1.5 µl
Primer reverse (1 mM)	1.5 µl
DEPC-H <sub>2</sub> O	3 µl

**Table 14: Amplification program for qPCR**

Step	Temperature	Time
<b>Initial Denaturation</b>	95°C	5 min
<b>40 x Cycles</b>	95°C	20 sec
	60°C	15 sec
	72°C	20 sec
<b>Cooling</b>	40°C	30 sec

## 2.2.7 Transcriptomic analysis

### 2.2.7.1 Treatment of streptococci with CPP-PNA

4 h cultures of *S. pneumoniae* was diluted 1:200 in in THY medium. *S. pyogenes* overnight culture was diluted 1:1000 in THY medium. Aliquots of 450 µl diluted bacteria (~ 10<sup>6</sup> CFU/ml) were incubated with 50 µl of the compound of interest (CPP-PNA, CPP-scrPNA, CPP, or Ampuwa® (mock control)). *S. pneumoniae* was incubated with 7.5 µM CPP-PNA or CPP, respectively, for 5 h at 37°C at 7 rpm. *S. pyogenes* was treated with 4 µM CPP-PNA or CPP, respectively, for 6 h at 37°C, 7 rpm. After incubation, seven aliquots of *S. pneumoniae* or five aliquots of *S. pyogenes* per treatment condition were centrifuged (13 000 g, 10 min, 4°C), washed with cold PBS, and pooled. The samples were centrifuged again, the supernatant was removed, and the pellets were frozen in liquid nitrogen and stored at -80°C.

### 2.2.7.2 RNA isolation

RNA was isolated from bacterial pellets after treatment with the FastRNA™ Pro Blue Kit (MP Biomedicals) according to the manufacturer's manual. To enhance lysis of bacteria prior to RNA isolation, *S. pneumoniae* pellets were treated with 6 µl polyiosinic acid (10 mg/ml) and *S. pyogenes* pellets with 3 µl, respectively.

### 2.2.7.3 Cleaning RNA, determination of quality and quantity of RNA, and target gene expression

Genomic DNA was removed from the RNA samples and the quality and quantity of the RNA was controlled as described in 2.2.6.3. To determine the relative target gene expression, cDNA was synthesized (see 2.2.6.4) and quantitative PCR was performed (see 2.2.6.5).

#### **2.2.7.4 Transcriptomic analysis**

RNA isolated of CPP-PNA treated *S. pyogenes* and *S. pneumoniae* and the respective control samples was analyzed in collaboration with Prof. Dr. Jörg Vogel and coworkers (Helmholtz Institute for RNA-based Infection Research, Würzburg). cDNA library preparation and sequencing was done at the Core Unit Systems Medicine, University of Würzburg. After RNA-sequencing, reads were trimmed, filtered and mapped against the respective reference genome (genome accession of *S. pyogenes* 591: NZ CP077685.1; *S. pneumoniae* TIGR4: NC 003028.3). All bioinformatic analyses of the data, such as normalization, analyses of differential expression, and KEGG pathway enrichment analysis of differentially expressed genes, were conducted by the cooperation-partner Jakob Jung at the Helmholtz Institute for RNA-based Infection Research, Würzburg.

#### **2.2.8 Cell-based infection system**

##### **2.2.8.1 Detroit 562 cultivation and maintenance**

For maintenance, the human pharynx carcinoma epithelial cell line Detroit 562 (ATCC CCL138) was cultivated in Dulbecco's modified eagle medium (DMEM)/F12 (1:1) (supplemented with 10 % FBS) at 37°C and 5 % CO<sub>2</sub>, and passaged every 3 days. For that, cell culture medium was removed, cells were washed with PBS, and detached from T75 flask by incubation for 15 min at 37°C with 2.5 ml Accutase™ solution. The reaction was stopped with 7.5 ml cell culture medium. Detached cells were diluted 1:2 in fresh medium, transferred into new T75 flasks, and incubated at 37°C, 5 % CO<sub>2</sub>.

##### **2.2.8.2 Antimicrobial effects of CPP-PNA conjugates in cell based infection model**

Confluent Detroit 562 cells were seeded ( $7.5 \times 10^4$  cells in 150 µl cell culture medium) into 96-well plates (flat bottom) and incubated overnight at 37°C, 5 % CO<sub>2</sub>. Afterwards, the culture was infected with *S. pneumoniae* TIGR4 at multiplicity of infection (MOI) of 5 (added in 40 µl cell culture medium), treated with 10 µM CPP-PNA or 1 µg levofloxacin (provided in 10 µl Ampuwa®), and incubated for 3 h at 37°C, 5 % CO<sub>2</sub>. The supernatant was collected, adherent cells were detached using Accutase™ solution, and the samples were combined, centrifuged (4000 g, 10 min), and washed twice in PBS. The pellet was then suspended in PBS, and serial dilutions of the sample were plated to determine the CFU.

##### **2.2.8.3 Viability of Detroit 562 cells: LDH leakage assay and crystal violet staining**

To determine the viability of Detroit 562 after treatment with CPP-PNA, LDH-leakage assay and crystal violet staining of cells were performed.  $7.5 \times 10^4$  Detroit 562 cells were seeded into 96-well plates, incubated for 24 h at 37°C, 5 % CO<sub>2</sub>, treated with 20 µM CPP-PNAs or 1 µg

levofloxacin, and incubated for 3 h at 37°C, 5 % CO<sub>2</sub>. Lactate dehydrogenase (LDH) leakage is a measure of compromised cell membranes and was determined using the CyQUANT™ LDH Cytotoxicity Assay Kit (Thermo Fisher Scientific, Darmstadt) according to the manufacturer's manual. As dead cells exhibit reduced adhesion, resulting in detachment, viability can be determined by staining cells that remained bound to the culture wells using crystal violet. Cells were washed with PBS, fixed with 100 µl methanol for 10 min, washed with PBS supplemented with 0.005 % Tween 20, and then incubated with 0.1 % crystal violet solution for 10 min. The cells were washed with Ampuwa®, and the remaining crystal violet was solved in 100 µl of 33 % acetic acid for 10 min. 70 µl of this solution was transferred to fresh wells, and the optical density at 600 nm was measured with a plate reader.

## 2.2.9 Infection model organism *Galleria mellonella* larvae

### 2.2.9.1 Maintenance of *G. mellonella* larvae

The larvae of the greater wax moth *Galleria mellonella* were obtained from Bugs-International GmbH (Irsingen, Germany). The larvae were stored and fed in a wheat bran mixture (Table 15).

**Table 15: Feed of *G. mellonella* larvae**

Ingredient	Amount
Wheat bran	125 g
Oatmeal	Two small hands full
Brewer's yeast	Two tablespoons (TB)
Milk powder	Two TB
Honey	4 TB
Glycerol	4 TB

Larvae with a weight of 0.15 – 0.2 g were used for infection and treatment; when weight was below 0.15 g, the larvae were incubated with food at 37°C until the optimal weight was reached; larvae above 0.2 g and pupa were frozen at -20° C for 10 h and discarded.

### 2.2.9.2 Infection and treatment of *G. mellonella* larvae

For infection of *G. mellonella* larvae with *S. pneumoniae* TIGR4, 10 ml of a 5 h culture were centrifuged at 4000 g for 10 min, the pellet was washed with 0.9 % NaCl and centrifuged again. The bacterial pellet was suspended in 0.9 % NaCl and diluted to OD<sub>600</sub> = 1.4. Serial dilution was plated out on THY agar to determine the CFU/ml (2.2 – 6.6 x 10<sup>8</sup> CFU/mL). For infection of larvae with *S. pyogenes* 591, 10 ml of a bacterial culture (max. 16 h) were centrifuged (4000 g for 10 min), washed with 0.9 % NaCl, diluted to OD<sub>600</sub> = 1.2, and plated out for determination of the CFU/ml (2.5 – 4 x 10<sup>8</sup> CFU/ml).

10  $\mu$ l of the bacterial suspension was injected into a *G. mellonella* larvae with a fine dosage syringe (Omnican®-F, 0.01 – 1 ml, 0.3 x 12 mm, B. Braun AG, Melsungen, Germany) using a microapplicator (World Precision Instruments, Sarasota, USA). The injection site was between the last two pairs of pro-legs of the larvae into its midgut (Figure 4).

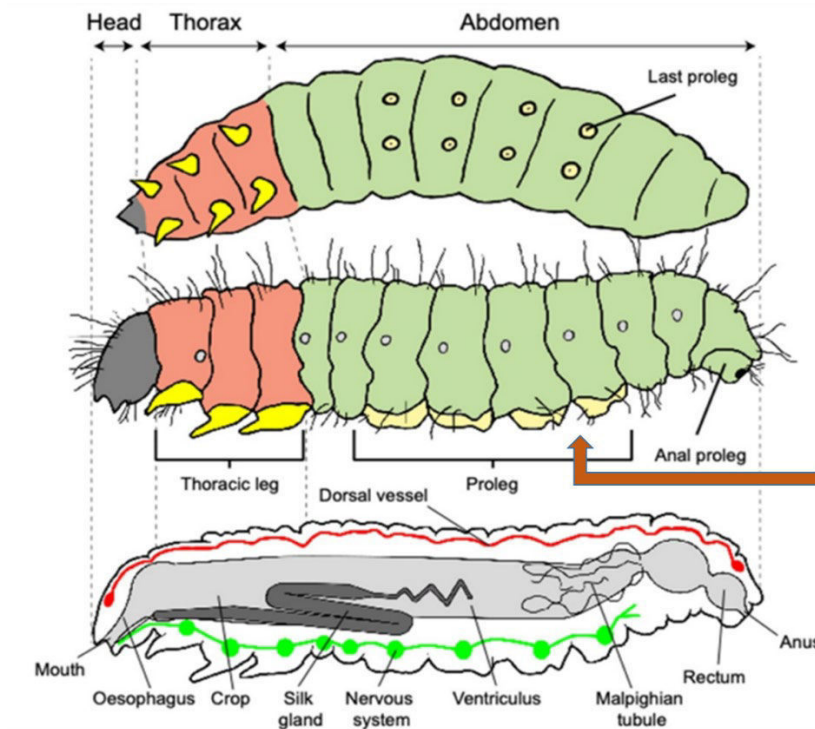


**Figure 4: Anatomy of *G. mellonella* larvae (adapted from Durieux et al., 2021; Singkum et al., 2019; Engel and Moran, 2013; Singkum et al., 2019). A red arrow shows the injection site.**

After 30 min, 10 nmol of CPP-PNA in 0.9 % NaCl or 1 – 10  $\mu$ g levofloxacin in 0.9 % NaCl with 3 % DMSO were injected close to the infection site. As mock control, 0.9 % NaCl and 0.9 % NaCl with 3 % DMSO were used, respectively. Larvae were then incubated with feed at 37°C. For determination of survival rates, larvae were checked daily for one week. Larvae were considered alive when they responded to light touch with tweezers. Pupae were recorded as alive and discarded.

### 2.2.9.3 Determination of bacteria load in *G. mellonella* larvae

To measure the bacterial load in infected *G. mellonella*, larvae were homogenized and serial dilutions of the homogenate were plated out on selective medium. To confirm bacterial species identity, colony PCR was performed.

#### 2.2.9.3.1 Homogenization of *G. mellonella* larvae

For determination of the bacterial load per larvae, infected and treated larvae were cooled at the time points indicated for 10 min at 4°C and transferred to 2 ml screw cap tubes with 850  $\mu$ l cold PBS and a homogenization bead (diameter  $\sim$  0.5 cm). The larvae were homogenized with the

Precellys 24 Tissue Homogenizer at 5000 rpm for 4 x 20 sec, a serial dilution of the content was plated out onto Columbia CNA agar with 5 % sheep blood and incubated over night at 37° C with 5 % CO<sub>2</sub>.

*S. pneumoniae* colonies grown on selective Columbia CNA agar were easily distinguished from other colony types by their brownish-grey coloration. Additionally, colony PCR was performed to proof colony identity.

### 2.2.9.3.2 Colony PCR

For colony PCR a single colony was picked, suspended in 8 µl Ampuwa<sup>®</sup> with 2 µl polyiosinic acid (10 mg/ml) and heated for 15 min at 98° C to release the template DNA. For detection of *S. pneumoniae*, the gene encoding pneumolysin (*ply*) was amplified. *S. pyogenes* was identified by amplifying the gene encoding the M protein. The composition of the reaction mixture and the amplification program are provided in Table 16 and Table 17.

The PCR products were separated on a 1 % Agarose gel by electrophoresis at 100 V in TAE buffer. Per well, 10 µl PCR sample and 2 µl of 6 x loading dye were loaded onto the gel. GeneRuler 1 kb DNA-Ladder (Thermo Fisher Scientific, Waltham, USA) was used to determine the size of the PCR product.

**Table 16: Reaction mixture for colony PCR**

Component	Amount	Final concentration
10 x Taq reaction buffer	2.5 µl	1 x
10 mM dNTPs	0.5 µl	200 µM
10 mM reverse primer	0.5 µl	0.2 µM
10 mM forward primer	0.5 µl	0.2 µM
Taq DNA Polymerase	0.12 µl	1.25 units
Template DNA	2.5 µl	variable
Nuclease free water ad. 25 µl		

**Table 17: Amplification program for colony PCR**

Step	Temperature	Time
<b>Initial denaturation</b>	94°C	5 min
<b>30 Cycles</b>	94°C	30 sec
	45°C / 56°C ( <i>S. pneumoniae</i> / <i>S. pyogenes</i> )	30 sec
	72°C	2 min
<b>Final Extension</b>	72°C	10 min
<b>Hold</b>	4°C	

#### **2.2.9.4 Proteomics analysis of the immune response of infected *G. mellonella* larvae**

Per experimental run, 45 larvae were infected with *S. pyogenes* 591 with the optimal infection dose ( $2.5 - 4 \times 10^6$  CFU/larva) and 30 larvae with 0.9 % NaCl (mock control) (see 2.2.9.1). Hemolymph was extracted after 4 h, 24 h, and 72 h from 15 infected larvae and 10 non-infected larvae per time point.

##### **2.2.9.4.1 Extraction of hemolymph**

The larva was chilled at 4° C for 15 min before the head was carefully dissected with a scalpel on a disinfected surface. Approximately 30 µl of hemolymph were extracted cautiously from the decapitated larvae and mixed with an anticoagulant solution previously added to the tube, a spatula tip of N-phenylthiourea, 1.5 µl EDTA (10 mM) and 1.5 µl sodium citrate (30 mM) (Wrońska AK et al., 2022). Per time point, the hemolymph of all 15 infected or 10 uninfected larvae, respectively, were collected into one tube.

The protein concentration of the hemolymph was determined using Pierce™ Coomassie (Bradford) Protein-Assay-K (Thermo Fisher Scientific, Waltham, USA), according to the manufacturer's manual.

To separate the hemocytes from the hemolymph, the samples were centrifuged (200 xg, 8°C, 15 min), the supernatant was transferred to fresh tube, centrifuged again (20 000 g, 3 min), and transferred to a new tube. The cell pellet, containing the hemocytes, was washed with 0.9 % NaCl, centrifuged (200 g, 15 min, 8°C), and suspended in PBS with 5 µM glucose. The cell-free hemolymph and the hemocyte samples were stored at -20°C.

##### **2.2.9.4.2 Proteomics analysis: mass spectroscopy**

The mass spectrometric analysis was carried out in the Core Facility Proteome Analysis of the Rostock University Medical Center by Dr. Mikkat, using the Synapt G2-S mass spectrometer, which was coupled to the nanoAcquity ULC system. Additionally, trypsinized peptides were separated by reverse phase UPLC and analyzed in data-independent mode (HDMS<sup>E</sup>). Label-free mass spectrometric quantification and expression analysis was performed with Progenesis QI for Proteomics (Nonlinear Dynamics, Newcastle upon Tyne, UK).



### 3. Results

#### 3.1 Antimicrobial effect of antisense CPP-PNAs on *Streptococcus pneumoniae*

In this work, the specific antimicrobial activity of CPP-PNA conjugates against *S. pneumoniae* was determined. The conjugates were optimized by varying the PNA target and the carrier system. The antimicrobial activity was examined with regard to kill kinetics and the target specificity of the PNA molecule. Furthermore, CPP-PNA effectiveness was investigated in a cell-based system and the constructs were tested as a therapeutic in an invertebrate model organism.

##### 3.1.1 Identification of effective CPP-PNA conjugates

Barkowsky and coworkers identified effective CPP-PNA conjugates with antibacterial activity in *Streptococcus pyogenes*. The PNA in these conjugates is complementary to the start region of the *gyrA* gene, encoding the subunit A of the essential topoisomerase gyrase. Carrier peptides mediating the uptake in *S. pyogenes* are (RXR)<sub>4</sub>XB, TAT, and K8 (Barkowsky et al., 2019). On this basis, these three CPPs were investigated for their ability to mediate uptake of a PNA cargo in *S. pneumoniae*. The CPP-PNA conjugates were incubated in different doses with the pneumococcal strains TIGR4, D39, and 19F. In addition, the antimicrobial activity of two different PNA targets *gyrA* and *rpoB* was compared. The essential gene *rpoB* encodes the subunit B of the RNA polymerase.

CPP-scrambled PNA (CPP-scrPNA) constructs were used to control for sequence specificity. A scrPNA has the same base composition as the specific antisense PNA, but in a randomized order. Prior to synthesis, the sequences of all PNAs and scrPNAs were checked using BLAST® (Altschul et al., 1997) to rule out complementarity to the start region of the mRNA sequence of another essential gene in *S. pneumoniae*.

In the experimental setting, bacteria were incubated under conditions that allowed slight growth over the course of the experiment (Barkowsky et al., 2020). Bacteria were incubated for 6 h with 2.5 – 20 µM CPP-PNA conjugates. The colony count reduction of *S. pneumoniae* TIGR4 upon incubation with the different tested CPP-PNA conjugates are shown in Figure 5. The antibacterial effect of the constructs on the strains D39 and 19F are provided in the appendix (Figure 35 and Figure 36, respectively).

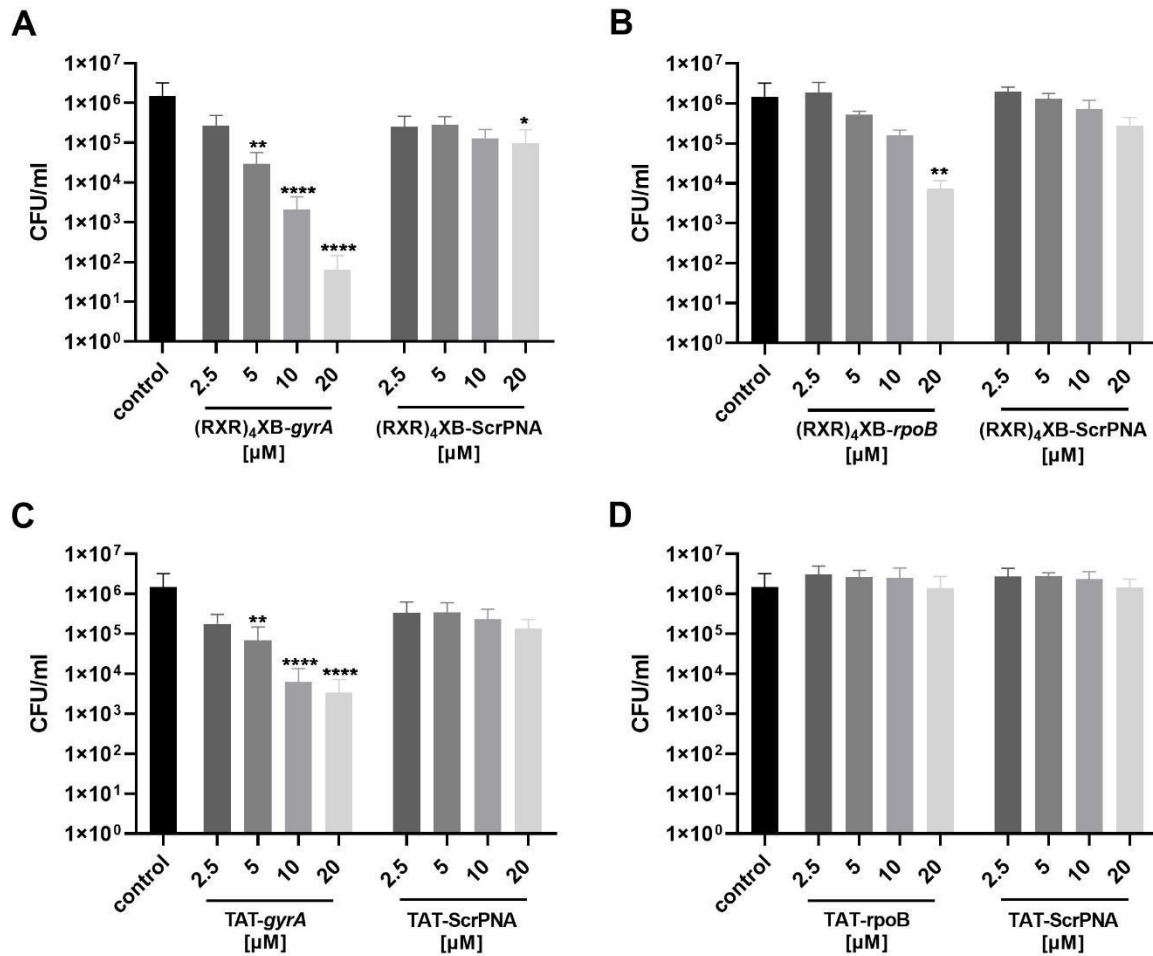


**Figure 5: Concentration-dependent reduction of bacterial cell count following treatment of *S. pneumoniae* TIGR4 with cell-penetrating peptide (CPP)-antisense PNAs for 6 h.** scrPNA, scrambled PNA controls. Treatment with (A) (RXXR)<sub>4</sub>XB-anti-*gyrA* PNAs, (B) (RXXR)<sub>4</sub>XB-anti-*rpoB* PNAs, (C) TAT-anti-*gyrA* PNAs, and (D) TAT-anti-*rpoB* PNAs. Data are presented as means and standard deviation. Statistical significance was determined by one-way analysis of variance (ANOVA) with multiple comparisons. Differences between PNA conjugate samples and mock control are shown as:  $p \leq 0.05$  (\*);  $p \leq 0.01$  (\*\*);  $p \leq 0.0001$  (\*\*\*\*). Sample size:  $n = 5$ ; (Barkowsky et al., 2022).

Testing different concentrations of the CPP-PNA conjugates on *S. pneumoniae* TIGR4 revealed a significant dose-dependent reduction of cell counts with (RXXR)<sub>4</sub>XB-anti-*gyrA* PNA and TAT-anti-*gyrA* PNA, while K8-anti-*gyrA* PNA had no effect (data not shown). (RXXR)<sub>4</sub>XB-PNA caused a stronger CFU reduction than TAT-PNA. The control CPP-scrPNAs had only small effects on the survival of *S. pneumoniae* TIGR4. Antimicrobial activity of CPP-scrPNA indicate sequence-independent effects of the conjugates, especially due to toxicity of the carrier molecule. The specific antimicrobial effect of CPP-PNAs is calculated as difference of the log<sub>10</sub> reduction caused by the CPP-antisense PNA and the log<sub>10</sub> reduction of the CPP-scrPNA. In the further work, it is referred to as  $\Delta\log_{10}$  reduction.

The toxicity of the CPPs (RXR)<sub>4</sub>XB and TAT was tested in *S. pneumoniae* TIGR4 (Figure 6). With a log<sub>10</sub> CFU reduction of 2, these CPPs alone caused a higher antimicrobial effect than the corresponding CPP-scrPNAs (Figure 5). Therefore, CPP-scrPNAs that have the same chemical characteristics as the CPP-antisense PNA represent a more suitable control than the CPP alone.

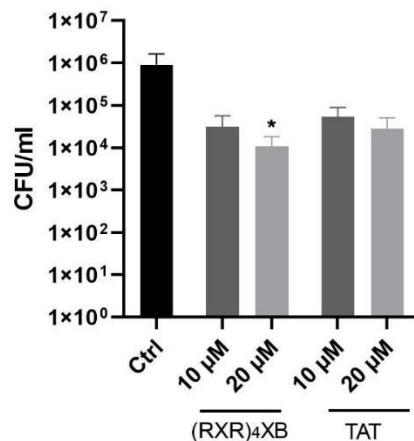


**Figure 6: Toxicity of CPPs (RXR)<sub>4</sub>XB and TAT in *S. pneumoniae* strain TIGR4.** Colony count reduction after 6 h incubation of *S. pneumoniae* TIGR4 with 10 and 20 μM of the CPPs (RXR)<sub>4</sub>XB and TAT. Data are presented as mean values with standard deviation. Statistical significance was determined using Kruskal-Wallis test. Differences between CPP samples and mock control are expressed as:  $p \leq 0.05$  (\*). Sample size:  $n = 3$  (Barkowsky et al., 2022).

Comparison of the antimicrobial effect of CPP-anti-*gyrA* PNAs with CPP-anti-*rpoB* PNAs showed, that CPP-PNAs targeting *gyrA* were more effective than those targeting *rpoB* (Figure 5). Accordingly, treatment with TAT-*rpoB*, combining both, the less effective carrier molecule and PNA target, had no effect on pneumococcal survival. The *gyrA* sequence is therefore considered a more suitable target for antisense PNAs than *rpoB* in *S. pneumoniae*.

Similar results were obtained in the other pneumococcal strains tested: (RXR)<sub>4</sub>XB- and TAT-anti-*gyrA* PNA caused a high and significant  $\Delta$ log<sub>10</sub> CFU reduction, while K8 was no effective carrier. PNA complementary to the start region of *gyrA* mRNA was more effective than *rpoB*-antisense PNA. *S. pneumoniae* D39 was affected to a comparable extent as TIGR4 by CPP-antisense PNA treatment, while 19F was rather less sensitive (Figure 35 and Figure 36, respectively).

Attempting to improve the antimicrobial effect by enhancing the uptake of PNAs, different carriers were screened. Several carriers have been tested that have either been shown to translocate cargos in other bacterial species or eukaryotic cells, or have been predicted to enhance uptake (Table 11). In total, 22 conjugates with different carriers linked to anti-*gyrA* PNA were examined for their antimicrobial effect in *S. pneumoniae* TIGR4. Several were additionally

tested in 19F. The colony count reduction of the conjugates is listed as log<sub>10</sub> CFU reduction in Table 18. For comparison, the effect of (RXR)<sub>4</sub>XB-anti-*gyrA* is provided.

**Table 18: Antimicrobial effect of CPP-PNAs on *S. pneumoniae* strain TIGR4 and strain 19F.** Incubation time: 6 h.

CPP- <i>gyrA</i> PNA [10 μM]	TIGR4 Log <sub>10</sub> CFU reduction	19F Log <sub>10</sub> CFU reduction
(RXR) <sub>4</sub> XB-anti- <i>gyrA</i>	3.21	2.3
(RFR) <sub>4</sub> XB-anti- <i>gyrA</i>	5.1	3.61
PenArg-anti- <i>gyrA</i>	2.9	n.d.
AB2-anti- <i>gyrA</i>	2.83	1.83
R9-anti- <i>gyrA</i>	1.82	n.d.
TP10-anti- <i>gyrA</i>	1.14	1.1
R9-TAT-anti- <i>gyrA</i>	1.1	1.07
Sc18-anti- <i>gyrA</i>	0.92	n.d.
HIV-1Rev-anti- <i>gyrA</i>	0.47	0.84
pANTpHD-anti- <i>gyrA</i>	0.43	1.06
gH625-MK-anti- <i>gyrA</i>	0.4	n.d.
gH625-MR-anti- <i>gyrA</i>	0.4	n.d.
TLM-anti- <i>gyrA</i>	0.33	n.d.
SynB3-anti- <i>gyrA</i>	0.31	0.78
pVec (truncated)-anti- <i>gyrA</i>	0.16	0.73
AmiA-anti- <i>gyrA</i>	0	n.d.
Bac7(15-24)-anti- <i>gyrA</i>	0	n.d.
BUF 5-19-anti- <i>gyrA</i>	0	n.d.
CADY-anti- <i>gyrA</i>	0	n.d.
K8-anti- <i>gyrA</i>	0	0
PDESTK-anti- <i>gyrA</i>	0	0.62
RSV-A9-anti- <i>gyrA</i>	0	n.d.
SARS-CoV-2 predicted Seq.-anti- <i>gyrA</i>	0	n.d.

Of the CPP-PNAs tested, 6 had an antimicrobial effect (log CFU reduction > 1) on *S. pneumoniae* TIGR4. With the exception of (RFR)<sub>4</sub>XB-anti-*gyrA*, no construct caused a higher cell count reduction than (RXR)<sub>4</sub>XB-anti-*gyrA*. For several CPP-PNAs, exhibiting a strong antimicrobial effect, the Δlog<sub>10</sub> CFU reduction was determined using CPP-scrPNA. None of the tested conjugates had a higher Δlog<sub>10</sub> reduction than (RXR)<sub>4</sub>XB-anti-*gyrA* (2.71 Δlog<sub>10</sub> CFU reduction). The necessity to determine the Δlog<sub>10</sub> is highlighted by (RFR)<sub>4</sub>XB-anti-*gyrA*, which was identified as unsuitable construct: causing a log<sub>10</sub> CFU reduction of 5.1, the Δlog<sub>10</sub> reduction was only 1.0. This indicates a strong toxic effect of the carrier.

Due to the high and specific antimicrobial effect of the conjugates (RXR)<sub>4</sub>XB-anti-*gyrA* PNA and TAT-anti-*gyrA* PNA, they were used for further investigation.

### 3.1.2 Kill kinetics of (RXR)<sub>4</sub>XB- and TAT-PNA

The kill kinetics of the antimicrobial constructs (RXR)<sub>4</sub>XB-anti-*gyrA* PNA and TAT-anti-*gyrA* PNA were examined (Figure 7). *S. pneumoniae* TIGR4 was incubated with 10 μM of CPP-PNA and the colony count was determined every 2 h for 12 h.

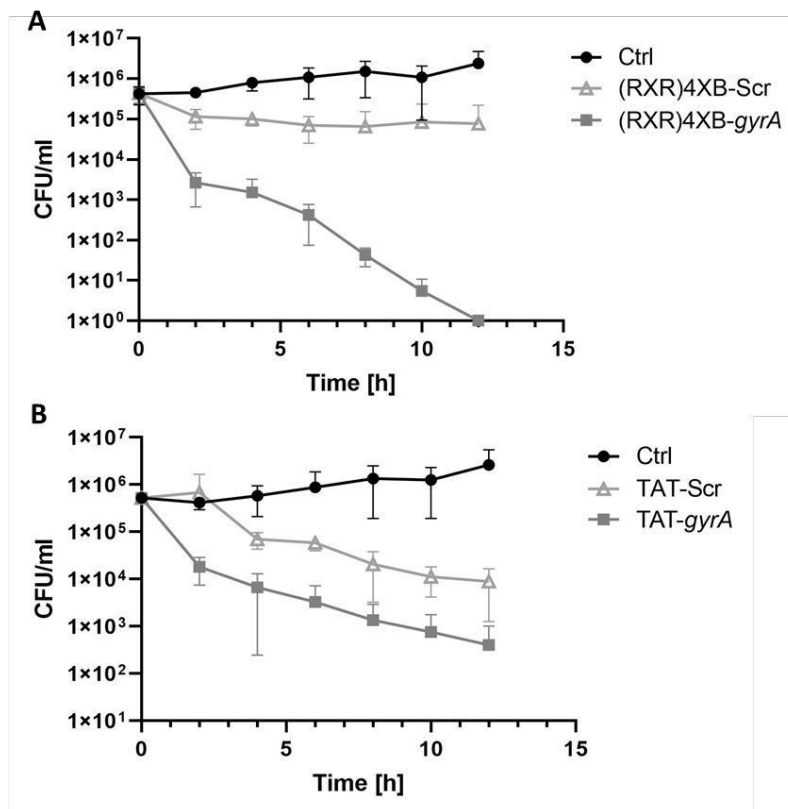


**Figure 7: Killing kinetics of CPP-anti-*gyrA* PNA treatment in *S. pneumoniae* strain TIGR4.** (A) Bacterial counts following treatment with 10 μM (RXR)<sub>4</sub>XB-anti-*gyrA* PNA and or (RXR)<sub>4</sub>XB-scrPNA. (B) Bacterial counts following treatment with 10 μM TAT-anti-*gyrA* PNA or TAT-scrPNA. Data are presented as mean values with standard deviation (±). Sample size n = 3 (Barkowsky et al., 2022).

(RXR)<sub>4</sub>XB-anti-*gyrA* caused a specific, strong, and constant CFU reduction over time, leading to complete eradication of pneumococci after 12 h. The (RXR)<sub>4</sub>XB-scrPNA control did not cause reduction of CFU. The effect of TAT-anti-*gyrA* PNA was less strong, and continuous CFU reduction in the presence of TAT-scrPNA indicated unspecific toxicity of the carrier on pneumococci.

### 3.1.3 Target specificity

The target specificity of the CPP-PNA conjugates was investigated by measuring the relative transcript abundance of the target gene after CPP-PNA treatment. For that, *S. pneumoniae* TIGR4 was incubated with 7.5  $\mu$ M CPP-anti-*gyrA* or 10  $\mu$ M CPP-anti-*rpoB* for 6 h in BHI. Within this experimental setting these concentrations were sublethal. Total RNA was isolated, cDNA synthesized, and the relative quantity of the respective target gene in treated bacteria compared to untreated pneumococci was determined using qPCR. For normalization, the transcript abundance of the 5S rRNA gene was used. As illustrated in Figure 8A, treatment of *S. pneumoniae* TIGR4 with 7.5  $\mu$ M (RXR)<sub>4</sub>XB- and TAT-anti-*gyrA* PNA caused significant reduction of the *gyrA* transcript abundance to 45 % and 29 %, respectively, compared to the untreated control. Incubation with 10  $\mu$ M of (RXR)<sub>4</sub>XB- and TAT-anti-*rpoB* PNA reduced relative *rpoB* transcript levels to 51 % and 45 %, respectively (Figure 8B).

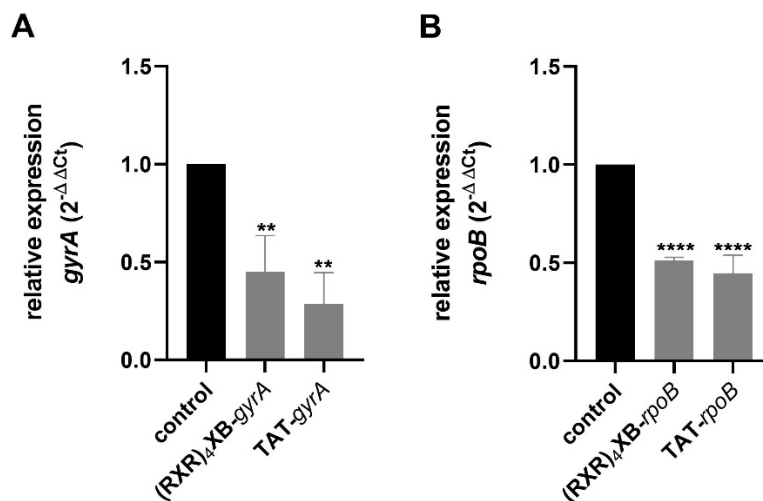


**Figure 8: Relative expression of target genes in *S. pneumoniae* strain TIGR4 following treatment with CPP-antisense PNAs.** The 5S rRNA gene served as internal control. Relative expression was calculated using the threshold cycle ( $2^{-\Delta\Delta C_t}$ ) method. (A) Treatment with 7.5  $\mu$ M TAT-anti-*gyrA* PNAs and 7.5  $\mu$ M (RXR)<sub>4</sub>XB-anti-*gyrA* PNAs. Relative expression of *gyrA*. (B) Treatment with 10  $\mu$ M TAT-anti-*rpoB* PNAs and 10  $\mu$ M (RXR)<sub>4</sub>XB-anti-*rpoB* PNAs. Relative expression of *rpoB*. Data are presented as means and standard deviation. Statistical significance was determined by one-way ANOVA with multiple comparisons. Differences between PNA conjugate samples and the mock control are shown as:  $p \leq 0.01$  (\*\*) and  $p \leq 0.0001$  (\*\*\*\*). Sample size:  $n = 3$  (Barkowsky et al., 2022).

Further, the transcript abundance of the two virulence genes *ply* and *pspA* was determined in CPP-anti-*rpoB* PNA treated pneumococci (Figure 9). As *rpoB* encodes the subunit of RNA polymerase, reduced *rpoB* levels are expected to impact overall gene expression. *Ply* encodes the cytolytic and proinflammatory toxin pneumolysin (Nishimoto et al., 2020; van Pee et al., 2016). Treatment with (RXR)<sub>4</sub>XB- and TAT-anti-*rpoB* PNA resulted in significant reduction of the relative expression of *ply* to 56 % and 45 %, respectively. *PspA* encodes the pneumococcal surface protein A, which is an important virulence factor of pneumococci

involved in adhesion to host cells and protection from host immune response (Hammerschmidt et al., 1999; Park et al.). The expression level of *pspA* was reduced by TAT-anti-*rpoB* PNA treatment to 57 %, while in contrast, it was not affected by (RXR)<sub>4</sub>XB-anti-*rpoB* PNA.

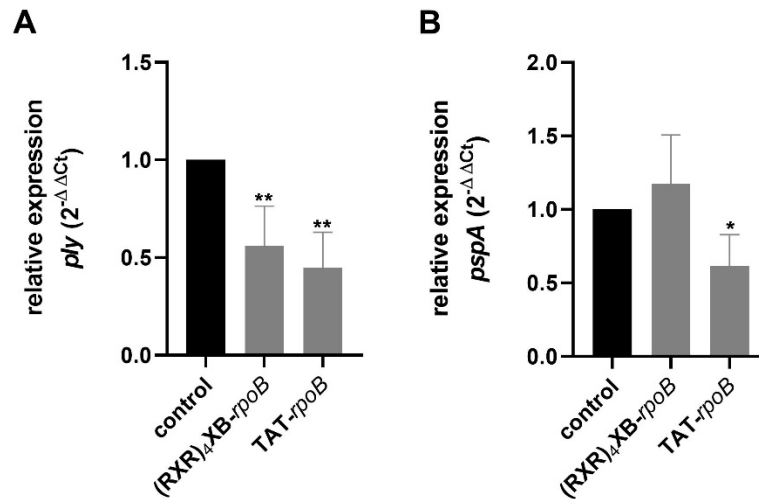


**Figure 9: Relative expression of virulence genes in *S. pneumoniae* strain TIGR4 following treatment with CPP-anti-*rpoB* PNAs.** The 5S rRNA gene served as internal control. Relative expression was calculated using the threshold cycle ( $2^{-\Delta\Delta C_t}$ ) method. (A) Treatment with 10  $\mu$ M TAT-anti-*rpoB* PNAs and (RXR)<sub>4</sub>XB-anti-*rpoB* PNAs. Relative expression of *ply*. (B) Treatment with 10  $\mu$ M TAT-anti-*rpoB* PNAs and (RXR)<sub>4</sub>XB-anti-*rpoB* PNAs. Relative expression of *pspA*. Data are presented as means and standard deviation. Statistical significance was determined by one-way ANOVA with multiple comparisons. Differences between PNA conjugate samples and the mock control (untreated) are shown as:  $p \leq 0.05$  (\*) and  $p \leq 0.01$  (\*\*). Sample size:  $n = 4$  (Barkowsky et al., 2022).

### 3.1.4 CPP-PNA in a cell-based infection system

To investigate antimicrobial effects of CPP-PNA on pneumococci in a cell-based infection system, Detroit 562 human pharyngeal epithelial cells were incubated with *S. pneumoniae* TIGR4 at a multiplicity of infection (MOI) of 5. After incubation with 20  $\mu$ M (RXR)<sub>4</sub>XB-anti-*gyrA* PNA for 3 h, the CFU were determined (Figure 10). As control (RXR)<sub>4</sub>XB-scrPNA was applied, and for comparison 1  $\mu$ g levofloxacin ( $\sim 2.5 \times$  MIC) was used.

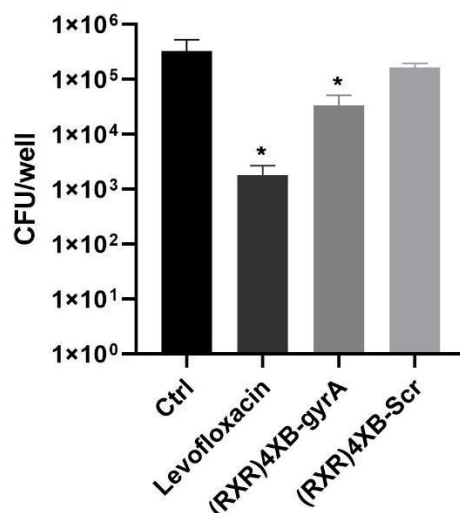


**Figure 10: Antimicrobial effect of (RXR)<sub>4</sub>XB-anti-*gyrA* PNA in a cell-based infection system.** Detroit 562 cells were infected with *S. pneumoniae* strain TIGR4 and subsequently treated with 1 µg levofloxacin, or 20 µM (RXR)<sub>4</sub>XB-anti-*gyrA* PNA, or 20 µM (RXR)<sub>4</sub>XB-scrPNA, respectively. Data are presented as means and standard deviation. Statistical significance was determined with one-way ANOVA with multiple comparisons. Differences between PNA conjugate samples and mock control (untreated) are shown as:  $p \leq 0.05$  (\*). Sample size:  $n = 3$  (Barkowsky et al., 2022).

Treatment of pneumococci in the cell-based infection system with (RXR)<sub>4</sub>XB-anti-*gyrA* PNA resulted in a log<sub>10</sub> reduction of cell count, while the CPP-scrPNA control had no effect. Addition of 1 µg levofloxacin caused a 2 log<sub>10</sub> CFU reduction.

Further, potential cytotoxic effects of the CPP-PNA conjugates on the human pharyngeal epithelial cell line Detroit 562 were examined. After incubation of the cells with 20 µM (RXR)<sub>4</sub>XB-PNA or TAT-PNA, cell viability was determined by measuring lactate dehydrogenase (LDH) leakage and by staining viable adherent cells with crystal violet. Completely lysed cells served as positive control.

LDH leakage upon treatment with CPP-PNAs was compared to maximal LDH release of lysed cells and is given in percent (Table 19). This experiment revealed low cytotoxicity of (RXR)<sub>4</sub>XB-PNA and TAT-PNA conjugates.

**Table 19: Relative LDH release of Detroit 562 cells upon CPP-PNA treatment.** LDH release upon treatment compared to LDH release of lysed cells in percent. Cells were incubated with 20 µM CPP-PNAs or 1 µg levofloxacin for 3 h. Statistical significance was determined by one-way ANOVA, multiple comparisons. Differences between LDH release of samples and maximum LDH release are expressed as:  $p \leq 0.0001$  (\*\*\*\*). Sample size:  $n = 4$ .

Concentration/Amount	Compound	LDH leakage compared to maximal leakage
20 µM	(RXR) <sub>4</sub> XB-PNA	5 % (****)
20 µM	TAT-PNA	6 % (****)
1 µg	Levofloxacin	3 % (****)



Viable cells were determined by staining with crystal violet. Crystal violet which had bound to the cells was extracted and the optical density (OD<sub>600</sub>) was measured (Figure 11). Treatment of the cells with 20  $\mu$ M of the CPP-PNA conjugates resulted in similar high OD<sub>600</sub> values as incubation with 1  $\mu$ g levofloxacin. Both, LDH release measurement and crystal violet staining, revealed low cytotoxicity of the tested CPP-PNA conjugates.

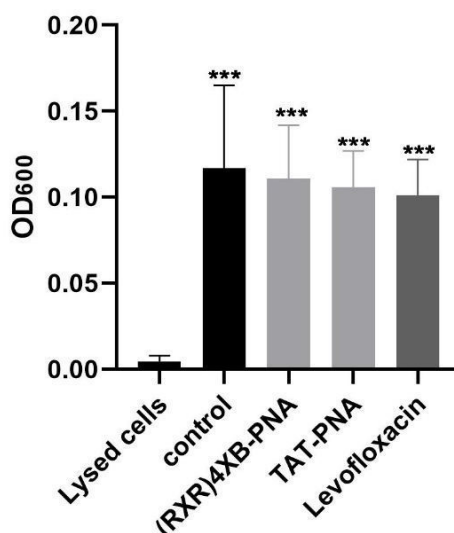


**Figure 11: Cell viability of Detroit 562 cells upon treatment with CPP-PNAs.** Detroit 562 cells were lysed and treated with 20  $\mu$ M (RXR)<sub>4</sub>XB-PNA or 20  $\mu$ M TAT-PNA, respectively. Biomass was stained with crystal violet, bound crystal violet was extracted, and the optical density of the solution was measured at 600 nm. Data are presented as means and standard deviation. Statistical significance was determined by one-way ANOVA with multiple comparisons. Differences between samples and maximal cell lysis are shown as  $p \leq 0.001$  (\*\*\*). Sample size:  $n = 4$ , (Barkowsky et al., 2022).

### 3.1.5 CPP-PNA as therapeutic in the infection model organism

#### *Galleria mellonella*

To determine potential therapeutic effects of the CPP-PNAs (RXR)<sub>4</sub>XB- and TAT-anti-*gyrA*, larvae of the invertebrate infection model organism *Galleria mellonella* were used. For this purpose, an infection dosis of pneumococci causing death of  $\sim 80\%$  of *G. mellonella* larvae over seven days was injected into the larval midgut. Subsequently, 10 nmol of CPP-PNA were injected close to the infection site, and survival of the larvae was monitored for a week. As a positive control larvae were treated with levofloxacin. Gina Barkowsky and Irina Pöhner contributed to the data collection in this experiment.

As shown in Figure 12A, treatment of infected larvae with 1  $\mu$ g levofloxacin increased survival rates from 19% to 40%, and 10  $\mu$ g levofloxacin elevated the survival rate to over 70%. Injection of 10 nmol (RXR)<sub>4</sub>XB-anti-*gyrA* PNA and TAT-anti-*gyrA* PNA increased the survival rates of infected larvae by 22% (Figure 12B) and by 25% (Figure 12B), respectively.

The CPP-scrPNA had no effect on the survival rates. These experiments showed, that (RXR)<sub>4</sub>XB- and TAT-anti-*gyrA* PNA improved larval survival rates, and that 1 µg levofloxacin and 10 nmol of the tested CPP-PNAs had comparable effects *in vivo*. Treatment of infected larvae with (RXR)<sub>4</sub>XB-anti-*rpoB* PNA and TAT-anti-*rpoB* PNA conjugates did not increase larval survival rates (data not shown).

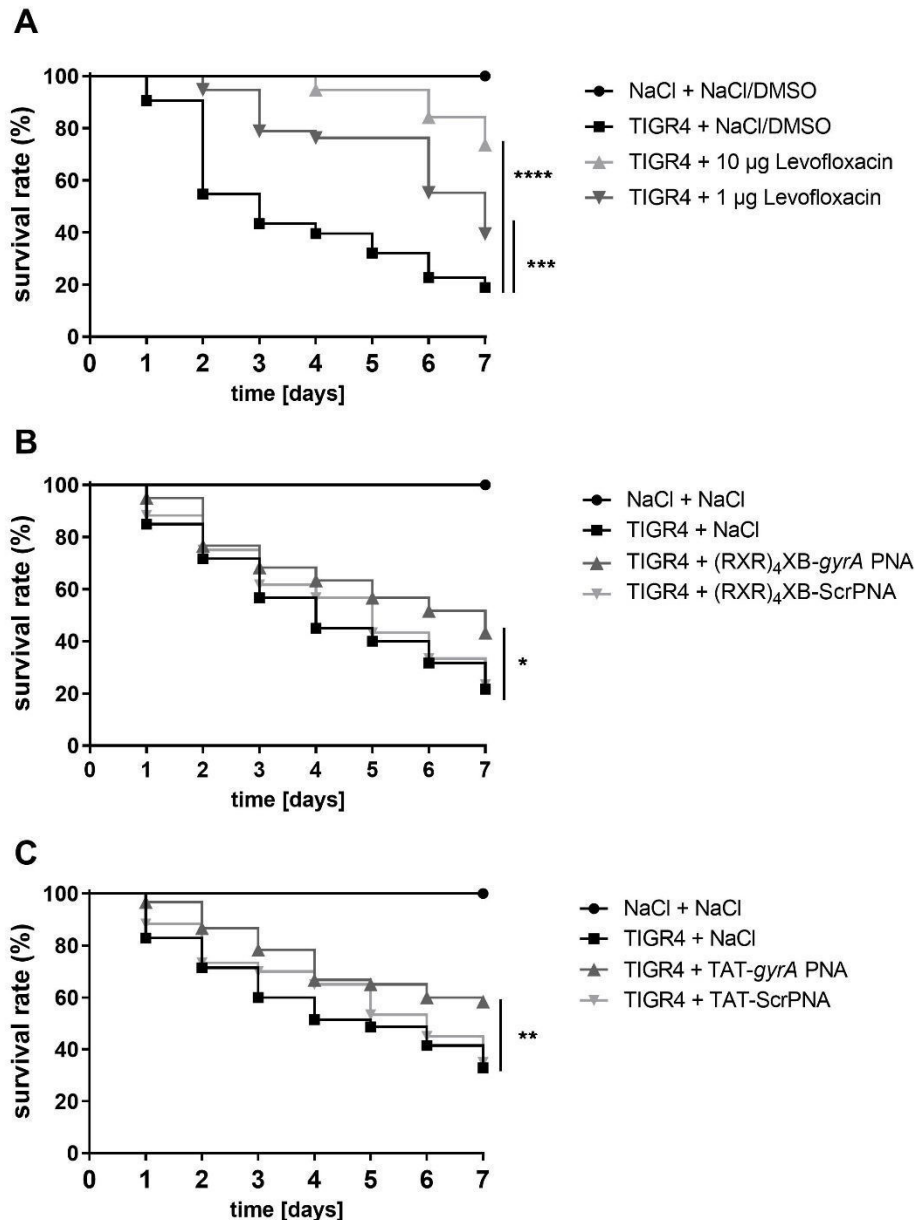


**Figure 12: Survival of *Galleria mellonella* larvae treated with 10 nmol CPP-PNAs following infection with *S. pneumoniae* strain TIGR4.** (A) *G. mellonella* larvae infected with *S. pneumoniae* TIGR4 and subsequently treated with 10 or 1 µg levofloxacin. Sample size: n = 40 larvae per group. (B) *G. mellonella* larvae infected with *S. pneumoniae* TIGR4 and subsequently treated with TAT-anti-*gyrA* PNA or TAT-scrPNA, respectively. Sample size: n = 60 larvae per group. (C) *G. mellonella* larvae infected with *S. pneumoniae* TIGR4 and subsequently treated with (RXR)<sub>4</sub>XB-anti-*gyrA* PNA or (RXR)<sub>4</sub>XB-scrPNA, respectively. Sample size: n = 60 larvae per group. Statistical significance was determined using the log-rank test. Differences between curves are shown as: p ≤ 0.05 (\*); p ≤ 0.01 (\*\*); p ≤ 0.001 (\*\*\*); p ≤ 0.0001 (\*\*\*\*). (Barkowsky et al., 2022).

Further, the antimicrobial effect of (RXR)<sub>4</sub>XB-anti-*gyrA* PNA was examined *in vivo*. Larvae were infected with *S. pneumoniae* TIGR4 and subsequently treated with 10 nmol (RXR)<sub>4</sub>XB-anti-*gyrA*. As positive control 1 µg and 10 µg levofloxacin were used. After 24 h, larvae were homogenized and the pneumococcal colony count was determined. The bacterial load of the larvae is shown in Figure 13.

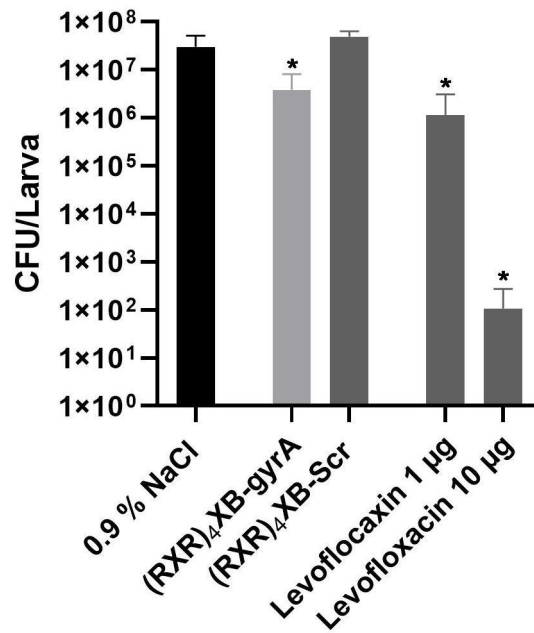


**Figure 13: Bacterial load of *G. mellonella* larvae infected with *S. pneumoniae* strain TIGR4 and treated with (RXR)<sub>4</sub>XB-*gyrA* PNA.** *G. mellonella* larvae were infected with *S. pneumoniae* TIGR4 and subsequently treated with 10 nmol (RXR)<sub>4</sub>XB-anti-*gyrA*, or 10 nmol (RXR)<sub>4</sub>XB-scrPNA, 1 µg or 10 µg levofloxacin. After 24 h, larvae were homogenized and CFU of pneumococci was determined (selective medium and colony PCR). Data are presented as means and standard deviation. Statistical significance was determined by one-way ANOVA with multiple comparisons. Differences between treated samples and mock control are expressed as  $p \leq 0.05$  (\*). Sample size: four larvae per group in three independent experiments; (Barkowsky et al., 2022).

Treatment of infected larvae by injection of 10 nmol (RXR)<sub>4</sub>XB-anti-*gyrA* PNA reduced bacterial load of larvae by 1 log<sub>10</sub> CFU; the CPP-scrPNA control had no effect on the colony count. Injection of 1 µg levofloxacin caused a log<sub>10</sub> CFU reduction of 1.2, and 10 µg of the antibiotic mediated a log<sub>10</sub> CFU reduction of 5.2.

It was shown that 10 nmol (RXR)<sub>4</sub>XB-anti-*gyrA* PNA has an antimicrobial activity *in vivo* and a therapeutic effect on *S. pneumoniae*-infected larvae, comparable to the effect of 1 µg levofloxacin.

### 3.2 Improving the antimicrobial effect of CPP-PNA with pyrenebutyrate

In this part of the work, possible beneficial effects of the counterion pyrenebutyrate (PB) on the uptake of CPP-PNA, and consequently increased antimicrobial activity of the conjugates, were investigated. Since PB has only been used in eukaryotes but not in bacteria, different concentrations of PB were first tested to determine toxicity in streptococci. Therefore,  $8 \times 10^5$  CFU/ml *S. pneumoniae* TIGR4 or  $5 \times 10^5$  CFU/ml *S. pyogenes* 591 were incubated with PB concentrations from 50  $\mu$ M to 400  $\mu$ M for 6 h and the bacterial count was determined (Figure 14). The concentrations tested are based on the amount of PB used in similar experiments in cell culture (Takeuchi et al., 2006).

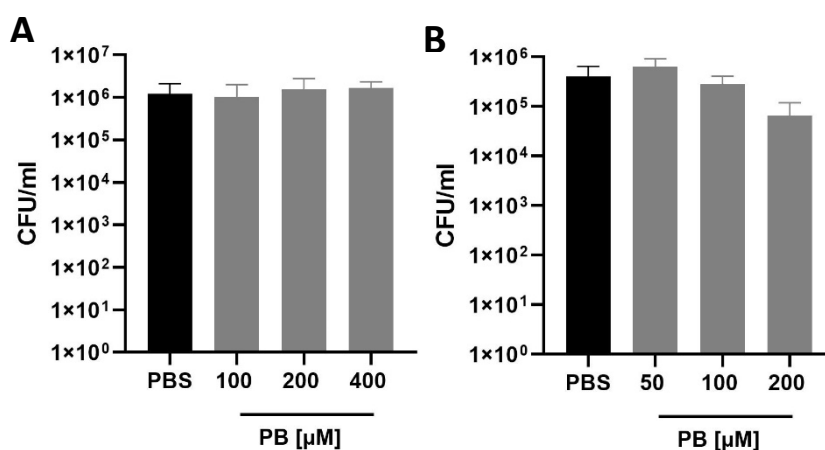


**Figure 14: Effect of different concentrations of pyrenebutyrate on bacterial cell count of (A) *S. pneumoniae* TIGR4 and (B) *S. pyogenes* 591.** Incubation for 6 h; control: PBS. Data are shown as mean with standard deviation. Sample size:  $n = 2 - 4$ .

*S. pneumoniae* was not affected by PB at concentrations up to 400  $\mu$ M, whereas 200  $\mu$ M PB resulted in a reduction of the *S. pyogenes* colony count of 0.5 log<sub>10</sub> of CFU/ml. For the following experiments with *S. pneumoniae* 200  $\mu$ M PB, and with *S. pyogenes* 100  $\mu$ M PB were used.

To observe effects of PB on the antimicrobial activity of CPP-PNA, bacteria were pre-incubated for 10 min with PB. Afterwards, kill assays with different CPP-PNA conjugates were carried out. Increased antimicrobial effects of CPP-antisense PNA in presence of PB would indicate, that PB supports uptake of the conjugates. The results of the kill assays with pneumococci and GAS are illustrated in Figure 15. Since previous studies with eukaryotic cells only determined effects of PB with arginine-rich CPPs, the number of positive amino acid residues of the carriers studied in this work are listed in Table 20 for comparison.

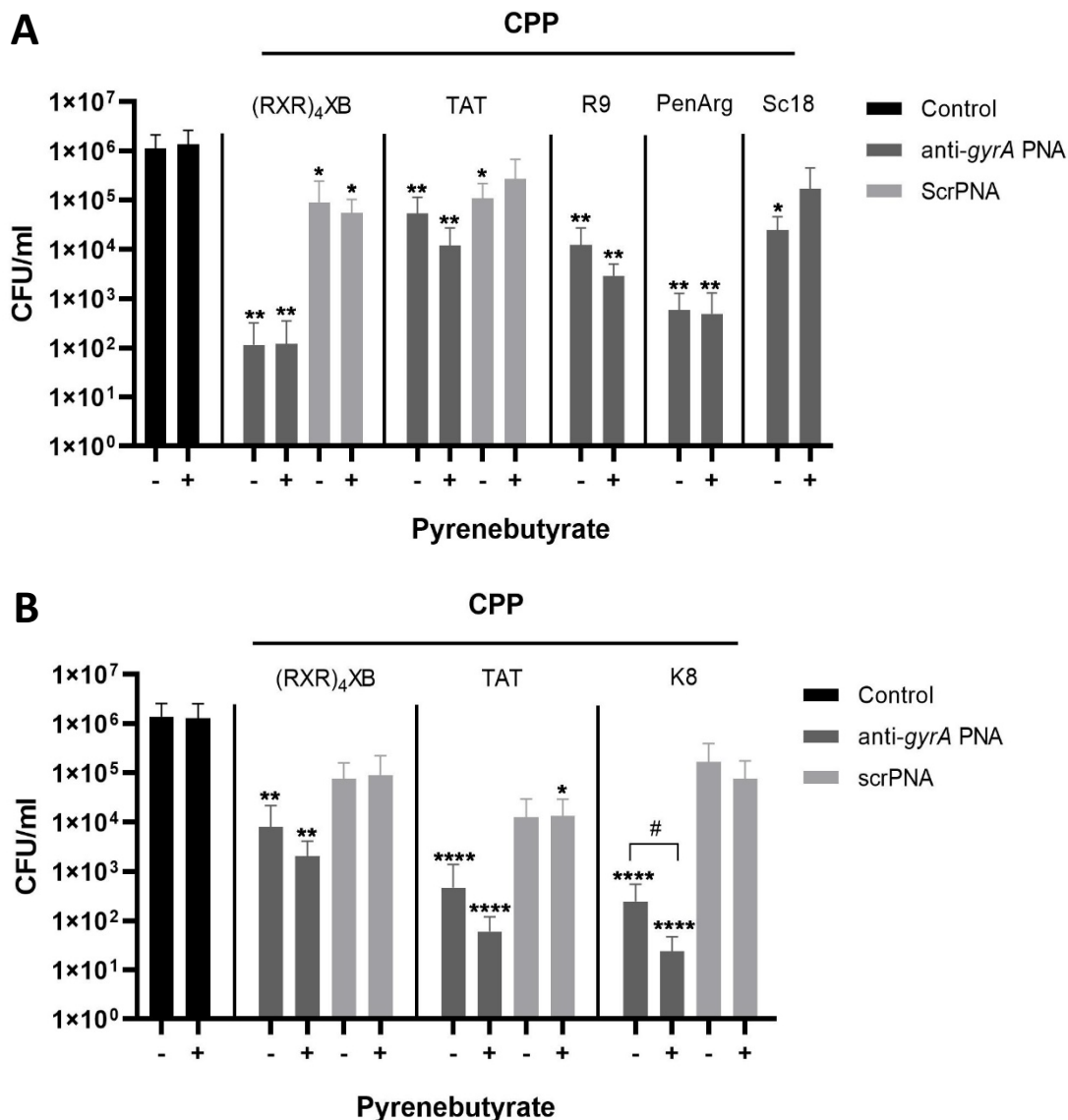


**Figure 15: Effect of pyrenebutyrate on cell count reduction of CPP-PNA on streptococci.** The number of CFU/ml was determined after 6 h incubation of (A) *S. pneumoniae* TIGR4 and (B) *S. pyogenes* 591 with different CPP-PNA in absence (-) and presence (+) of PB. Antisense PNAs: anti-*gyrA* PNA and scrPNA (randomized sequence). Concentrations used with *S. pneumoniae*: CPP-PNA: 10  $\mu$ M, PB: 200  $\mu$ M; with *S. pyogenes*: CPP-PNA: 5  $\mu$ M, PB: 100  $\mu$ M. Data are presented as mean value and standard deviation. Statistical significance was determined using Kruskal-Wallis test. Differences between CPP-PNA samples and mock control (Ampuwa®) were expressed as:  $p \leq 0.05$  (\*),  $p \leq 0.01$  (\*\*),  $p \leq 0.0001$  (\*\*\*\*). Differences between CPP-PNA samples with and without PB are expressed as  $p \leq 0.05$  (#). Sample size: *S. pneumoniae*:  $n = 3 - 5$ ; *S. pyogenes*:  $n = 5 - 9$ .

**Table 20: Positive amino acid residues per CPP**

CPP	Arginine residues	Lysine residues	Proportion of positively charged amino acids
PenArg	4	5	7/16 (44%)
Sc18	4	5	9/16 (56%)
(RXR) <sub>4</sub> XB	8	0	8/14 (57%)
TAT	6	3	9/12 (75%)
R9	9	0	9/9 (100%)
K8	0	8	8/8 (100%)

## Results

Pre-incubating *S. pneumoniae* TIGR4 with PB did not increase the antimicrobial activity of (RXR)<sub>4</sub>XB-anti-*gyrA* PNA and PenArg-anti-*gyrA* PNA, and even mitigated the cell count reduction of Sc18-anti-*gyrA* PNA. The cell count reduction of TAT-anti-*gyrA* PNA and R9-anti-*gyrA* PNA conjugates increased in the presence of PB. These results indicate that the positive charge of a carrier might be important for the effect of PB on CPP-PNA in pneumococci, as TAT and R9 are both more positively charged than the other CPPs tested, whose activity was not affected by the counterion.

In *S. pyogenes* 591, addition of PB resulted in increased antimicrobial activity of all three tested CPP-PNAs (RXR)<sub>4</sub>XB-, TAT-, and K8-anti-*gyrA*. The effect increased as a function of the positive charge of the CPPs. The difference observed between samples with and without pre-incubation with PB was significant for K8-anti-*gyrA* treatment. Therefore, kill kinetics of K8-anti-*gyrA* PNA in the presence and absence of PB were investigated in *S. pyogenes* (Figure 16).

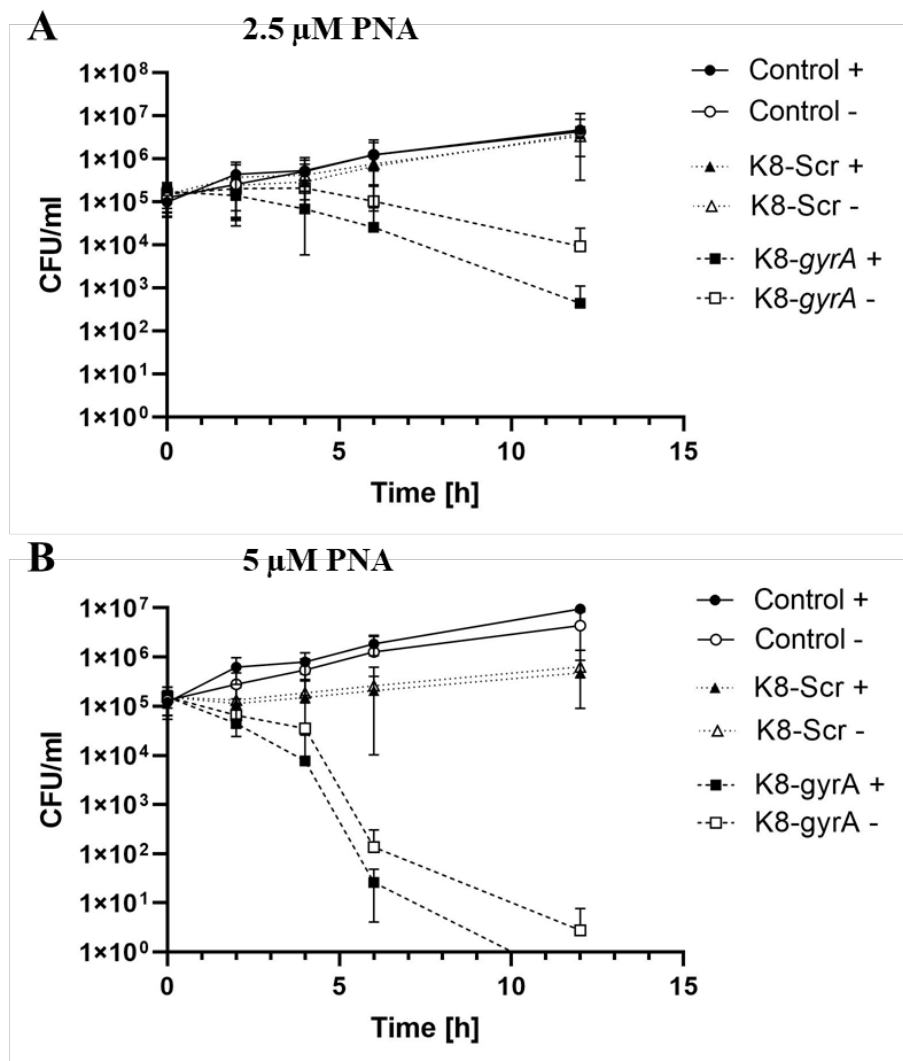


**Figure 16: Kinetics of effect of pyrenebutyrate on antimicrobial cell count reduction of CPP-PNA on *S. pyogenes* 591.** The number of CFU/ml was determined over 12 h incubation with K8-anti-*gyrA* PNA and K8-scrPNA (randomized sequence) in absence (-) and presence (+) of PB. Mock control: Ampuwa®. Concentration of PB: 100  $\mu\text{M}$ ; CPP-PNA concentration (A) 2.5  $\mu\text{M}$  and (B) 5  $\mu\text{M}$ . Data are presented as mean value and standard deviation. Sample size:  $n = 5$ .

Pre-incubation with 100  $\mu\text{M}$  PB before treatment with 2.5  $\mu\text{M}$  K8-anti-*gyrA* PNA resulted in an increase of its antimicrobial activity. After 12 h, the colony count reduction was 1.5 log<sub>10</sub> higher than without PB (Figure 16A). Treatment with 5  $\mu\text{M}$  K8-anti-*gyrA* PNA in the presence of PB resulted after 12 h in complete eradication of *S. pyogenes*, which was not achieved in absence of the counterion (Figure 16B).

To investigate, whether the effect of PB on the antimicrobial activity of CPP-PNAs was caused by improved peptide uptake, fluorescently labeled K8 was applied. K8-FITC uptake in *S. pyogenes* 591 was measured in presence and absence of PB. After pre-incubation for 10 min with PB, K8-FITC was added for 30 min to *S. pyogenes*, and the intracellular fluorescence

intensity at 490 nm was determined. The experiment was carried out by Jana Bull and the result is illustrated in Figure 17.

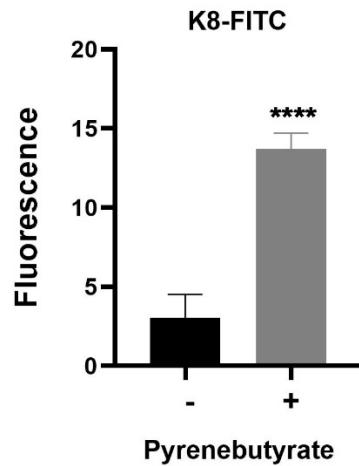


**Figure 17: Uptake of K8-FITC into in *S. pyogenes* in presence and absence of PB.** After pre-incubation of *S. pyogenes* 591 with 100  $\mu$ M PB, 10  $\mu$ M K8-FITC were added for 30 min. Bacteria were washed, lysed, and the amount of K8-FITC in the supernatant was determined via measurement of fluorescence at 490 nm. Data are presented as mean value and standard deviation. Statistical significance was determined using unpaired t-test. Difference between samples without (-) and with (+) PB is expressed as:  $p \leq 0.0001$  (\*\*\*\*). Sample size:  $n = 4$ , data were collected by Jana Bull.

In the presence of PB a 4.5-fold increase of intracellular K8-FITC in *S. pyogenes* 591 was observed compared to samples that were not pre-treated with PB. It can therefore be concluded, that pre-incubation of *S. pyogenes* with PB increases the uptake of conjugates in dependence of the carrier. The data indicate that CPPs containing a high proportion of the positively charged amino acid residues arginine and lysine are preferentially taken up in the presence of the counterion.



### 3.3 Transcriptomic analyses of CPP-PNA treated streptococci

For the investigation of target gene specificity and putative off target effects of CPP-PNA treatment in streptococci, transcriptomic analyses were performed. For this purpose, RNA was isolated from CPP-PNA treated streptococci, and after cleaning and quality control, sent to the Core Unit Systems Medicine of the University of Würzburg. From the RNA samples, a cDNA library was prepared and sequenced. After quality control the reads were mapped against the respective reference genomes (genome accession of *S. pyogenes* 591: NZ CP077685.1; *S. pneumoniae* TIGR4: NC 003028.3). Differential gene expression analyses and pathway enrichment analyses were done by Jacob Jung (Helmholtz Institute for RNA-based Infection Research, Würzburg).

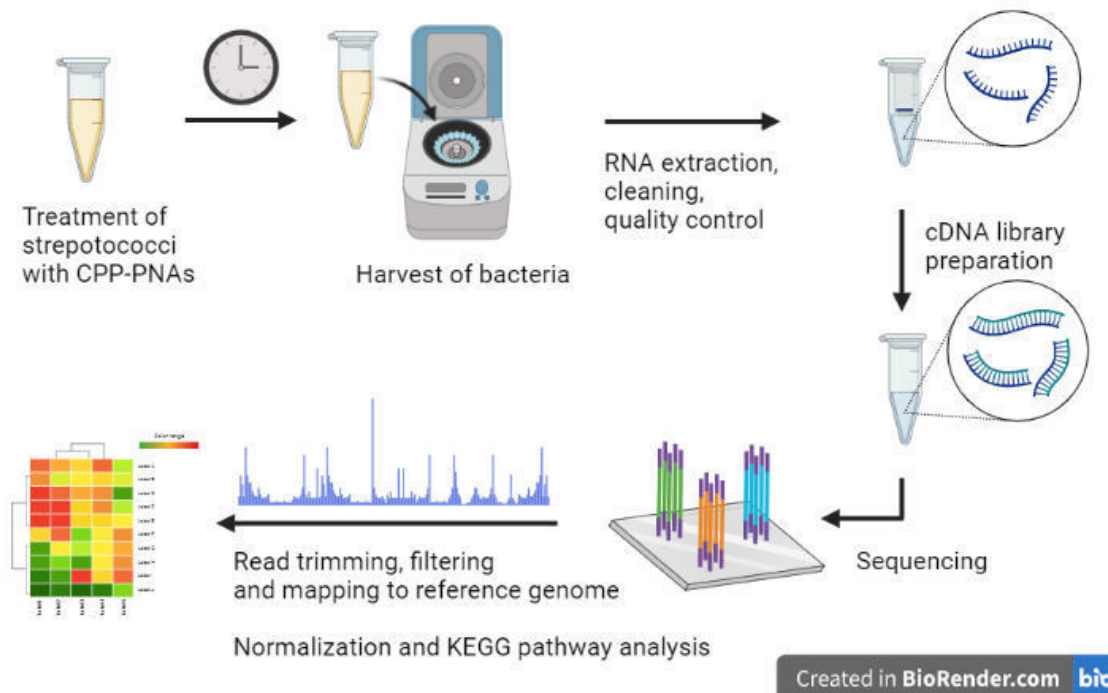


**Figure 18: Workflow for the investigation of transcriptomic effects of CPP-PNA or CPP treatment on streptococcal species.** Streptococci were incubated with CPP-PNA or CPP for 5 h (*S. pneumoniae* TIGR4) or 6 h (*S. pyogenes* 591). Bacteria were harvested and washed via centrifugation. RNA was isolated, cleaned, and after quality control sent to the Core Unit Systems Medicine, University of Würzburg. From the template RNA, a cDNA library was prepared and sequenced. The reads were trimmed, filtered, and mapped against the reference genomes. After normalization, differential gene expression, and pathway enrichment analysis was performed. Analyses programs: packages of R/Bioconductor; read count: edgeR (v3.30.0); Pathway enrichment analysis: EggNOG (5.0.0). The figure was created with BioRender.

First, optimal treatment settings were determined. Principally, there are two different approaches to achieve moderate transcriptomic changes upon application of a stressor: short pulse with high concentration or longer incubation with sublethal concentrations. Application

of high doses of CPP-PNA (4 - 10  $\mu$ M) for a short incubation period (10 - 30 min) resulted in morphologically altered bacterial pellets after centrifugation. RNA isolated from streptococci after this treatment contained a higher proportion of small RNA species with accumulation of RNA fragments of the size of 25 nucleotides (nt), which may represent degradation products or enrichment of naturally occurring small sRNAs. These changes appeared to coincide with increases in CPP-PNA conjugate concentration (Figure 37 in appendix). They occurred with (RXR)<sub>4</sub>XB-antisense PNA and -scrPNA, as well as TAT-antisense PNA and -scrPNA, and K8-antisensePNA and -scrPNA treatment, but not with CPPs without cargo. It is of note, that this effect was related to the peptide-coupled PNA molecules, independent of their antisense properties. CPP-scrPNAs do not cause CFU reduction under the conditions tested here, but lead to the same pellet morphology changes and to low RNA sample quality as their antisense-PNA counterparts. A similar phenomenon was observed by Popella and coworkers when isolating RNA of *Salmonella enterica* after treatment with lethal concentration of CPP-PNA. They compared seven RNA isolation protocols for possible enrichment of larger and undegraded RNA molecules, of which two were found suitable (Popella et al., 2021). In this work, we tested several different protocols, but were not able to identify a method leading to improved RNA quality following incubation with high CPP-PNA concentration. Due to the accumulation of short RNA fragments and the apparently reduced RNA integrity following treatment with lethal CPP-PNA concentration, bacteria were treated with sublethal concentrations for a longer incubation period.

In order to verify target gene transcript reduction under these conditions, relative transcript levels were determined by qPCR. Treatment of pneumococci with (RXR)<sub>4</sub>XB-anti-*gyrA* PNA significantly decreased relative target gene transcript levels to 63 % compared to untreated control, while (RXR)<sub>4</sub>XB-scrPNA and CPP alone did not affect *gyrA* mRNA levels. In *S. pyogenes*, (RXR)<sub>4</sub>XB- and TAT-anti-*gyrA* PNA reduced relative target gene transcript level to 63 % and 65 %, respectively, compared to untreated control. The controls (RXR)<sub>4</sub>XB-scrPNA, TAT-scrPNA, and the unconjugated CPP (RXR)<sub>4</sub>XB did not alter *gyrA* mRNA levels.

### 3.3.1 Transcriptomic response of *Streptococcus pneumoniae*

Transcriptomic profiling of *S. pneumoniae* after incubation for 5 h with sublethal concentrations (7.5  $\mu$ M) of CPP-PNA, CPP-scrPNA and CPP was performed by Core Unit Systems Medicine, University of Würzburg. For quality control, the four biologically independent samples per treatment condition were plotted two-dimensionally with the principal component analysis

(PCA). After removal of batch effects, distinct clusters for each treatment condition were detected (Figure 19).

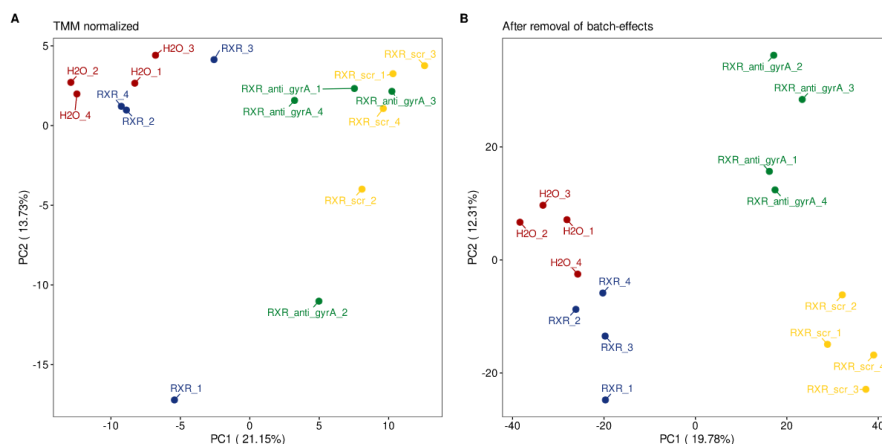


**Figure 19: Principal component analysis (PCA) of the different treatment conditions with *S. pneumoniae*.** Four independent biological replicates (a) after TMM normalization and (b) after additional removal of batch effects. The figure was generated by Jakob Jung.

The numbers of differentially expressed genes upon CPP-PNA treatment compared to untreated control are listed in Table 21.

**Table 21: Number of differentially expressed genes in *S. pneumoniae* TIGR4 after treatment with CPP-PNA, CPP-scrPNA and CPP.** Genes were considered significantly differentially expressed when the total fold change > 2 and p-value < 0.001.

	(RXR) <sub>4</sub> XB- anti- <i>gyrA</i>	(RXR) <sub>4</sub> XB- scrPNA	(RXR) <sub>4</sub> XB
<b>Number of genes with significantly altered transcript abundance:</b>	42	72	8
<b>Upregulated</b>	41	71	8
<b>downregulated</b>	1	1	0

(RXR)<sub>4</sub>XB-scrPNA treatment resulted in the highest number of differentially expressed genes, while the CPP (RXR)<sub>4</sub>XB had the lowest effect on expression profile. Generally, the transcriptomic change is low and almost all significantly influenced genes are upregulated.

The transcriptomic responses are illustrated as volcano plots (Figure 20). There was no alteration of target gene *gyrA* transcript level detected upon (RXR)<sub>4</sub>XB-anti-*gyrA* PNA treatment. Most of the genes that were significantly upregulated after treatment with the CPP-PNAs and CPPs were involved in carbohydrate uptake and metabolism. The gene with second highest upregulation upon (RXR)<sub>4</sub>XB-anti-*gyrA* PNA is *nanB*, encoding neuraminidase B. Almost all genes for which expression levels were affected by (RXR)<sub>4</sub>XB-scrPNA treatment were also similarly affected by (RXR)<sub>4</sub>XB-anti-*gyrA* PNA treatment and vice versa, although not always to a significant extent.

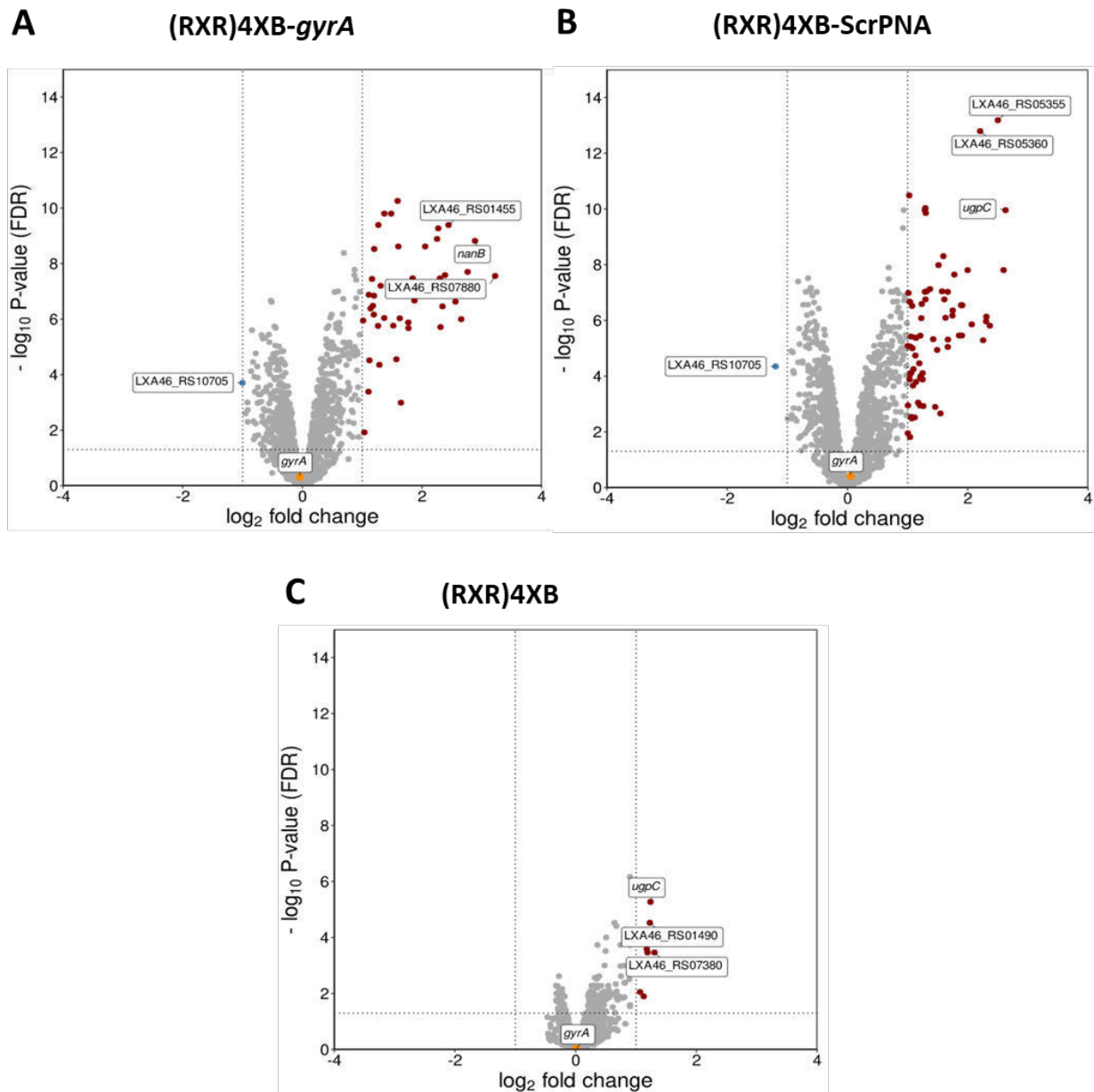


**Figure 20: Transcriptomic responses of *S. pneumoniae* strain TIGR4 upon CPP-PNA and CPP treatment.** Volcano plots show changes in transcript abundance as log<sub>2</sub> fold changes with false discovery rate (FDR)-adjusted  $-\log_{10}$  p-value *S. pneumoniae* strain TIGR4 treated for 5 h with 7.5  $\mu$ M of (A) (RXR)<sub>4</sub>XB-anti-*gyrA*, (B) (RXR)<sub>4</sub>XB-scrPNA and (C) (RXR)<sub>4</sub>XB, versus untreated control. Genes with a fold change of transcript abundance > 2 and FDR-adjusted p-value < 0.001 were considered as significantly differentially regulated. Significantly upregulated genes (red) and downregulated genes (blue) are marked; the three most differentially expressed genes are named in the figure. The figure was generated by Jakob Jung.

After pathway enrichment analysis, a heat map was generated (Figure 21) showing the transcriptomic changes under the treatment conditions tested. Most pathways upregulated by CPP-PNA and CPP-scrPNA treatment were metabolic pathways, especially those involved in uptake and metabolism of carbohydrates. Among them, expression of proteins of bacterial phosphotransferase systems (PTSs), which are essential in sugar uptake, were highly induced.

Also, genes with sequence similarity to genes involved in *E. coli* biofilm formation are upregulated after CPP-PNA treatment. Only a few pathways were downregulated, among them are mismatch repair nucleotide excision repair, DNA replication, peptidoglycan biosynthesis, two-component systems, and cationic antimicrobial peptide (CAMP) resistance.

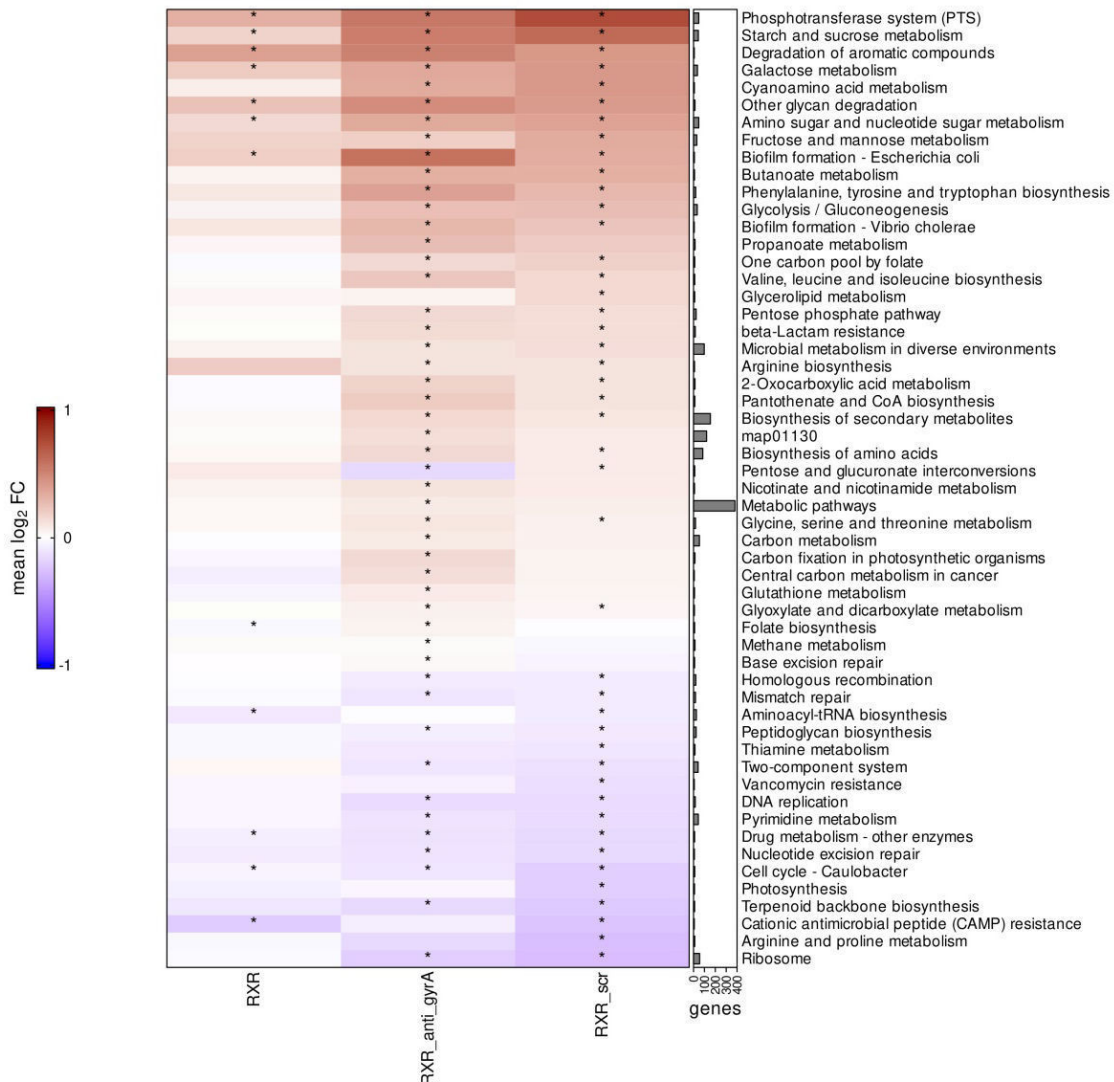


**Figure 21: Pathways with differentially expressed genes of *S. pneumoniae* strain TIGR4 upon CPP-PNA and CPP treatment.** The heat map was generated with RNA Seq. data of 10<sup>6</sup> CFU/ml bacteria treated for 5 h with 7.5 μM of (RXR)<sub>4</sub>XB, (RXR)<sub>4</sub>XB-anti-*gyrA*, and (RXR)<sub>4</sub>XB-scrPNA. Log<sub>2</sub> fold changes (FC) of gene transcript abundances compared to untreated (water) sample are displayed in blue (downregulation) and red (upregulation). Genes were considered significantly differentially expressed (\*) when FC > 2 and FDR-adjusted p-value < 0.001. The figure was generated by Jakob Jung.

### 3.3.2 Transcriptomic response of *Streptococcus pyogenes*

Transcriptomic analysis of *S. pyogenes* treated with 4 μM (RXR)<sub>4</sub>XB, (RXR)<sub>4</sub>XB-anti-*gyrA* PNA and -scrPNA, TAT-anti-*gyrA* PNA and -scrPNA for 6 h was performed by the Core Unit Systems Medicine, University of Würzburg.

## Results

Principal component analysis (PCA) shows the respective clusters of the four independent samples per CPP-PNA/ CPP (Figure 22). The numbers of differentially expressed genes per treatment condition compared to the untreated (water) control are listed in Table 22.

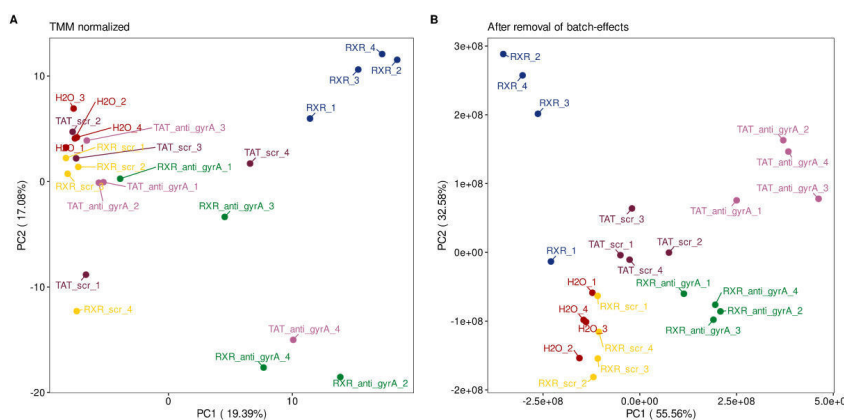


**Figure 22: Principal component analysis (PCA) of the different treatment conditions of *S. pyogenes*.** Four independent biological replicates (a) after TMM normalization and (b) after additional removal of batch effects. The figure was generated by Jakob Jung.

**Table 22: Number of differentially expressed genes in *S. pyogenes* 591 after treatment with CPP-PNA, CPP-scrPNA and CPP.** Genes were considered significantly differentially expressed when total fold change > 2 and p-value < 0.001.

	(RXR) <sub>4</sub> XB- <i>gyrA</i>	(RXR) <sub>4</sub> XB-scrPNA	(RXR) <sub>4</sub> XB	TAT- <i>gyrA</i>	TAT-scrPNA
<b>Number of genes with significantly altered transcript abundance:</b>	3	0	26	6	4
<b>Upregulated</b>	3	0	10	4	4
<b>Downregulated</b>	0	0	16	2	0

The number of genes that were significantly differentially expressed was low. The changes in transcript abundance of genes are displayed with volcano plots in Figure 23. No target gene specificity was measured, as mRNA level of *gyrA* were not significantly affected by (RXR)<sub>4</sub>XB-anti-*gyrA* PNA or TAT-anti-*gyrA* PNA treatment. Incubation of *S. pyogenes* with (RXR)<sub>4</sub>XB-scrPNA resulted in no significant change of transcript abundance. In contrast to the results obtained with *S. pneumoniae*, following treatment with the CPP (RXR)<sub>4</sub>XB the highest number of genes was differentially expressed in GAS in comparison to the other treatment conditions. Further, the affected genes were unique compared to treatment with the other molecules. Among them were genes involved in carbohydrate uptake, in peptidoglycan biosynthesis, and genes encoding the general stress response protein *csbD* and the competence-associated protein *coiA*.

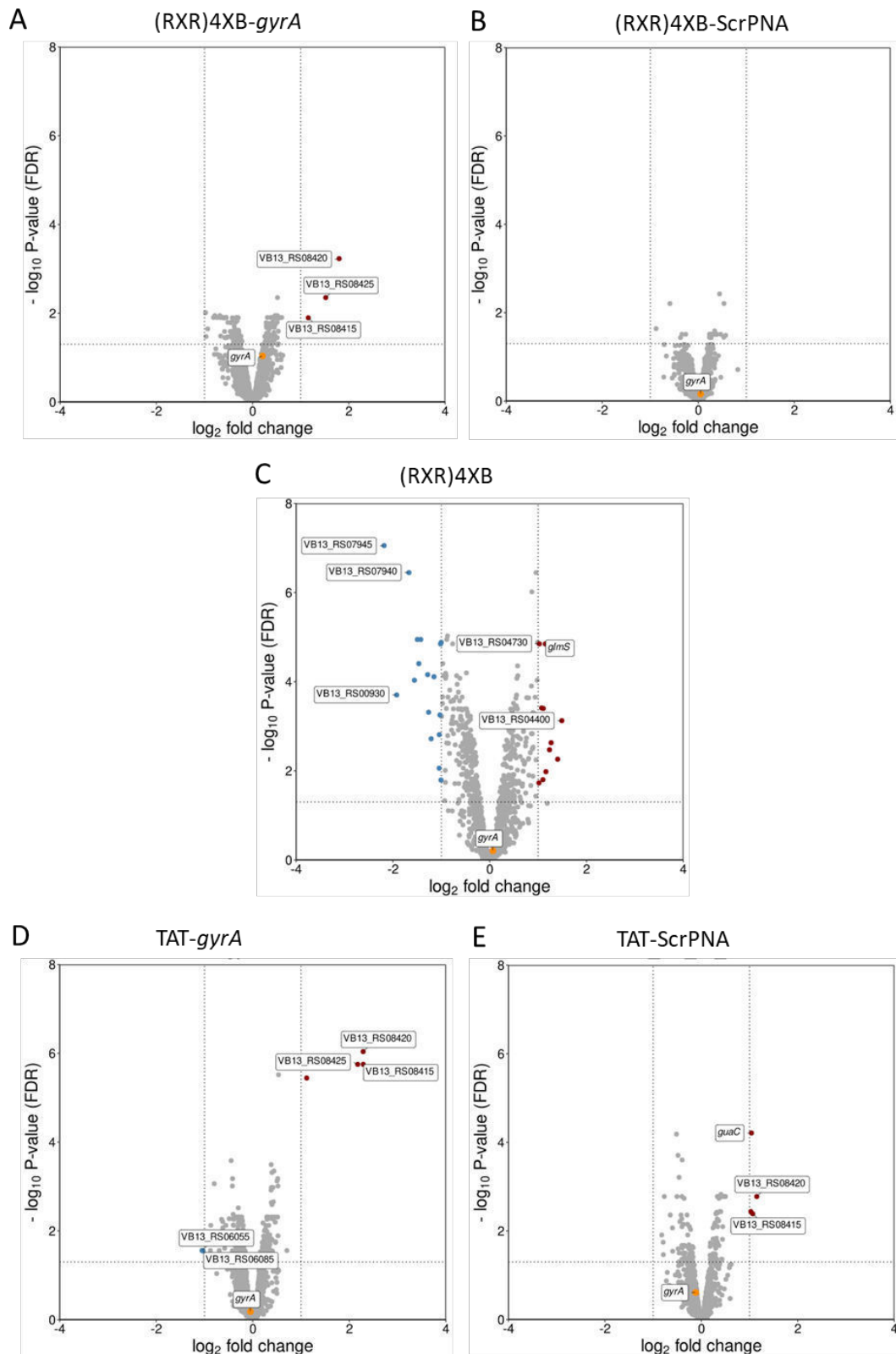


**Figure 23: Transcriptomic responses of *S. pyogenes* upon CPP-PNA and CPP treatment.** Volcano plots show changes in transcript abundance as  $\log_2$  fold changes and false discovery rate (FDR)-adjusted  $-\log_{10}$  p-value. Data were generated of  $10^6$  CFU/ml bacteria treated for 6 h with  $4 \mu\text{M}$  of (A)  $(\text{RXR})_4\text{XB}$ -anti-*gyrA* PNA, (B)  $(\text{RXR})_4\text{XB}$ -scrPNA (randomized sequence), (C)  $(\text{RXR})_4\text{XB}$ , (D) TAT-anti-*gyrA* PNA, and (E) TAT-scrPNA, versus untreated (water) control. Genes with a fold change  $> 2$  and FDR-adjusted p-value  $< 0.001$  of transcript abundances were considered as significantly differentially regulated. Significantly upregulated genes (red) and downregulated genes (blue) are marked; the three most differentially expressed genes are named in the figure. The figure was generated by Jakob Jung.

## Results

Of the genes with significantly changed expression levels after (RXR)<sub>4</sub>XB-anti-*gyrA* PNA treatment, two were genes of domains with unknown function (DUF), and one was encoding a protein of the PadR family of transcriptional regulators. These three genes were also upregulated after incubation with TAT-anti-*gyrA* PNA and TAT-scrPNA. However, they were not affected by treatment with (RXR)<sub>4</sub>XB-scrPNA or (RXR)<sub>4</sub>XB. Additionally, the TAT-coupled PNAs led to increased *guaC* expression, which encodes a GMP reductase. The only significantly downregulated genes were two hypothetical proteins, one of which is potentially involved in DNA repair.

Pathway enrichment analysis (Figure 24) reveals the low transcriptomic changes upon the treatment conditions tested. Incubation of GAS with (RXR)<sub>4</sub>XB resulted in decreased biosynthesis of aminoacyl-tRNA and fatty acid, which was not observed under the other conditions tested.



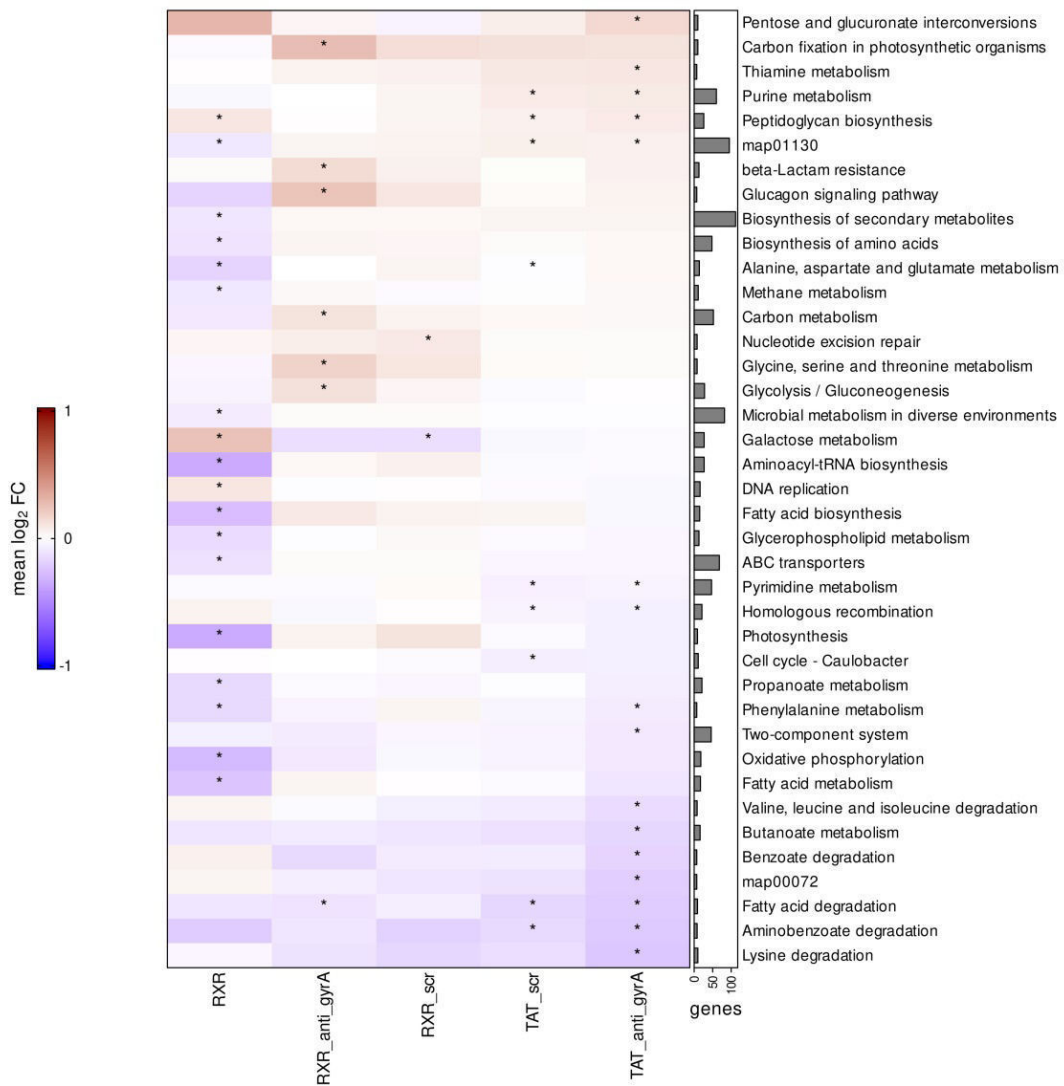
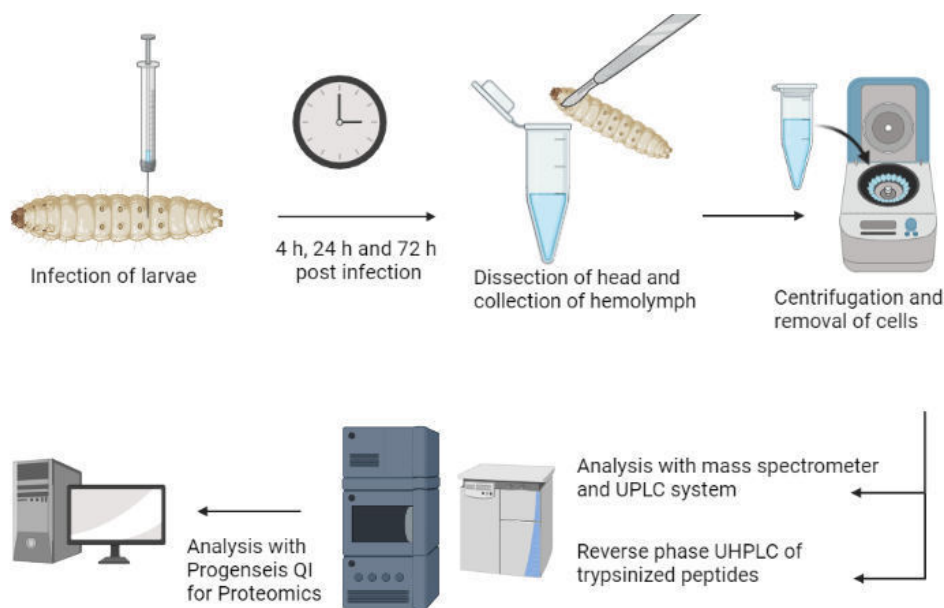


**Figure 24: Pathways with differentially expressed genes of *S. pyogenes* upon CPP-PNA and CPP treatment.** The heat map was generated with RNA Seq. data of  $10^6$  CFU/ml bacteria treated for 6 h with 4  $\mu$ M of (RXR)<sub>4</sub>XB, (RXR)<sub>4</sub>XB-anti-*gyrA* PNA, (RXR)<sub>4</sub>XB-scrPNA, TAT-anti-*gyrA* PNA and TAT-scrPNA. Log<sub>2</sub> fold changes (FC) of gene transcript abundances compared to untreated (water) sample are displayed with blue (downregulation) and red (upregulation). Genes were considered significantly differentially expressed (\*) when FC > 2 and FDR-adjusted p-value < 0.001. The figure was generated by Jakob Jung.

### 3.4 Investigation of the immune response of *Galleria mellonella* to *Streptococcus pyogenes* infection using a proteomics approach

*Galleria mellonella* is an increasingly popular invertebrate infection model organism (Jorjão et al., 2018; Wojda et al., 2020), especially due to the similarity of its immune system to the innate immune system of mammals (Pereira et al., 2018). The aim of this work was the investigation of the transferability of the immune response (IR) of *G. mellonella* to mammals and especially humans. Therefore, a proteomics analysis of the IR of *G. mellonella* to *S. pyogenes* infection was performed.  $2 - 4 \times 10^6$  CFU GAS M49 strain 591 were injected per larva. This dose resulted in a constant mortality rate over 7 days, leading to the death of around 80 % of larvae during the course of the experiment (Figure 38, appendix). The workflow of the experiment is shown in Figure 25. Cell-free hemolymph of infected larvae was collected at time points 4, 24, and 72 h post-infection (p.i.). Mock-infected larvae served as control.



Created in BioRender.com bio

**Figure 25: Workflow of proteomics analysis of cell-free hemolymph of infected *G. mellonella* larvae.** Larvae were infected with  $2 - 4 \times 10^6$  CFU *S. pyogenes* 519. 4 h, 24 h, and 72h post infection (p.i.) hemolymph was collected, pooled and protected with an anticoagulant mixture. Cells were removed via centrifugation. Mass spectrometric analysis was carried out by Dr. Mikkat using the Synapt G2-S mass spectrometer and nanoAcquity UPLC. Trypsinized peptides were additionally separated by reverse phase UHPLC. Analysis was performed with Progenesis QI for Proteomics. Figure was created with BioRender.

### 3.4.1 Infection of *Galleria mellonella* with *S. pyogenes* caused changes of the protein abundance over time

Cell-free hemolymph of infected and non-infected larvae was analysed by Dr. Mikkat (Core Facility Proteomics, University of Rostock) with label-free mass spectroscopy and UPLC. The number of proteins identified in infected larvae with altered abundance compared to non-infected larvae is shown in Table 24.

**Table 23: Proteins with altered amount in cell-free hemolymph 4, 24, and 72h p.i..** Proteins abundance was considered as significantly changed at a fold change  $> 2$  and  $p < 0.05$  (ANOVA).

		<b>4 h</b>	<b>24 h</b>	<b>72 h</b>
<b>Total number of proteins with changed abundance:</b>		249	250	246
	Increased in infected	160	186	168
	Reduced in infected	89	64	78
<b>Number of proteins with significantly changed abundance:</b>		43	153	163
	Increased in infected	30	143	121
	Reduced in infected	13	10	42
<b>Among them: uncharacterized proteins with significantly changed abundance</b>		5	14	32
	Increased in infected	4	12	22
	Reduced in infected	1	2	10

The overall proteomic response of *G. mellonella* larvae to infection with *S. pyogenes* is presented in volcano plots (Figure 26) displaying significance over fold-change of protein quantity. Protein abundances with a max fold change of  $> 2$  with a statistical significance of  $p < 0.05$  (ANOVA) were considered as significantly changed in this work.

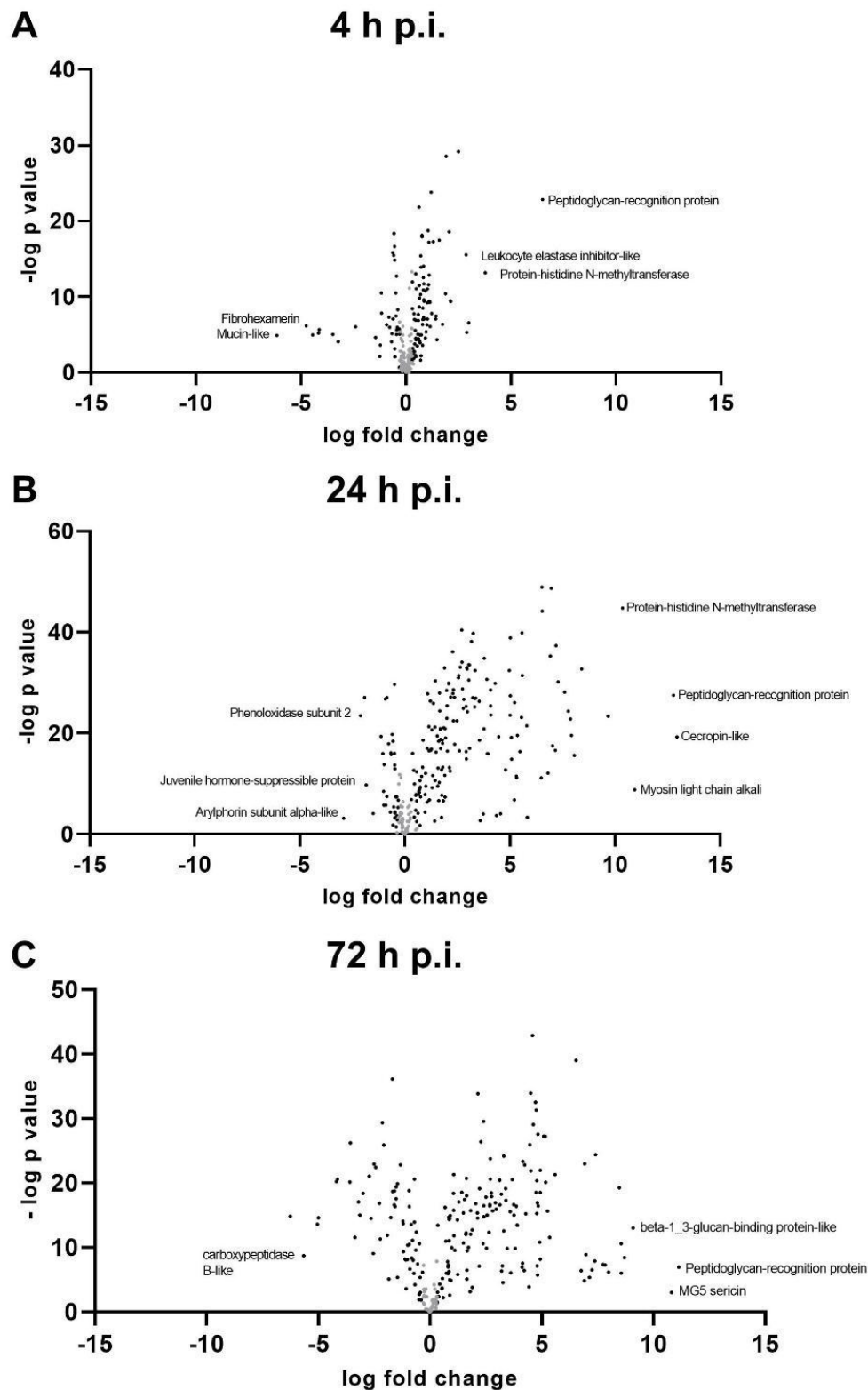


**Figure 26: Proteomic response of *Galleria mellonella* larvae infected with  $2 - 4 \times 10^6$  CFU of *S. pyogenes* 591 after (A) 4 h, (B) 24 h, and (C) 72 h p.i..** The volcano plots show the differences of protein amount between infected and control larvae as log fold change and the significance of change as - log p-value (ANOVA). Black dots present proteins with significantly altered abundance, grey dots present proteins that were not significantly changed.

Four hours p.i., only 43 proteins with significantly changed abundance were detected. Among them were proteins for recognition of foreign surfaces, serine proteases which can be easily generated from circulating zymogens, and an enzyme catalysing posttranslational modification contributing to cytoskeleton integrity (Protein-histidine N-methyltransferase). After 24 h, the number of proteins that occurred with increased amounts in the hemolymph was higher than after the other two time points studied. 72 h p.i., many of the proteins present at reduced levels compared to non-infected larvae were involved in development and metabolism.

Proteins with different concentration in infected and control larvae were grouped based on their biological function either stated by UniProt or inferred from the literature. A table listing the accession number, protein description and significant fold change between infected and control larvae at different time points of all grouped proteins in this work is provided in the appendix (Table 27).

Overall, proteins associated with humoral and cellular immune response showed altered abundance following infection.

### **3.4.1 Proteins of the humoral immune response**

The amount of proteins associated with non-self recognition and of opsonins that increased upon *S. pyogenes* infection is plotted over time (Figure 27). Among those were eight peptidoglycan recognition proteins (PGRPs) (strongest increase of an PGRP at 24 h: 7058-fold; another at 72 h: 2238-fold), seven  $\beta$ -1,3-glucan recognition proteins (strongest increase measured at 72 h: 555-fold), hemolin (24 h: 2.7-fold) and hemicentin 1-like (24 h: 92-fold). The strongest rise of recognition proteins following infection was observed between four and 24 h p.i.. The levels of the opsonin cationic peptide 8 (GmCP8) and C-type lectins remained constant in infected larvae.

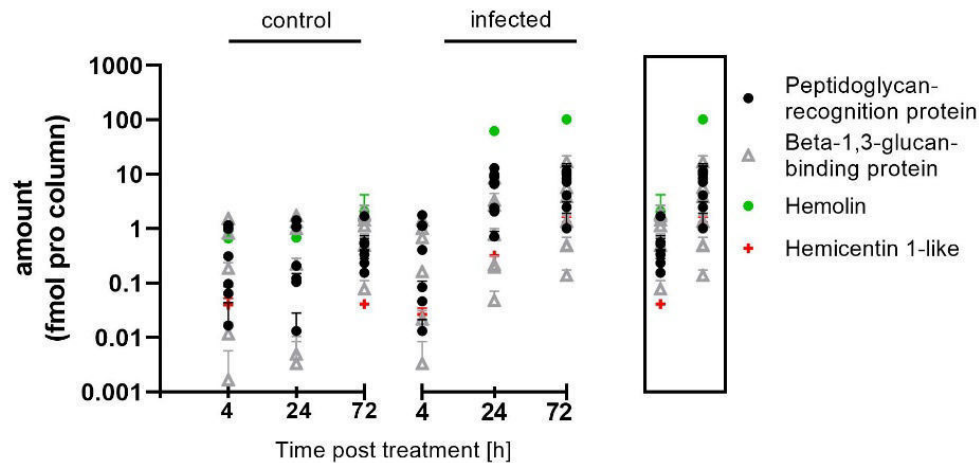


**Figure 27: Proteins associated with non-self recognition.** The amount of protein detected in the cell-free hemolymph of control and infected larvae at 4, 24, and 72 h p.i. is displayed. In the box, the quantity of proteins in control larvae (left) and infected larvae (right) at 72 h p.i. is shown in direct comparison. Only proteins with significantly altered concentrations (fold change  $\geq 2$  and  $p < 0.05$  (ANOVA)) compared to untreated control are displayed. The data of four independent biological replicates are illustrated as mean value with standard deviation.

A gustatory receptor candidate protein and several chemosensory and odorant binding proteins were present at different abundance in infected larvae compared to non-infected larvae. A very strong increase was measured for gustatory receptor candidate 59 (4 h: 7.4-fold; 24 h: infinity; 72 h: 254.2-fold). Two odorant binding proteins were elevated, while one was reduced in infected larvae. Chemosensory proteins (CPs) with increased amount in GAS infection were CP 15 (24 h: 818-fold change), CP 14, 8, 6, and 3, while CP 16 decreased (72 h: -4.4-fold). The inconsistent expression of these proteins indicates that they play different roles during infection.

The phenol oxidase system is a fast response to injury and invading pathogens. The cascade results in production of the polymer melanin, which clots the wounds and traps invading microorganisms. It is further involved in cellular immune response mechanisms as encapsulation (Eleftherianos and Revenis, 2011). Upon activation by binding of surface compounds of pathogens or components of destructed tissue by recognition proteins, serine proteases cleave the zymogen prophenol oxidase to phenol oxidase (PO). PO oxidizes phenols to quinones, that are polymerized to melanin (González-Santoyo and Córdoba-Aguilar, 2012; Jiang et al., 1997). Dopachrome tautomerase are further enzymes involved in biosynthesis of melanin (Barek et al., 2022; Xia et al., 2006). In infected larvae, the abundance of two prophenol oxidases decreased (24 h: 4-fold; 72 h: 5-fold), while the levels a PO activating enzyme (24 h: 37-fold; 72 h: 27-fold) and two dopachrome tautomerase (one identified via blasting the sequence) increased (24 h: 3- and 15-fold; 72 h: 6.5- and 17.8-fold). The data are therefore consistent with the activation of this immune cascade.

The large repertoire of antimicrobial peptides (AMPs) of *G. mellonella* is crucial for its immune response by directly killing invading microorganisms. *G. mellonella* is known to distinguish between different pathogen types and is able to express a relatively specific AMP response (Mak et al., 2010). GAS infection led to increased levels of 16 AMPs of nine classes. They are listed with corresponding fold changes in Table 24 and illustrated in Figure 28. Most AMPs were absent in non-infected larvae. Strongest increase of AMP levels were observed 24 h p.i.. The AMP classes with highest fold change of abundance were gloverins, cecropins, the inducible metalloproteinase inhibitor (IMPI), and the silk protein seroin. Gloverins and cecropins are typical antibacterial peptides (Asai et al., 2021; Brady et al., 2019; Wang et al., 2018). IMPI is a well characterized and important antimicrobial agent with broad range of action (Clermont et al., 2004; Vertyporokh and Wojda, 2017; Wedde et al., 1998), while seroin is a less described antibacterial peptide (Nirmala, Mita et al., 2001; Singh et al., 2014; Zhu, H. et al., 2020). These data show, that AMP production, which is the most essential part of defence, is activated by GAS infection.

**Table 24: Accession number and description of putative antimicrobial peptides (AMPs) with fold changes at three different time points in infected larvae compared to control.** Only significant fold changes (fold change > 2 and  $p < 0.05$  (ANOVA)) are listed.

Accession number	Description	Fold change		
		4 h	24 h	72 h
A0A6J1X9I2;Q8ITT0	Gloverin		235	166.5
A0A6J1W9I9	Gloverin-like		121.1	354.6
A0A6J1WQI3	Gloverin-like		146.1	4.6
P85210	Cecropin-D-like peptide		Infinity	Infinity
A0A6J1WJ15	Cecropin-like	Infinity	7873	417.7
A0A6J1WAG2	Lysozyme		7.8	24.6
A0A6J1WSB4;P82174	Lysozyme		8.4	14.5
A0A6J1W7W4	Lysozyme		3.4	3.7
C9WHZ7;P85211;P85214	Proline-rich protein		48	19.4
A0A6J3CC84	Inducible metalloproteinase inhibitor protein		130.8	376.5
A0A6J1X0P3;A0A6J3C8K9	Seroin isoform X2	21.6	37.1	228.7
Q8ITT4;A0A6J1X5W9	6tox		32.5	38.2
A0A6J1W9L8	Apolipoprotein D-like	2.1	7.7	6.7
A0A6J1X1K1	Apolipophorins-like			2.1
A0A6J3C047	Apolipophorins-like			2.1
A0A3G1T196;P85216	Anionic antimicrobial peptide 2		2.5	

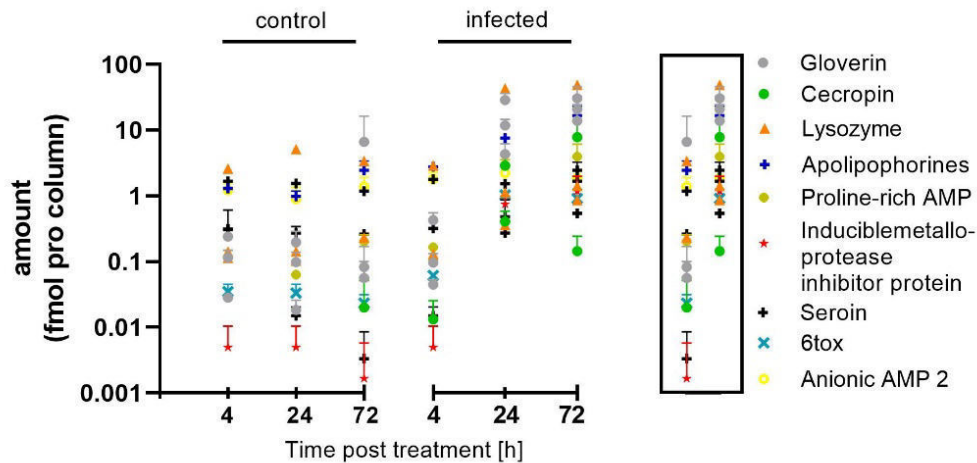


**Figure 28: Antimicrobial peptides (AMPs).** The amount of protein detected in the cell-free hemolymph of control and infected larvae at 4, 24, and 72 h p.i. is displayed. In the box, the quantity of proteins in control larvae (left) and infected larvae (right) at 72 h p.i. is shown in direct comparison. Only proteins with significantly altered concentrations (fold change  $\geq 2$  and  $p < 0.05$  (ANOVA)) compared to untreated control are displayed. The data of four independent biological replicates are illustrated as mean value with standard deviation.

In this study, upregulation of several heat shock proteins (HSP) was observed in *G. mellonella* following GAS infection: small HSP20 and small HSP21.4 (24 h: 15.5- and 9.5-fold, respectively), as well as the HSP27.4 and 70 (24 h: 7.5- and 6.6-fold). HSPs are known to be modulators of mammalian immune response (Pockley, 2003; Srivastava et al., 1998; Wrońska and Boguś, 2020) and important for protection of insects against environmental stress, including pathogens (Guz et al., 2020; Iryani et al., 2017; Wrońska and Boguś, 2020).

Serine proteases (SPs) are essential in larval food digestion and have multiple functions in the IR (Kanost and Jiang, 2015; Patel, 2017), such as activation of the phenol oxidase system resulting in melanisation (Kanost, M. R., Gorman, M. J., 2008). Within the large group of SPs, especially CLIP SPs are important immune factors, as they are rapidly activated upon recognition of foreign material and cleave the cytokine Spätzle, which is the ligand for the Toll signalling cascade (An et al., 2010; Jang et al., 2006; Roh et al., 2009). SPs activation and inhibition is strictly regulated (Silverman et al., 2001). Here, four non-dietary SPs and eight SP inhibitors showed elevated levels upon infection. Among them were two CLIP SPs (24 h: 10.4- and 8.5-fold; 72 h: 26.7- and 10.5-fold) and two inhibitors which were identified as leukocyte elastase inhibitor-likes (24 h: 339.4- and 9.4-fold; 72 h: 13.5- and 22.6-fold). Most SP inhibitors were already upregulated at 4 h p.i., indicating a role during the early immune response.

Further, putative immune-relevant proteins and peptides with changed abundance upon GAS infection were identified (Figure 29).



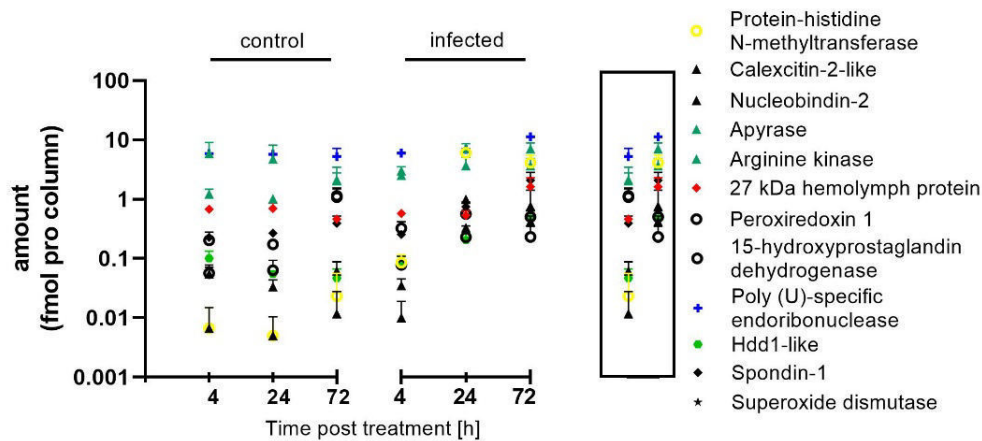


**Figure 29: Putative immune-relevant proteins.** The amount of protein detected in the cell-free hemolymph of control and infected larvae at 4, 24, and 72 h p.i. is displayed. In the box, the quantity of proteins in control larvae (left) and infected larvae (right) at 72 h p.i. is shown in direct comparison. Only proteins with significantly altered concentrations (fold change  $\geq 2$  and  $p < 0.05$  (ANOVA)) compared to untreated control are displayed. The data of four independent biological replicates are illustrated as mean value with standard deviation.

Among them were two negative regulators of IR: Peroxiredoxin and 15-hydroxyprostaglandin dehydrogenase, which initially increased (3.2- and 3.6-fold, respectively) until 24 h and then decreased (-2.3- and - 4.7-fold, respectively) until 72 h p.i.. Further, two extracellular ATP-level modulating proteins were detected in increased amounts in infected larvae: ATPase apyrase (72 h: 3.3-fold) and arginine kinase (24 h: 7-fold).

Enzymes involved in production and regulation of reactive oxygen species (ROS) displayed significantly changed levels in the larval hemolymph following infection. Superoxide dismutase (24 h: 243-fold), which produces hydrogen peroxide ( $H_2O_2$ ), and sulfhydryl oxidase (72 h: 5.7-fold), generating  $H_2O_2$  as by-product during catalysis of protein folding by forming disulphide bonds, were present at elevated levels. The amount of the antioxidant catalase was diminished by half at 72 h p.i., while the level of thioredoxin (24 h: 5.9-fold), involved in ROS homeostasis, was raised.

### 3.4.2 Proteins of cellular immune response

In addition to components of the humoral branch also proteins involved in cellular IR were elevated following GAS infection.

The calcium-binding protein calnexin (24 h: 156-fold), and nucleobindin-2 (72 h: 12.2-fold) which is involved in calcium homeostasis via storage and release, were increased. Both proteins are associated with phagocytosis and inflammation (Boullaran and Kehrl, 2014; Huang et al., 2016; Stendahl et al., 1994).

One uncharacterized protein (A0A6J1X587) which was 20-fold increased 72 h p.i. was identified via sequence comparison using BLAST® (Altschul et al., 1997) as Hdd1-like. Noduler Hdd1 and Hdd11 are considered to be essential for crosslinking of hemocytes and pathogens to encapsulate foreign material (Sheehan et al., 2020).

Furthermore, a putative endonuclease (A0A6J1WSG1) (72 h: 2.2-fold) with high sequence similarity (83 % identities) to poly (U)-specific endoribonuclease P102 of *Heliothis virescens* (Lepidoptera: Nocturidae) was identified. P102 was shown to be involved in formation of amyloid fibrils and thereby contributing to encapsulation (Pascale et al., 2014). The sequence alignment of the putative endonuclease and P102 of *Heliothis virescens* is depicted in Figure 30.

Score	Expect	Method	Identities	Positives	Gaps
632 bits(1631)	0.0	Compositional matrix adjust.	291/349(83%)	323/349(92%)	0/349(0%)
Query 1	MKIIFIFLLCLVACRADDIAHAAGQIFNSILPNLITNSVTGQQGNTGANTLQQIGTVVGG				60
Sbjct 16	MK+ + L CL CRADD+AHAAGQIFN+ILPNLITNSVTGQQGNT NTLQQIGTVVGG				75
Query 61	VVDYAKKKSIEDLLKQVQDSTDDDLRLSEEMFNGDVNNAFYIEVNLQKTSAMTKND				120
Sbjct 76	VVDYAKKKSIEDLLRQVQDSTTDEDILRVSEEMFNADINMALAYIQVNLQKTSPLSKDD				135
Query 121	QAQNLLNVPDAVWNGPTIKPFVALFDNYHKNVIRPEFVTPNEESEQTTFFINTILATGPI				180
Sbjct 136	+A NLL+VP+ VWNGPTI+PF ALFDNYHKNVIRPEFVTPNEE+EQ TFINTILATGPI				195
Query 181	RSLMAFLVNKGLTQLNEYEQVELLRKIWFTKYARHWTGICKCSCAFENIFMAELKSDQV				240
Sbjct 196	RSLM FLV+KGLTQ+NEYEQVELL+KIWFTKYARHWTG+CKCSCAFENIFMAELKS+ V				255
Query 241	LGLHSWLFFAKRELDHKANYLGYIDKLDLSGKGLILKQHSILSETKDAPEVTMFGVTSPE				300
Sbjct 256	LGLHSWLFFAKRE D KANYLGY+DKLDLSGKG+ILKQHSILSETKDAPEVTMFGVTSPE				315
Query 301	LETALYTLCFMARPDPRCKLRYNNVNFVIQTKTIRSDNPLIDTGYPMF				349
Sbjct 316	LE ALYT+CFMARPDPRC+LRYNN+NF IQTKT++SDN+ LIDT YP +				364

**Figure 30: Sequence alignment of endonucleases. Endonuclease of *G. mellonella* (A0A6J1WSG1) (Query 1) and poly (U)-specific endoribonuclease P102 of *Heliothis virescens* (F6IA34) (Sbjct) are aligned using BLAST® (Altschul et al., 1997).**

A putative immune-relevant protein in *G. mellonella* with a rapid and very high increase in abundance during infection is a protein-histidine N-methyltransferase (4 h: 13.7-fold; 24 h: 1309.3-fold; 72 h: 170.3-fold). It catalyses actin modification via peptidyl-histidine methylation, which is a posttranslational modification regulating actin polymerization dynamics.

### 3.4.3 Proteins not associated with the immune response

Besides proteins directly involved in the IR, the level of tissue components, especially cytoskeletal and muscular proteins, was also elevated. The alteration of concentration over time is illustrated in Figure 31. Some of the peptides were already increased after 4 h, the strongest

fold change was observed between four and 24 h, e.g. myosin light chain alkali (1970-fold) and tropomyosin-2 (266.7-fold).

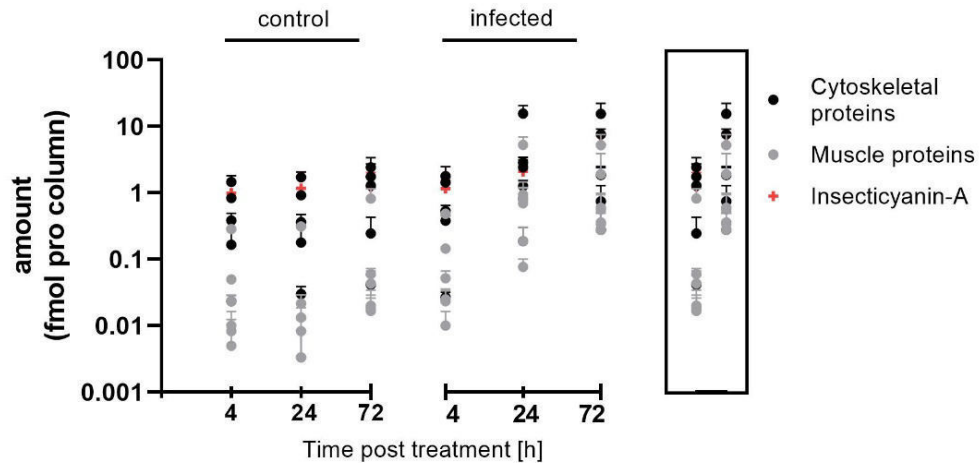


**Figure 31: Tissue proteins.** The amount of protein detected in the cell-free hemolymph of control and infected larvae at 4, 24, and 72 h p.i. is displayed. In the box, the quantity of proteins in control larvae (left) and infected larvae (right) at 72 h p.i. is shown in direct comparison. Only proteins with significantly altered concentrations (fold change  $\geq 2$  and  $p < 0.05$  (ANOVA)) compared to untreated control are displayed. The data of four independent biological replicates are illustrated as mean value with standard deviation.

In infected larvae, the amount of twelve dietary gut enzymes in the hemolymph was strongly elevated. Among them were several trypsins and chymotrypsins, proteinases as papain-like cysteine proteases and cathepsin L, and pancreatic-like lipases. Furthermore, a chitin deacetylase 8 (72 h: 15-fold) was identified via sequence comparison using BLAST® (Altschul et al., 1997), which is associated with modification of the peritrophic membrane of the midgut (Liu et al., 2019). However, despite caution, contamination of the hemolymph with gut enzymes during the decapitation of the larvae cannot be ruled out.

The amount of silk fibers (fibroins), glue-like protein sericin, and the antimicrobial silk protein seroin was reduced dramatically over time in control larvae, while increasing in infected larvae to a similar extent (Figure 32). Differences in the amount at 72 h for fibers were 28.2 – 375-fold, for seroin 228.7-fold, while the changes of sericin level were not significant due to the high variance between samples.

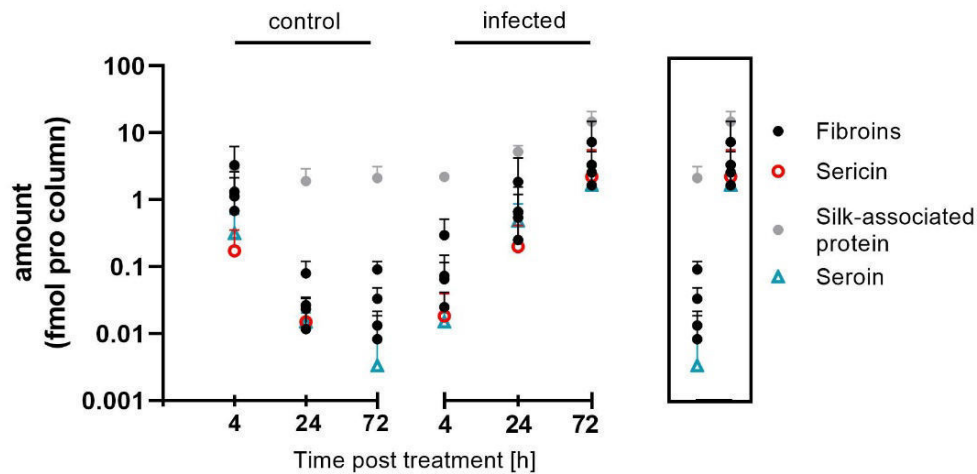


**Figure 32: Silk proteins.** The amount of protein detected in the cell-free hemolymph of control and infected larvae at 4, 24, and 72 h p.i. is displayed. In the box, the quantity of proteins in control larvae (left) and infected larvae (right) at 72 h p.i. is shown in direct comparison. Only proteins with significantly altered concentrations (fold change  $\geq 2$  and  $p < 0.05$  (ANOVA)) compared to untreated control are displayed. The data of four independent biological replicates are illustrated as mean value with standard deviation.

Further, proteins of metabolic and developmental pathways were affected by GAS infection. The abundance of nine carboxylases and three glutathione-S-transferases, which are generally associated with xenobiotic detoxification, increased strongly in infected larvae. In contrast, the amount of proteins involved in metabolic pathways rose in non-infected larvae between 24 and 72 h, whereas they remained constant or decreased in infected larvae (Figure 33).

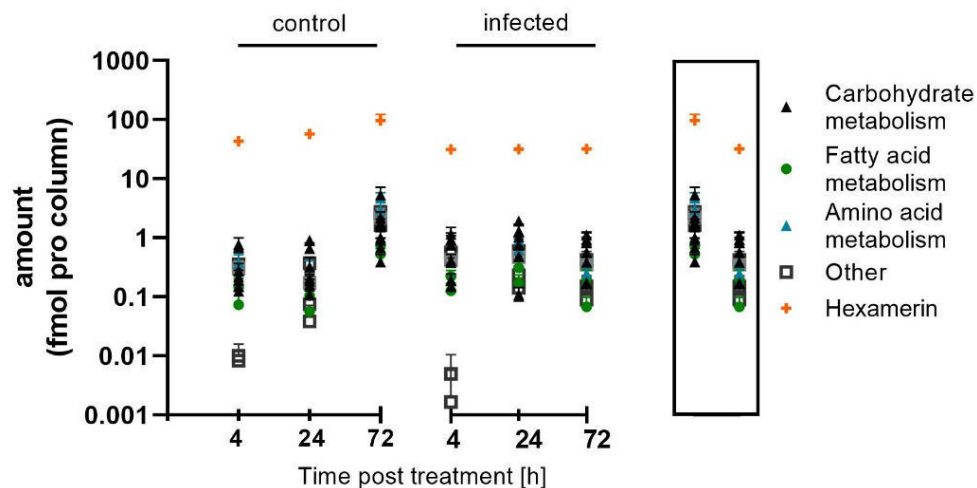


**Figure 33: Proteins involved in metabolism.** The amount of protein detected in the cell-free hemolymph of control and infected larvae at 4, 24, and 72 h p.i. is displayed. In the box, the quantity of proteins in control larvae (left) and infected larvae (right) at 72 h p.i. is shown in direct comparison. Only proteins with significantly altered concentrations (fold change  $\geq 2$  and  $p < 0.05$  (ANOVA)) compared to untreated control are displayed. The data of four independent biological replicates are illustrated as mean value with standard deviation.

Proteins associated with growth or known to be essential for metamorphosis were found with elevated or constant levels in non-infected larvae, while they were reduced in infected larvae.

## Results

At 72 h p.i. two juvenile hormone (JH)-suppressible proteins (-2.7- and -3.2-fold), three spermine oxidases (-2.5-, -2.9- and -3.2-fold), vitellogenin (-2.3-fold), carboxylpeptidase B-like (-50.6-fold), sericotropin (-33-fold), and a subunit of arylphorin (-31.9-fold) were reduced. The only exception was a JH esterase-like protein (24 h: 33.4-fold; 72 h: 121.4-fold) which had increased levels in infected larvae but was constant in the control.

In summary, proteins not associated with the IR with increased abundance in the hemolymph upon GAS infection were tissue components, dietary gut enzymes, silk-associated proteins, and enzymes involved in xenobiotic detoxification. In contrast, proteins of metabolic pathways and developmental processes were decreased in infected larvae.

## 4 Discussion

### 4.1 Antimicrobial effect of antisense CPP-PNAs on *Streptococcus pneumoniae*

Antisense technology for treatment of diseases is an emerging field. Several synthetic antisense oligonucleotides have been approved by FDA (United States Food and Drug Administration) and EMA (European Medicines Agency) as therapeutics within the last years (Kulkarni et al., 2021). Examples are the medication Amondys 45 to treat Duchenne muscular dystrophy (Shirley, 2021; U.S. Food and Drug Administration, 2021), Spinraza to medicate spinal muscular atrophy (Chiriboga, 2017; U.S. Food and Drug Administration, 2016), and Kynamro for hypercholesterolemia (Hair et al., 2013). PNAs have several advantages compared to other antisense oligonucleotides due to their stable structure and their high affinity to complementary nucleic acid sequences. For carrier-coupled-antisense PNAs to be used as antimicrobial agents, they need to enter bacteria, which have more surface barriers than human cells.

In this work, CPP-PNA conjugates with antimicrobial activity against clinically relevant *S. pneumoniae* strains were identified. The activity and kill kinetics were investigated, and additionally the specific effects were determined in a cell-based system. Further, the target specificity of the PNA molecules was proven by determination of the reduction of target transcript levels. The effectiveness of the conjugates was demonstrated *in vivo*, using the invertebrate model organism *Galleria mellonella*.

#### 4.1.1 CPP-PNA conjugates with antimicrobial activity in *S. pneumoniae*

(RXR)<sub>4</sub>XB- and TAT-anti-*gyrA* PNA conjugates mediated significant dose-dependent CFU reduction at concentrations of 5 – 20  $\mu$ M in *S. pneumoniae* TIGR4. Treatment of *S. pneumoniae* TIGR4 with 10  $\mu$ M (RXR)<sub>4</sub>XB-anti-*gyrA* PNA resulted in continuous CFU reduction and complete eradication of the pathogen after 12 h. In contrast, the antibacterial effect of TAT-anti-*gyrA* PNA was lower and the TAT-scrPNA control caused a continuously increasing toxic effect. As scrPNA exhibit a randomized sequence of the bases of the antisense PNA sequence, and are not complementary to the start region of any essential gene in pneumococci, bactericidal activity of CPP-scrPNA indicate unspecific toxic effects of the molecule. Such are most likely caused by the carrier molecule (Abushahba, Mohammad, Thangamani et al., 2016; El-Andaloussi et al., 2007; Langel, 2019). The data presented here show that the strong bactericidal effect of the (RXR)<sub>4</sub>XB-anti-*gyrA* PNA conjugate was caused sequence-specifically by the

antisense PNA and identifies (RXR)<sub>4</sub>XB as effective carrier for PNAs in pneumococci. This CPP is also more effective as carrier of PNAs than TAT in *S. pyogenes* and in *Listeria monocytogenes* (Abushahba, Mohammad, Thangamani et al., 2016; Barkowsky et al., 2019). Unspecific toxicity of TAT-scrPNA was also observed in *S. pyogenes* and was even stronger than in pneumococci (Barkowsky et al., 2019).

There were more differences observed in CPP-PNA activity between the two streptococcal species, as antisense PNAs conjugated to the oligolysine K8 had no antimicrobial activity in pneumococci, although K8 had been shown to be an effective carrier of PNA in *S. pyogenes*. In contrast, the oligoarginine R9-anti-*gyrA* PNA conjugate caused CFU reduction in pneumococci, while PNA conjugates with the CPPs R6 and R10 were not bactericidal in *S. pyogenes* (Barkowsky et al., 2019). The uptake of CPP-coupled PNAs is not only species-specific but can also depend on the strain. CFU reduction caused by (RXR)<sub>4</sub>XB-anti-*gyrA* and TAT-anti-*gyrA* PNA conjugates was similar for pneumococcal strains TIGR4 and D39, but strain 19F was less sensitive. Differences of the antimicrobial activity of CPP-PNAs between strains were also observed in *S. pyogenes* and *L. monocytogenes*. In *L. monocytogenes* the MIC of (RXR)<sub>4</sub>XB-PNA varied among different strains between 0.25 and 4 µM (Abushahba, Mohammad, Thangamani et al., 2016). In *S. pyogenes*, serotype M18 was not affected at all by 5 µM TAT-PNA, while other serotypes were reduced by 2.5 log<sub>10</sub> CFU at the same concentration. It is likely that the presence of a capsule influences the sensitivity of bacteria to CPP-PNA. The MIC of CPP-PNAs was lower in *L. monocytogenes*, which lack a capsule (McLaughlin et al., 2014), than in *S. pyogenes* (Abushahba, Mohammad, Thangamani et al., 2016; Barkowsky et al., 2019). A comparably high concentration of CPP-PNAs was necessary in pneumococci, which produce a thick polysaccharide capsule (Hyams et al., 2009). The capsule of *S. pneumoniae* TIGR4 is relatively thick, approximately twice as thick as that of strains D39 and 19F (Hyams et al., 2009; Moorthy et al., 2016; Zafar, Hamaguchi et al., 2017).

In general, the differences between the serotypes investigated in this study point out the importance to test potentially antimicrobial CPP-PNA conjugates in several different strains. The pneumococcal strains used were selected, because all three are highly virulent. The clinical isolate TIGR4 (serotype 4) causes severe pneumonia and, as D39 (serotype 2), invasive diseases in mice (Aaberge et al., 1995; Lanie et al., 2006; van Ginkel et al., 2003). *S. pneumoniae* 19F is commonly found as asymptomatic colonizer of the nasopharynx, but is also associated with severe disease, especially meningitis with high case fatality rates (Brueggemann et al., 2004; Cohen et al., 2015; Grabenstein and Musey, 2014; Müller et al., 2020). Consequently,

serotype 2 is covered in the pneumococcal polysaccharide vaccine PPSV-23, and serotypes 4 and 19F additionally also in the pneumococcal conjugate vaccines PCV-7, -13, and -20 (Hall E. et al., 2021; U.S. Food and Drug Administration, 2018, 2019, 2022).

In this work, anti-*gyrA* PNA was compared with anti-*rpoB* PNA and *gyrA* was identified as more suitable target for antisense PNA in pneumococci. Both genes are essential and were shown to be effective targets for antisense PNA in different bacterial species (Abushahba, Mohammad, Seleem, 2016; Abushahba, Mohammad, Thangamani et al., 2016; Kurupati et al., 2007; Patenge et al., 2013). It is not yet known what makes a gene a particularly efficient target for antisense PNAs. Popella and coworkers showed, that transcript abundance is not predictive of the target's vulnerability (Popella et al., 2021).

Several more carriers were screened that were either described to be effective in mediating uptake of cargos into other bacterial species or into cell lines, or described as sequences with potential translocating activity. One example was a predicted CPP sequence obtained from SARS-CoV-2 (Kardani und Bolhassani 2021). In addition to CPPs with translocating activity, an AmiA ligand was tested as possible carrier as it is actively taken up by an ABC transporter. AmiA is an oligopeptide permease binding the peptide AKTIKITQTR extracellularly and transporting it into the cytoplasm (Nasher et al. 2018). The AKTIKITQTR-anti-*gyrA* PNA construct had no antimicrobial activity, indicating that the transporter does not recognize the molecule coupled to the cargo or is unable to transport this larger molecule. None of the 22 carrier-PNA conjugates tested in this study had a higher specific antimicrobial activity than (RXR)<sub>4</sub>XB-anti-*gyrA*.

The CPPs (RXR)<sub>4</sub>XB and TAT alone caused a stronger unspecific antibacterial effect in pneumococci than the corresponding PNA-constructs. A similar observation was made by El-Andaloussi and coworkers when comparing the cytotoxicity of unbound CPPs and CPP-cargo conjugates. Free TAT caused a higher membrane disturbance of HeLa cells than TAT coupled to a cargo, and different cargo types influenced the degree of toxicity as well (El-Andaloussi et al. 2007). Together, these data support the usefulness of CPP-scrPNA as control rather than the CPPs alone, since they are chemically comparable to the CPP-antisense PNA molecules. In general, CPP-scrPNAs are considered a more suitable control than free CPPs (Jones et al., 2005; Popella et al., 2022; Stein, 1999).

#### **4.1.2 Target specificity of PNAs**

Treatment of pneumococci with sublethal concentrations of CPP-anti-*gyrA* PNA and CPP-anti-*rpoB* PNA conjugates significantly reduced the relative abundance of target gene transcripts. A



higher concentration of CPP-anti-*rpoB* PNA conjugates was needed for a target transcript reduction comparable to treatment with CPP-anti-*gyrA* PNA conjugates. This is in accordance with the higher antimicrobial activity of CPP-anti-*gyrA* PNA conjugates.

The gene *rpoB* encodes the  $\beta$ -subunit of the RNA polymerase, which is essential for gene transcription. Consequently, diminished expression of the RNA polymerase due to CPP-anti-*rpoB* PNA treatment resulted in reduced transcript abundance of the two virulence genes *pspA* and *ply*, which encode the pneumococcal surface protein A and pneumolysin, respectively. Although TAT-anti-*rpoB* PNA did not exhibit antimicrobial activity at the concentrations tested, it caused significant reduction of *ply* mRNA levels at sublethal concentrations. Reduced expression of pneumolysin following treatment with CPP-*rpoB* PNA might attenuate pneumococcal virulence, as the toxin pneumolysin is crucial for inflammation and transmission of the pathogen (Pereira et al., 2022; Zafar, Wang et al., 2017). Similar downstream knockdown effects were observed by Abushahba and coworkers, where treatment of *L. monocytogenes* with TAT-anti-*rpoA* PNA caused significant reduction of the transcript level of *rpoA*, which encodes the  $\alpha$ -subunit of RNA polymerase. In a concentration-dependent manner, TAT-anti-*rpoA* PNA treatment resulted in a decrease of the transcripts of three other virulence genes studied (Abushahba, Mohammad, Thangamani et al., 2016).

Some antisense oligonucleotides act by inducing RNase H activity, which cleaves the RNA sequence of the oligonucleotide-mRNA duplex (Liang et al., 2017). PNA activity is RNase H-independent, causing translational repression by sterically blocking target mRNA translation (Ray and Nordén, 2000). How sequestration of the ribosomal binding site of mRNA of a target gene results in alteration of the steady state levels of the target transcripts by PNA is not understood. However, reduced target mRNA levels were measured upon antisense PNA treatment in this work, which was also observed in several other bacterial species, including *L. monocytogenes*, *Klebsiella pneumoniae*, *E. coli*, and *S. pyogenes* (Abushahba, Mohammad, Thangamani et al., 2016; Bai et al., 2012; Barkowsky et al., 2019). Popella and coworkers treated *Salmonella enterica* with CPP-PNA, which resulted in rapid target mRNA decay. They considered that ribonucleases, induced by natural small RNAs (sRNAs), might cause decay of mRNA bound by antisense PNA. However, they have not yet been able to identify a ribonuclease induced by PNA-mRNA duplexes (Popella et al., 2021).

### 4.1.3 Evaluation of CPP-PNAs *in vivo* using an infection model organism

The larvae of the wax worm *Galleria mellonella* are increasingly popular as pre-screening infection model organism to investigate potential therapeutics (Jorjão et al., 2018; Wojda et al., 2020). In this work, larvae were infected with a dosis of *S. pneumoniae* TIGR4 resulting in death of ~ 80 % of infected larvae after 7 days. Treatment with 10 nmol (RXR)<sub>4</sub>XB- and TAT-anti-*gyrA* PNA increased survival rates by 22 % and 25 %, respectively. The efficacy of these constructs was comparable to 1 µg levofloxacin (2.5 x MIC). 24 h after treatment with (RXR)<sub>4</sub>XB-anti-*gyrA* PNA, the bacterial load of infected larvae was significantly reduced in comparison to untreated larvae.

In contrast, treatment with (RXR)<sub>4</sub>XB-anti-*rpoB* PNA did not improve larval survival rates, although the conjugate has an antibacterial effect *in vitro*, and sublethal treatment with CPP-anti-*rpoB* PNA was shown to reduce the expression of pneumolysin *in vitro*. Even though pneumolysin is crucial for inflammation (Nishimoto et al., 2020; Pereira et al., 2022), no effect of the possibly reduced *ply* transcript levels was observed here.

Although the antimicrobial activity of (RXR)<sub>4</sub>XB-anti-*gyrA* PNA was higher than the effect of TAT-anti-*gyrA* PNA *in vitro*, larval survival rates were comparable following treatment with TAT-anti-*gyrA* and (RXR)<sub>4</sub>XB-anti-*gyrA* PNA. Undesirable interactions of small molecule drugs with other off-target molecules can strongly influence its pharmacokinetic (Metz and Hajduk, 2010; Rao et al., 2019). CPP-PNAs were injected close to the infection site, avoiding long routes through the larval body and delivering the therapeutic directly to the pathogen. Yet, the larval midgut is a complex environment that offers many opportunities for CPP-PNA interactions, potentially reducing its effectiveness. In future experiments, pneumococcal pneumonia in mammalian infection models could be treated with CPP-PNAs in the dosage form of an inhalant. Inhalation offers the advantage of site-directed delivery of the CPP-PNAs allowing to decrease the dose.

In general, the invertebrate model *G. mellonella* could be used to demonstrate, that the tested CPP-PNAs (RXR)<sub>4</sub>XB- and TAT-anti-*gyrA* PNA exhibit antibacterial activity *in vivo*.

#### 4.1.4 Perspective of CPP-PNA treatment in pneumococci

In order to be able to use carrier-coupled antisense PNAs as a therapeutic agent for the treatment of pneumococcal infections, more suitable conjugates must be identified. Potential strategies are testing novel PNA targets or improving the uptake of the antisense molecules.

Essential genes that were shown to be effective targets for antibacterial antisense PNAs in different species are, among others, *acpP* encoding a crucial gene for fatty acid synthesis (Popella et al., 2021; Popella et al., 2022), genes of 16s and 23s rRNA (Good and Nielsen, 1998b), or *ftsZ* and *dnaB* encoding a cell division protein and a helicase essential for replication (Popella et al., 2022). Next to essential genes, pneumococcal virulence genes could be targeted. The knock down of pneumolysin is particularly promising, since the cytotoxin plays several crucial roles in pneumococcal pathogenesis. It mediates bacterial spread through the host body, damages cells by its pore-forming activity, contributes to inflammation, blocks complement activation, and is further involved in bacterial transmission (Alcantara et al., 2001; Berry et al., 1989; Berry and Paton, 2000; Nishimoto et al., 2020; Zafar, Wang et al., 2017). Therefore, inhibiting translation of the toxin might greatly reduce the ability of the pathogen to cause severe infection and allow the host immune response to defeat the pathogen.

Further, combination of antisense PNAs and antibiotics could reduce the concentration of antibiotics needed for treatment of pneumococci. Combination of CPP-anti-*gyrA* conjugates with levofloxacin was shown to have a synergistic effect on treatment of *S. pyogenes* and *S. aureus in vitro* (Dryselius et al., 2005; Patenge et al., 2013). Combination of 1 µg levofloxacin with 4 nmol TAT-anti-*gyrA* PNA improved survival rates of GAS infected *G. mellonella* larvae to a comparable extent as treatment with 15 µg levofloxacin (Barkowsky et al., 2019). Furthermore, it could be considered to combine antibiotics with antisense PNA targeting antibiotic resistance genes. Nezhadi and coworkers were able to re-sensitize *E. coli* to colistin with PNA targeting the corresponding resistance gene *mcr-1* (Nezhadi et al., 2019). PNA hybridizing to transcripts of a β-lactamase-resistance gene restored sensitivity of the *E. coli* isolates to cefotaxime (Readman et al., 2016). As antimicrobial resistance in *S. pneumoniae* increases (Cherazard et al., 2017), re-sensitizing the pathogen to antibiotics by addition of suitable CPP-PNAs might be a promising therapeutic approach.

The antimicrobial activity of antisense PNAs could be also improved by increasing their uptake. New CPPs are constantly being identified which can be examined for their translocation activity in pneumococci. CPPs have been identified from various origins and a large proportion of these are viral peptides (Milletti, 2012) such as TAT, which is derived from the transactivating

transcriptional activator of the human immunodeficiency virus 1 (Frankel and Pabo, 1988). Viral peptides constitute a large unexploited repertoire and harbor a variety of putative CPP sequences. Many researchers such as Kardani and coworkers are screening viral genomes for possible CPPs, such as SARS-CoV-2 (Kardani and Bolhassani, 2021). A possible CPP of SARS-CoV-2 was examined in this work for its ability to transport PNAs in pneumococci, but turned out to be ineffective. In addition to CPPs, other carrier systems should be considered. PNAs could be linked to molecules that are actively transported into bacteria with an uptake system. Równicki and coworkers conjugated PNA to vitamin B12, which is an essential molecule in many bacterial species. The conjugate was successfully taken up via a receptor uptake system in *E. coli* and *S. enterica* (Równicki et al., 2017). Although *S. pyogenes* has a relatively high B12 uptake rate, such is not known for *S. pneumoniae*, and there is no evidence, that pneumococci use B12 at all (Giannella et al., 1971). Next to vitamins, one could consider the use of siderophores as carriers. Pneumococci meet their iron demand by secretion of high affinity iron-binding proteins and take up of those siderophores. (Brown et al., 2001; Brown et al., 2002; Cheng et al., 2013; Honsa et al., 2013). Prerequisites for the selection of a suitable carrier molecule are the intake of sufficiently large quantities, and above all the ability of the transporter system to recognize the carrier despite the presence of the cargo and to translocate the construct regardless of the increased size. The absence of any of these requirements could be the reason why the AmiA ligand did not mediate uptake of the PNA cargo by the AmiA/AmiB permease into pneumococci.

Another alternative for the transport of PNAs into *S. pneumoniae* could be the use of nanoparticles (NPs). Several types of NPs, such as liposomal NPs (Daeihamed et al., 2017), solid lipid NPs (Naseri et al., 2015), or polymer-based NPs (Abed and Couvreur, 2014) have been tested as carriers of antibiotics into cells (Wang et al., 2017). Especially ultrasmall nanoparticles (< 2 nm) are considered suitable for translocation through bacterial surfaces (Gupta et al., 2019), and it was shown that fluorescently labeled ultrasmall gold nanoparticles effectively penetrate *E. coli* (Białas et al., 2022). A further promising approach are anionic liposomes as delivery system. Antisense oligonucleotides targeting transcripts of *mecA*, which encodes a penicillin-binding protein, were efficiently delivered by anionic liposomes into methicillin-resistant *S. aureus* and re-sensitized the pathogen to methicillin. Combinatory treatment of infected mice with the liposome-encapsulated antisense agent and antibiotics increased survival rates of septic mice by 50 % compared to treatment with antibiotic only or empty liposomes (Meng et al., 2009).

In summary, it was shown in this work that carrier-coupled antisense PNAs are a promising therapeutic approach for the treatment of pneumococci with a great potential to increase the efficiency of PNAs by choosing optimal gene targets and more efficient carriers.

## **4.2 Improving the antimicrobial effect of CPP-PNA with pyrenebutyrate**

The counterion PB can be employed as translocation catalyst accelerating the direct translocation of arginine-rich CPPs in various cell lines (Guterstam et al., 2009; Katayama et al., 2013; Takeuchi et al., 2006). In this work, the effect of PB on the antimicrobial activity of CPP-PNAs was shown in bacteria. In presence of PB, uptake of K8-FITC conjugates into *S. pyogenes* was strongly elevated, and the antibacterial effect of CPP-PNA on *S. pneumoniae* and *S. pyogenes* was increased. Thus, this work showed that the action of PB is not limited to eukaryotes but is also effective in a bacterial species, despite difference in composition and charge of the membranes, and the presence of cell wall and capsule in streptococci. The necessary concentrations employed in the tested streptococcal species were comparable to those used in cells (Guterstam et al., 2009; Takeuchi et al., 2006). The counterion itself had no effect on bacterial cell counts at the used concentrations, nor did it increase toxic effects of CPP-scrPNA controls.

The improvement of the antimicrobial effect of CPP-PNA on streptococci by PB seems to depend on the proportion of positively charged amino acid residues of the carriers. In pneumococci, CPP-PNAs with a proportion of arginine and lysines below 57 % ((RXR)<sub>4</sub>XB- and PenArg-anti-*gyrA* PNA) were not improved by PB, while the conjugates TAT-anti-*gyrA* PNA (75 %) and R9-anti-*gyrA* PNA (100 %) had increased antibacterial activity in presence of PB.

The strongest effect of PB on CPP-PNAs antimicrobial activity was measured with K8-PNA in GAS. Until now, it was assumed that the guanidinium cations of arginine residues of CPPs are particularly important for improved uptake via counteranions (Futaki et al., 2004; Katayama et al., 2013; Sakai and Matile, 2003; Takeuchi et al., 2006). Oligolysine K8 is a cationic CPP as oligoarginines, yet it lacks a guanidinium moiety. Therefore, interactions of PB with guanidinium cations of the CPPs do not appear to be essential to increase the translocation into bacteria. It seems likely that a general interaction of positively charged CPPs with negatively charged PB is sufficient to increase the accumulation of CPPs on the membrane surface. In turn, the interaction of CPPs with a membrane increases efficiency of CPP uptake. Furthermore,

Katayama and coworkers showed that PB enhances direct translocation of oligoarginines through artificial membranes not only due to electrostatic interaction with the CPP, but also indirectly by increasing membrane fluidity and formation of membrane curvatures (Katayama et al., 2013). Cellular and bacterial membranes are not uniform in composition and charge, but some areas are more fluid than others. In general, the translocation of cationic CPPs is higher in more fluid domains compared to more static ones (Duchardt et al., 2007; Lamazière et al., 2010; Säälük et al., 2011). Incubation with PB was shown to disperse phase separation and increase fluidity of negatively charged artificial membranes, which might result in enhanced translocation of cationic CPPs. Additionally, PB caused formation of inward tubular structures on artificial membranes, which disappeared upon addition of oligoarginines. Formation of curvatures and recovery might enhance the uptake of CPPs (Katayama et al., 2013). Whether one of these effects of PB detected with artificial membranes or the combination of these effects enhances uptake of positively charged oligopeptides in bacteria, is not known. It has also not yet been tested, if PB increases the uptake of oligolysines not only into *S. pyogenes* but also in eukaryotic cells.

The effect of PB was stronger in GAS than in pneumococci. The efficiency of different carriers varies generally between the two streptococcal species, such as K8 is a very efficient CPP in GAS, but not effective at all in pneumococci. As surface structures as the capsule may play an role in uptake of carriers (Good et al., 2000; Good et al., 2001; Good and Nielsen, 1998a; Wojciechowska et al., 2020), they could also influence activity of the counterion. Pneumococci generally have a thick capsule and especially the capsule of *S. pneumoniae* TIGR4 is relatively wide with 185 nm (thickness of D39 capsule: 104 nm) (Hyams et al., 2009; Zafar, Hamaguchi et al., 2017). The capsules of the streptococcal species differ not only in thickness but also in composition. GAS capsules are composed of hyaluronic acid (N-acetylglucosamine and glucuronic acid), whereas pneumococcal capsules consist of 2 – 8 saccharides that are often substituted with O-acetyl, phosphoglycerol, or pyruvyl acetal residues (Ashbaugh et al., 1998; Calix et al., 2012; Wessels, 2019). Based on that, it would further be interesting if PB has an effect on the uptake of CPP-PNAs in other bacterial species. Gram-negative bacteria differ greatly in their surface from gram-positive streptococci. Especially, while the peptidoglycan layer is less thick, there is an additional outer membrane layer. Whether this is an obstacle to PB remains to be investigated.

A limitation of the use of PB is, that pre-treatment of cell with the counterion is not effective in presence of medium or serum. This is thought to be due to competition of ionic species in

medium with the carrier for interaction with PB (Takeuchi et al., 2006). Use of the counterion is consequently restricted to application in PBS. Therefore, the approach is to use PB *in vitro* to increase CPP-PNA uptake and thus the necessary amount of CPP-PNA can be reduced. This would reduce the costs when characterizing the antibacterial activity *in vitro*, or when knock down effects of specific genes with CPP-PNAs are investigated. To enable the use of PB *in vivo*, Mishra and coworkers tested an approach in which they covalently coupled PB to a CPP-cargo molecule. Compared to CPP alone, the uptake of the PB-CPP-cargo conjugates into cells was increased 4-5-fold and shown to be independent of medium, as the amount of conjugates taken up in the presence of medium was just as high as without medium (Mishra et al., 2009). It is possible that interaction of PB with the membrane, in addition to the interaction of positive CPPs themselves with the membrane, increases accumulation and thus uptake. It could be tested, whether linking PB to CPP-PNA might result in a conjugate with improved activity in bacteria.

In summary, it was shown in this work that the use of PB strongly increased the uptake of some CPP-cargo conjugates in *S. pyogenes* and consequently enhances the specific antimicrobial activity of the CPP-PNAs. Furthermore, the effect of PB was not limited to arginine-rich CPPs but was also mediated with lysine-rich oligopeptides. Based on these findings, the addition of PB could be used to significantly reduce the amount of CPP-cargos in *S. pyogenes in vitro*, as uptake can be increased by more than 4-fold.

### **4.3 Transcriptomic analyses of CPP-PNA treated streptococci**

The transcriptomic changes after treatment with CPP-PNA conjugates were investigated to detect possible knockdown and off-target effects, activation of particular stress resistance pathways, and possible mechanisms for development of CPP-PNA resistance in the streptococcal species. Although with the protocol applied in this work, no reduction in the expression level of the target gene *gyrA* after CPP-antisense PNA treatment was measured, a limited number of transcriptomic changes could be detected.

#### **4.3.1 Transcriptomic changes in pneumococci after (RXR)<sub>4</sub>XB-PNA treatment**

Transcriptomic changes in pneumococci after treatment with (RXR)<sub>4</sub>XB-anti-*gyrA* PNA and with CPP-scrPNA were very similar. Fewer genes were differentially expressed after (RXR)<sub>4</sub>XB treatment, which were further not unique for the CPP but also altered after

incubation with (RXR)<sub>4</sub>XB-PNAs. The majority of genes with altered expression levels after treatment with (RXR)<sub>4</sub>XB-PNA, e.g. the gene with the highest fold change *ugpA* encoding a sugar transporter permease, were involved in carbohydrate metabolism and sugar uptake. The second most upregulated gene upon (RXR)<sub>4</sub>XB-anti-*gyrA* PNA treatment was *nanB*, which encodes the neuraminidase B. Neuraminidases are involved in infection, modulation of host innate immunity, and required to use sialic acid as carbon and energy source (Corfield, 1992; Iijima et al., 2004; Powell and Varki, 2001; Sudhakara et al., 2019). Increase of its expression might be due to its role in metabolism. Upregulation of metabolic pathways was also observed by Popella and coworkers in CPP-PNA treated *S. enterica* (Popella et al., 2021).

The function of a upregulated YhcH/Yjgk/YiaL family protein is less understood. Yjgk is part of a stress response via a toxin-antitoxin system and related to biofilm formation (Kim et al., 2009), while YhcH is involved in sialic acid metabolism (Teplyakov et al., 2005). Further RelE and Xre family genes, which are part of toxin-antitoxin systems, were upregulated. Both systems are thought to act as modulators of protein synthesis upon stress (Alkhalili et al., 2019; Hu et al., 2019; Nieto et al., 2010). The results indicate that the CPP-PNA were recognized as putative stressor by pneumococci, independently of the antisense activity. Activation of stress pathways could lead to development of resistance towards the CPP-PNA molecules. Also in CPP-PNA treated *S. enterica*, pathways involved in stress and envelope homeostasis were found upregulated. This was independent of the antisense activity of the CPP-PNA conjugates, but did not occur after treatment with unbound CPPs. Especially the PhoP/Q stress response, which is involved in modification of the bacterial membrane to provide e.g. resistance to AMPs, was induced in *S. enterica* (Popella et al., 2021). As PhoP/Q regulates lipid and protein modification in the outer membrane, gram-positive bacteria lack this system. Whether the CPP-PNA induced stress pathways in pneumococci also affect the envelope composition is not known yet, but it represents a common resistance mechanism to AMPs (Joo et al., 2016).

Noticeable, also the lantibiotic two-peptide bacteriocin components PneA1 and PneA2 were upregulated after CPP-PNA treatment and not affected by unconjugated (RXR)<sub>4</sub>XB. So far it is not known which conditions induce expression and antimicrobial activity of this AMP (Majchrzykiewicz et al., 2010; Majchrzykiewicz, 2011). The expression of the bacteriocin could be a defense mechanism of the pneumococci against hostile AMP-producing bacteria, which is activated when CPP-PNAs are perceived as possible AMPs. However, the cationic antimicrobial peptides (CAMPs) resistance was downregulated. CAMP resistance mechanisms include electrostatic repulsion of the cationic peptides, proteolytic cleavage or trapping by



CAMP-binding proteins, or export via efflux pumps (Kraus and Peschel, 2006). It would be very advantageous if the CPP-PNA conjugates were not recognized by the streptococci as CAMP, and therefore no pre-existing resistance mechanism to the conjugates is activated.

Further downregulated pathways were DNA repair, homologous recombination, and mismatch repair. Reduction of DNA repair results in increased mutation rates. It is known that bacterial stress response to antibiotics is linked to emergence of antibiotic resistance because of increased mutagenesis (Baharoglu and Mazel, 2011; Gutierrez et al., 2013; Kohanski et al., 2010). Treatment of *S. pneumoniae* with subinhibitory levels of ciprofloxacin and streptomycin resulted in an increase of mismatch repair mutants and in increased mutation frequency (Henderson-Begg et al., 2006). Especially low concentrations of antibiotics can induce mutagenesis and consequently emerge of *de novo* antibiotics resistance (Baharoglu and Mazel, 2011; Henderson-Begg et al., 2006; Wu et al., 1999). Reduced expression of genes involved in mismatch repair was also observed in *S. enterica* treated with (RXR)<sub>4</sub>XB- and TAT-PNA (Popella et al., 2021). Since the sublethal concentrations of CPP-PNA have led to a downregulation of DNA repair mechanisms, it can be assumed that this might result in development of *de novo* resistance mechanisms against CPP-PNA due to elevated mutagenesis. In summary, treatment of pneumococci with sublethal concentrations of (RXR)<sub>4</sub>XB-PNA resulted in increased expression of genes involved in stress response, and in reduced DNA repair. This indicates that (RXR)<sub>4</sub>XB-PNAs were recognized by pneumococci as putative stressors, and that there is potential for *de novo* resistance development against the CPP-PNAs. The transcriptional responses to CPP-PNA treatment appear to be off-target effects, independent of the antisense effect of the PNAs but to be due to the chemical structure of the conjugates. As the transcriptional response to CPP-PNAs differed from that to uncoupled CPPs, the findings underline that CPP-scrPNA are better suited as controls than CPPs.

#### **4.3.2 Transcriptomic changes in *S. pyogenes* treated with (RXR)<sub>4</sub>XB- and TAT-PNA**

In GAS, the three most upregulated genes after (RXR)<sub>4</sub>XB-anti-*gyrA* PNA, TAT-anti-*gyrA* PNA and TAT-scrPNA treatment were the same. Their expression was not altered by treatment with (RXR)<sub>4</sub>XB and (RXR)<sub>4</sub>XB-scrPNA. Two of them were genes with unknown function (domains of unknown function (DUFs)), and one encoded a PadR transcription factor. PadR family members are found in multiple species and are involved in detoxification, multidrug recognition and resistance, stress response, and virulence (Agustiandari et al., 2008; Dale et al.; Fibriansah et al., 2012; Grande Burgos et al., 2009; Isom et al., 2016; Silva et al., 2005).

Pneumococcal PadR *PtvR* regulates the operon responsible for phenotypic tolerance to vancomycin (*ptv*), which is inducible by stress conditions including vancomycin (Liu et al., 2017), while other PadR members in streptococci are involved in multiple environmental stress tolerance (Lee et al., 2021). Upregulation of a PadR transcription factor might be a resistance mechanism of *S. pyogenes* against (RXR)<sub>4</sub>XB- and TAT-anti-*gyrA* PNA conjugates and should be further investigated.

TAT-anti-*gyrA* PNA treatment resulted in downregulation of two genes encoding hypothetical proteins. One of them is located in a region encoding the endodeoxyribonuclease RuvA involved in DNA repair, the other is considered to be part of the poorly characterized Rrf2 family. Reduced DNA repair upon TAT-anti-*gyrA* PNA treatment was also observed in pneumococci and *S. enterica* (Popella et al., 2021). It is striking that the transcriptomic profiles after TAT-anti-*gyrA* and -scrPNA were almost identical, while it differed greatly between (RXR)<sub>4</sub>XB-anti-*gyrA* PNA and its controls. This fits into the observations that the TAT-conjugates tend to be more toxic, whereby TAT-scrPNA also leads to upregulation of the PadR family regulator, for example. Further, coupling a PNA cargo to (RXR)<sub>4</sub>XB seemed to reduce its toxicity.

Treatment of GAS with the peptide (RXR)<sub>4</sub>XB resulted in the upregulation of many genes, which were not affected by the peptide conjugates. Genes upregulated exclusively by (RXR)<sub>4</sub>XB were mainly genes which are considered to be involved in stress response. Among them was a gene encoding csbD (pfam05532), a protein of general stress response in *Bacillus subtilis* and activated upon multiple stress stimuli (Reder et al., 2012). Also the expression of the competence protein *coiA* was upregulated by (RXR)<sub>4</sub>XB, which is required for transformation and a putative transcription factor in GAS. The relationship between competence and stress response are of interest and interconnections between these mechanisms in gram-positive bacteria are known, but poorly understood (Claverys et al., 2006; Dagkessamanskaia et al., 2004). While (RXR)<sub>4</sub>XB treatment resulted in increased expression of genes involved in stress resistance, coupling the CPP to a PNAs appeared to reduce recognition and responses. Fewer activated stress responses are advantageous, as development of resistance mechanisms might be slower.

It is striking, how different the transcriptional response of the two streptococcal species was. While most genes with altered expression in pneumococci were involved in metabolism, this played a minor role in GAS. Also, treatment with (RXR)<sub>4</sub>XB had a low impact on the pneumococcal transcriptome, whereas GAS upregulated a variety of genes, which were unique

compared to the other conjugates. It seems unlikely that the activation of a single and dominant resistance mechanism against CPP-PNA is imminent in the two species. In *S. enterica*, Popella and coworkers detected a strong activation of the PhoP/Q pathway in response to several CPP-PNA conjugates, which is only present in gram-negative bacteria, that might mediate resistance to certain CPP-PNAs (Popella et al., 2021).

### **4.3.3 Limitations of the experimental setting and prospect of improvement**

In this work, bacteria were treated with sublethal concentrations over a prolonged incubation period. The relative target transcript abundance measured with RT qPCR decreased upon CPP-anti-*gyrA* treatment to 65 %, which is in accordance with target mRNA decay observed under similar conditions (Abushahba, Mohammad, Thangamani et al., 2016; Barkowsky et al., 2019; Barkowsky et al., 2022). However, target gene transcript reduction could not be confirmed in the transcriptomic analysis. For comparison, Popella and coworkers performed transcriptomic profiling of *S. enterica* with a lethal CPP-PNA concentration (1x MIC) for 15 min. In this setting, the target gene transcript abundance was reduced compared to control by 4.5 – 5-fold using (RXR)<sub>4</sub>XB-PNA, and 3-fold using TAT-PNA (Popella et al., 2021). Consequently, in future experiments the dose should be increased to cause comparably strong effects on the target gene expression.

A low number of genes were significantly altered in their expression profile. In *S. enterica*, treatment under the previously described conditions resulted in 409 differently expressed genes upon (RXR)<sub>4</sub>XB-PNA treatment and 508 genes upon TAT-PNA (Popella et al., 2021). In contrast, (RXR)<sub>4</sub>XB-PNA altered the expression of only 42 genes in pneumococci, and 3 genes in *S. pyogenes*. The CPPs (RXR)<sub>4</sub>XB and TAT without coupled PNA influenced the expression of 26 and 97 gene, respectively, in *S. enterica* (Popella et al., 2021). In this work, (RXR)<sub>4</sub>XB resulted in altered transcript levels of 8 and 26 genes in pneumococci and GAS, respectively. A low level of transcriptomic change by CPP-PNA is not generally associated with a low target gene decrease. Treatment of *S. enterica* with (KFF)<sub>3</sub>K-PNA, which resulted in reduction of transcript levels of the target gene by 4.5 – 5 fold, altered the expression of only 5 genes (Popella et al., 2021). Extent of transcriptomic change seems to be, among others, influenced by the respective CPP-PNA and the species.

Furthermore, Roth and coworkers showed the correlation of treatment time with the extent of transcriptional change. Incubation of *E. coli* with a sublethal concentration of hydrogen peroxide resulted in a significant change of 12 % of all bacterial genes after 10 min of treatment,

whereas only 2.4 % were altered after 60 minutes. Potential reasons for the differences between the two conditions are, on the one hand, that the bacteria in the early sample were in the exponential phase, while in the later sample they were already entering the early stationary phase. On the other hand, hydrogen peroxide is quickly broken down by *E. coli*, which can lead to regrowth in the subsequent sample (Roth et al., 2022). The experiments should therefore be repeated with a reduced treatment time and increased CPP-PNA concentration to generate an experimental setting appropriate for investigating effects of CPP-PNA on the transcriptome.

In this work, streptococci were treated with sublethal CPP-PNA concentrations over a prolonged incubation time, since the quality of the RNA isolated from samples following treatment with lethal CPP-PNA concentrations was reduced. The RNA integrity was low and RNA molecules with a length of approximately 25 nt accumulated. Similar observations were reported by Popella and coworkers when applying lethal concentrations of CPP-PNAs. Comparing different RNA isolation methods, they found a method to isolate RNA from lethal and short-term treated *S. enterica* (Popella et al., 2021). In future experiments, a suitable RNA isolation protocol for the streptococcal species should be developed for samples, which have been treated with high concentrations of CPP-PNAs.

In summary, after identification of a suitable method for isolation of RNA, streptococci should be treated with lethal concentration of CPP-PNA in a short pulse. Transcriptomic changes under these conditions could then be compared to the results of this work and will help to identify activated stress responses and putative resistance mechanisms upon CPP-PNA treatment.

#### **4.4 Proteome profiling of model organism *G. mellonella* during GAS infection**

In this part of the work, the suitability of *Galleria mellonella* as a model organism was investigated. The focus was on the specific immune response to an *S. pyogenes* infection, and whether the findings on induced immune processes and pathways can be extrapolated to the mammalian innate immune system. Examination of the proteome of cell-free hemolymph of infected larvae compared to non-infected larvae revealed three main features of the insect's immune response: relative specificity, similarity to the mammalian innate immune system, and complexity.

#### 4.4.1 Specificity of *G. mellonella* immune response

It is known, that the immune system of *G. mellonella* is able to distinguish between different pathogens and to carry out a relatively specific response (Mak et al., 2010). The relative specificity is reflected by the proteins that recognize the pathogen, by the antimicrobial peptides that are expressed, and by specific heat shock proteins and chemosensory proteins that are present in changing levels in infected larvae compared to healthy controls.

##### **Proteins associated with non-self recognition**

Pathogens and foreign surfaces are recognized by pathogen-associated molecular pattern (PAMPs) and indirectly also via damage-associated molecular patterns (DAMPs) by binding to pattern recognition receptors (PRRs). Recognition leads to induction of signaling cascades as Toll, IMD or JAK-STAT, resulting most importantly in upregulation of antimicrobial peptides (AMPs), NADPH oxidase complex dependent production of reactive oxygen species or reactive nitrogen species (ROS/RNS) and hydrogen peroxide (H<sub>2</sub>O<sub>2</sub>), and start of the phenol oxidase (PO) cascade (Sheehan, Garvey et al., 2018). Opsonization has furthermore phagocytosis-promoting activity on hemocytes (Aathmanathan et al. 2018) and stimulates aggregation of hemocytes for encapsulation of pathogens (Asai et al., 2021; Jung et al., 2019; Sheehan, Garvey et al., 2018).

The main PRR in lepidoptera are peptidoglycan recognition proteins (PGRPs),  $\beta$ -1,3-glucan binding proteins ( $\beta$ -1,3-glucan BPs), hemolin, gram-negative bacteria binding proteins (GNBs), C-type-lectins (CTLs), and cationic peptide 8 (GmCP8) (Dubovskiy et al., 2016; Jiang et al., 2010; Kim et al., 2010; Zhang et al., 2015; Zhu et al., 2010). This work revealed that the recognition proteins, expressed in *G. mellonella* upon *S. pyogenes* infection are eight different PGRPs, seven  $\beta$ -1,3-glucan BPs, hemolin, and less-likely hemicentin 1-like and GmCP8. No increase was measured for GNBs (such as A0A6J1X3L8) or CTLs.

PGRPs are among the most common PRRs in insects (Wang et al., 2019), but the differences between distinct PGRPs or  $\beta$ -1,3-glucan BPs are less characterized. Whether the expressed pattern of PGRP types upon GAS infection is unique compared to other pathogens is not yet known. Generally, increased PGRPs level were also measured in *G. mellonella* larvae infected with gram-positive *Staphylococcus aureus* (Sheehan et al., 2019) and in larvae infected with the fungus *Candida albicans* (Vertyporokh and Wojda, 2020), whose surface lacks PG. Vice versa, GAS surface does not contain  $\beta$ -1,3-glucan, although  $\beta$ -1,3-glucan BPs were induced upon infection. Such was also observed in *G. mellonella* infected with *S. aureus* (Sheehan et al., 2019). Recognition of fungi and gram-positive bacteria result in activation of the same

signalling cascade. While the IMD cascade is activated after recognition of mostly gram-negative and only a few gram-positive bacterial species (e.g. *Bacillus*), the Toll signalling cascade is activated after recognition of gram-positive bacteria and fungi (via the cytokine Spätzle) (Burger et al., 1991; Schleifer and Kandler, 1972). Further it was shown, that several  $\beta$ -1,3-glucan BPs can bind also to lipoteichoic acid (LTA), but not lipopolysaccharides (LPS) (Jiang et al., 2004; Lee et al., 2004). Taken together, these two recognition protein types are able to bind to surface structures of both fungi and gram-positive bacteria.

The non-self-recognition molecule hemolin is a member of the Ig superfamily and similar to mammalian immunoglobulin (Bettencourt et al., 1997; Shaik and Sehnal, 2009; Zhang et al., 2011). This opsonin, present as soluble molecule or bound to the surface of hemocytes (Bettencourt et al. 2002), binds to the bacterial cell wall components LTA and LPS. Increased hemolin levels were measured after infection of the wax moth with *C. albicans* (Vertyporokh and Wojda, 2020), *S. aureus* (Sheehan et al., 2019), and *Mycobacterium bovis* (Asai et al., 2021).

In summary, *G. mellonella* uses for recognition of *S. pyogenes* primarily the most important PRRs for detection PGRPs,  $\beta$ -1,3-glucan BP, and hemolin, but does not use CTLs or PRRs that explicitly only bind LPS, such as GNBs. The different PGRP types cannot be distinguished and compared with PGRP types expressed upon infection with other microbes so far, but an even more specific recognition of GAS seems likely. In this study it was further shown that GmCP8 and hemicentin might rather be involved in different functions than recognition of GAS.

### **Antimicrobial peptides (AMPs)**

AMPs are upregulated upon activation of the pathways Toll and IMD. Some AMPs are regulated by both pathways, some can be cross-regulated, and others are strictly separated (Nishide et al., 2019; Tanji et al., 2007). This experiment revealed which of the ~ 20 members of AMPs of *G. mellonella* known so far (Kordaczuk et al., 2022) are upregulated in GAS infection. The amount of most AMPs was very low in non-infected larvae leading to strong fold changes, particularly at 24 and 72 h post infection. AMPs that were induced by GAS infection were gloverins, cecropins, lysozymes, a proline-rich protein, inducible metalloproteinase inhibitor (IMPI), the silk protein seroin, and 6tox.

Gloverins and cecropins, which were among the most highly increased AMPs in GAS infection, are induced by a broad range of pathogens as *M. bovis* (Asai et al., 2021), *S. aureus*, and *Aspergillus fumigatus* (Sheehan, Clarke, Kavanagh, 2018). In contrast, moricin-like peptides

are absent in GAS infected *G. mellonella*, although they were increased by gram-positive *S. aureus*, gram-negative *Pseudomonas aeruginosa*, and in *C. albicans* (Andrejko et al., 2021; Sheehan et al., 2019; Turrís et al., 2021). Also proline-rich and anionic peptides, which are important AMPs in the IR to *P. aeruginosa* (Andrejko et al., 2021), seem to play a minor role in GAS infection. And despite cross-reactivity of pathways and shared signaling pathways, exclusively antifungal AMPs like gallerimycin and galiomycin were absent.

The silk protein seroin has a strong antimicrobial activity, which might protect the pupa. It was also shown to be strongly upregulated in bacterially infected larvae (Nirmala, Mita et al., 2001; Singh et al., 2014; Zhu, H. et al., 2020). Upon wounding it was expressed also in the fat body (Korayem et al., 2007). Rarely described and insufficiently explored is 6tox, a member of the defensin-derived family X-tox so far only known in Lepidoptera and Hymenoptera species (Girard et al., 2008; Tian et al., 2010). *G. mellonella* 6-tox structure contains six characteristic conserved tandem repeats of cysteine-stabilized  $\alpha\beta$  motifs, which are also found in invertebrate defensins and in scorpion toxins (Vogel et al., 2011). Its expression was shown to be induced in *Galleria* upon *E. coli* infection after 6 h in larval fat bodies, hemocytes, and midgut (JH Lee, SM Park, KS Chae, IH Lee, Korean Society of Sericultural Science, 2010). X-tox expression in *Spodoptera exigua* was found to be induced by infection with gram-positive and negative bacteria, fungi and viruses (Girard et al., 2008). The role of the atypical protein in immune response is not understood. Although it is often classified as putative AMP, its direct antibacterial effect was not shown yet, and it is speculated, that it might rather act as effector of hemocyte-mediated processes (d'Alençon et al., 2013; Girard et al., 2008; JH Lee, SM Park, KS Chae, IH Lee, Korean Society of Sericultural Science, 2010).

Specificity was further indicated by heat shock proteins (HSPs), which are important for protection of insects against multiple stressors (Guz et al., 2020). In mammals, HSPs are modulators of the IR and considered to link innate and adaptive immune system, as they are involved in multiple responses such as immune cell activation and maturation (Wrońska and Boguś, 2020). Mammalian HSPs involved in IR are HSP90, 70, and 60 (Bausinger et al., 2002; Binder, 2014; van Noort et al., 2012). In this study, HSP20, 21.4, 27.4, and 70 were shown to be increased in response to GAS infection. While the functions of HSP20 and HSP21 were not described yet, HSP27 was already shown to be involved in *G. mellonella* response against fungi. HSP70, playing an important role in the mammalian IR, was not upregulated in *G. mellonella* after fungal infection, but increased upon GAS infection in this work (Wrońska and Boguś, 2020), indicating also specificity of HSP expression.

Further, a strong increase in a gustatory receptor candidate 59 (GRC) upon infection was observed. During infection of the wax moth larvae with *Aspergillus fumigatus*, GRC 25 was the protein with the greatest increase in abundance (Sheehan, Clarke, Kavanagh, 2018), which was also observed during infection of larvae with heat-killed *C. albicans* (Vertyporokh and Wojda, 2020), and *S. aureus* (Sheehan et al., 2019). Mc Namara and coworkers discussed two theories on the increase in gustatory receptor proteins: first, as infection are energy and nutrient consuming, larvae might compensate the rising demand by increasing the receptor (Mc Namara et al., 2017; Moret and Schmid-Hempel, 2000). Second, the increase of this receptor might be a toxin avoidance reaction. *Drosophila* are able to detect smallest concentrations of an insect repellent and suppress feeding via avoidance gustatory receptors (Chapman, 2003). *Drosophila* eating bacterial contaminated food reacted within one hour after ingestion with upregulation of expression of the gustatory receptor 66a (Charroux et al., 2020). The second theory is in accordance with the data of this work, as *G. mellonella* had 4 h post infection already amounts of the GRC 59 while none was measured in the control larvae. In *Drosophila*, GR59c is suggested to detect aversive compounds as a bitter receptor, yet it is not proven (Shim et al., 2015). This data indicate that *G. mellonella* larvae detect *S. pyogenes* components with a gustatory receptor and that GR59c is an avoidance receptor that might suppress feeding behaviour of the infected larvae.

The increased abundance of specific recognition proteins, chemosensory proteins, AMPs, and HSPs reveal a relative specificity of the *G. mellonella* IR to GAS. Although some PRRs opsonize a wide range of pathogens and some AMPs have a broad spectrum of activity, *G. mellonella* appears to recognize and target GAS relative specifically. This is particularly evident from the fact that after recognition of *G. mellonella*, no AMPs with exclusively antifungal activity are expressed. Even more, the distinct AMP response upon GAS infection is reflected in low levels of AMPs that were shown to be important in response to gram-negative bacteria, such as *Pseudomonas*. In order to be able to prove the specificity of the chemosensory molecules and HSPs, more comparative data with other pathogens would be needed, since they have hardly been examined so far. This work provides a basis and contribution for that approach.

#### **4.4.2 Similarity of the *G. mellonella* immune response and the mammalian innate immune system**

The cellular IR of insect hemocytes and mammalian neutrophils share the main processes. Neutrophils are involved in phagocytosis, encapsulation, reactive oxygen species (ROS)



production, and enzyme release of granules (Sheehan, Garvey et al., 2018). In this work, proteins involved in these processes were detected in infected larvae. Among them are the calcium-binding proteins calyculin and nucleobindin-2, which increased during infection. Inflammation and phagocytosis are calcium-dependent, as phagocytosis requires calcium-dependent rearrangement of the actin cytoskeleton (Melendez AJ., 2000-2013). Calyculin is involved in phagocytic activity of neutrophils (Stendahl et al., 1994). Stimulation of cells of the crab *Eriocheir sinensis* with LPS lead to increased expression of calyculin-1, while knock down of the putative immune signalling protein resulted in disruption of phagocytosis (Huang et al., 2016). Furthermore, Bidoli and coworkers observed increased transcription of calyculin-1 upon LPS stimulation in the stick insect *Bacillus rossius*. They speculated that it might play a role in the cellular IR of insects and is involved in phagocytosis (Bidoli et al., 2022). In this work, calyculin was detected for the first time in association with the IR in *G. mellonella*. Nucleobindin-2 is involved in insect calcium homeostasis via calcium storage and release (Kawano et al., 2000). Mammalian nucleobindin-2 is highly expressed in neutrophils (Boullaran and Kehrl, 2014). Its role in the mammalian and insect IR is not fully understood yet. The presence of the two calcium-binding proteins indicate induction of phagocytosis upon GAS infection *G. mellonella*.

An endonuclease with high sequence similarity to poly (U)-specific endoribonuclease P102 of *Heliothis virescens* (Lepi., Nocturidae) was detected. This endonuclease forms amyloid fibrils (Pascale et al., 2014). Insects accumulate amyloid fibrils intracellularly and release them during infection. The fibrils form a layer around foreign surfaces and act as scaffold for melanin synthesis and for adhesion of hemocytes around it (Falabella et al., 2012). This endoribonuclease of *G. mellonella* might promote phagocytosis during infection. In mammalian infection, amyloid fibrils have pro-inflammatory roles and are involved in the activation of innate immunity. They are protective against pathogens, yet most studies focus on roles of amyloid fibrils in human disorders as the Alzheimer's disease (Huang et al., 2019).

The enzymes superoxide dismutase and sulfhydryl oxidase, involved in ROS homeostasis and production, were increased in GAS infected larvae, while antioxidant catalase was decreased. ROS have also multiple and important roles in the innate immune response of mammals, as they are second messengers and regulators of inflammation, and perform direct killing of pathogens (Di Marzo et al., 2018; Lee and Song, 2021; Moghadam et al., 2021).

Analogous to mammalian IR, accumulation of serine proteases (SPs) and subsequent inhibitors was observed after infection of *G. mellonella*. As expected, SP and among them CLIP SPs

levels rose rapidly in infected larvae. Circulating as inactive zymogens in the hemolymph, they are quickly activated upon recognition of damaged tissue or microbial polysaccharides (Gettins, 2002; Kanost and Jiang, 2015; Silverman et al., 2001). CLIP SPs are important immune factors in insects with unique protein architecture absent in vertebrates. The main function of CLIP SPs is cleavage of the cytokine Spätzle, which then acts as ligand for activation of the Toll cascade, and activation of the PO pathway. SP activities are regulated tightly via inhibitors (Kanost and Jiang, 2015). Interesting proteins in this context are the leukocyte elastase inhibitor-like enzymes, two of them being strongly increased. Little is known about the action of the leukocyte elastase-like SP and its inhibitor in insects. Human leukocyte elastase, also known as neutrophil elastase, acts during inflammation as hydrolyzing enzyme within neutrophil lysosomes, but it also secreted and degrades components of the extracellular matrix and surface components of gram-negative bacteria (Belaouaj et al., 2000; Pham, 2006; Sonawane et al., 2006). The mode of action and possible activity against gram-positive bacteria of the homologue insect leukocyte elastase-like enzyme and inhibitor are not investigated yet.

A strong increase during infection was measured for a protein-histidine N-methyltransferase. This enzyme catalyses actin modification via peptidyl-histidine methylation, which is a posttranslational modification in eukaryotes and an important regulatory mechanism (Kwiatkowski and Drozak, 2020). Human SETD3 (actin histidine methyltransferase) and SETD2 (actin lysine methyltransferase) are evolutionary highly conserved. Sequence comparison of the histidine methyltransferase of *G. mellonella* with human SETD3 (Q86TU7) via BLAST® (Altschul et al., 1997) revealed 37 % identity with 55 % positives. Both histidine and lysine modification of actin result in increased actin polymerization (Kwiatkowski et al., 2018; Seervai et al., 2020). Filamentous actin (F-actin) is essential in many fundamental processes (Wickramarachchi et al., 2010). It is known to play an important role in vertebrate wound healing and IR, as it is involved in cell migration, cell-cell interaction and endocytic processes, e.g. engulfing foreign material (Bunnell et al., 2011; Wickramarachchi et al., 2010). Knockdown of SETD2 resulted in impaired cell migration (Seervai et al., 2020). This work indicates involvement of actin methylation in insect IR and that increased F-actin rates are important in both, vertebrate and invertebrate IR.

In summary, the proteomic analysis showed the strong similarity of the IR of *G. mellonella* and the innate IR of mammals. The fundamental mammalian innate IR mechanisms of recognition, coating, phagocytosing, and direct killing of bacteria e.g. via ROS, were all detected in this study. However, an essential component of mammalian IR is the production of pro-

inflammatory cytokines (Carrillo et al., 2017; Fieber and Kovarik, 2014). Few lepidopteran cytokines with stimulatory activity on immune cells are well studied and neither growth blocking peptide and plasmatocyte-spreading factor nor others were expressed in an increased during GAS infection (Aizawa et al., 2001; Matsumoto et al., 2003; Strand and Clark, 1999). In general, no elevated cytokine levels have been reported in comparable experiments from other studies, such as infections of *G. mellonella* with various pathogens (Sheehan et al., 2019; Sheehan, Clarke, Kavanagh, 2018; Vertyporokh and Wojda, 2020). In addition, the formation of neutrophil extracellular traps (NETs) is an essential part of the mammalian innate IR against GAS infections (Fieber and Kovarik, 2014). In *G. mellonella*, oenocytoids are able to form NET-like coagulation structures (Altincicek et al., 2008). However, since NETs consist mainly of nucleic acids and the protein components of NETs in insects are not known so far, this work could not examine whether these extracellular structures also play an important role in *G. mellonella* response to GAS.

#### 5.4.3 Complexity of *G. mellonella* immune response

Complexity and similarity to the mammalian IR was further observed as two proteins regulating extracellular ATP were increased in infected larvae: apyrase and arginine kinase. Apyrase is an ATP and ADP hydrolysing enzyme ubiquitous in all organisms (Moo-Young and Butler, 2011; Plesner, 1995). Arginine kinase is essential for maintaining and buffering constant ATP levels in invertebrates and has indirect effects on the IR of oyster. The enzyme binds to LPS, which inhibits the ATP hydrolytic activity leading to increased levels of extracellular ATP. Increased concentrations of extracellular ATP activate in oyster purinergic signalling pathways, enhance calcium influx, production of ROS, and lysosome release of hemocytes (Jiang et al., 2016). Increased levels of arginine kinase was also measured in *G. mellonella* larvae infected with *M. bovis* (Asai et al., 2021). Arginine kinase is absent in vertebrates, yet the protein creatine kinase has the same biochemical function (Dossey AT, Morales-Ramos JA, Guadalupe Rojas M, 2016). Creatine kinase of the fish *Bronchiostema* was also shown to be inducible by LPS. Recombinant creatine kinase of *Bronchiostema* exhibited LPS-binding activity and bacteriostatic activity against *E. coli* (An et al., 2009). It is not known, whether arginine kinase of *G. mellonella* or creatine kinase of mammals have binding activity towards LPS, LTA or other bacterial surface structures. However, extracellular ATP is most certainly a pro-inflammatory molecule in humans (Faas et al., 2017), as it is a universal and ubiquitous DAMP (Di Virgilio et al., 2020). The extracellular ATP level represent a marker for cellular breakdown and might induce IR pathways in both, vertebrates and invertebrates.

The abundance of several cytoskeleton-associated compounds and especially muscular protein was strongly elevated in the hemolymph. The general increase of those compounds might result from cellular breakdown caused by the infection directly due to the pathogens (Nash et al., 2015) and by destructive processes of the IR (Sadd and Siva-Jothy, 2006). Levels of extracellular actin, the most abundant protein in nearly all eukaryotic cells (Dominguez and Holmes, 2011), can act as marker for damaged cells. Such was also observed in *Drosophila* larvae, where a tenfold increase of extracellular actin was measured within 4 h after bacterial infection compared to control larvae (Vierstraete et al., 2004). Actin is involved in phagocytosis, as this mechanism requires actin cytoskeleton rearrangement. Also, actin secreted by immune competent cells can bind to bacterial surface components, mediate phagocytosis (May and Machesky, 2001) and direct killing of bacteria (Sandiford et al., 2015).

A strong increase in the amount of silk proteins was detected in the hemolymph of infected larvae. *G. mellonella* silk is composed of heavy chain, light chain, and P25 (hexafibroin) fibers, and the bioadhesive sericin holding the fibers together (Zurovec et al., 1998; Zurovec and Sehnal, 2002). During infection, silk glands were shown to secrete the opsonin hemolin to a similar extent as the fat body (Shaik and Sehnal, 2009). Silk glands also produced several other proteins that might be involved in the IR (Nirmala, Kodrik et al., 2001; Nirmala, Mita et al., 2001). In turn, Korayem and coworkers showed that silk proteins were constantly produced in midgut, fat body, yet to lesser extent as in the silk gland (Korayem et al., 2007). Furthermore, they detected that clots formed after injury of *G. mellonella* contain fibroins, indicating a role of silk proteins in coagulation. Therefore, increased amounts of fibroins might be explained by their role in clotting as reaction to tissue damage, while the extent of increase during infection is enabled by expression of these compounds in several tissues in addition to silk glands. The data from this work indicate a relevant role of silk proteins in the IR that needs to be further investigated.

Besides proteomic changes due to the immune response, the data also show, that infection affects larval metabolism and development. In infected larvae, the amount of many proteins involved in metabolism was reduced. Also hexamerins, which are storage proteins in the hemolymph and an important amino acid source (Munn and Greville, 1969; Sheehan et al., 2020), declined during infection. As *G. mellonella* does not feed during metamorphosis and adulthood (Boggs and Freeman, 2005; Wojda et al., 2020), all energy must be acquired during the larval stages. The energy is mostly stored in cells of the fat body (Boggs and Freeman, 2005; Hoshizaki, 2005), an organ with homologous functions to mammalian liver and adipose tissue

(Azeez et al., 2014). Consequently, prepupal larvae have high metabolic rates (Merkey et al., 2011). Activation of immune responses in infected larvae are energy-consuming and nutrient-demanding. Infection results in a systemic switch where nutrients are directed to cellular immune tasks. In the fat body, storage of energy is replaced by synthesis of molecules such as AMPs (Arnold et al., 2013; Dolezal et al., 2019; Wagner, 2005). The metabolic switch with redirection of energy sources and reduction of enzymes required e.g. for biosynthesis of vitamins and cofactors, could be observed in this experiment.

Many proteins that promote development or accumulate before metamorphosis did not increase in infected larvae, such as vitellogenin, spermine oxidases, and sericotropin. The larval state is maintained by the juvenile hormone (JH), while dropping of its titre induces metamorphosis. The titre drop is achieved via reduced JH biosynthesis, by increase of JH catabolism mostly mediated by JH esterases (Kamita and Hammock, 2010), or JH suppression (Jones et al., 1993). Two JH-suppressible proteins were found increased in amount in control larvae. JH-suppressible proteins are storage proteins accumulating in developing larvae, suppressing JH and leading at high amounts to induction of metamorphosis (Cheon et al., 2002; Jones et al., 1993). In contrast, a strong increase of a predicted JH esterase-like protein was measured in infected larvae, which would indicate the imminent start of the metamorphosis. Since infected larvae were small, dark colored, and on the verge of dying, while healthy larvae were bigger, yellow and prepupal, the sequence of the predicted JH-esterase-like protein compared with proteins in other species. This revealed indeed similarities to the juvenile hormone esterase-like protein in *Spodoptera frugiperda* (73 % positives), but also acylcarnitine hydrolase-like protein of *Amyelois transitella* (76 % positives) and acetylcholinesterase of *Manduca sexta* (70 % positives), indicating that this protein might be no JH esterase.

#### **4.4.4 *G. mellonella* as a model organism for the investigation of immune responses**

This work demonstrated relative specificity of *G. mellonella* IR towards GAS infection by choice of recognition proteins, AMP production, chemosensory and heat shock proteins. Several proteins detected in this study were identified based on similarities with components of the mammalian immune system or with members of the IR of distantly related invertebrates. Mostly, they have been poorly investigated in insects and some even not at all in *G. mellonella*. This indicates that the insect IR is more complex than appreciated today. Many processes and proteins need to be further investigated, such as arginine kinase, the calcium-binding proteins calyculin and nucleobindin-2, and the putative P102-like endoribonuclease. This work points

out similarities of the IR of *G. mellonella* to the mammalian innate IR. It demonstrates that all cellular IR processes mediated by neutrophils in mammals are also involved in *G. mellonella* with GAS infection, and that also fundamental processes of the humoral response are similar.

Despite differences in the spectrum of AMPs produced and their respective mode of action, several AMPs are evolutionally conserved, e.g. c-lysozyme, cationic peptides and defensins in mammals (Sheehan, Garvey et al., 2018; Smith and Casadevall, 2021). Recognition results in activation of orthologous signal cascades, which are both functionally and structurally similar. Coagulation and clotting, despite fundamental differences, for instance the role of melanin in the PO system in insects, are based on the same processes. The results of this work highlight that information about the IR in insects is still limited. An example for the gaps that remain to be filled is the role of silk fibers in the clotting cascade.

Furthermore, this work demonstrates that results obtained with this model organism allow to extrapolate questions about the functions of orthologue proteins, processes and pathways in mammals. Examples are the role of extracellular ATP and the importance of actin and its polymerization in the immune response. It thereby points out the great potential of this invertebrate model and the need to obtain further information about this relatively organism.

The main points of this work are illustrated in a simplified overview graphic (Figure 34).

Despite the lack of an adaptive immune response, the fast and complex first line reaction of the *G. mellonella* immune system is comparable to the mammalian innate immune response and qualifies the insect organism a simplified model for GAS infection.

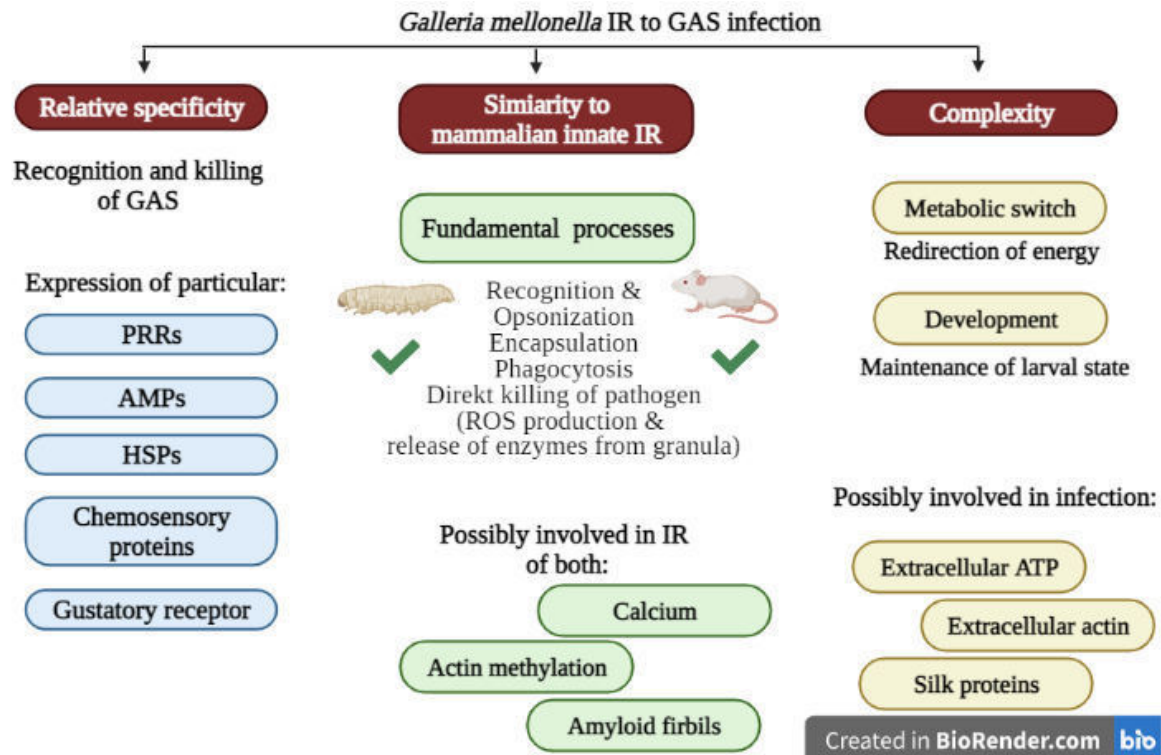


**Figure 34: Overview of main findings of the work: The *G. mellonella* immune response to GAS infection concerning the relative specificity, similarity to the mammalian innate immune response, and complexity.** Relative specificity of the larval immune response (IR) was displayed by proteins expressed for recognition and killing of GAS: Pattern recognition receptors (PRRs), antimicrobial peptides (AMPs), heat shock proteins (HSPs), chemosensory proteins, and a gustatory receptor candidate. Fundamental processes of mammalian innate IR (recognition, encapsulation, phagocytosis, and direct killing of pathogens using reactive oxygen species (ROS) and enzymes released from granules of hemocytes and neutrophils) were found in infected larvae. Proteins were detected indicating involvement of calcium, actin methylation, and amyloid fibrils, also in the IR of larvae. Complexity of larval response to infection was displayed in switches of metabolism and development of larvae. This work indicated further roles of extracellular ATP and actin, and silk proteins in larval IR. The figure was created using BioRender.com.

## References

- Aaberge, I. S., Eng, J., Lermark, G. and Løvik, M. (1995) 'Virulence of *Streptococcus pneumoniae* in mice: a standardized method for preparation and frozen storage of the experimental bacterial inoculum', *Microbial pathogenesis*, vol. 18, no. 2, pp. 141–152.
- Abed, N. and Couvreur, P. (2014) 'Nanocarriers for antibiotics: a promising solution to treat intracellular bacterial infections', *International journal of antimicrobial agents*, vol. 43, no. 6, pp. 485–496.
- Abes, R., Moulton, H. M., Clair, P., Yang, S.-T., Abes, S., Melikov, K., Prevot, P., Youngblood, D. S., Iversen, P. L., Chernomordik, L. V. and Lebleu, B. (2008) 'Delivery of steric block morpholino oligomers by (R-X-R)<sub>4</sub> peptides: structure-activity studies', *Nucleic acids research*, vol. 36, no. 20, pp. 6343–6354.
- Abushahba, M., Mohammad, H. and Seleem, M. (2016) 'Targeting Multidrug-resistant Staphylococci with an anti-rpoA Peptide Nucleic Acid Conjugated to the HIV-1 TAT Cell Penetrating Peptide', *Molecular therapy. Nucleic acids*, vol. 5, no. 7, e339.
- Abushahba, M., Mohammad, H., Thangamani, S., Hussein, A. and Seleem, M. (2016) 'Impact of different cell penetrating peptides on the efficacy of antisense therapeutics for targeting intracellular pathogens', *Scientific reports*, vol. 6, p. 20832.
- Agustiandari, H., Lubelski, J., van Berg Saparoea, H. B., Kuipers, O. P. and Driessen, A. J. M. (2008) 'LmrR is a transcriptional repressor of expression of the multidrug ABC transporter LmrCD in *Lactococcus lactis*', *Journal of bacteriology*, vol. 190, no. 2, pp. 759–763.
- Aizawa, T., Hayakawa, Y., Ohnishi, A., Fujitani, N., Clark, K. D., Strand, M. R., Miura, K., Koganesawa, N., Kumaki, Y., Demura, M., Nitta, K. and Kawano, K. (2001) 'Structure and activity of the insect cytokine growth-blocking peptide. Essential regions for mitogenic and hemocyte-stimulating activities are separate', *The Journal of biological chemistry*, vol. 276, no. 34, pp. 31813–31818.
- Alajlouni, R. A. and Seleem, M. N. (2013) 'Targeting *Listeria Monocytogenes* rpoA and rpoD Genes Using Peptide Nucleic Acids', *Nucleic Acid Therapeutics*, vol. 23, no. 5, pp. 363–367.
- Alaybeyoglu, B., Sariyar Akbulut, B. and Ozkirimli, E. (2018) 'pVEC hydrophobic N-terminus is critical for antibacterial activity', *Journal of peptide science : an official publication of the European Peptide Society*, vol. 24, no. 6, e3083.
- Alcantara, R. B., Preheim, L. C. and Gentry-Nielsen, M. J. (2001) 'Pneumolysin-induced complement depletion during experimental pneumococcal bacteremia', *Infection and immunity*, vol. 69, no. 6, pp. 3569–3575.
- Alkhalili, R. N., Wallenius, J. and Canbäck, B. (2019) 'Towards Exploring Toxin-Antitoxin Systems in *Geobacillus*: A Screen for Type II Toxin-Antitoxin System Families in a Thermophilic Genus', *International journal of molecular sciences*, vol. 20, no. 23.
- Allolio, C., Magarkar, A., Jurkiewicz, P., Baxová, K., Javanainen, M., Mason, P. E., Šachl, R., Cebecauer, M., Hof, M., Horinek, D., Heinz, V., Rachel, R., Ziegler, C. M., Schröfel, A. and Jungwirth, P. (2018) 'Arginine-rich cell-penetrating peptides induce membrane multilamellarity and subsequently enter via formation of a fusion pore', *Proceedings of the National Academy of Sciences of the United States of America*, vol. 115, no. 47, pp. 11923–11928.
- AlonsoDeVelasco, E., Verheul, A. F., Verhoef, J. and Snippe, H. (1995) 'Streptococcus pneumoniae: virulence factors, pathogenesis, and vaccines', *Microbiological reviews*, vol. 59, no. 4, pp. 591–603.
- Altincicek, B., Stötzel, S., Wygrecka, M., Preissner, K. T. and Vilcinskis, A. (2008) 'Host-derived extracellular nucleic acids enhance innate immune responses, induce coagulation, and prolong survival upon infection in insects', *Journal of immunology (Baltimore, Md. : 1950)*, vol. 181, no. 4, pp. 2705–2712.
- Altschul, S. F., Madden, T. L., Schäffer, A. A., Zhang, J., Zhang, Z., Miller, W. and Lipman, D. J. (1997) 'Gapped BLAST and PSI-BLAST: a new generation of protein database search programs', *Nucleic acids research*, vol. 25, no. 17, pp. 3389–3402.
- Alves, I. D., Jiao, C.-Y., Aubry, S., Aussedat, B., Burlina, F., Chassaing, G. and Sagan, S. (2010) 'Cell biology meets biophysics to unveil the different mechanisms of penetratin internalization in cells', *Biochimica et biophysica acta*, vol. 1798, no. 12, pp. 2231–2239.
- An, C., Jiang, H. and Kanost, M. R. (2010) 'Proteolytic activation and function of the cytokine Spätzle in the innate immune response of a lepidopteran insect, *Manduca sexta*', *The FEBS journal*, vol. 277, no. 1, pp. 148–162.



## References

- An, Y., Fan, N. and Zhang, S. (2009) 'Creatine kinase is a bacteriostatic factor with a lectin-like activity', *Molecular immunology*, vol. 46, no. 13, pp. 2666–2670.
- Andrejko, K., Whittles, L. K. and Lewnard, J. A. (2022) 'Health-Economic Value of Vaccination Against Group A Streptococcus in the United States', *Clinical infectious diseases : an official publication of the Infectious Diseases Society of America*, vol. 74, no. 6, pp. 983–992.
- Andrejko, M., Mak, P., Siemińska-Kuczer, A., Iwański, B., Wojda, I., Suder, P., Kuleta, P., Regucka, K. and Cytryńska, M. (2021) 'A comparison of the production of antimicrobial peptides and proteins by *Galleria mellonella* larvae in response to infection with two *Pseudomonas aeruginosa* strains differing in the profile of secreted proteases', *Journal of Insect Physiology*, vol. 131, p. 104239.
- (2019) *Antibiotic resistance threats in the United States, 2019*, Centers for Disease Control and Prevention (U.S.).
- Arnold, P. A., Johnson, K. N. and White, C. R. (2013) 'Physiological and metabolic consequences of viral infection in *Drosophila melanogaster*', *The Journal of experimental biology*, vol. 216, Pt 17, pp. 3350–3357.
- Arrighi, R. B. G., Ebikeme, C., Jiang, Y., Ranford-Cartwright, L., Barrett, M. P., Langel, U. and Faye, I. (2008) 'Cell-penetrating peptide TP10 shows broad-spectrum activity against both *Plasmodium falciparum* and *Trypanosoma brucei brucei*', *Antimicrobial agents and chemotherapy*, vol. 52, no. 9, pp. 3414–3417.
- Asai, M., Sheehan, G., Li, Y., Robertson, B. D., Kavanagh, K., Langford, P. R. and Newton, S. M. (2021) 'Innate Immune Responses of *Galleria mellonella* to *Mycobacterium bovis* BCG Challenge Identified Using Proteomic and Molecular Approaches', *Frontiers in cellular and infection microbiology*, vol. 11.
- Ashbaugh, C. D., Moser, T. J., Shearer, M. H., White, G. L., Kennedy, R. C. and Wessels, M. R. (2000) 'Bacterial determinants of persistent throat colonization and the associated immune response in a primate model of human group A streptococcal pharyngeal infection', *Cellular microbiology*, vol. 2, no. 4, pp. 283–292.
- Ashbaugh, C. D., Warren, H. B., Carey, V. J. and Wessels, M. R. (1998) 'Molecular analysis of the role of the group A streptococcal cysteine protease, hyaluronic acid capsule, and M protein in a murine model of human invasive soft-tissue infection', *Journal of Clinical Investigation*, vol. 102, no. 3, pp. 550–560.
- Askari, F. K. and McDonnell, W. M. (1996) 'Antisense-oligonucleotide therapy', *The New England journal of medicine*, vol. 334, no. 5, pp. 316–318.
- Azeez, O. I., Meintjes, R. and Chamunorwa, J. P. (2014) 'Fat body, fat pad and adipose tissues in invertebrates and vertebrates: the nexus', *Lipids in health and disease*, vol. 13, p. 71.
- Baharoglu, Z. and Mazel, D. (2011) 'Vibrio cholerae triggers SOS and mutagenesis in response to a wide range of antibiotics: a route towards multiresistance', *Antimicrobial agents and chemotherapy*, vol. 55, no. 5, pp. 2438–2441.
- Bai, H., You, Y., Yan, H., Meng, J., Xue, X., Hou, Z., Zhou, Y., Ma, X., Sang, G. and Luo, X. (2012) 'Antisense inhibition of gene expression and growth in gram-negative bacteria by cell-penetrating peptide conjugates of peptide nucleic acids targeted to rpoD gene', *Biomaterials*, vol. 33, no. 2, pp. 659–667.
- Baldassarri, L., Creti, R., Recchia, S., Imperi, M., Facinelli, B., Giovanetti, E., Pataracchia, M., Alfarone, G. and Orefici, G. (2006) 'Therapeutic failures of antibiotics used to treat macrolide-susceptible *Streptococcus pyogenes* infections may be due to biofilm formation', *Journal of clinical microbiology*, vol. 44, no. 8, pp. 2721–2727.
- Barek, H., Zhao, H., Heath, K., Veraksa, A. and Sugumaran, M. (2022) '*Drosophila* yellow-h encodes dopaminechrome tautomerase: A new enzyme in the eumelanin biosynthetic pathway', *Pigment cell & melanoma research*, vol. 35, no. 1, pp. 26–37.
- Barkowsky, G., Abt, C., Pöhner, I., Bieda, A., Hammerschmidt, S., Jacob, A., Kreikemeyer, B. and Patenge, N. (2022) 'Antimicrobial Activity of Peptide-Coupled Antisense Peptide Nucleic Acids in *Streptococcus pneumoniae*', *Microbiology spectrum*, vol. 10, no. 6, e0049722.
- Barkowsky, G., Kreikemeyer, B. and Patenge, N. (2020) 'Validation of Suitable Carrier Molecules and Target Genes for Antisense Therapy Using Peptide-Coupled Peptide Nucleic Acids (PNAs) in Streptococci', *Methods in molecular biology (Clifton, N.J.)*, vol. 2136, pp. 339–345.
- Barkowsky, G., Lemster, A.-L., Pappesch, R., Jacob, A., Krüger, S., Schröder, A., Kreikemeyer, B. and Patenge, N. (2019) 'Influence of Different Cell-Penetrating Peptides on the Antimicrobial Efficiency of PNAs in *Streptococcus pyogenes*', *Molecular therapy. Nucleic acids*, vol. 18, pp. 444–454.
- Bausinger, H., Lipsker, D. and Hanau, D. (2002) 'Heat-shock proteins as activators of the innate immune system', *Trends in immunology*, vol. 23, no. 7, pp. 342–343.

## References

- Belaouaj, A., Kim, K. S. and Shapiro, S. D. (2000) 'Degradation of outer membrane protein A in Escherichia coli killing by neutrophil elastase', *Science (New York, N.Y.)*, vol. 289, no. 5482, pp. 1185–1188.
- Bennett, C. F. and Swayze, E. E. (2010) 'RNA targeting therapeutics: molecular mechanisms of antisense oligonucleotides as a therapeutic platform', *Annual review of pharmacology and toxicology*, vol. 50, pp. 259–293.
- Berry, A. M. and Paton, J. C. (2000) 'Additive attenuation of virulence of Streptococcus pneumoniae by mutation of the genes encoding pneumolysin and other putative pneumococcal virulence proteins', *Infection and immunity*, vol. 68, no. 1, pp. 133–140.
- Berry, A. M., Yother, J., Briles, D. E., Hansman, D. and Paton, J. C. (1989) 'Reduced virulence of a defined pneumolysin-negative mutant of Streptococcus pneumoniae', *Infection and immunity*, vol. 57, no. 7, pp. 2037–2042.
- Bettencourt, R., Lanz-Mendoza, H., Lindquist, K. R. and Faye, I. (1997) 'Cell adhesion properties of hemolin, an insect immune protein in the Ig superfamily', *European journal of biochemistry*, vol. 250, no. 3, pp. 630–637.
- Bhattacharya, S. (2010) 'The facts about penicillin allergy: a review', *Journal of advanced pharmaceutical technology & research*, vol. 1, no. 1, pp. 11–17.
- Białas, N., Sokolova, V., van der Meer, S. B., Knuschke, T., Ruks, T., Klein, K., Westendorf, A. M. and Epple, M. (2022) 'Bacteria (E. coli ) take up ultrasmall gold nanoparticles (2 nm) as shown by different optical microscopic techniques (CLSM, SIM, STORM)', *Nano Select*, vol. 3, no. 10, pp. 1407–1420.
- Bidoli, C., Miccoli, A., Buonocore, F., Fausto, A. M., Gerdol, M., Picchietti, S. and Scapigliati, G. (2022) 'Transcriptome Analysis Reveals Early Hemocyte Responses upon In Vivo Stimulation with LPS in the Stick Insect Bacillus rossius (Rossi, 1788)', *Insects*, vol. 13, no. 7.
- Binder, R. J. (2014) 'Functions of heat shock proteins in pathways of the innate and adaptive immune system', *Journal of immunology (Baltimore, Md. : 1950)*, vol. 193, no. 12, pp. 5765–5771.
- Bisno, A. L., Gerber, M. A., Gwaltney, J. M., Kaplan, E. L. and Schwartz, R. H. (2002) 'Practice guidelines for the diagnosis and management of group A streptococcal pharyngitis. Infectious Diseases Society of America', *Clinical infectious diseases : an official publication of the Infectious Diseases Society of America*, vol. 35, no. 2, pp. 113–125.
- Boggs, C. L. and Freeman, K. D. (2005) 'Larval food limitation in butterflies: effects on adult resource allocation and fitness', *Oecologia*, vol. 144, no. 3, pp. 353–361.
- Böhmová, E., Machová, D., Pechar, M., Pola, R., Venlíková, K., Janoušková, O. and Etrych, T. (2018) 'Cell-penetrating peptides: a useful tool for the delivery of various cargoes into cells', *Physiological research*, vol. 67, Suppl 2, S267-S279.
- Boullaran, C. and Kehrl, J. H. (2014) 'Implications of non-canonical G-protein signaling for the immune system', *Cellular signalling*, vol. 26, no. 6, pp. 1269–1282.
- Brady, D., Grapputo, A., Romoli, O. and Sandrelli, F. (2019) 'Insect Cecropins, Antimicrobial Peptides with Potential Therapeutic Applications', *International journal of molecular sciences*, vol. 20, no. 23.
- Brakel, C. L. (1989) *Discoveries in antisense nucleic acids*, The Woodlands, Tex., Portfolio Publ. Co. u.a.
- Breaker, R. R. and Joyce, G. F. (1994) 'A DNA enzyme that cleaves RNA', *Chemistry & biology*, vol. 1, no. 4, pp. 223–229.
- Brouwer, S., Rivera-Hernandez, T., Curren, B. F., Harbison-Price, N., Oliveira, D. M. P. de, Jespersen, M. G., Davies, M. R. and Walker, M. J. (2023) 'Pathogenesis, epidemiology and control of Group A Streptococcus infection', *Nature reviews. Microbiology*, pp. 1–17.
- Brown, A. O., Mann, B., Gao, G., Hankins, J. S., Humann, J., Giardina, J., Faverio, P., Restrepo, M. I., Halade, G. V., Mortensen, E. M., Lindsey, M. L., Hanes, M., Happel, K. I., Nelson, S., Bagby, G. J., Lorent, J. A., Cardinal, P., Granados, R., Esteban, A., LeSaux, C. J., Tuomanen, E. I. and Orihuela, C. J. (2014) 'Streptococcus pneumoniae translocates into the myocardium and forms unique microlesions that disrupt cardiac function', *PLoS pathogens*, vol. 10, no. 9, e1004383.
- Brown, J. S., Gilliland, S. M. and Holden, D. W. (2001) 'A Streptococcus pneumoniae pathogenicity island encoding an ABC transporter involved in iron uptake and virulence', *Molecular microbiology*, vol. 40, no. 3, pp. 572–585.
- Brown, J. S., Gilliland, S. M., Ruiz-Albert, J. and Holden, D. W. (2002) 'Characterization of pit, a Streptococcus pneumoniae iron uptake ABC transporter', *Infection and immunity*, vol. 70, no. 8, pp. 4389–4398.

## References

- Brueggemann, A. B., Peto, T. E. A., Crook, D. W., Butler, J. C., Kristinsson, K. G. and Spratt, B. G. (2004) 'Temporal and geographic stability of the serogroup-specific invasive disease potential of *Streptococcus pneumoniae* in children', *The Journal of infectious diseases*, vol. 190, no. 7, pp. 1203–1211.
- Buccini, D. F., Cardoso, M. H. and Franco, O. L. (2020) 'Antimicrobial Peptides and Cell-Penetrating Peptides for Treating Intracellular Bacterial Infections', *Frontiers in cellular and infection microbiology*, vol. 10, p. 612931.
- Bunnell, T. M., Burbach, B. J., Shimizu, Y. and Ervasti, J. M. (2011) ' $\beta$ -Actin specifically controls cell growth, migration, and the G-actin pool', *Molecular biology of the cell*, vol. 22, no. 21, pp. 4047–4058.
- Burger, H. G., Yamada, Y., Bangah, M. L., McCloud, P. I. and Warne, G. L. (1991) 'Serum gonadotropin, sex steroid, and immunoreactive inhibin levels in the first two years of life', *The Journal of clinical endocrinology and metabolism*, vol. 72, no. 3, pp. 682–686.
- Calix, J. J., Porambo, R. J., Brady, A. M., Larson, T. R., Yother, J., Abeygunwardana, C. and Nahm, M. H. (2012) 'Biochemical, Genetic, and Serological Characterization of Two Capsule Subtypes among *Streptococcus pneumoniae* Serotype 20 Strains: DISCOVERY OF A NEW PNEUMOCOCCAL SEROTYPE\*', *The Journal of biological chemistry*, vol. 287, no. 33, pp. 27885–27894.
- Carapetis, J. R., Steer, A. C., Mulholland, E. K. and Weber, M. (2005) 'The global burden of group A streptococcal diseases', *The Lancet Infectious Diseases*, vol. 5, no. 11, pp. 685–694.
- Carney, T. J., Feitosa, N. M., Sonntag, C., Slanchev, K., Kluger, J., Kiyozumi, D., Gebauer, J. M., Coffin Talbot, J., Kimmel, C. B., Sekiguchi, K., Wagener, R., Schwarz, H., Ingham, P. W. and Hammerschmidt, M. (2010) 'Genetic analysis of fin development in zebrafish identifies furin and hemicentin1 as potential novel fraser syndrome disease genes', *PLoS genetics*, vol. 6, no. 4, e1000907.
- Carrillo, J. L. M., Rodríguez, F. P. C., Coronado, O. G., García, M. A. M. and Cordero, J. F. C. (2017) 'Physiology and Pathology of Innate Immune Response Against Pathogens', in Rezaei, N. (ed) *Physiology and Pathology of Immunology*, InTech.
- Center for Disease Control and Prevention (2022) *Group A Streptococcal (GAS) Disease: Scarlet Fever: All You Need to Know* [Online]. Available at <https://www.cdc.gov/groupastrep/diseases-public/scarlet-fever.html> (Accessed 27 February 2022).
- Centers for Disease Control and Prevention (U.S.) (ed) (2021) *Epidemiology and prevention of vaccine-preventable diseases: Chapter 17: Pneumococcal disease*, 14th edn, Washington, D.C., Public Health Foundation.
- Chan, T., Tay, M. Z., Kyaw, W. M., Chow, A. and Ho, H. J. (2020) 'Epidemiology, vaccine effectiveness, and risk factors for mortality for pneumococcal disease among hospitalised adults in Singapore: a case-control study', *BMC infectious diseases*, vol. 20, no. 1, p. 423.
- Chandra, M., Sachdeva, A. and Silverman, S. K. (2009) 'DNA-catalyzed sequence-specific hydrolysis of DNA', *Nature chemical biology*, vol. 5, no. 10, pp. 718–720.
- Chapman, R. F. (2003) 'Contact chemoreception in feeding by phytophagous insects', *Annual review of entomology*, vol. 48, pp. 455–484.
- Charroux, B., Daian, F. and Royet, J. (2020) 'Drosophila Aversive Behavior toward *Erwinia carotovora* carotovora Is Mediated by Bitter Neurons and Leukokinin', *iScience*, vol. 23, no. 6, p. 101152.
- Chen, S., Liu, M., Li, Y., Zhou, X., Hou, Y. and Gong, J. (2016) 'Molecular Identification and Expression Patterns of Apolipoprotein D From *Bombyx mori* (Lepidoptera: Bombycidae) in Response to Oxidative Stress and Bacterial Challenge', *Annals of the Entomological Society of America*, vol. 109, no. 5, pp. 759–767.
- Cheng, W., Li, Q., Jiang, Y.-L., Zhou, C.-Z. and Chen, Y. (2013) 'Structures of *Streptococcus pneumoniae* PiaA and its complex with ferrichrome reveal insights into the substrate binding and release of high affinity iron transporters', *PloS one*, vol. 8, no. 8, e71451.
- Cheon, H.-M., Hwang, S.-J., Kim, H.-J., Jin, B. R., Chae, K.-S., Yun, C.-Y. and Seo, S.-J. (2002) 'Two juvenile hormone suppressible storage proteins may play different roles in *Hyphantria cunea* Drury', *Archives of insect biochemistry and physiology*, vol. 50, no. 4, pp. 157–172.
- Cherazard, R., Epstein, M., Doan, T.-L., Salim, T., Bharti, S. and Smith, M. A. (2017) 'Antimicrobial Resistant *Streptococcus pneumoniae*: Prevalence, Mechanisms, and Clinical Implications', *American journal of therapeutics*, vol. 24, no. 3, e361-e369.
- Chiriboga, C. A. (2017) 'Nusinersen for the treatment of spinal muscular atrophy', *Expert review of neurotherapeutics*, vol. 17, no. 10, pp. 955–962.

## References

- Chithrani, D. B., Dunne, M., Stewart, J., Allen, C. and Jaffray, D. A. (2010) 'Cellular uptake and transport of gold nanoparticles incorporated in a liposomal carrier', *Nanomedicine : nanotechnology, biology, and medicine*, vol. 6, no. 1, pp. 161–169.
- Chochua, S., Metcalf, B. J., Li, Z., Rivers, J., Mathis, S., Jackson, D., Gertz, R. E., Srinivasan, V., Lynfield, R., van Beneden, C., McGee, L. and Beall, B. (2017) 'Population and Whole Genome Sequence Based Characterization of Invasive Group A Streptococci Recovered in the United States during 2015', *mBio*, vol. 8, no. 5.
- Cillóniz, C., Garcia-Vidal, C., Ceccato, A. and Torres, A. (2018) 'Antimicrobial Resistance Among *Streptococcus pneumoniae*', in Fong, I. W., Shlaes, D. and Drlica, K. (eds) *Antimicrobial Resistance in the 21st Century*, Cham, Springer International Publishing, pp. 13–38.
- Claverys, J.-P., Prudhomme, M. and Martin, B. (2006) 'Induction of competence regulons as a general response to stress in gram-positive bacteria', *Annual review of microbiology*, vol. 60, pp. 451–475.
- Clermont, A., Wedde, M., Seitz, V., Podsiadlowski, L., Lenze, D., Hummel, M. and Vilcinskis, A. (2004) 'Cloning and expression of an inhibitor of microbial metalloproteinases from insects contributing to innate immunity', *The Biochemical journal*, vol. 382, Pt 1, pp. 315–322.
- Cohen, C., Naidoo, N., Meiring, S., Gouveia, L. de, Mollendorf, C. von, Walaza, S., Naicker, P., Madhi, S. A., Feldman, C., Klugman, K. P., Dawood, H. and Gottberg, A. von (2015) 'Streptococcus pneumoniae Serotypes and Mortality in Adults and Adolescents in South Africa: Analysis of National Surveillance Data, 2003 - 2008', *PloS one*, vol. 10, no. 10, e0140185.
- Coleman, J. L. and Benach, J. L. (1999) 'Use of the plasminogen activation system by microorganisms', *The Journal of laboratory and clinical medicine*, vol. 134, no. 6, pp. 567–576.
- Collin, F., Karkare, S. and Maxwell, A. (2011) 'Exploiting bacterial DNA gyrase as a drug target: current state and perspectives', *Applied microbiology and biotechnology*, vol. 92, no. 3, pp. 479–497.
- Corfield, T. (1992) 'Bacterial sialidases--roles in pathogenicity and nutrition', *Glycobiology*, vol. 2, no. 6, pp. 509–521.
- Daeihamed, M., Dadashzadeh, S., Haeri, A. and Akhlaghi, M. F. (2017) 'Potential of Liposomes for Enhancement of Oral Drug Absorption', *Current drug delivery*, vol. 14, no. 2, pp. 289–303.
- Dagkessamanskaia, A., Moscoso, M., Hénard, V., Guiral, S., Overweg, K., Reuter, M., Martin, B., Wells, J. and Claverys, J.-P. (2004) 'Interconnection of competence, stress and CiaR regulons in *Streptococcus pneumoniae*: competence triggers stationary phase autolysis of ciaR mutant cells', *Molecular microbiology*, vol. 51, no. 4, pp. 1071–1086.
- Dai, H., Rayaprolu, S., Gong, Y., Huang, R., Prakash, O. and Jiang, H. (2008) 'Solution structure, antibacterial activity, and expression profile of Manduca sexta moricin', *Journal of peptide science : an official publication of the European Peptide Society*, vol. 14, no. 7, pp. 855–863.
- Dale, J., Batzloff, Cleary, P. and et al (eds) (2016) *Current Approaches to Group A Streptococcal Vaccine Development* (In: Ferretti JJ, Stevens DL, Fischetti VA, editors. *Streptococcus pyogenes : Basic Biology to Clinical Manifestations* [Internet]).
- Dale, J., Batzloff, Cleary, P. and et al. *Current Approaches to Group A Streptococcal Vaccine Development*.
- Dale, J. B. and Walker, M. J. (2020) 'Update on group A streptococcal vaccine development', *Current opinion in infectious diseases*, vol. 33, no. 3, pp. 244–250.
- d'Alençon, E., Bierne, N., Girard, P.-A., Magdelenat, G., Gimenez, S., Seninet, I. and Escoubas, J.-M. (2013) 'Evolutionary history of x-tox genes in three lepidopteran species: origin, evolution of primary and secondary structure and alternative splicing, generating a repertoire of immune-related proteins', *Insect Biochemistry and Molecular Biology*, vol. 43, no. 1, pp. 54–64.
- Demidov, V. V., Potaman, V. N., Frank-Kamenetskii, M. D., Egholm, M., Buchard, O., Sönnichsen, S. H. and Nielsen, P. E. (1994) 'Stability of peptide nucleic acids in human serum and cellular extracts', *Biochemical pharmacology*, vol. 48, no. 6, pp. 1310–1313.
- DeMuri, G. P. and Wald, E. R. (2014) 'The Group A Streptococcal Carrier State Reviewed: Still an Enigma', *Journal of the Pediatric Infectious Diseases Society*, vol. 3, no. 4, pp. 336–342.
- Derossi, D., Joliot, A. H., Chassaing, G. and Prochiantz, A. (1994) 'The third helix of the Antennapedia homeodomain translocates through biological membranes', *The Journal of biological chemistry*, vol. 269, no. 14, pp. 10444–10450.

## References

- Dhawan, R., Gupta, K., Kajla, M., Kakani, P., Choudhury, T. P., Kumar, S., Kumar, V. and Gupta, L. (2017) 'Apolipoprotein-III Acts as a Positive Regulator of Plasmodium Development in Anopheles stephensi', *Frontiers in Physiology*, vol. 8.
- Di Marzo, N., Chisci, E. and Giovannoni, R. (2018) 'The Role of Hydrogen Peroxide in Redox-Dependent Signaling: Homeostatic and Pathological Responses in Mammalian Cells', *Cells*, vol. 7, no. 10.
- Di Virgilio, F., Sarti, A. C. and Coutinho-Silva, R. (2020) 'Purinergic signaling, DAMPs, and inflammation', *American journal of physiology. Cell physiology*, vol. 318, no. 5, C832-C835.
- Dolezal, T., Krejcová, G., Bajgar, A., Nedbalová, P. and Strasser, P. (2019) 'Molecular regulations of metabolism during immune response in insects', *Insect Biochemistry and Molecular Biology*, vol. 109, pp. 31–42.
- Dominguez, R. and Holmes, K. C. (2011) 'Actin Structure and Function', *Annual review of biophysics*, vol. 40, pp. 169–186.
- Donkor, E. S. (2013) 'Understanding the pneumococcus: transmission and evolution', *Frontiers in cellular and infection microbiology*, vol. 3, p. 7.
- Dossey AT, Morales-Ramos JA, Guadalupe Rojas M (2016) *Insects as Sustainable Food Ingredients*, Elsevier.
- Drin, G., Cottin, S., Blanc, E., Rees, A. R. and Tamsamani, J. (2003) 'Studies on the internalization mechanism of cationic cell-penetrating peptides', *The Journal of biological chemistry*, vol. 278, no. 33, pp. 31192–31201.
- Dryselius, R., Aswasti, S. K., Rajarao, G. K., Nielsen, P. E. and Good, L. (2003) 'The translation start codon region is sensitive to antisense PNA inhibition in Escherichia coli', *Oligonucleotides*, vol. 13, no. 6, pp. 427–433.
- Dryselius, R., Nekhotiaeva, N. and Good, L. (2005) 'Antimicrobial synergy between mRNA- and protein-level inhibitors', *The Journal of antimicrobial chemotherapy*, vol. 56, no. 1, pp. 97–103.
- Dubovskiy, I. M., Kryukova, N. A., Glupov, V. V. and Ratcliffe, N. A. (2016) 'Encapsulation and nodulation in insects'.
- Duchardt, F., Fotin-Mleczek, M., Schwarz, H., Fischer, R. and Brock, R. (2007) 'A comprehensive model for the cellular uptake of cationic cell-penetrating peptides', *Traffic (Copenhagen, Denmark)*, vol. 8, no. 7, pp. 848–866.
- Durieux, M.-F., Melloul, É., Jemel, S., Roisin, L., Dardé, M.-L., Guillot, J., Dannaoui, É. and Botterel, F. (2021) 'Galleria mellonella as a screening tool to study virulence factors of Aspergillus fumigatus', *Virulence*, vol. 12, no. 1, pp. 818–834.
- Efimova, S. S., Schagina, L. V. and Ostroumova, O. S. (2014) 'Channel-forming activity of cecropins in lipid bilayers: effect of agents modifying the membrane dipole potential', *Langmuir : the ACS journal of surfaces and colloids*, vol. 30, no. 26, pp. 7884–7892.
- El-Andaloussi, S., Järver, P., Johansson, H. J. and Langel, U. (2007) 'Cargo-dependent cytotoxicity and delivery efficacy of cell-penetrating peptides: a comparative study', *The Biochemical journal*, vol. 407, no. 2, pp. 285–292.
- Eleftherianos, I. and Revenis, C. (2011) 'Role and importance of phenoloxidase in insect hemostasis', *Journal of innate immunity*, vol. 3, no. 1, pp. 28–33.
- Ellis, J. D., Graham, J. R. and Mortensen, A. (2013) 'Standard methods for wax moth research', *Journal of Apicultural Research*, vol. 52, no. 1, pp. 1–17.
- El-Sawaf, S. K. (1950) 'The Life-history of the Greater Wax-moth (Galleria mellonella L.) In Egypt, with special Reference to the Morphology of the mature Larva (Lepidoptera : Pyralidae).', *Bulletin de la Societe Fouad Ier d'entomologie*.
- Engel, P. and Moran, N. A. (2013) 'The gut microbiota of insects - diversity in structure and function', *FEMS microbiology reviews*, vol. 37, no. 5, pp. 699–735.
- European Medicines Agency (2016) *Principles of replacement, reduction and refinement (3R): (CPMP/SWP/728/95)*.
- Faas, M. M., Saez, T. and Vos, P. de (2017) 'Corrigendum to "Extracellular ATP and adenosine: The yin and yang in immune responses?" Molecular Aspects of Medicine 55 (2017) 9-19', *Molecular aspects of medicine*, vol. 57, p. 30.
- Falabella, P., Riviello, L., Pascale, M., Di Lelio, I., Tettamanti, G., Grimaldi, A., Iannone, C., Monti, M., Pucci, P., Tamburro, A. M., Deeguileor, M., Gigliotti, S. and Pennacchio, F. (2012) 'Functional amyloids in insect immune response', *Insect Biochemistry and Molecular Biology*, vol. 42, no. 3, pp. 203–211.

## References

- Falanga, A., Valiante, S., Galdiero, E., Franci, G., Scudiero, O., Morelli, G. and Galdiero, S. (2017) 'Dimerization in tailoring uptake efficacy of the HSV-1 derived membranotropic peptide gH625', *Scientific reports*, vol. 7, no. 1, p. 9434.
- Fenske, D. B. and Cullis, P. R. (2005) 'Entrapment of small molecules and nucleic acid-based drugs in liposomes', *Methods in enzymology*, vol. 391, pp. 7–40.
- Fibriansah, G., Kovács, Á. T., Pool, T. J., Boonstra, M., Kuipers, O. P. and Thunnissen, A.-M. W. H. (2012) 'Crystal structures of two transcriptional regulators from *Bacillus cereus* define the conserved structural features of a PadR subfamily', *PLoS one*, vol. 7, no. 11, e48015.
- Fieber, C. and Kovarik, P. (2014) 'Responses of innate immune cells to group A *Streptococcus*', *Frontiers in cellular and infection microbiology*, vol. 4, p. 140.
- Fischetti, V. A. (1989) 'Streptococcal M protein: molecular design and biological behavior', *Clinical microbiology reviews*, vol. 2, no. 3, pp. 285–314.
- Fischetti, V. A. (2016) *Streptococcus pyogenes : Basic Biology to Clinical Manifestations: M Protein and Other Surface Proteins on Streptococci*, Oklahoma City (OK).
- Frankel, A. D. and Pabo, C. O. (1988) 'Cellular uptake of the tat protein from human immunodeficiency virus', *Cell*, vol. 55, no. 6, pp. 1189–1193.
- Futaki, S., Niwa, M., Nakase, I., Tadokoro, A., Zhang, Y., Nagaoka, M., Wakako, N. and Sugiura, Y. (2004) 'Arginine carrier peptide bearing Ni(II) chelator to promote cellular uptake of histidine-tagged proteins', *Bioconjugate chemistry*, vol. 15, no. 3, pp. 475–481.
- Futaki, S., Suzuki, T., Ohashi, W., Yagami, T., Tanaka, S., Ueda, K. and Sugiura, Y. (2001) 'Arginine-rich peptides. An abundant source of membrane-permeable peptides having potential as carriers for intracellular protein delivery', *The Journal of biological chemistry*, vol. 276, no. 8, pp. 5836–5840.
- Gettins, P. G. W. (2002) 'Serpin structure, mechanism, and function', *Chemical reviews*, vol. 102, no. 12, pp. 4751–4804.
- Giannella, R. A., Broitman, S. A. and Zamcheck, N. (1971) 'Vitamin B12 uptake by intestinal microorganisms: mechanism and relevance to syndromes of intestinal bacterial overgrowth', *Journal of Clinical Investigation*, vol. 50, no. 5, pp. 1100–1107.
- Girard, P.-A., Boublik, Y., Wheat, C. W., Volkoff, A.-N., Cousserans, F., Brehélin, M. and Escoubas, J.-M. (2008) 'X-tox: an atypical defensin derived family of immune-related proteins specific to Lepidoptera', *Developmental and comparative immunology*, vol. 32, no. 5, pp. 575–584.
- Gjonbalaj, M., Keith, J. W., Do, M. H., Hohl, T. M., Pamer, E. G. and Becattini, S. (2020) 'Antibiotic Degradation by Commensal Microbes Shields Pathogens', *Infection and immunity*, vol. 88, no. 4.
- González-Santoyo, I. and Córdoba-Aguilar, A. (2012) 'Phenoloxidase: a key component of the insect immune system', *Entomologia Experimentalis et Applicata*, vol. 142, no. 1, pp. 1–16.
- Good, L., Awasthi, S. K., Dryselius, R., Larsson, O. and Nielsen, P. E. (2001) 'Bactericidal antisense effects of peptide-PNA conjugates', *Nature biotechnology*, vol. 19, no. 4, pp. 360–364.
- Good, L. and Nielsen, P. E. (1998a) 'Antisense inhibition of gene expression in bacteria by PNA targeted to mRNA', *Nature biotechnology*, vol. 16, no. 4, pp. 355–358.
- Good, L. and Nielsen, P. E. (1998b) 'Inhibition of translation and bacterial growth by peptide nucleic acid targeted to ribosomal RNA', *Proceedings of the National Academy of Sciences of the United States of America*, vol. 95, no. 5, pp. 2073–2076.
- Good, L., Sandberg, R., Larsson, O., Nielsen, P. E. and Wahlestedt, C. (2000) 'Antisense PNA effects in *Escherichia coli* are limited by the outer-membrane LPS layer', *Microbiology (Reading, England)*, 146 (Pt 10), pp. 2665–2670.
- Grabenstein, J. D. and Klugman, K. P. (2012) 'A century of pneumococcal vaccination research in humans', *Clinical microbiology and infection : the official publication of the European Society of Clinical Microbiology and Infectious Diseases*, 18 Suppl 5, pp. 15–24.
- Grabenstein, J. D. and Musey, L. K. (2014) 'Differences in serious clinical outcomes of infection caused by specific pneumococcal serotypes among adults', *Vaccine*, vol. 32, no. 21, pp. 2399–2405.
- Grande Burgos, M. J., Kovács, A. T., Mirończuk, A. M., Abriouel, H., Gálvez, A. and Kuipers, O. P. (2009) 'Response of *Bacillus cereus* ATCC 14579 to challenges with sublethal concentrations of enterocin AS-48', *BMC microbiology*, vol. 9, p. 227.

## References

- Green, M. and Loewenstein, P. M. (1988) 'Autonomous functional domains of chemically synthesized human immunodeficiency virus tat trans-activator protein', *Cell*, vol. 55, no. 6, pp. 1179–1188.
- Gupta, A., Mumtaz, S., Li, C.-H., Hussain, I. and Rotello, V. M. (2019) 'Combatting antibiotic-resistant bacteria using nanomaterials', *Chemical Society reviews*, vol. 48, no. 2, pp. 415–427.
- Guterstam, P., Madani, F., Hirose, H., Takeuchi, T., Futaki, S., El Andaloussi, S., Gräslund, A. and Langel, U. (2009) 'Elucidating cell-penetrating peptide mechanisms of action for membrane interaction, cellular uptake, and translocation utilizing the hydrophobic counter-anion pyrenebutyrate', *Biochimica et biophysica acta*, vol. 1788, no. 12, pp. 2509–2517.
- Gutierrez, A., Laureti, L., Crussard, S., Abida, H., Rodríguez-Rojas, A., Blázquez, J., Baharoglu, Z., Mazel, D., Darfeuille, F., Vogel, J. and Matic, I. (2013) 'β-Lactam antibiotics promote bacterial mutagenesis via an RpoS-mediated reduction in replication fidelity', *Nature communications*, vol. 4, p. 1610.
- Guz, N., Dageri, A., Altincicek, B. and Aksoy, S. (2020) 'Molecular characterization and expression patterns of heat shock proteins in *Spodoptera littoralis*, heat shock or immune response?', *Cell Stress & Chaperones*, vol. 26, no. 1, pp. 29–40.
- Hair, P., Cameron, F. and McKeage, K. (2013) 'Mipomersen sodium: first global approval', *Drugs*, vol. 73, no. 5, pp. 487–493.
- Hall E., Wodi PA., Hamborsky J., Morelli V. and Schillie S. (2021) *Centers for Disease Control and Prevention. Epidemiology and Prevention of Vaccine-Preventable Diseases.: Chapter 17: Pneumococcal diseases. Pneumococcal Vaccine Characteristics*, 14th edn, Washington, D.C., Public Health Foundation.
- Hallas, G. (1985) 'The production of pyrogenic exotoxins by group A streptococci', *The Journal of hygiene*, vol. 95, no. 1, pp. 47–57.
- Halwani, A. E., Niven, D. F. and Dunphy, G. B. (2000) 'Apolipoprotein III and the interactions of lipoteichoic acids with the immediate immune responses of *Galleria mellonella*', *Journal of invertebrate pathology*, vol. 76, no. 4, pp. 233–241.
- Hammerschmidt, S., Bethe, G., H. Remane, P. and Chhatwal, G. S. (1999) 'Identification of Pneumococcal Surface Protein A as a Lactoferrin-Binding Protein of *Streptococcus pneumoniae*', *Infection and immunity*, vol. 67, no. 4, pp. 1683–1687.
- Hammond, S. M., Bernstein, E., Beach, D. and Hannon, G. J. (2000) 'An RNA-directed nuclease mediates post-transcriptional gene silencing in *Drosophila* cells', *Nature*, vol. 404, no. 6775, pp. 293–296.
- Hansen, M., Kilk, K. and Langel, U. (2008) 'Predicting cell-penetrating peptides', *Advanced drug delivery reviews*, vol. 60, 4-5, pp. 572–579.
- Hatamoto, M., Ohashi, A. and Imachi, H. (2010) 'Peptide nucleic acids (PNAs) antisense effect to bacterial growth and their application potentiality in biotechnology', *Applied microbiology and biotechnology*, vol. 86, no. 2, pp. 397–402.
- Hayes, A., Lacey, J. A., Morris, J. M., Davies, M. R. and Tong, S. Y. C. (2020) 'Restricted Sequence Variation in *Streptococcus pyogenes* Penicillin Binding Proteins', *mSphere*, vol. 5, no. 2.
- Hegarty, J. P. and Stewart, D. B. (2018) 'Advances in therapeutic bacterial antisense biotechnology', *Applied microbiology and biotechnology*, vol. 102, no. 3, pp. 1055–1065.
- Henderson-Begg, S. K., Livermore, D. M. and Hall, L. M. C. (2006) 'Effect of subinhibitory concentrations of antibiotics on mutation frequency in *Streptococcus pneumoniae*', *The Journal of antimicrobial chemotherapy*, vol. 57, no. 5, pp. 849–854.
- Henriques-Normark, B. and Tuomanen, E. I. (2013) 'The pneumococcus: epidemiology, microbiology, and pathogenesis', *Cold Spring Harbor perspectives in medicine*, vol. 3, no. 7.
- Herce, H. D., Garcia, A. E., Litt, J., Kane, R. S., Martin, P., Enrique, N., Rebolledo, A. and Milesi, V. (2009) 'Arginine-Rich Peptides Destabilize the Plasma Membrane, Consistent with a Pore Formation Translocation Mechanism of Cell-Penetrating Peptides', *Biophysical Journal*, vol. 97, no. 7, pp. 1917–1925.
- Holgerson, E. M., Gandhi, S., Zhou, Y., Kim, J., Vaz, B., Bogojeski, J., Bugno, M., Shalev, Z., Cheung-Ong, K., Gonçalves, J., O'Hara, M., Kron, K., Verby, M., Sun, M., Kakaradov, B., Delong, A., Merico, D. and Deshwar, A. G. (2021) 'Transcriptome-Wide Off-Target Effects of Steric-Blocking Oligonucleotides', *Nucleic Acid Therapeutics*, vol. 31, no. 6, pp. 392–403.
- Honsa, E. S., Johnson, M. D. L. and Rosch, J. W. (2013) 'The roles of transition metals in the physiology and pathogenesis of *Streptococcus pneumoniae*', *Frontiers in cellular and infection microbiology*, vol. 3, p. 92.

## References

- Hoshizaki, D. K. (2005) 'Fat-Cell Development', in *Comprehensive Molecular Insect Science*, Elsevier, pp. 315–345.
- Hossain, Z. (2014) 'Bacteria: Streptococcus', in *Encyclopedia of Food Safety*, Elsevier, pp. 535–545.
- Hoyer, J., Schatzschneider, U., Schulz-Siegmund, M. and Neundorff, I. (2012) 'Dimerization of a cell-penetrating peptide leads to enhanced cellular uptake and drug delivery', *Beilstein journal of organic chemistry*, vol. 8, pp. 1788–1797.
- Hu, Y., Hu, Q., Wei, R., Li, R., Zhao, D., Ge, M., Yao, Q. and Yu, X. (2019) 'The XRE Family Transcriptional Regulator SrtR in *Streptococcus suis* Is Involved in Oxidant Tolerance and Virulence', *Frontiers in cellular and infection microbiology*, vol. 8.
- Huang, Y., Hui, K., Jin, M., Yin, S., Wang, W. and Ren, Q. (2016) 'Two endoplasmic reticulum proteins (calnexin and calreticulin) are involved in innate immunity in Chinese mitten crab (*Eriocheir sinensis*)', *Scientific reports*, vol. 6, p. 27578.
- Huang, Y.-M., Hong, X.-Z., Shen, J., Geng, L.-J., Pan, Y.-H., Ling, W. and Zhao, H.-L. (2019) 'Amyloids in Site-Specific Autoimmune Reactions and Inflammatory Responses', *Frontiers in immunology*, vol. 10, p. 2980.
- Hutter, H., Vogel, B. E., Plenefisch, J. D., Norris, C. R., Proenca, R. B., Spieth, J., Guo, C., Mastwal, S., Zhu, X., Scheel, J. and Hedgecock, E. M. (2000) 'Conservation and novelty in the evolution of cell adhesion and extracellular matrix genes', *Science (New York, N.Y.)*, vol. 287, no. 5455, pp. 989–994.
- Hyams, C., Camberlein, E., Cohen, J. M., Bax, K. and Brown, J. S. (2009) 'The *Streptococcus pneumoniae* Capsule Inhibits Complement Activity and Neutrophil Phagocytosis by Multiple Mechanisms', *Infection and immunity*, vol. 78, no. 2, pp. 704–715.
- Iijima, R., Takahashi, H., Namme, R., Ikegami, S. and Yamazaki, M. (2004) 'Novel biological function of sialic acid (N-acetylneuraminic acid) as a hydrogen peroxide scavenger', *FEBS letters*, vol. 561, 1-3, pp. 163–166.
- Iryani, M. T. M., MacRae, T. H., Panchakshari, S., Tan, J., Bossier, P., Wahid, M. E. A. and Sung, Y. Y. (2017) 'Knockdown of heat shock protein 70 (Hsp70) by RNAi reduces the tolerance of *Artemia franciscana* nauplii to heat and bacterial infection', *Journal of Experimental Marine Biology and Ecology*, vol. 487, pp. 106–112.
- Isom, C. E., Menon, S. K., Thomas, L. M., West, A. H., Richter-Addo, G. B. and Karr, E. A. (2016) 'Crystal structure and DNA binding activity of a PadR family transcription regulator from hypervirulent *Clostridium difficile* R20291', *BMC microbiology*, vol. 16.
- Iubatti, M., Gabas, I. M., Cavaco, L. M., Mood, E. H., Lim, E., Bonanno, F., Yavari, N., Brolin, C. and Nielsen, P. E. (2022) 'Antisense Peptide Nucleic Acid-Diaminobutanoic Acid Dendron Conjugates with SbmA-Independent Antimicrobial Activity against Gram-Negative Bacteria', *ACS infectious diseases*, vol. 8, no. 5, pp. 1098–1106.
- Jang, I.-H., Chosa, N., Kim, S.-H., Nam, H.-J., Lemaitre, B., Ochiai, M., Kambris, Z., Brun, S., Hashimoto, C., Ashida, M., Brey, P. T. and Lee, W.-J. (2006) 'A Spätzle-processing enzyme required for toll signaling activation in *Drosophila* innate immunity', *Developmental cell*, vol. 10, no. 1, pp. 45–55.
- JH Lee, SM Park, KS Chae, IH Lee, Korean Society of Sericultural Science (2010) 'Galleria mellonella 6-Tox Gene, Putative Immune Related Molecule in Lepidoptera', *International Journal of Industrial Entomology*, Volume 21 Issue 1, pp. 127–132.
- Jha, D., Mishra, R., Gottschalk, S., Wiesmüller, K.-H., Ugurbil, K., Maier, M. E. and Engelmann, J. (2011) 'CyLoP-1: a novel cysteine-rich cell-penetrating peptide for cytosolic delivery of cargoes', *Bioconjugate chemistry*, vol. 22, no. 3, pp. 319–328.
- Jiang, H., Ma, C., Lu, Z.-Q. and Kanost, M. R. (2004) 'Beta-1,3-glucan recognition protein-2 (betaGRP-2) from *Manduca sexta*; an acute-phase protein that binds beta-1,3-glucan and lipoteichoic acid to aggregate fungi and bacteria and stimulate prophenoloxidase activation', *Insect Biochemistry and Molecular Biology*, vol. 34, no. 1, pp. 89–100.
- Jiang, H., Vilcinskas, A. and Kanost, M. R. (2010) 'Immunity in lepidopteran insects', *Advances in experimental medicine and biology*, vol. 708, pp. 181–204.
- Jiang, H., Wang, Y., Ma, C. and Kanost, M. R. (1997) 'Subunit composition of pro-phenol oxidase from *Manduca sexta*: molecular cloning of subunit ProPO-P1', *Insect Biochemistry and Molecular Biology*, vol. 27, no. 10, pp. 835–850.
- Jiang, S., Jia, Z., Chen, H., Wang, L. and Song, L. (2016) 'The modulation of haemolymph arginine kinase on the extracellular ATP induced bactericidal immune responses in the Pacific oyster *Crassostrea gigas*', *Fish & shellfish immunology*, vol. 54, pp. 282–293.



## References

- Johnson, A. F. and LaRock, C. N. (2021) 'Antibiotic Treatment, Mechanisms for Failure, and Adjunctive Therapies for Infections by Group A Streptococcus', *Frontiers in microbiology*, vol. 12, p. 760255.
- Jones, G., Venkataraman, V., Manczak, M. and Schelling, D. (1993) 'Juvenile hormone action to suppress gene transcription and influence message stability', *Developmental genetics*, vol. 14, no. 4, pp. 323–332.
- Jones, S. W., Christison, R., Bundell, K., Voyce, C. J., Brockbank, S. M. V., Newham, P. and Lindsay, M. A. (2005) 'Characterisation of cell-penetrating peptide-mediated peptide delivery', *British journal of pharmacology*, vol. 145, no. 8, pp. 1093–1102.
- Joo, H.-S., Fu, C.-I. and Otto, M. (2016) 'Bacterial strategies of resistance to antimicrobial peptides', *Philosophical transactions of the Royal Society of London. Series B, Biological sciences*, vol. 371, no. 1695.
- Jorjão, A. L., Oliveira, L. D., Scorzoni, L., Figueiredo-Godoi, L. M. A., Cristina A Prata, M., Jorge, A. O. C. and Junqueira, J. C. (2018) 'From moths to caterpillars: Ideal conditions for *Galleria mellonella* rearing for in vivo microbiological studies', *Virulence*, vol. 9, no. 1, pp. 383–389.
- Jung, J., Popella, L., Do, P. T., Pfau, P., Vogel, J. and Barquist, L. (2023) 'Design and off-target prediction for antisense oligomers targeting bacterial mRNAs with the MASON web server', *RNA (New York, N.Y.)*, vol. 29, no. 5, pp. 570–583.
- Jung, J., Sajjadian, S. M. and Kim, Y. (2019) 'Hemolin, an immunoglobulin-like peptide, opsonizes nonself targets for phagocytosis and encapsulation in *Spodoptera exigua*, a lepidopteran insect', *Journal of Asia-Pacific Entomology*, vol. 22, no. 3, pp. 947–956.
- Kamita, S. G. and Hammock, B. D. (2010) 'Juvenile hormone esterase: biochemistry and structure', *Journal of pesticide science*, vol. 35, no. 3, pp. 265–274.
- Kanost, M. R. and Jiang, H. (2015) 'Clip-domain serine proteases as immune factors in insect hemolymph', *Current opinion in insect science*, vol. 11, pp. 47–55.
- Kanost, M. R., Gorman, M. J. (2008) 'Phenoloxidasen in insect immunity', *Insect Immunology.*, B978-012373976.
- Kanwal, S. and Vaitla, P. (2022) *StatPearls: Streptococcus Pyogenes*, Treasure Island (FL).
- Kardani, K. and Bolhassani, A. (2021) 'Exploring novel and potent cell penetrating peptides in the proteome of SARS-COV-2 using bioinformatics approaches', *PloS one*, vol. 16, no. 2, e0247396.
- Karkare, S. and Bhatnagar, D. (2006) 'Promising nucleic acid analogs and mimics: characteristic features and applications of PNA, LNA, and morpholino', *Applied microbiology and biotechnology*, vol. 71, no. 5, pp. 575–586.
- Katayama, S., Nakase, I., Yano, Y., Murayama, T., Nakata, Y., Matsuzaki, K. and Futaki, S. (2013) 'Effects of pyrenebutyrate on the translocation of arginine-rich cell-penetrating peptides through artificial membranes: recruiting peptides to the membranes, dissipating liquid-ordered phases, and inducing curvature', *Biochimica et biophysica acta*, vol. 1828, no. 9, pp. 2134–2142.
- Kawano, J., Kotani, T., Ogata, Y., Ohtaki, S., Takechi, S., Nakayama, T., Sawaguchi, A., Nagaike, R., Oinuma, T. and Suganuma, T. (2000) 'CALNUC (nucleobindin) is localized in the Golgi apparatus in insect cells', *European journal of cell biology*, vol. 79, no. 3, pp. 208–217.
- Kersemans, V., Kersemans, K. and Cornelissen, B. (2008) 'Cell penetrating peptides for in vivo molecular imaging applications', *Current pharmaceutical design*, vol. 14, no. 24, pp. 2415–2447.
- Khil, J., Im, M., Heath, A., Ringdahl, U., Mundada, L., Cary Engleberg, N. and Fay, W. P. (2003) 'Plasminogen enhances virulence of group A streptococci by streptokinase-dependent and streptokinase-independent mechanisms', *The Journal of infectious diseases*, vol. 188, no. 4, pp. 497–505.
- Kim, C. H., Shin, Y. P., Noh, M. Y., Jo, Y. H., Han, Y. S., Seong, Y. S. and Lee, I. H. (2010) 'An insect multiligand recognition protein functions as an opsonin for the phagocytosis of microorganisms', *The Journal of biological chemistry*, vol. 285, no. 33, pp. 25243–25250.
- Kim, Y., Wang, X., Ma, Q., Zhang, X.-S. and Wood, T. K. (2009) 'Toxin-antitoxin systems in *Escherichia coli* influence biofilm formation through YjgK (TabA) and fimbriae', *Journal of bacteriology*, vol. 191, no. 4, pp. 1258–1267.
- Klugman, K. P. and Black, S. (2018) 'Impact of existing vaccines in reducing antibiotic resistance: Primary and secondary effects', *Proceedings of the National Academy of Sciences of the United States of America*, vol. 115, no. 51, pp. 12896–12901.

## References

- Knudsen, H. and Nielsen, P. E. (1996) 'Antisense properties of duplex- and triplex-forming PNAs', *Nucleic acids research*, vol. 24, no. 3, pp. 494–500.
- Kohanski, M. A., DePristo, M. A. and Collins, J. J. (2010) 'Sublethal antibiotic treatment leads to multidrug resistance via radical-induced mutagenesis', *Molecular cell*, vol. 37, no. 3, pp. 311–320.
- Konate, K., Crombez, L., Deshayes, S., Decaffmeyer, M., Thomas, A., Brasseur, R., Aldrian, G., Heitz, F. and Divita, G. (2010) 'Insight into the cellular uptake mechanism of a secondary amphipathic cell-penetrating peptide for siRNA delivery', *Biochemistry*, vol. 49, no. 16, pp. 3393–3402.
- Korayem, A. M., Hauling, T., Lesch, C., Fabbri, M., Lindgren, M., Loseva, O., Schmidt, O., Dushay, M. S. and Theopold, U. (2007) 'Evidence for an immune function of lepidopteran silk proteins', *Biochemical and biophysical research communications*, vol. 352, no. 2, pp. 317–322.
- Kordaczuk, J., Sułek, M., Mak, P., Zdybicka-Barabas, A., Śmiałek, J. and Wojda, I. (2022) 'Cationic protein 8 plays multiple roles in *Galleria mellonella* immunity', *Scientific reports*, vol. 12, no. 1, p. 11737.
- Kraus, D. and Peschel, A. (2006) 'Molecular mechanisms of bacterial resistance to antimicrobial peptides', *Current topics in microbiology and immunology*, vol. 306, pp. 231–250.
- Krzyściak, W., Pluskwa, K. K., Jurczak, A. and Kościelniak, D. (2013) 'The pathogenicity of the *Streptococcus* genus', *European journal of clinical microbiology & infectious diseases : official publication of the European Society of Clinical Microbiology*, vol. 32, no. 11, pp. 1361–1376.
- Kulkarni, J. A., Witzigmann, D., Thomson, S. B., Chen, S., Leavitt, B. R., Cullis, P. R. and van der Meel, R. (2021) 'The current landscape of nucleic acid therapeutics', *Nature Nanotechnology*, vol. 16, no. 6, pp. 630–643.
- Kurupati, P., Tan, K. S. W., Kumarasinghe, G. and Poh, C. L. (2007) 'Inhibition of gene expression and growth by antisense peptide nucleic acids in a multiresistant beta-lactamase-producing *Klebsiella pneumoniae* strain', *Antimicrobial agents and chemotherapy*, vol. 51, no. 3, pp. 805–811.
- Kwiatkowski, S. and Drozak, J. (2020) 'Protein Histidine Methylation', *Current protein & peptide science*, vol. 21, no. 7, pp. 675–689.
- Kwiatkowski, S., Seliga, A. K., Vertommen, D., Terreri, M., Ishikawa, T., Grabowska, I., Tiebe, M., Teleman, A. A., Jagielski, A. K., Veiga-da-Cunha, M. and Drozak, J. (2018) 'SETD3 protein is the actin-specific histidine N-methyltransferase', *eLife*, vol. 7.
- Lamazière, A., Maniti, O., Wolf, C., Lambert, O., Chassaing, G., Trugnan, G. and Ayala-Sanmartin, J. (2010) 'Lipid domain separation, bilayer thickening and pearling induced by the cell penetrating peptide penetratin', *Biochimica et biophysica acta*, vol. 1798, no. 12, pp. 2223–2230.
- Langel, Ü. (2019) 'Toxicity and Immune Response', in Langel, Ü. (ed) *CPP, Cell-Penetrating Peptides*, Singapore, Springer Singapore, pp. 339–357.
- Lanie, J. A., Ng, W.-L., Kazmierczak, K. M., Andrzejewski, T. M., Davidsen, T. M., Wayne, K. J., Tettelin, H., Glass, J. I. and Winkler, M. E. (2006) 'Genome Sequence of Avery's Virulent Serotype 2 Strain D39 of *Streptococcus pneumoniae* and Comparison with That of Unencapsulated Laboratory Strain R6', *Journal of bacteriology*, vol. 189, no. 1, pp. 38–51.
- LaRock, D. L., Russell, R., Johnson, A. F., Wilde, S. and LaRock, C. N. (2020) 'Group A *Streptococcus* Infection of the Nasopharynx Requires Proinflammatory Signaling through the Interleukin-1 Receptor', *Infection and immunity*, vol. 88, no. 10.
- Lavine, M. D. and Strand, M. R. (2002) 'Insect hemocytes and their role in immunity', *Insect Biochemistry and Molecular Biology*, vol. 32, no. 10, pp. 1295–1309.
- Lee, J. and Song, C.-H. (2021) 'Effect of Reactive Oxygen Species on the Endoplasmic Reticulum and Mitochondria during Intracellular Pathogen Infection of Mammalian Cells', *Antioxidants*, vol. 10, no. 6.
- Lee, M. H., Osaki, T., Lee, J. Y., Baek, M. J., Zhang, R., Park, J. W., Kawabata, S., Söderhäll, K. and Lee, B. L. (2004) 'Peptidoglycan recognition proteins involved in 1,3-beta-D-glucan-dependent prophenoloxidase activation system of insect', *The Journal of biological chemistry*, vol. 279, no. 5, pp. 3218–3227.
- Lee, Y., Kim, N., Roh, H., Kim, A., Han, H.-J., Cho, M. and Kim, D.-H. (2021) 'Transcriptome analysis unveils survival strategies of *Streptococcus parauberis* against fish serum', *PLoS one*, vol. 16, no. 5.
- Liang, X.-H., Sun, H., Nichols, J. G. and Croke, S. T. (2017) 'RNase H1-Dependent Antisense Oligonucleotides Are Robustly Active in Directing RNA Cleavage in Both the Cytoplasm and the Nucleus', *Molecular therapy : the journal of the American Society of Gene Therapy*, vol. 25, no. 9, pp. 2075–2092.

## References

- Liu, L., Zhou, Y., Qu, M., Qiu, Y., Guo, X., Zhang, Y., Liu, T., Yang, J. and Yang, Q. (2019) 'Structural and biochemical insights into the catalytic mechanisms of two insect chitin deacetylases of the carbohydrate esterase 4 family', *The Journal of biological chemistry*, vol. 294, no. 15, pp. 5774–5783.
- Liu, X., Li, J.-W., Feng, Z., Luo, Y., Veening, J.-W. and Zhang, J.-R. (2017) 'Transcriptional Repressor PtvR Regulates Phenotypic Tolerance to Vancomycin in *Streptococcus pneumoniae*', *Journal of bacteriology*, vol. 199, no. 14.
- Loughran, A. J., Orihuela, C. J. and Tuomanen, E. I. (2019) 'Streptococcus pneumoniae: Invasion and Inflammation', *Microbiology spectrum*, vol. 7, no. 2.
- Luchini, A. and Vitiello, G. (2020) 'Mimicking the Mammalian Plasma Membrane: An Overview of Lipid Membrane Models for Biophysical Studies', *Biomimetics (Basel, Switzerland)*, vol. 6, no. 1.
- Lynch, J. P. and Zhanel, G. G. (2009) 'Streptococcus pneumoniae: does antimicrobial resistance matter?', *Seminars in respiratory and critical care medicine*, vol. 30, no. 2, pp. 210–238.
- Maimaiti, N., Ahmed, Z., Md Isa, Z., Ghazi, H. F. and Aljunid, S. (2013) 'Clinical Burden of Invasive Pneumococcal Disease in Selected Developing Countries', *Value in health regional issues*, vol. 2, no. 2, pp. 259–263.
- Majchrzykiewicz, J. A. (2011) *Bacteriocins of Streptococcus pneumoniae and its response to challenges by antimicrobial peptides*, University of Groningen.
- Majchrzykiewicz, J. A., Lubelski, J., Moll, G. N., Kuipers, A., Bijlsma, J. J. E., Kuipers, O. P. and Rink, R. (2010) 'Production of a class II two-component lantibiotic of *Streptococcus pneumoniae* using the class I nisin synthetic machinery and leader sequence', *Antimicrobial agents and chemotherapy*, vol. 54, no. 4, pp. 1498–1505.
- Mak, P., Zdybicka-Barabas, A. and Cytryńska, M. (2010) 'A different repertoire of *Galleria mellonella* antimicrobial peptides in larvae challenged with bacteria and fungi', *Developmental and comparative immunology*, vol. 34, no. 10, pp. 1129–1136.
- Manceur, A., Wu, A. and Audet, J. (2007) 'Flow cytometric screening of cell-penetrating peptides for their uptake into embryonic and adult stem cells', *Analytical biochemistry*, vol. 364, no. 1, pp. 51–59.
- Mańdziuk, J. and Kuchar, E. P. (2022) *StatPearls: Streptococcal Meningitis*, Treasure Island (FL).
- Martner, A., Dahlgren, C., Paton, J. C. and Wold, A. E. (2008) 'Pneumolysin released during *Streptococcus pneumoniae* autolysis is a potent activator of intracellular oxygen radical production in neutrophils', *Infection and immunity*, vol. 76, no. 9, pp. 4079–4087.
- Massé, E., Vanderpool, C. K. and Gottesman, S. (2005) 'Effect of RyhB Small RNA on Global Iron Use in *Escherichia coli*', *Journal of bacteriology*, vol. 187, no. 20, pp. 6962–6971.
- Matsumoto, Y., Oda, Y., Uryu, M. and Hayakawa, Y. (2003) 'Insect cytokine growth-blocking peptide triggers a termination system of cellular immunity by inducing its binding protein', *The Journal of biological chemistry*, vol. 278, no. 40, pp. 38579–38585.
- May, R. C. and Machesky, L. M. (2001) 'Phagocytosis and the actin cytoskeleton', *Journal of cell science*, vol. 114, Pt 6, pp. 1061–1077.
- Mc Namara, L., Carolan, J. C., Griffin, C. T., Fitzpatrick, D. and Kavanagh, K. (2017) 'The effect of entomopathogenic fungal culture filtrate on the immune response of the greater wax moth, *Galleria mellonella*', *Journal of Insect Physiology*, vol. 100, pp. 82–92.
- McLauchlin, J., Rees, C. E. D. and Dodd, C. E. R. (2014) '*Listeria monocytogenes* and the Genus *Listeria*', in Rosenberg, E., DeLong, E. F., Lory, S., Stackebrandt, E. and Thompson, F. (eds) *The Prokaryotes*, Berlin, Heidelberg, Springer Berlin Heidelberg, pp. 241–259.
- Melendez AJ. (ed) (2000-2013) *Calcium Signaling During Phagocytosis*. [Online], Austin (TX): Landes Bioscience, In: Madame Curie Bioscience Database [Internet]. Available at <https://www.ncbi.nlm.nih.gov/books/NBK5971/>.
- Meng, J., Wang, H., Hou, Z., Chen, T., Fu, J., Ma, X., He, G., Xue, X., Jia, M. and Luo, X. (2009) 'Novel anion liposome-encapsulated antisense oligonucleotide restores susceptibility of methicillin-resistant *Staphylococcus aureus* and rescues mice from lethal sepsis by targeting *mecA*', *Antimicrobial agents and chemotherapy*, vol. 53, no. 7, pp. 2871–2878.
- Merkey, A. B., Wong, C. K., Hoshizaki, D. K. and Gibbs, A. G. (2011) 'Energetics of metamorphosis in *Drosophila melanogaster*', *Journal of Insect Physiology*, vol. 57, no. 10, pp. 1437–1445.

## References

- Metz, J. T. and Hajduk, P. J. (2010) 'Rational approaches to targeted polypharmacology: creating and navigating protein–ligand interaction networks', *Current Opinion in Chemical Biology*, vol. 14, no. 4, pp. 498–504.
- Milletti, F. (2012) 'Cell-penetrating peptides: classes, origin, and current landscape', *Drug discovery today*, vol. 17, 15-16, pp. 850–860.
- Minoo, S. and Hosseininaveh, V. (2015) 'Destruction of peritrophic membrane and its effect on biological characteristics and activity of digestive enzymes in larvae of the Indian meal moth, *Plodia interpunctella* (Lepidoptera: Pyralidae)', *European Journal of Entomology*, vol. 112, no. 2, pp. 245–250.
- Mishra, R., Su, W., Pfeuffer, J., Ugurbil, K. and Engelmann, J. (2009) 'Covalent Pyrenebutyrate-Cell Penetrating Peptide Conjugates: Enhanced Direct Membrane Translocation of Coupled Molecular Imaging Agents.', *35th Annual Meeting and Exposition of the Controlled Release Society 2008* (pp. 817-818). Red Hook, NY, USA: Curran.
- Mitchell, D. J., Kim, D. T., Steinman, L., Fathman, C. G. and Rothbard, J. B. (2000) 'Polyarginine enters cells more efficiently than other polycationic homopolymers', *The journal of peptide research : official journal of the American Peptide Society*, vol. 56, no. 5, pp. 318–325.
- Mnich, M. E., van Dalen, R. and van Sorge, N. M. (2020) 'C-Type Lectin Receptors in Host Defense Against Bacterial Pathogens', *Frontiers in cellular and infection microbiology*, vol. 10.
- Moghadam, Z. M., Henneke, P. and Kolter, J. (2021) 'From Flies to Men: ROS and the NADPH Oxidase in Phagocytes', *Frontiers in cell and developmental biology*, vol. 9, p. 628991.
- Mondhe, M., Chessher, A., Goh, S., Good, L. and Stach, J. E. M. (2014) 'Species-selective killing of bacteria by antimicrobial peptide-PNAs', *PloS one*, vol. 9, no. 2, e89082.
- Montazersaheb, S., Hejazi, M. S. and Nozad Charoudeh, H. (2018) 'Potential of Peptide Nucleic Acids in Future Therapeutic Applications', *Advanced pharmaceutical bulletin*, vol. 8, no. 4, pp. 551–563.
- Mook-Kanamori, B. B., Geldhoff, M., van der Poll, T. and van de Beek, D. (2011) 'Pathogenesis and pathophysiology of pneumococcal meningitis', *Clinical microbiology reviews*, vol. 24, no. 3, pp. 557–591.
- Moorthy, A. N., Rai, P., Jiao, H., Wang, S., Tan, K. B., Qin, L., Watanabe, H., Zhang, Y., Teluguakula, N. and Chow, V. T. K. (2016) 'Capsules of virulent pneumococcal serotypes enhance formation of neutrophil extracellular traps during in vivo pathogenesis of pneumonia', *Oncotarget*, vol. 7, no. 15, pp. 19327–19340.
- Moo-Young, M. and Butler, M. (2011) *Comprehensive Biotechnology (Second Edition)*, Elsevier Science.
- Moret, Y. and Schmid-Hempel, P. (2000) 'Survival for immunity: the price of immune system activation for bumblebee workers', *Science (New York, N.Y.)*, vol. 290, no. 5494, pp. 1166–1168.
- Müller, A., Salmen, A., Aebi, S., Gouveia, L. de, Gottberg, A. von and Hathaway, L. J. (2020) 'Pneumococcal serotype determines growth and capsule size in human cerebrospinal fluid', *BMC microbiology*, vol. 20.
- Munn, E. A. and Greville, G. D. (1969) 'The soluble proteins of developing: *Calliphora erythrocephala*, particularly calliphorin, and similar proteins in other insects', *Journal of Insect Physiology*, vol. 15, no. 10, pp. 1935–1950.
- Musser, J. M., Beres, S. B., Zhu, L., Olsen, R. J., Vuopio, J., Hyyryläinen, H.-L., Gröndahl-Yli-Hannuksela, K., Kristinsson, K. G., Darenberg, J., Henriques-Normark, B., Hoffmann, S., Caugant, D. A., Smith, A. J., Lindsay, D. S. J., Boragine, D. M. and Palzkill, T. (2020) 'Reduced In Vitro Susceptibility of *Streptococcus pyogenes* to  $\beta$ -Lactam Antibiotics Associated with Mutations in the *pbp2x* Gene Is Geographically Widespread', *Journal of clinical microbiology*, vol. 58, no. 4.
- Naseri, N., Valizadeh, H. and Zakeri-Milani, P. (2015) 'Solid Lipid Nanoparticles and Nanostructured Lipid Carriers: Structure, Preparation and Application', *Advanced pharmaceutical bulletin*, vol. 5, no. 3, pp. 305–313.
- Nash, A. A., Dalziel, R. G. and Fitzgerald, J. R. (2015) 'Mechanisms of Cell and Tissue Damage', *Mims' Pathogenesis of Infectious Disease*, pp. 171–231.
- Nasher, F., Aguilar, F., Aebi, S., Hermans, P. W. M., Heller, M. and Hathaway, L. J. (2018) 'Peptide Ligands of AmiA, AliA, and AliB Proteins Determine Pneumococcal Phenotype', *Frontiers in microbiology*, vol. 9, p. 3013.
- Nelson, K. E., Levy, M. and Miller, S. L. (2000) 'Peptide nucleic acids rather than RNA may have been the first genetic molecule', *Proceedings of the National Academy of Sciences of the United States of America*, vol. 97, no. 8, pp. 3868–3871.
- Nelson, W. E. (2016) *Nelson textbook of pediatrics*, 20th edn, Philadelphia, Pennsylvania, Elsevier.

## References

- Nezhadi, J., Narenji, H., Soroush Barhaghi, M. H., Rezaee, M. A., Ghotaslou, R., Pirzadeh, T., Tanomand, A., Ganbarov, K., Bastami, M., Madhi, M., Yousefi, M. and Kafil, H. S. (2019) 'Peptide nucleic acid-mediated re-sensitization of colistin resistance Escherichia coli KP81 harboring mcr-1 plasmid', *Microbial pathogenesis*, vol. 135, p. 103646.
- Nielsen, P. E. and Egholm, M. (1999) 'An introduction to peptide nucleic acid', *Current issues in molecular biology*, vol. 1, 1-2, pp. 89–104.
- Nielsen, P. E., Egholm, M., Berg, R. H. and Buchardt, O. (1991) 'Sequence-selective recognition of DNA by strand displacement with a thymine-substituted polyamide', *Science (New York, N.Y.)*, vol. 254, no. 5037, pp. 1497–1500.
- Niere, M., Dettloff, M., Maier, T., Ziegler, M. and Wiesner, A. (2001) 'Insect immune activation by apolipoprotein III is correlated with the lipid-binding properties of this protein', *Biochemistry*, vol. 40, no. 38, pp. 11502–11508.
- Niere, M., Meisslitzer, C., Dettloff, M., Weise, C., Ziegler, M. and Wiesner, A. (1999) 'Insect immune activation by recombinant Galleria mellonella apolipoprotein III(1)', *Biochimica et biophysica acta*, vol. 1433, 1-2, pp. 16–26.
- Nieto, C., Sadowy, E., La Campa, A. G. de, Hryniewicz, W. and Espinosa, M. (2010) 'The relBE2Spn toxin-antitoxin system of Streptococcus pneumoniae: role in antibiotic tolerance and functional conservation in clinical isolates', *PLoS one*, vol. 5, no. 6, e11289.
- Nirmala, X., Kodrik, D., Zurovec, M. and Sehnal, F. (2001) 'Insect silk contains both a Kunitz-type and a unique Kazal-type proteinase inhibitor', *European journal of biochemistry*, vol. 268, no. 7, pp. 2064–2073.
- Nirmala, X., Mita, K., Vanisree, V., Zurovec, M. and Sehnal, F. (2001) 'Identification of four small molecular mass proteins in the silk of Bombyx mori', *Insect molecular biology*, vol. 10, no. 5, pp. 437–445.
- Nishide, Y., Kageyama, D., Yokoi, K., Jouraku, A., Tanaka, H., Futahashi, R. and Fukatsu, T. (2019) 'Functional crosstalk across IMD and Toll pathways: insight into the evolution of incomplete immune cascades', *Proceedings. Biological sciences*, vol. 286, no. 1897, p. 20182207.
- Nishimoto, A. T., Rosch, J. W. and Tuomanen, E. I. (2020) 'Pneumolysin: Pathogenesis and Therapeutic Target', *Frontiers in microbiology*, vol. 11.
- Numata, K., Horii, Y., Oikawa, K., Miyagi, Y., Demura, T. and Ohtani, M. (2018) 'Library screening of cell-penetrating peptide for BY-2 cells, leaves of Arabidopsis, tobacco, tomato, poplar, and rice callus', *Scientific reports*, vol. 8.
- O'Brien, K. L., Wolfson, L. J., Watt, J. P., Henkle, E., Deloria-Knoll, M., McCall, N., Lee, E., Mulholland, K., Levine, O. S. and Cherian, T. (2009) 'Burden of disease caused by Streptococcus pneumoniae in children younger than 5 years: global estimates', *Lancet (London, England)*, vol. 374, no. 9693, pp. 893–902.
- Oikawa, K., Islam, M. M., Horii, Y., Yoshizumi, T. and Numata, K. (2018) 'Screening of a Cell-Penetrating Peptide Library in Escherichia coli : Relationship between Cell Penetration Efficiency and Cytotoxicity', *ACS Omega*, vol. 3, no. 12, pp. 16489–16499.
- Paddock, F. (1918) 'The Beemoth Or Waxworm', *Texas Agricultural Experiment Station*, no. 231.
- Park, C. B., Yi, K. S., Matsuzaki, K., Kim, M. S. and Kim, S. C. (2000) 'Structure-activity analysis of buforin II, a histone H2A-derived antimicrobial peptide: the proline hinge is responsible for the cell-penetrating ability of buforin II', *Proceedings of the National Academy of Sciences of the United States of America*, vol. 97, no. 15, pp. 8245–8250.
- Park, S.-S., Gonzalez-Juarbe, N., Martínez, E., Hale, J. Y., Lin, Y.-H., Huffines, J. T., Kruckow, K. L., Briles, D. E. and Orihuela, C. J. 'Streptococcus pneumoniae Binds to Host Lactate Dehydrogenase via PspA and PspC To Enhance Virulence', *mBio*, vol. 12, no. 3.
- Pascale, M., Laurino, S., Vogel, H., Grimaldi, A., Monné, M., Riviello, L., Tettamanti, G. and Falabella, P. (2014) 'The Lepidopteran endoribonuclease-U domain protein P102 displays dramatically reduced enzymatic activity and forms functional amyloids', *Developmental and comparative immunology*, vol. 47, no. 1, pp. 129–139.
- Patel, S. (2017) 'A critical review on serine protease: Key immune manipulator and pathology mediator', *Allergologia et immunopathologia*, vol. 45, no. 6, pp. 579–591.
- Patenge, N., Pappesch, R., Krawack, F., Walda, C., Mraheil, M. A., Jacob, A., Hain, T. and Kreikemeyer, B. (2013) 'Inhibition of Growth and Gene Expression by PNA-peptide Conjugates in Streptococcus pyogenes', *Molecular therapy. Nucleic acids*, vol. 2, no. 11, e132-.

## References

- Pech, L. L. and Strand, M. R. (1996) 'Granular cells are required for encapsulation of foreign targets by insect haemocytes', *Journal of cell science*, 109 (Pt 8), pp. 2053–2060.
- Pellestor, F. and Paulasova, P. (2004) 'The peptide nucleic acids (PNAs), powerful tools for molecular genetics and cytogenetics', *European journal of human genetics : EJHG*, vol. 12, no. 9, pp. 694–700.
- Pereira, J. M., Xu, S., Leong, J. M. and Sousa, S. (2022) 'The Yin and Yang of Pneumolysin During Pneumococcal Infection', *Frontiers in immunology*, vol. 13, p. 878244.
- Pereira, T. C., Barros, P. P. de, Fugisaki, L. R. d. O., Rossoni, R. D., Ribeiro, F. d. C., Menezes, R. T. de, Junqueira, J. C. and Scorzoni, L. (2018) 'Recent Advances in the Use of *Galleria mellonella* Model to Study Immune Responses against Human Pathogens', *Journal of fungi (Basel, Switzerland)*, vol. 4, no. 4.
- Perret, F., Nishihara, M., Takeuchi, T., Futaki, S., Lazar, A. N., Coleman, A. W., Sakai, N. and Matile, S. (2005) 'Anionic fullerenes, calixarenes, coronenes, and pyrenes as activators of oligo/polyarginines in model membranes and live cells', *Journal of the American Chemical Society*, vol. 127, no. 4, pp. 1114–1115.
- Pham, C. T. N. (2006) 'Neutrophil serine proteases: specific regulators of inflammation', *Nature reviews. Immunology*, vol. 6, no. 7, pp. 541–550.
- Phillips, G. N., Flicker, P. F., Cohen, C., Manjula, B. N. and Fischetti, V. A. (1981) 'Streptococcal M protein: alpha-helical coiled-coil structure and arrangement on the cell surface', *Proceedings of the National Academy of Sciences of the United States of America*, vol. 78, no. 8, pp. 4689–4693.
- Plesner, L. (1995) 'Ecto-ATPases: identities and functions', *International review of cytology*, vol. 158, pp. 141–214.
- Pockley, A. G. (2003) 'Heat shock proteins as regulators of the immune response', *Lancet (London, England)*, vol. 362, no. 9382, pp. 469–476.
- Pooga, M. and Langel, Ü. (2015) 'Classes of Cell-Penetrating Peptides', *Methods in molecular biology (Clifton, N.J.)*, vol. 1324, pp. 3–28.
- Popella, L., Jung, J., Do, P. T., Hayward, R. J., Barquist, L. and Vogel, J. (2022) 'Comprehensive analysis of PNA-based antisense antibiotics targeting various essential genes in uropathogenic *Escherichia coli*', *Nucleic acids research*.
- Popella, L., Jung, J., Popova, K., Đurica-Mitić, S., Barquist, L. and Vogel, J. (2021) 'Global RNA profiles show target selectivity and physiological effects of peptide-delivered antisense antibiotics', *Nucleic acids research*, vol. 49, no. 8, pp. 4705–4724.
- Potaczek, D. P., Garn, H., Unger, S. D. and Renz, H. (2016) 'Antisense molecules: A new class of drugs', *The Journal of allergy and clinical immunology*, vol. 137, no. 5, pp. 1334–1346.
- Powell, L. D. and Varki, A. P. (2001) 'Sialidases', *Current protocols in molecular biology*, Chapter 17, Unit17.12.
- Pratt, C. C. and Weers, P. M. M. (2004) 'Lipopolysaccharide binding of an exchangeable apolipoprotein, apolipoprotein III, from *Galleria mellonella*', *Biological chemistry*, vol. 385, no. 11, pp. 1113–1119.
- Rao, M. S., Gupta, R., Liguori, M. J., Hu, M., Huang, X., Mantena, S. R., Mittelstadt, S. W., Blomme, E. A. G. and van Vleet, T. R. (2019) 'Novel Computational Approach to Predict Off-Target Interactions for Small Molecules', *Frontiers in Big Data*, vol. 2.
- Rawlings M, Cronan JE Jr. (1992) 'The gene encoding *Escherichia coli* acyl carrier protein lies within a cluster of fatty acid biosynthetic genes', *J Biol Chem*, Mar 25;267(9):5751-4.
- Ray, A. and Nordén, B. (2000) 'Peptide nucleic acid (PNA): its medical and biotechnical applications and promise for the future', *FASEB journal : official publication of the Federation of American Societies for Experimental Biology*, vol. 14, no. 9, pp. 1041–1060.
- Readman, J. B., Dickson, G. and Coldham, N. G. (2016) 'Translational Inhibition of CTX-M Extended Spectrum  $\beta$ -Lactamase in Clinical Strains of *Escherichia coli* by Synthetic Antisense Oligonucleotides Partially Restores Sensitivity to Cefotaxime', *Frontiers in microbiology*, vol. 7, p. 373.
- Reder, A., Höper, D., Gerth, U. and Hecker, M. (2012) 'Contributions of Individual  $\sigma$ B-Dependent General Stress Genes to Oxidative Stress Resistance of *Bacillus subtilis*', *Journal of bacteriology*, vol. 194, no. 14, pp. 3601–3610.
- Roh, K.-B., Kim, C.-H., Lee, H., Kwon, H.-M., Park, J.-W., Ryu, J.-H., Kurokawa, K., Ha, N.-C., Lee, W.-J., Lemaitre, B., Söderhäll, K. and Lee, B.-L. (2009) 'Proteolytic Cascade for the Activation of the Insect Toll

## References

- Pathway Induced by the Fungal Cell Wall Component', *The Journal of biological chemistry*, vol. 284, no. 29, pp. 19474–19481.
- Rossi, J. J. (1995) 'Therapeutic antisense and ribozymes', *British medical bulletin*, vol. 51, no. 1, pp. 217–225.
- Roth, A. F., Sullivan, D. M. and Davis, N. G. (1998) 'A large PEST-like sequence directs the ubiquitination, endocytosis, and vacuolar degradation of the yeast a-factor receptor', *The Journal of cell biology*, vol. 142, no. 4, pp. 949–961.
- Roth, M., Jaquet, V., Lemeille, S., Bonetti, E.-J., Cambet, Y., François, P. and Krause, K.-H. (2022) 'Transcriptomic Analysis of E. coli after Exposure to a Sublethal Concentration of Hydrogen Peroxide Revealed a Coordinated Up-Regulation of the Cysteine Biosynthesis Pathway', *Antioxidants*, vol. 11, no. 4.
- Rothbard, J. B., Jessop, T. C., Lewis, R. S., Murray, B. A. and Wender, P. A. (2004) 'Role of membrane potential and hydrogen bonding in the mechanism of translocation of guanidinium-rich peptides into cells', *Journal of the American Chemical Society*, vol. 126, no. 31, pp. 9506–9507.
- Roux, A. de, Schmöle-Thoma, B., Schmöle-Thoma, B., Siber, G. R., Hackell, J. G., Kuhnke, A., Ahlers, N., Baker, S. A., Razmpour, A., Emini, E. A., Fernsten, P. D., Gruber, W. C., Lockhart, S., Burkhardt, O., Welte, T. and Lode, H. M. (2008) 'Comparison of pneumococcal conjugate polysaccharide and free polysaccharide vaccines in elderly adults: conjugate vaccine elicits improved antibacterial immune responses and immunological memory', *Clinical infectious diseases : an official publication of the Infectious Diseases Society of America*, vol. 46, no. 7, pp. 1015–1023.
- Równicki, M., Dąbrowska, Z., Wojciechowska, M., Wierzba, A. J., Maximova, K., Gryko, D. and Trylska, J. (2019) 'Inhibition of Escherichia coli Growth by Vitamin B 12 –Peptide Nucleic Acid Conjugates', *ACS Omega*, vol. 4, no. 1, pp. 819–824.
- Równicki, M., Wojciechowska, M., Wierzba, A. J., Czarnecki, J., Bartosik, D., Gryko, D. and Trylska, J. (2017) 'Vitamin B12 as a carrier of peptide nucleic acid (PNA) into bacterial cells', *Scientific reports*, vol. 7, no. 1, p. 7644.
- Ruczyński, J., Rusiecka, I., Turecka, K., Kozłowska, A., Alenowicz, M., Gągało, I., Kawiak, A., Rekowski, P., Waleron, K. and Kocić, I. (2019) 'Transportan 10 improves the pharmacokinetics and pharmacodynamics of vancomycin', *Scientific reports*, vol. 9, no. 1, p. 3247.
- Säälik, P., Niinep, A., Pae, J., Hansen, M., Lubenets, D., Langel, Ü. and Pooga, M. (2011) 'Penetration without cells: membrane translocation of cell-penetrating peptides in the model giant plasma membrane vesicles', *Journal of controlled release : official journal of the Controlled Release Society*, vol. 153, no. 2, pp. 117–125.
- Sadd, B. M. and Siva-Jothy, M. T. (2006) 'Self-harm caused by an insect's innate immunity', *Proceedings. Biological sciences*, vol. 273, no. 1600, pp. 2571–2574.
- Sadler, K., Eom, K. D., Yang, J.-L., Dimitrova, Y. and Tam, J. P. (2002) 'Translocating proline-rich peptides from the antimicrobial peptide bactenecin 7', *Biochemistry*, vol. 41, no. 48, pp. 14150–14157.
- Sakai, N. and Matile, S. (2003) 'Anion-mediated transfer of polyarginine across liquid and bilayer membranes', *Journal of the American Chemical Society*, vol. 125, no. 47, pp. 14348–14356.
- Sakai, N., Sordé, N., Das, G., Perrottet, P., Gerard, D. and Matile, S. (2003) 'Synthetic multifunctional pores: deletion and inversion of anion/cation selectivity using pM and pH', *Organic & biomolecular chemistry*, vol. 1, no. 7, pp. 1226–1231.
- Sakai, N., Takeuchi, T., Futaki, S. and Matile, S. (2005) 'Direct observation of anion-mediated translocation of fluorescent oligoarginine carriers into and across bulk liquid and anionic bilayer membranes', *ChemBiochem : a European journal of chemical biology*, vol. 6, no. 1, pp. 114–122.
- Sandiford, S. L., Dong, Y., Pike, A., Blumberg, B. J., Bahia, A. C. and Dimopoulos, G. (2015) 'Cytoplasmic Actin Is an Extracellular Insect Immune Factor which Is Secreted upon Immune Challenge and Mediates Phagocytosis and Direct Killing of Bacteria, and Is a Plasmodium Antagonist', *PLoS pathogens*, vol. 11, no. 2.
- Sani, M.-A., Henriques, S. T., Weber, D. and Separovic, F. (2015) 'Bacteria May Cope Differently from Similar Membrane Damage Caused by the Australian Tree Frog Antimicrobial Peptide Maculatin 1.1\*', *The Journal of biological chemistry*, vol. 290, no. 32, pp. 19853–19862.
- Sattar, S. B. A. and Sharma, S. (2022) *StatPearls: Bacterial Pneumonia*, Treasure Island (FL).
- Schleifer, K. H. and Kandler, O. (1972) 'Peptidoglycan types of bacterial cell walls and their taxonomic implications', *Bacteriological Reviews*, vol. 36, no. 4, pp. 407–477.

## References

- Seervai, R. N. H., Jangid, R. K., Karki, M., Tripathi, D. N., Jung, S. Y., Kearns, S. E., Verhey, K. J., Cianfrocco, M. A., Millis, B. A., Tyska, M. J., Mason, F. M., Rathmell, W. K., Park, I. Y., Dere, R. and Walker, C. L. (2020) 'The Huntingtin-interacting protein SETD2/HYPB is an actin lysine methyltransferase', *Science Advances*, vol. 6, no. 40.
- Sela, S., Neeman, R., Keller, N. and Barzilai, A. (2000) 'Relationship between asymptomatic carriage of *Streptococcus pyogenes* and the ability of the strains to adhere to and be internalised by cultured epithelial cells', *Journal of medical microbiology*, vol. 49, no. 6, pp. 499–502.
- Shai, Y. (1999) 'Mechanism of the binding, insertion and destabilization of phospholipid bilayer membranes by alpha-helical antimicrobial and cell non-selective membrane-lytic peptides', *Biochimica et biophysica acta*, vol. 1462, 1-2, pp. 55–70.
- Shaik, H. A. and Sehna, F. (2009) 'Hemolin expression in the silk glands of *Galleria mellonella* in response to bacterial challenge and prior to cell disintegration', *Journal of Insect Physiology*, vol. 55, no. 9, pp. 781–787.
- Sheehan, G., Clarke, G. and Kavanagh, K. (2018) 'Characterisation of the cellular and proteomic response of *Galleria mellonella* larvae to the development of invasive aspergillosis', *BMC microbiology*, vol. 18, no. 1, p. 63.
- Sheehan, G., Dixon, A. and Kavanagh, K. (2019) 'Utilization of *Galleria mellonella* larvae to characterize the development of *Staphylococcus aureus* infection', *Microbiology (Reading, England)*, vol. 165, no. 8, pp. 863–875.
- Sheehan, G., Garvey, A., Croke, M. and Kavanagh, K. (2018) 'Innate humoral immune defences in mammals and insects: The same, with differences?', *Virulence*, vol. 9, no. 1, pp. 1625–1639.
- Sheehan, G., Konings, M., Lim, W., Fahal, A., Kavanagh, K. and van de Sande, W. W. J. (2020) 'Proteomic analysis of the processes leading to *Madurella mycetomatis* grain formation in *Galleria mellonella* larvae', *PLoS neglected tropical diseases*, vol. 14, no. 4, e0008190.
- Shen, D., Wang, L., Ji, J., Liu, Q. and An, C. (2018) 'Identification and Characterization of C-type Lectins in *Ostrinia furnacalis* (Lepidoptera: Pyralidae)', *Journal of insect science (Online)*, vol. 18, no. 2.
- Shen, W., Hoyos, C. L. de, Sun, H., Vickers, T. A., Liang, X.-H. and Crooke, S. T. (2018) 'Acute hepatotoxicity of 2' fluoro-modified 5-10-5 gapmer phosphorothioate oligonucleotides in mice correlates with intracellular protein binding and the loss of DBHS proteins', *Nucleic acids research*, vol. 46, no. 5, pp. 2204–2217.
- Shim, J., Lee, Y., Jeong, Y. T., Kim, Y., Lee, M. G., Montell, C. and Moon, S. J. (2015) 'The full repertoire of *Drosophila* gustatory receptors for detecting an aversive compound', *Nature communications*, vol. 6, p. 8867.
- Shirley, M. (2021) 'Casimersen: First Approval', *Drugs*, vol. 81, no. 7, pp. 875–879.
- Silva, R. S. de, Kovacicova, G., Lin, W., Taylor, R. K., Skorupski, K. and Kull, F. J. (2005) 'Crystal structure of the virulence gene activator AphA from *Vibrio cholerae* reveals it is a novel member of the winged helix transcription factor superfamily', *The Journal of biological chemistry*, vol. 280, no. 14, pp. 13779–13783.
- Silverman, G. A., Bird, P. I., Carrell, R. W., Church, F. C., Coughlin, P. B., Gettins, P. G., Irving, J. A., Lomas, D. A., Luke, C. J., Moyer, R. W., Pemberton, P. A., Remold-O'Donnell, E., Salvesen, G. S., Travis, J. and Whisstock, J. C. (2001) 'The serpins are an expanding superfamily of structurally similar but functionally diverse proteins. Evolution, mechanism of inhibition, novel functions, and a revised nomenclature', *The Journal of biological chemistry*, vol. 276, no. 36, pp. 33293–33296.
- Sims Sanyahumbi, A., Colquhoun, S., Wyber, R. and Carapetis, J. R. (2016) *Streptococcus pyogenes : Basic Biology to Clinical Manifestations: Global Disease Burden of Group A Streptococcus*, Oklahoma City (OK).
- Singh, C. P., Vaishna, R. L., Kakkar, A., Arunkumar, K. P. and Nagaraju, J. (2014) 'Characterization of antiviral and antibacterial activity of *Bombyx mori* seroin proteins', *Cellular microbiology*, vol. 16, no. 9, pp. 1354–1365.
- Singh, K., Sridevi, P. and Singh R. (2019.) 'Potential Applications of Peptide Nucleic Acid (PNA) in biomedical domain', *Authorea [Online]*. Available at DOI: 10.22541/au.157773086.64212371.
- Singh, S. K., Koshkin, A. A., Wengel, J. and Nielsen, P. (1998) 'LNA (locked nucleic acids): synthesis and high-affinity nucleic acid recognition', *Chemical Communications*, no. 4, pp. 455–456.
- Singkum, P., Suwanmanee, S., Pumeesat, P. and Luplertlop, N. (2019) 'A powerful in vivo alternative model in scientific research: *Galleria mellonella*', *Acta microbiologica et immunologica Hungarica*, vol. 66, no. 1, pp. 31–55.
- Slater, J. (2007) 'Bacterial Infections of the Equine Respiratory Tract', in *Equine Respiratory Medicine and Surgery*, Elsevier, pp. 327–353.



## References

- Smeesters, P. R., McMillan, D. J., Sriprakash, K. S. and Georgousakis, M. M. (2009) 'Differences among group A streptococcus epidemiological landscapes: consequences for M protein-based vaccines?', *Expert review of vaccines*, vol. 8, no. 12, pp. 1705–1720.
- Smith, D. and Casadevall, A. (2021) 'Fungal immunity and pathogenesis in mammals versus the invertebrate model organism *Galleria mellonella*', *Pathogens and disease*, vol. 79, no. 3.
- Sonawane, A., Jyot, J., During, R. and Ramphal, R. (2006) 'Neutrophil elastase, an innate immunity effector molecule, represses flagellin transcription in *Pseudomonas aeruginosa*', *Infection and immunity*, vol. 74, no. 12, pp. 6682–6689.
- Srivastava, P. K., Menoret, A., Basu, S., Binder, R. J. and McQuade, K. L. (1998) 'Heat shock proteins come of age: primitive functions acquire new roles in an adaptive world', *Immunity*, vol. 8, no. 6, pp. 657–665.
- Steer, A. C., Law, I., Matatolu, L., Beall, B. W. and Carapetis, J. R. (2009) 'Global emm type distribution of group A streptococci: systematic review and implications for vaccine development', *The Lancet. Infectious diseases*, vol. 9, no. 10, pp. 611–616.
- Stein, C. A. (1999) 'Two problems in antisense biotechnology: in vitro delivery and the design of antisense experiments', *Biochimica et biophysica acta*, vol. 1489, no. 1, pp. 45–52.
- Stendahl, O., Krause, K. H., Krischer, J., Jerström, P., Theler, J. M., Clark, R. A., Carpentier, J. L. and Lew, D. P. (1994) 'Redistribution of intracellular Ca<sup>2+</sup> stores during phagocytosis in human neutrophils', *Science (New York, N.Y.)*, vol. 265, no. 5177, pp. 1439–1441.
- Strahl, H. and Errington, J. (2017) 'Bacterial Membranes: Structure, Domains, and Function', *Annual review of microbiology*, vol. 71, pp. 519–538.
- Strand, M. R. and Clark, K. D. (1999) 'Plasmatocyte spreading peptide induces spreading of plasmatocytes but represses spreading of granulocytes', *Archives of insect biochemistry and physiology*, vol. 42, no. 3, pp. 213–223.
- Sudhakara, P., Sellamuthu, I. and Aruni, A. W. (2019) 'Bacterial sialoglycosidases in Virulence and Pathogenesis', *Pathogens*, vol. 8, no. 1.
- Szabó, I., Yousef, M., Soltész, D., Bató, C., Mező, G. and Bánóczy, Z. (2022) 'Redesigning of Cell-Penetrating Peptides to Improve Their Efficacy as a Drug Delivery System', *Pharmaceutics*, vol. 14, no. 5.
- Takeuchi, T., Kosuge, M., Tadokoro, A., Sugiura, Y., Nishi, M., Kawata, M., Sakai, N., Matile, S. and Futaki, S. (2006) 'Direct and rapid cytosolic delivery using cell-penetrating peptides mediated by pyrenebutyrate', *ACS chemical biology*, vol. 1, no. 5, pp. 299–303.
- Tang, H. (2009) 'Regulation and function of the melanization reaction in *Drosophila*', *Fly*, vol. 3, no. 1, pp. 105–111.
- Tanji, T., Hu, X., Weber, A. N. R. and Ip, Y. T. (2007) 'Toll and IMD Pathways Synergistically Activate an Innate Immune Response in *Drosophila melanogaster*', *Molecular and Cellular Biology*, vol. 27, no. 12, pp. 4578–4588.
- Tarle, M. and Radoś, N. (1991) 'Investigation on serum neurone-specific enolase in prostate cancer diagnosis and monitoring: comparative study of a multiple tumor marker assay', *The Prostate*, vol. 19, no. 1, pp. 23–33.
- Temsamani, J. G. P. (1997) 'Antisense oligonucleotides: a new therapeutic approach', *Biotechnol Appl Biochem.*, Oct;26(2):65-71.
- Teplyakov, A., Obmolova, G., Toedt, J., Galperin, M. Y. and Gilliland, G. L. (2005) 'Crystal structure of the bacterial Yhch protein indicates a role in sialic acid catabolism', *Journal of bacteriology*, vol. 187, no. 16, pp. 5520–5527.
- Thadchanamoorthy, V. and Dayasiri, K. (2021) 'Review on Pneumococcal Infection in Children', *Cureus*, vol. 13, no. 5, e14913.
- Tian, C., Gao, B., Fang, Q., Ye, G. and Zhu, S. (2010) 'Antimicrobial peptide-like genes in *Nasonia vitripennis*: a genomic perspective', *BMC genomics*, vol. 11, p. 187.
- Todar, K. (2015) *The Good, the Bad, and the Deadly: Streptococci*, <https://textbookofbacteriology.net/index.html>.
- Tojo, S., Naganuma, F., Arakawa, K. and Yokoo, S. (2000) 'Involvement of both granular cells and plasmatocytes in phagocytic reactions in the greater wax moth, *Galleria mellonella*', *Journal of Insect Physiology*, vol. 46, no. 7, pp. 1129–1135.

## References

- Tsai, C. J.-Y., Loh, J. M. S. and Proft, T. (2016) 'Galleria mellonella infection models for the study of bacterial diseases and for antimicrobial drug testing', *Virulence*, vol. 7, no. 3, pp. 214–229.
- Turris, S., Lund, A., Munn, M. B., Chasmar, E., Rabb, H., Callaghan, C. W., Ranse, J. and Hutton, A. (2021) 'Measuring the Masses: Domains Driving Data Collection and Analysis for the Health Outcomes of Mass Gatherings (Paper 3)', *Prehospital and disaster medicine*, vol. 36, no. 2, pp. 211–217.
- U.S. Food and Drug Administration (2016) *FDA approves first drug for spinal muscular atrophy; 2016.12.23* [Online]. Available at <https://www.fda.gov/news-events/press-announcements/fda-approves-first-drug-spinal-muscular-atrophy> (Accessed 27 February 2022).
- U.S. Food and Drug Administration (2018) *Prevnar 7- Pneumococcal 7-valent Conjugate Vaccine (Diphtheria CRM197 Protein). STN: 103905* [Online]. Available at <http://www.fda.gov/vaccines-blood-biologics/vaccines/prevnar> (Accessed 27 February 2023).
- U.S. Food and Drug Administration (2019) *Prevnar 13- Pneumococcal 13-valent Conjugate Vaccine (Diphtheria CRM197 Protein). STN#: 125324* [Online]. Available at <https://www.fda.gov/vaccines-blood-biologics/vaccines/prevnar-13> (Accessed 27 February 2023).
- U.S. Food and Drug Administration (2021) *FDA Approves Targeted Treatment for Rare Duchenne Muscular Dystrophy Mutation;: Press announcement 2021.02.25* [Online]. Available at <https://www.fda.gov/news-events/press-announcements/fda-approves-targeted-treatment-rare-duchenne-muscular-dystrophy-mutation-0> (Accessed 22 February 2023).
- U.S. Food and Drug Administration (2022) *Prevnar 20- Pneumococcal 20-valent Conjugate Vaccine. STN: 125731* [Online]. Available at <https://www.fda.gov/vaccines-blood-biologics/vaccines/prevnar-20> (Accessed 27 February 2023).
- Umezawa, N., Gelman, M. A., Haigis, M. C., Raines, R. T. and Gellman, S. H. (2002) 'Translocation of a beta-peptide across cell membranes', *Journal of the American Chemical Society*, vol. 124, no. 3, pp. 368–369.
- van Ginkel, F. W., McGhee, J. R., Watt, J. M., Campos-Torres, A., Parish, L. A. and Briles, D. E. (2003) 'Pneumococcal carriage results in ganglioside-mediated olfactory tissue infection', *Proceedings of the National Academy of Sciences of the United States of America*, vol. 100, no. 24, pp. 14363–14367.
- van Noort, J. M., Bsibsi, M., Nacken, P., Gerritsen, W. H. and Amor, S. (2012) 'The link between small heat shock proteins and the immune system', *The international journal of biochemistry & cell biology*, vol. 44, no. 10, pp. 1670–1679.
- van Pee, K., Mulvihill, E., Müller, D. J. and Yildiz, Ö. (2016) 'Unraveling the Pore-Forming Steps of Pneumolysin from *Streptococcus pneumoniae*', *Nano letters*, vol. 16, no. 12, pp. 7915–7924.
- Vertyporokh, L. and Wojda, I. (2017) 'Expression of the insect metalloproteinase inhibitor IMPI in the fat body of *Galleria mellonella* exposed to infection with *Beauveria bassiana*', *Acta biochimica Polonica*, vol. 64, no. 2, pp. 273–278.
- Vertyporokh, L. and Wojda, I. (2020) 'Immune response of *Galleria mellonella* after injection with non-lethal and lethal dosages of *Candida albicans*', *Journal of invertebrate pathology*, vol. 170, p. 107327.
- Vierstraete, E., Verleyen, P., Baggerman, G., D'Hertog, W., van den Bergh, G., Arckens, L., Loof, A. de and Schoofs, L. (2004) 'A proteomic approach for the analysis of instantly released wound and immune proteins in *Drosophila melanogaster* hemolymph', *Proceedings of the National Academy of Sciences of the United States of America*, vol. 101, no. 2, pp. 470–475.
- Vivès, E., Brodin, P. and Lebleu, B. (1997) 'A truncated HIV-1 Tat protein basic domain rapidly translocates through the plasma membrane and accumulates in the cell nucleus', *The Journal of biological chemistry*, vol. 272, no. 25, pp. 16010–16017.
- Vogel, B. E. and Hedgecock, E. M. (2001) 'Hemicentin, a conserved extracellular member of the immunoglobulin superfamily, organizes epithelial and other cell attachments into oriented line-shaped junctions', *Development (Cambridge, England)*, vol. 128, no. 6, pp. 883–894.
- Vogel, H., Altincicek, B., Glöckner, G. and Vilcinskas, A. (2011) 'A comprehensive transcriptome and immune-gene repertoire of the lepidopteran model host *Galleria mellonella*', *BMC genomics*, vol. 12, p. 308.
- Wagner, A. (2005) 'Energy constraints on the evolution of gene expression', *Molecular biology and evolution*, vol. 22, no. 6, pp. 1365–1374.
- Wang, L., Hu, C. and Shao, L. (2017) 'The antimicrobial activity of nanoparticles: present situation and prospects for the future', *International journal of nanomedicine*, vol. 12, pp. 1227–1249.

## References

- Wang, Q., Guo, P., Wang, Z., Liu, H., Zhang, Y., Jiang, S., Han, W., Xia, Q. and Zhao, P. (2018) 'Antibacterial Mechanism of Gloverin2 from Silkworm, *Bombyx mori*', *International journal of molecular sciences*, vol. 19, no. 8.
- Wang, Q., Ren, M., Liu, X., Xia, H. and Chen, K. (2019) 'Peptidoglycan recognition proteins in insect immunity', *Molecular immunology*, vol. 106, pp. 69–76.
- Wedde, M., Weise, C., Kopacek, P., Franke, P. and Vilcinskas, A. (1998) 'Purification and characterization of an inducible metalloprotease inhibitor from the hemolymph of greater wax moth larvae, *Galleria mellonella*', *European journal of biochemistry*, vol. 255, no. 3, pp. 535–543.
- Weinberger, D. M., Malley, R. and Lipsitch, M. (2011) 'Serotype replacement in disease after pneumococcal vaccination', *The Lancet*, vol. 378, no. 9807, pp. 1962–1973.
- Wesolowski, D., Tae, H. S., Gandotra, N., Llopis, P., Shen, N. and Altman, S. (2011) 'Basic peptide-morpholino oligomer conjugate that is very effective in killing bacteria by gene-specific and nonspecific modes', *Proceedings of the National Academy of Sciences of the United States of America*, vol. 108, no. 40, pp. 16582–16587.
- Wessels, M. R. (2019) 'Capsular polysaccharide of group A *Streptococcus*', *Microbiology spectrum*, vol. 7, no. 1.
- Whitten, M. M. A., Tew, I. F., Lee, B. L. and Ratcliffe, N. A. (2004) 'A novel role for an insect apolipoprotein (apolipoprotein III) in beta-1,3-glucan pattern recognition and cellular encapsulation reactions', *Journal of immunology (Baltimore, Md. : 1950)*, vol. 172, no. 4, pp. 2177–2185.
- Wickramarachchi, D., Theofilopoulos, A. N. and Kono, D. H. (2010) 'Immune Pathology Associated with Altered Actin Cytoskeleton Regulation', *Autoimmunity*, vol. 43, no. 1, pp. 64–75.
- Wojciechowska, M., Równicki, M., Mieczkowski, A., Miskiewicz, J. and Trylska, J. (2020) 'Antibacterial Peptide Nucleic Acids—Facts and Perspectives', *Molecules*, vol. 25, no. 3.
- Wojda, I., Staniec, B., Sulek, M. and Kordaczuk, J. (2020) 'The greater wax moth *Galleria mellonella*: biology and use in immune studies', *Pathogens and disease*, vol. 78, no. 9.
- Wolfe, J. M., Fadzen, C. M., Choo, Z.-N., Holden, R. L., Yao, M., Hanson, G. J. and Pentelute, B. L. (2018) 'Machine Learning To Predict Cell-Penetrating Peptides for Antisense Delivery', *ACS central science*, vol. 4, no. 4, pp. 512–520.
- World Health Organization (2003) *Pneumococcal vaccines - WHO position paper* [Online].
- World Health Organization (2005) *The current evidence for the burden of Group A Streptococcal diseases*. World Health Organization (WHO/FCH/CAH/05.07), <https://apps.who.int/iris/handle/10665/69063>.
- World Health Organization (2007) *Pneumococcal conjugate vaccine for childhood immunization-WHO position paper* [Online]. Available at <https://apps.who.int/iris/handle/10665/240901>.
- World Health Organization (2017) *Prioritization of pathogens to guide discovery, research and development of new antibiotics for drug-resistant bacterial infections, including tuberculosis* [Online], Geneva.
- World Health Organization (2018) *Rheumatic fever and rheumatic heart disease. Report by the Director General. Seventy-First World Health Assembly*.
- World Health Organization (2021) *Pneumonia* [Online]. Available at <https://www.who.int/news-room/fact-sheets/detail/pneumonia>.
- Wright, L. R., Rothbard, J. B. and Wender, P. A. (2003) 'Guanidinium rich peptide transporters and drug delivery', *Current protein & peptide science*, vol. 4, no. 2, pp. 105–124.
- Wrońska, A. K. and Boguś, M. I. (2020) 'Heat shock proteins (HSP 90, 70, 60, and 27) in *Galleria mellonella* (Lepidoptera) hemolymph are affected by infection with *Conidiobolus coronatus* (Entomophthorales)', *PLoS one*, vol. 15, no. 2.
- Wrońska AK, Kaczmarek A, Kazek M, Boguś MI (2022) 'Infection of *Galleria mellonella* (Lepidoptera) Larvae With the Entomopathogenic Fungus *Conidiobolus coronatus* (Entomophthorales) Induces Apoptosis of Hemocytes and Affects the Concentration of Eicosanoids in the Hemolymph'. *Front Physiol*. 2022 Jan 6;12:774086.
- Wu, G., Liu, Y., Ding, Y. and Yi, Y. (2016) 'Ultrastructural and functional characterization of circulating hemocytes from *Galleria mellonella* larva: Cell types and their role in the innate immunity', *Tissue & cell*, vol. 48, no. 4, pp. 297–304.

## References

- Wu, Y. L., Scott, E. M., Po, A. L. and Tariq, V. N. (1999) 'Development of resistance and cross-resistance in *Pseudomonas aeruginosa* exposed to subinhibitory antibiotic concentrations', *APMIS : acta pathologica, microbiologica, et immunologica Scandinavica*, vol. 107, no. 6, pp. 585–592.
- Xia, A.-H., Zhou, Q.-X., Yu, L.-L., Li, W.-G., Yi, Y.-Z., Zhang, Y.-Z. and Zhang, Z.-F. (2006) 'Identification and analysis of YELLOW protein family genes in the silkworm, *Bombyx mori*', *BMC genomics*, vol. 7, p. 195.
- Xia, X., You, M., Rao, X.-J. and Yu, X.-Q. (2018) 'Insect C-type lectins in innate immunity', *Developmental and comparative immunology*, vol. 83, pp. 70–79.
- Xu, X. and Vogel, B. E. (2011) 'A Secreted Protein Promotes Cleavage Furrow Maturation during Cytokinesis', *Current biology : CB*, vol. 21, no. 2, pp. 114–119.
- Xu, X., Xu, M., Zhou, X., Jones, O. B., Moharomd, E., Pan, Y., Yan, G., Anthony, D. D. and Isaacs, W. B. (2013) 'Specific structure and unique function define the hemicentin', *Cell & Bioscience*, vol. 3, p. 27.
- Yang, L., Harroun, T. A., Weiss, T. M., Ding, L. and Huang, H. W. (2001) 'Barrel-stave model or toroidal model? A case study on melittin pores', *Biophysical Journal*, vol. 81, no. 3, pp. 1475–1485.
- Yavari, N., Goltermann, L. and Nielsen, P. E. (2021) 'Uptake, Stability, and Activity of Antisense Anti-acpP PNA-Peptide Conjugates in *Escherichia coli* and the Role of SbmA', *ACS chemical biology*, vol. 16, no. 3, pp. 471–479.
- Yoshida, T., Naito, Y., Yasuhara, H., Sasaki, K., Kawaji, H., Kawai, J., Naito, M., Okuda, H., Obika, S. and Inoue, T. (2019) 'Evaluation of off-target effects of gapmer antisense oligonucleotides using human cells', *Genes to Cells*, vol. 24, no. 12, pp. 827–835.
- Zafar, M. A., Hamaguchi, S., Zangari, T., Cammer, M. and Weiser, J. N. (2017) 'Capsule Type and Amount Affect Shedding and Transmission of *Streptococcus pneumoniae*', *mBio*, vol. 8, no. 4.
- Zafar, M. A., Wang, Y., Hamaguchi, S. and Weiser, J. N. (2017) 'Host-to-Host Transmission of *Streptococcus pneumoniae* Is Driven by Its Inflammatory Toxin, Pneumolysin', *Cell host & microbe*, vol. 21, no. 1, pp. 73–83.
- Zdbicka-Barabas, A. and Cytrynska, M. (2013) 'Apolipoproteins and insects immune response', *Invertebr. Surviv. J.*, vol. 10, pp. 58–68.
- Zhang, S., Gunaratna, R. T., Zhang, X., Najjar, F., Wang, Y., Roe, B. and Jiang, H. (2011) 'Pyrosequencing-based expression profiling and identification of differentially regulated genes from *Manduca sexta*, a lepidopteran model insect', *Insect Biochemistry and Molecular Biology*, vol. 41, no. 9, pp. 733–746.
- Zhang, X., He, Y., Cao, X., Gunaratna, R. T., Chen, Y., Blissard, G., Kanost, M. R. and Jiang, H. (2015) 'Phylogenetic analysis and expression profiling of the pattern recognition receptors: Insights into molecular recognition of invading pathogens in *Manduca sexta*', *Insect Biochemistry and Molecular Biology*, vol. 62, pp. 38–50.
- Zhu, H., Zhang, X., Lu, M., Chen, H., Chen, S., Han, J., Zhang, Y., Zhao, P. and Dong, Z. (2020) 'Antibacterial Mechanism of Silkworm Serpins', *Polymers*, vol. 12, no. 12.
- Zhu, Y., Ragan, E. J. and Kanost, M. R. (2010) 'Leureptin: a soluble, extracellular leucine-rich repeat protein from *Manduca sexta* that binds lipopolysaccharide', *Insect Biochemistry and Molecular Biology*, vol. 40, no. 10, pp. 713–722.
- Zhu, Y., Yu, X. and Cheng, G. (2020) 'Insect C-Type Lectins in Microbial Infections', *Advances in experimental medicine and biology*, vol. 1204, pp. 129–140.
- Zurovec, M., Kodrik, D., Yang, C., Sehnal, F. and Scheller, K. (1998) 'The P25 component of *Galleria* silk', *Molecular & general genetics : MGG*, vol. 257, no. 3, pp. 264–270.
- Zurovec, M. and Sehnal, F. (2002) 'Unique molecular architecture of silk fibroin in the waxmoth, *Galleria mellonella*', *The Journal of biological chemistry*, vol. 277, no. 25, pp. 22639–22647.

## Appendix

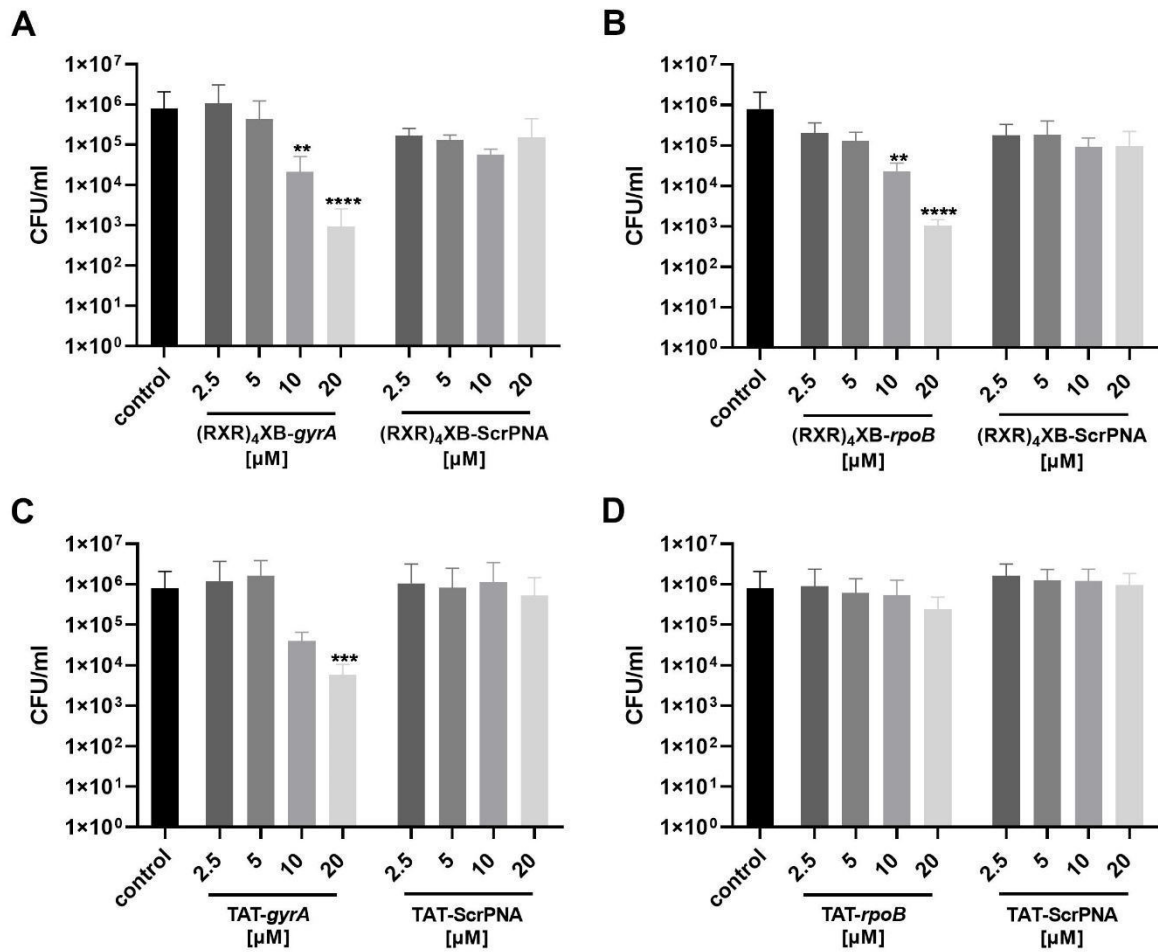


**Figure 35: Concentration-dependent reduction of bacterial cell count following treatment of *S. pneumoniae* D39 with cell-penetrating peptide (CPP)-antisense PNAs for 6 h.** scrPNA, scrambled PNA controls. Treatment with (A) (RXXR)<sub>4</sub>XB-anti-*gyrA* PNAs, (B) (RXXR)<sub>4</sub>XB-anti-*rpoB* PNAs, (C) TAT-anti-*gyrA* PNAs, and (D) TAT-anti-*rpoB* PNAs. Data are presented as means and standard deviation. Statistical significance was determined by one-way analysis of variance (ANOVA) with multiple comparisons. Differences between PNA conjugate samples and mock control (untreated) are shown as:  $p \leq 0.01$  (\*\*);  $p \leq 0.001$  (\*\*\*);  $p \leq 0.0001$  (\*\*\*\*). Sample size:  $n = 5$ , (Barkowsky et al., 2022).

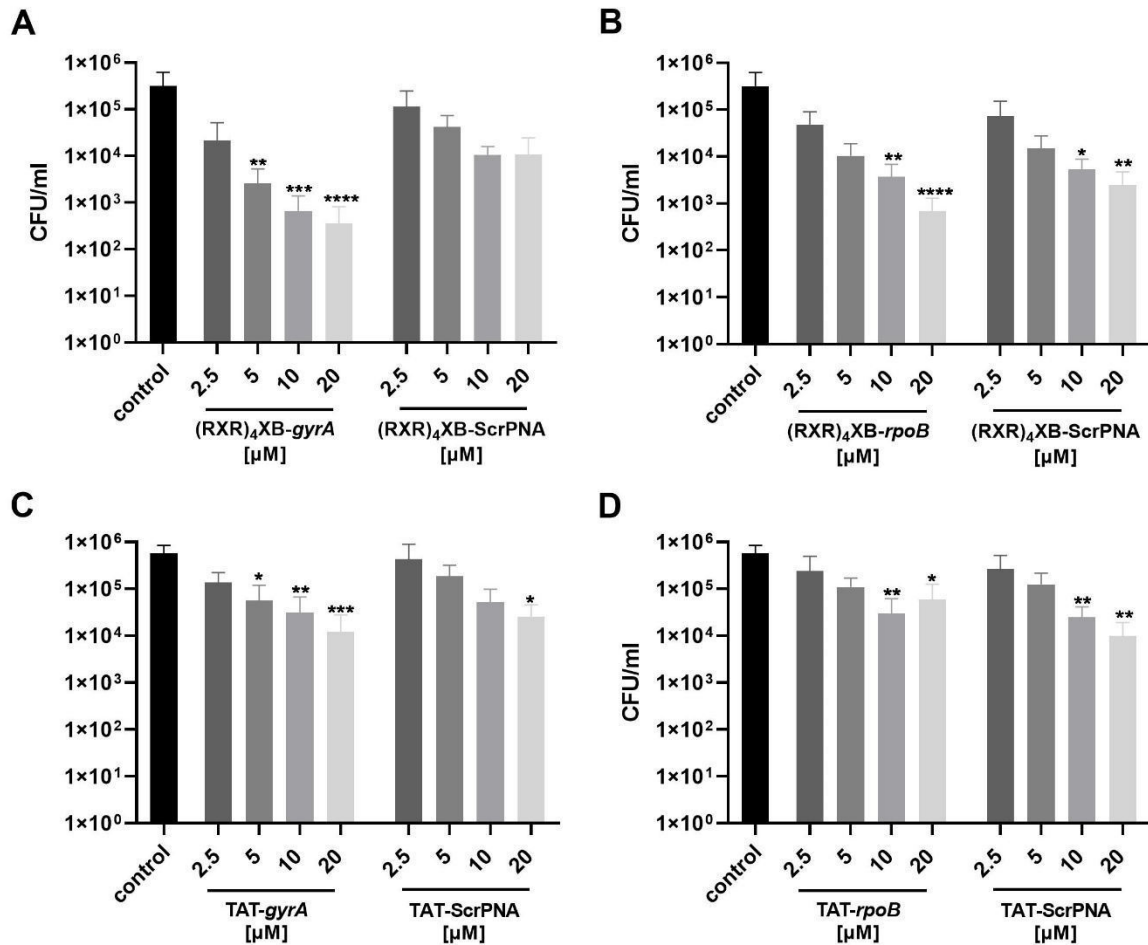


**Figure 36: Concentration-dependent reduction of bacterial cell count following treatment of *S. pneumoniae* 19F with cell-penetrating peptide (CPP)-antisense PNAs for 6 h.** scrPNA, scrambled PNA controls. Treatment with (A) (RXR)<sub>4</sub>XB-anti-*gyrA* PNAs, (B) (RXR)<sub>4</sub>XB-anti-*rpoB* PNAs, (C) TAT-anti-*gyrA* PNAs, and (D) TAT-anti-*rpoB* PNAs. Data are presented as means and standard deviation. Statistical significance was determined by one-way analysis of variance (ANOVA) with multiple comparisons. Differences between PNA conjugate samples and mock control (untreated) are shown as:  $p \leq 0.05$  (\*);  $p \leq 0.01$  (\*\*);  $p \leq 0.0001$  (\*\*\*). Sample size:  $n = 5$ , (Barkowsky et al., 2022).

**Table 25: Effect of pyrenebutyrate on antimicrobial cell count reduction of CPP-PNA on *S. pneumoniae*.** Log<sub>10</sub> cell count reduction of different CPP-PNA in absence (-) and presence (+) of pyrenebutyrate (PB), compared to untreated control. Increased (positive numbers) or reduced (negative numbers) effects of PB are listed. Numbers are calculated from mean values.  $n = 4-5$ .

CPP-PNA	Log <sub>10</sub> reduction - PB	Log <sub>10</sub> reduction + PB	$\Delta$ Log <sub>10</sub> reduction - PB	$\Delta$ Log <sub>10</sub> reduction + PB	Increased specific AMP effect by PB [log <sub>10</sub> CFU reduction]
(RXR) <sub>4</sub> XB- <i>gyrA</i>	4.1	4.0	2.87	2.42	- 0.45
(RXR) <sub>4</sub> XB-scrPNA	1.23	1.58			
TAT- <i>gyrA</i>	1.59	2.0	0.49	1.18	0.69
TAT-scrPNA	1.1	0.85			
					<b>Increased effect with PB [log<sub>10</sub> CFU reduction]</b>
R9- <i>gyrA</i>	2.0	2.83			0.83
PenArg- <i>gyrA</i>	3.54	3.63			0.09
Sc18- <i>gyrA</i>	1.88	0.95			- 0.93

**Table 26: Effect of pyrenebutyrate on antimicrobial cell count reduction of CPP-PNA on *S. pyogenes*.** Log<sub>10</sub> cell count reduction of different CPP-PNA in absence (-) and presence (+) of pyrenebutyrate (PB), compared to untreated control (Ampuwa®). Used concentration: 5 μM CPP-PNA; 100 μM PB. The specific reduction ( $\Delta$  log<sub>10</sub> reduction) considers the unspecific toxicity of CPP-scrPNA and is calculated as: log CFU reduction of CPP-antisensePNA – log reduction of CPP-scrPNA. The specific effect of PB is the difference of the  $\Delta$  log<sub>10</sub> reduction in presence and absence of PB (positive numbers are increased cell count reduction). Numbers are calculated from mean values. n = 7 – 8 (except TAT-anti-*gyrA*: n = 5)

CPP-PNA	Log <sub>10</sub> reduction - PB	Log <sub>10</sub> reduction + PB	$\Delta$ Log <sub>10</sub> reduction - PB	$\Delta$ Log <sub>10</sub> reduction + PB	Specific effect of PB [ $\Delta$ log <sub>10</sub> CFU reduction]
(RXR) <sub>4</sub> XB- <i>gyrA</i>	2.37	2.93	0.99	1.4	0.41
(RXR) <sub>4</sub> XB-scrPNA	1.38	1.23			
TAT- <i>gyrA</i>	3.67	4.53	2.66	3.53	0.89
TAT-scrPNA	1.01	1.00			
K8- <i>gyrA</i>	3.89	4.90	2.92	3.52	0.60
K8-scrPNA	0.97	1.38			

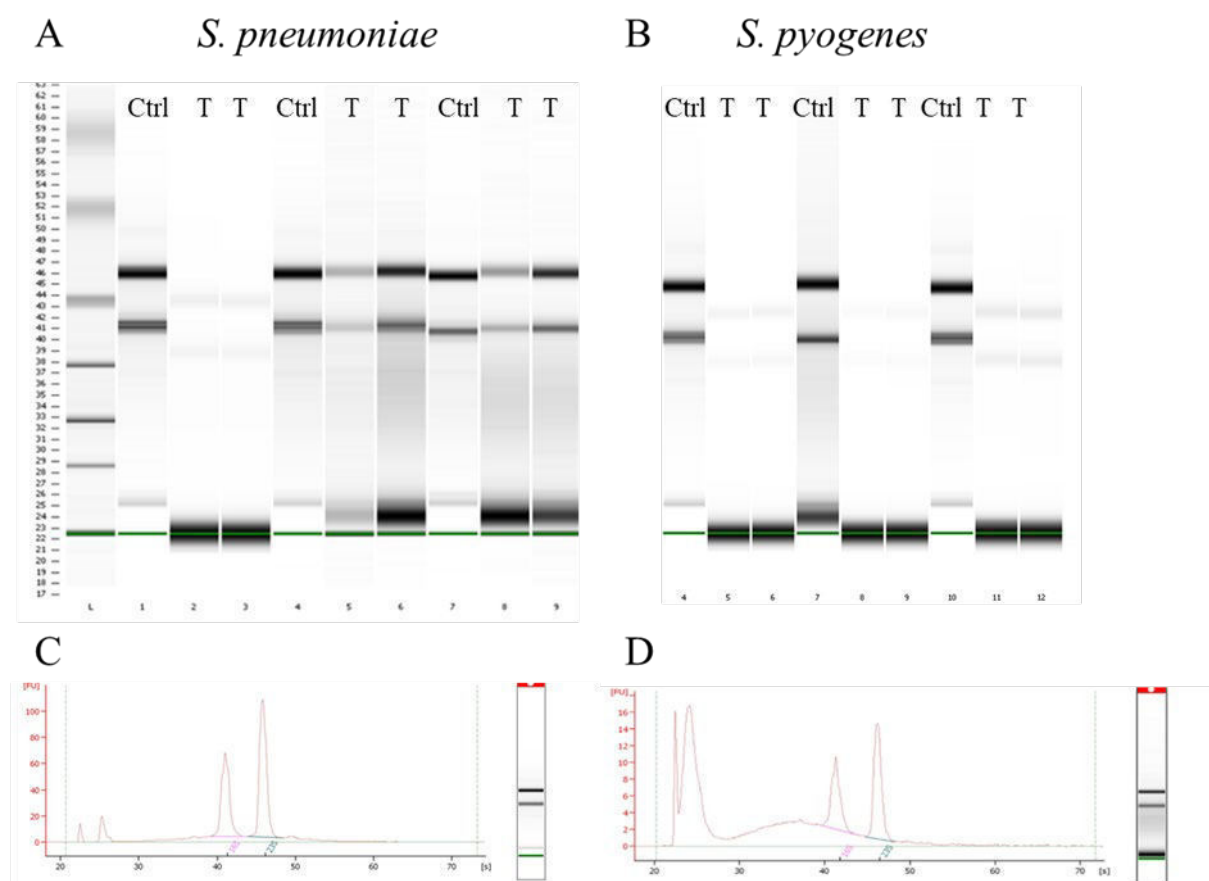


**Figure 37: RNA isolated of streptococci after treatment with lethal concentration of CPP-PNA.** RNA isolated from streptococci after short pulse (30 min) with lethal concentrations of CPP-PNA (T) or water control (Ctrl), and analysed with the Agilent 2100 Bioanalyser using the Agilent RNA 6000 Nano Kit. (A) Gel image of RNA isolated from *S. pneumoniae* TIGR4 after treatment with 10 μM CPP-PNA. (B) Gel image of RNA isolated from *S. pyogenes* 591 after treatment with 7.5 μM CPP-PNA. (C) Electropherogram of RNA isolated from *S. pneumoniae* TIGR4 incubated with a water control. (D) Electropherogram of RNA isolated from *S. pneumoniae* treated with 10 μM CPP-PNA. Ladder (L): size in nucleotides [nt]. Data from Tim Dannenberg.

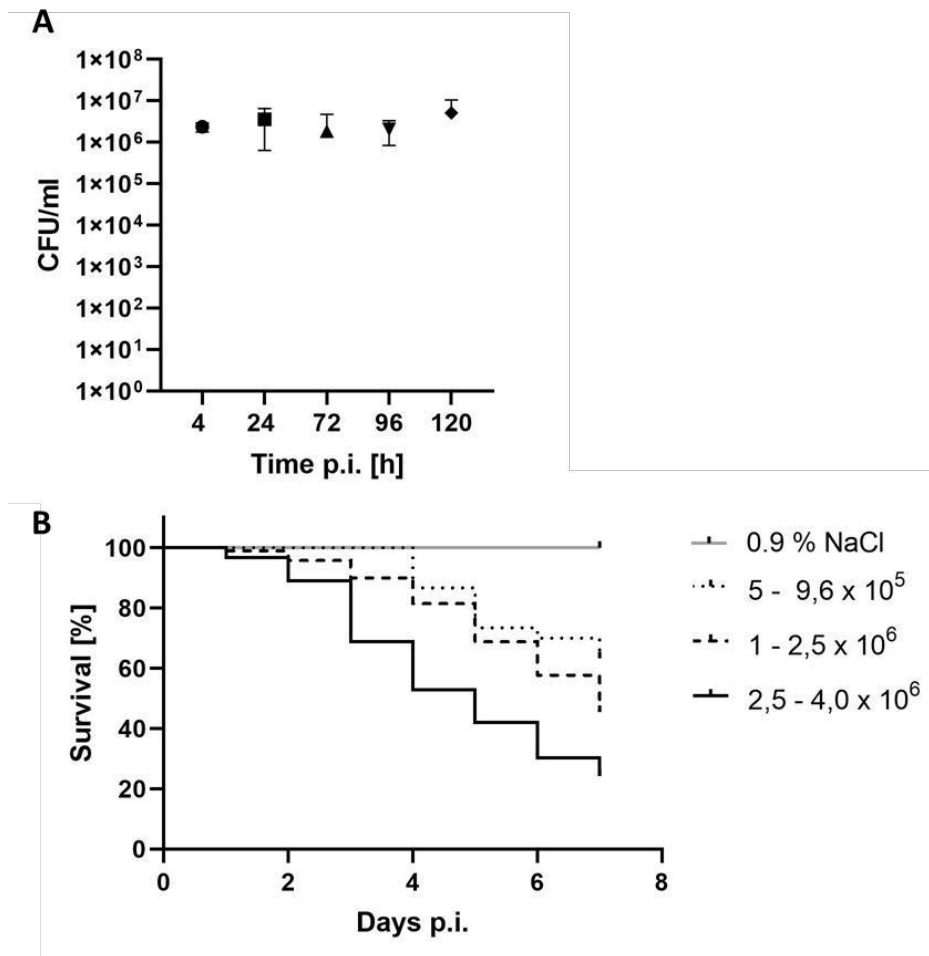


**Figure 38: Bacterial load and survival rate of *G. mellonella* infected with *S. pyogenes* 591.** (A) Bacterial load and persistence of *S. pyogenes* 591 injected with  $2.5 - 4 \times 10^6$  CFU/larvae in *G. mellonella* over 120 h p.i.. Data are presented as mean values with standard deviation. Sample size: in three independent runs, at 4 h: n = 12; 24 h: n = 7; 72 h: n = 5; 120 h: n = 3. (B) Kaplan Meier curve of survival rate of *G. mellonella* larvae infected with different dosages of *S. pyogenes* 591 over 7 days p.i.. Sample size: treated with 0.9 % NaCl: n = 40;  $5 - 9.6 \times 10^5$  CFU/larvae: n = 30;  $1 - 2.5 \times 10^6$  CFU/larvae: n = 170;  $2.5 - 4 \times 10^6$  CFU/larvae: n = 120.



**Table 27: Proteins with altered abundance in infected larvae compared to control larvae at 4, 24, and 72 h post infection.** Black numbers: increased abundance in infected larvae; blue numbers: reduced levels in infected larvae. Proteins are grouped based on suggested roles. Only fold changes < 2 and with p-values (ANOVA) < 0.05 are listed.

Accession	Description	Fold change		
		4 h	24h	72h
<b>Olfactory, gustatory, chemosensory protein</b>				
A0A6J1WTK1	Gustatory receptor candidate 59	7.4	Infinity	254.2
A0A6J1WG93	Odorant binding protein		1.9	10.4
A0A6J1WFB4	Odorant binding protein			9.1
A0A6J1WFP6	Odorant binding protein			2.7
A0A5C0E4H9	Chemosensory protein 15	3.4	817.8	9.4
A0A5C0E3Y6	Chemosensory protein 14	2.7	40.9	28.6
A0A5C0E221;A0A6J1X1V3	Chemosensory protein 8	2	11.6	30.1
A0A5C0E3E0;A0A6J3BZE6	Chemosensory protein 6		8.9	3.0
A0A5C0E2H9	Chemosensory protein 3		3.2	
A0A5C0E3F0;A0A6J1X7W1	Chemosensory protein 16		2	4.4
<b>Recognition/Opsonization</b>				
A0A6J1WRG3	Peptidoglycan recognition protein	91.1	7058.4	Infinity
A0A6J3BSP3;A0A6J3BXH7	Peptidoglycan recognition protein		55.6	2238.1
A0A6J1WIFY4	Peptidoglycan recognition protein	4.2	124.7	35.8
A0A6J1X3D5	Peptidoglycan recognition protein		8.2	18.9
Q8ITT1	Peptidoglycan recognition protein		6.2	12.8
A0A6J1WTH3;Q8ITT5	Peptidoglycan recognition protein		4.9	6.5
A0A6J1WPB8	Peptidoglycan recognition protein		17.1	26.3
A0A6J3BWU0;M1FW43	Peptidoglycan recognition protein	5.7	47.5	34
A0A6J1WC08;A0A6J1WC96	$\beta$ -1,3-glucan recognition protein		32.2	554.5
A0A6J1WHB6	$\beta$ -1,3-glucan recognition protein		90	
A0A6J1X8E9	$\beta$ -1,3-glucan recognition protein		39.5	
Q0E666;A0A6J3CBF7	$\beta$ -1,3-glucan recognition protein		4.9	9.8
A0A6J1WBD0;A0A6J1X785	$\beta$ -1,3-glucan recognition protein		3.5	
A0A6J1WNB4	$\beta$ -1,3-glucan recognition protein		2.5	3
A0A6J1X4Z5	$\beta$ -1,3-glucan recognition protein		2.7	2.7
C7ASJ3	Hemolin		92	48.4
A0A6J1WDH4	Hemicentin 1-like		3.1	30.7
A0A6J1WFM3	MD-2-related lipid-recognition protein-like			3.0
<b>Phenoloxidase system</b>				
A0A6J1WSG2;Q6UEH6	Prophenoloxidase subunit 2		- 4.3	- 5.4
Q964D5;Q9TWE9	Prophenoloxidase		- 3.8	- 5.7
A0A6J1W753	Phenoloxidase activating	2.1	37.4	27.4
A0A6J1WR80	L-dopachrome tautomerase yellow-f2-like		3.0	6.5
A0A6J1WEQ1;A0A6J1WLI8	Protein yellow-like		15.0	17.8
<b>Non-food digestive serine proteases</b>				
A0A6J1WWN6;A0A6J1X3N4	CLIP domain-containing serine protease		10.3	26.7
A0A6J1WFH8;A0A6J3C1Z9	Modular serine protease-like		8.5	10.5
A0A6J1WMH8	CLIP domain-containing serine protease		4.0	5.3
A0A6J1WLM8	Serine protease gd-like		2.4	3.2
A0A6J1WUY6	Scolexin B-like			2.1
<b>Serine protease inhibitors</b>				
A0A6J1W8F4	Serpin	2.2	3.4	22.6
A0A6J3CD34	Serpin; leukocyte elastase inhibitor-like		9.4	4.7
A0A6J1WYU5	Serpin; leukocyte elastase inhibitor-like	7.3	339.4	13.5
A0A6J1W790	Serine protease inhibitor 77Ba-like	3.8	32.4	28.4
A0A6J1WUP5	Serine protease inhibitor dipetalogastin-like		9.5	22.1
A0A6J1WBF9	Phosphatidylethanolamine-binding protein 1-like	2.0	7.8	3.6
A0A6J1W8F4	Serine-type endopeptidase inhibitor activity	2.2	3.4	22.6
A0A6J1WD23;A0A6J1WC71;	Alaserpin-like isoform			2.3

Accession	Description	Fold change		
		4 h	24h	72h
<b>Cytoskeleton and muscle components</b>				
A0A6J1WV96;A0A6J3CGX9	Myosin light chain alkali		1970.1	Infinity
A0A6J1X818	Elastin-like		15.1	108.3
A0A6J1WA54	Tropomyosin-2 isoform	4.4	266.7	17.3
A0A6J1W9N2;A0A4P8D336;A0A6J3BWD8	Tropomyosin-1 isoform X1	2.7	112.4	18.5
A0A6J1W617	Troponin I isoform X8	2.2	44.5	9.2
A0A6J1WM33	Myophilin	3	40	14
A0A6J1WIL1;A0A6J3BTM2	Troponin T skeletal muscle isoform		27.6	17.6
A0A6J1X2Z5	Actin muscle		17	6.4
A0A3G1T170	Actin 3		17	6.4
A0A6J1X611	Transgelin	2.3	13.6	7.6
A0A3G1T187;A0A6J1WVK1	Tubulin alpha chain		5.6	
A0A6J1WHZ4	Tubulin beta chain		3.5	
A0A6J1WGF3	Cofilin/actin-depolymerizing factor homolog		6.9	
A0A6J1X8E0	Insecticyanin-A-like			4.4
A0A6J1WRF1	Insecticyanin-A or 2			4.4
<b>Silk fibers and components</b>				
A0A6J1X4G6;Q9GUB5	Fibroin heavy chain	17.9		375.1
A0A6J1WD63;Q26427	Fibroin light chain	11.2	23.4	214.8
A0A6J1WHS7	Fibrohexamerin	27		141.2
A0A6J1WAR2;O62605	Fibrohexamerin	17.5		28.2
A0A6J1X1A8;A0A385JC11	Keratin-associated protein 19-2		2.7	7
A0A6J1X0P3;A0A6J3C8K9	Seroin	21.6	37.1	228.7
<b>Metabolism</b>				
A0A6J1WJM9	Fructose-bisphosphate aldolase		4.0	
A0A6J1W9W1	Fructose-bisphosphatase		3.2	
A0A6J1WK99;A0A6J3BVA9	Fructose-bisphosphate aldolase		3.8	
A0A6J1X640	Phosphopyruvate hydratase	2.2	8.3	
A0A6J1WYK7	Putative hydroxypyruvate isomerase			- 2.3
A0A6J1X4T9	Probable alpha-mannosidase At5g66150			- 9.2
A0A6J3C1Z4	Alpha-mannosidase			- 10.3
A0A6J1WL51;A0A6J1WLC5	Pyruvate kinase		4.5	
A0A6J1X517	Transketolase-like protein 2		2.9	- 4.8
A0A6J1WZX5;A0A6J3C9F4	Ornithine aminotransferase		5.0	- 12
A0A6J1WLD3;A0A6J1WEP3	Aldehyde dehydrogenase			- 11.8
A0A3G1T1B1;A0A6J1WJ94	Lambda-crystallin homolog		2.9	- 3.8
A0A6J1X3S6;A0A6J3C7U7	N-acetylneuraminatase lyase-like		3.1	- 8
A0A6J1WEK4	Retinal dehydrogenase 1-like		2.7	- 6.2
A0A3G1T199	Beta-ureidopropionase-like			- 6.6
A0A6J1WS44	Malate dehydrogenase	4.3	194.1	3.1
Q24997	Hexamerin			- 3
A0A6J1WGW2	Luciferin 4-monooxygenase-like		3	- 17.6
A0A6J1WVI3	Luciferin 4-monooxygenase-like		3.8	- 18.3
<b>Digestive gut enzyme</b>				
A0A6J3C399	Chymotrypsin-like elastase		2.2	4.1
A0A6J1WE27	Pancreatic lipase-related protein 1-like	2.1	22.1	27.8
A0A6J1WJA5	Lipase			9.6
A0A6J1W9E7	Lipase 3-like		4.2	13.4
A0A6J1WR81	Digestive cysteine proteinase 2-like	2.2		5.8
A0A6J1WUV4	Carboxypeptidase B-like			- 50.6
A0A6J1WGT9;A0A6J1WHZ1	Trypsin 3A1-like isoform X1		143	126.1
Q961Y0;A0A6J1WP58	Trypsin-like protein		5.2	
A0A6J1WTL2	Trypsin CFT-1-like			11
A0A6J3C399	Chymotrypsin-like elastase		2.2	4.1
A0A6J1X5J9	Papain-like cystein protease	2.3	19.7	12

Accession	Description	Fold change		
		4 h	24h	72h
A0A6J1W7W7	Cathepsin L		2.2	2.4
A0A6J1WPB0	Chitin deacetylase 8			15
A0A3G1T1P7;A0A6J3C4K6	Mucin-like	-71.2		119.8
<b>Carboxylester hydrolases</b>				
A0A6J3C7U2	Carboxylic ester hydrolase		10.1	26.9
A0A6J1WDQ7;A0A6J3C429	Carboxylic ester hydrolase		6.1	22.9
A0A6J1WG21;A0A6J3CBU5	Carboxylic ester hydrolase		6.7	6.7
A0A6J1W716	Carboxylic ester hydrolase		2.7	4.8
A0A6J1W743	Carboxylic ester hydrolase		2.1	5.3
A0A6J1WVD2	Carboxylesterase 1E; serine esterase,	2.8	218.9	30.5
A0A6J1W7L5;A0A6J1W707	Carboxylic ester hydrolase		13.7	24.1
A0A6J1WRD5	Venom carboxylesterase-6-like		93.1	92.7
A0A6J1W9F9	Carboxylic ester hydrolase		11.7	15
<b>Glutathione-S-transferase</b>				
Q964D6;A0A6J1X241	Glutathione-S-transferase-like protein	2.2	10.2	1.7
A0A6J1W9D2	Glutathione S-transferase-like		2.6	2.9
A0A6J1WGB7	Glutathione S-transferase 2-like		7.5	ns
<b>Development</b>				
A0A6J3C2I3	Juvenile hormone esterase-like		33.4	121.4
A0A6J1WMG8	Basic juvenile hormone-suppressible protein 2-like		-3.6	-2.7
A0A6J1WN20	Acidic juvenile hormone-suppressible prot. 1			-3.2
A0A6J1WQX3	Hemolymph juvenile hormone bp	2	31.5	40.9
A0A6J1WJG7	Spermine oxidase			-2.9
A0A6J3C2B6	Spermine oxidase-like			-3.2
A0A6J1W995	Spermine oxidase-like			-2.5
A0A6J1WG68	Vitellogenin			-2.3
<b>Antimicrobial peptides</b>				
A0A6J1X9I2;Q8ITT0	Gloverin		235	166.5
A0A6J1W9I9	Gloverin-like		121.1	354.6
A0A6J1WQI3	Gloverin-like		146.1	4.6
P85210	Cecropin-D-like peptide		Infinity	Infinity
A0A6J1WJ15	Cecropin-like	Infinity	7873	417.7
A0A6J1WAG2	Lysozym		7.8	24.6
A0A6J1WSB4;P82174	Lysozyme		8.4	14.5
A0A6J1W7W4	Lysozyme		3.4	3.7
C9WHZ7;P85211;P85214	Proline-rich protein		48	19.4
A0A6J3CC84	Inducible metalloproteinase inhibitor protein		130.8	376.5
A0A6J1X0P3;A0A6J3C8K9	Seroin isoform X2	21.6	37.1	228.7
Q8ITT4;A0A6J1X5W9	6tox		32.5	38.2
A0A6J1W9L8	Apolipoprotein D-like	2.1	7.7	6.7
A0A6J1X1K1	Apolipophorins-like			2.1
A0A6J3C047	Apolipophorins-like			2.1
A0A3G1T196;P85216	Anionic antimicrobial peptide 2		2.5	
A0A6J3BWC0;A5Z1R7	Superoxide dismutase	3.7	243.4	
<b>Heat shock proteins</b>				
A0A3G1T1G8;A0A6J1WTU8	Small HSP20		15.5	7.8
A0A3G1T1A3;A0A6J3BX10	Small HSP21.4		9.5	2.8
A0A3G1T1F5;A0A6J1WNJ3	HSP27.2		7.5	5.8
A0A3G1T1I1;A0A6J1X5C5	HSP70		6.6	
<b>Putative immune relevant</b>				
A0A6J1WA04	Calexitin-2-like		156.2	36
A0A6J1WUS2	Nucleobindin-2		10	12.2
A0A3G1T1Q5;A0A6J3BXS6	Apyrase-like			3.3
A0A6J1WLS9;A0A6J1WMA8	Arginine Kinase	2.5	7	
A0A6J1WFW3	Protein-histidine N-methyltransferase	13.7	1309.8	170.3
A0A6J1WIP1	27kDa hemolymph protein			3.5

## Appendix

Accession	Description	Fold change		
		4 h	24h	72h
A0A6J1X587	Hdd1-like		3.7	9.9
A0A6J3BX75	Spondin-1		2.8	5.3
A0A6J1WT50	Endoribonuclease		6.5	8.7
A0A6J1WSG1	Endoribonuclease			2.2
A0A3G1T1K4	Nucleoside diphosphate kinase		3.1	
A0A6J1X3S8	inter- $\alpha$ -trypsin inhibitor heavy chain H4-like		3.7	3.5
A0A3G1T1C0	Thioredoxin		5.9	2
A0A6J1X7S2	Sulfhydryl oxidase			5.7
A0A6J1X0T9	Catalase			- 2
A0A6J1WZW5	Trans-1_2-dihydrobenzene-1_2-diol dehydrogenase-like		- 3.6	- 3.4
A0A3G1T1I6;A0A6J3CAI3	Peroxiredoxin		3.2	- 2.3
A0A6J1WH84	15-hydroxyprostaglandin dehydrogenase [NAD(+)]-like		3.6	- 4.7
A0A6J1WHD9	GILT-like protein 1		- 2.1	- 8.8
Q9GQW5	Ferritin		2.3	
A0A6J1W8K3;A0A6J3C1B1	Ferritin		2.1	
A0A6J3BT64	Vainin-like protein 2		3.8	8.7
A0A6J3CA50;A0A6J1X7U6	N-acetylneuraminate 9-O-acetyltransferase			2.1